Imperial College London

Bacteriophage-guided cancer immunotherapy

Sajee Waramit

A thesis submitted to Imperial College London
for the degree of Doctor of Philosophy

Imperial College London

Faculty of Medicine

Division of Brain Sciences

Declaration

I hereby declare that the work presented in this thesis was conducted entirely by myself under the supervision of Dr. Amin Hajitou at the Department of Medicine, Faculty of Medicine, Imperial College London, during the year 2015-2019.

This thesis is submitted to Imperial College London for the degree of Doctor of Philosophy. No part of this thesis has already been, or is presently being, submitted for any other degree.

I confirm that the work reported herein is my own, and the work of others has been appropriately credited and referenced within this thesis. The contribution of other researchers work is indicated below:

The work presented in Figure 2.4 (chapter 2) and 3.5 (chapter 3) were performed with the assistance of Dr. Mariam Al-Bahrani, a previous PhD student at the Phage Therapy Group, Department of Medicine, Imperial College London.

The work presented in Figure 2.5 (chapter 2) was performed with the assistance of Dr.Keittisak Suwan, a research associate at the Phage Therapy Group, Department of Medicine, Imperial College London.

The work presented in Figure 3.7 and 3.8 (chapter 3) was performed with the assistance of Mr.Aittiphon Chongchai, a PhD student in the Department of Biochemistry, Faculty of Medicine, Chiang Mai University, Chiang Mai, Thailand.

Sajee Waramit
Imperial College London
May 2019

Copyright Declaration

Abstract

Over the past decades, gene delivery has become a powerful tool for treating many diseases; therefore, a wide range of delivery systems, simply categorised into viral and non-viral vectors, have been developed and applied in both research and clinical translation. In spite of high transduction efficacy, viral vectors encounter a number of limitations regarding their native entities. A hybrid bacteriophage vector has been successfully developed by our Phage Virotherapy group by integrating AAV elements into the filamentous bacteriophage genome. In doing so, the new vector, named adeno-associated phagemid-based vector (PAAV), is able to overcome limitations associated with AAV native tropism by using advantages of bacteriophages that lack native tropism for mammalian cells and tissues. PAAV vector has been applied in a few research areas including cancer therapy. To systemically target solid tumours, the vector is displayed cyclic RGD4C (CDCRGDCFC) ligands on the pIII capsids allowing it to specifically target the $\alpha_V\beta_3$ integrin receptors overexpressed on tumour cell surface and tumour blood vessels.

In this study, PAAV vector has been further refined to display the endosomal escape peptide (H5WYG) on the recombinant pVIII capsids to enhance endosomal escape and transgene expression. The PAAV displaying H5WYG peptide showed great buffering capacity at mild acidic pH relating to the situation that occurs during endosomal maturation and subsequently enhanced luciferase reporter gene expression in numerous human cancer cell lines, including lung carcinoma (A549), melanoma (M21) and meduloblastoma (UW228). Importantly, the modified vector remained safe for normal cells. H5WYG peptide facilitated endosomal escape through a proton sponge effect mechanism as PAAV-mediated gene expression decreased when applying the vascuolar ATPase inhibitor (bafilomycin A1) during vector transduction. Furthermore, displaying H5WYG peptide on the PAAV capsid augmented the secreted TNFα gene expression resulting in a greater cell death of A549, M21 and UW228 cells.

The PAAV gene delivery vector was tested in various applications in this thesis. Firstly, the vector was applied as a delivery tool to express the tumour associated antigens (MUC1 and PSMA) which are common target antigens for CAR T cell therapy. PAAV vector augmented MUC1 and PSMA expression in A549, Suit2 and UW228 cells. Although CAR T cells were not applied here, the strategy based on PAAV vector to enhance antigen expression can make the tumours more visible for CAR T cells and might be useful for CAR T cell therapy in solid tumours. Secondly, PAAV was applied on cancer vaccination in combination with a malaria vaccine. The vector was used to deliver a malarial epitope, Pb9, to present on tumour cell surfaces via restricted H2-K^d MHC class I molecules while adenoviral vector encoding a malaria sequence (ME.TRAP) was used to induce an immune response against Pb9. It is shown here that PAAV vector mediated Pb9 expression in EF43.fgf4 breast tumours. The ME.TRAP vaccine stimulated immune response according to *ex vivo* investigations of specific effector cell proliferation, activation and function. Pb9-specific tumour cell killing was also found both *ex vivo* and *in vivo*. The tumour cell death was mediated through caspase-3 dependent apoptosis. All these findings indicate the efficiency and numerous applications of PAAV-mediated gene delivery for cancer treatment.

Acknowledgment

I would like to express my appreciation and deep gratitude to many people who in one way or another have contributed in making this study possible and my working experience valuable.

First and foremost, my deepest appreciation goes to my supervisor, Dr. Amin Hajitou, for giving me the opportunity to join his research team and for his patient guidance, encouragement and invaluable support throughout my time as his student. I could not have imagined having a better advisor and mentor for my PhD study.

Besides my supervisor, my special gratitude goes to Dr. Keittisak Suwan for his generous understanding and unconditional support since the first day we met.

I would like to thank the amazing Phage Therapy members, past and present, Mariam AlBahrani, Paladd Asavarut, Grace Chu, Grace Yan, Justyna Przystal and Efi Tsafa for their friendship, kindness and personal support.

I am grateful for the Development and Promotion of Science and Technology Talents Project (DPST) and the Royal Thai Government for all the support throughout my study. Also, my special thanks goes to Dr. Teerapong Yata and Dr. Mesayamas Kongsema for introducing me to the Phage Therapy group.

My thanks to special friends, Chonlawan and Chaniga, whom I have shared moments of deep anxiety but also of big excitement during this PhD journey. Thank you for their listening, understanding and support as always. Mika, my first housemate and friend in London, who encouraged me to step out of my comfort zone. Phitsanu and Tim Tuft, for the wonderful times we shared at home. Maria Cencioni, for her help with FACs issues and keeping me company when working after-hours in the lab. Thank you for all the support.

Above all, I am extremely grateful to my parents, grandmother and families for their unconditional love and support. Thank you for always be there and believed in me. Without you, I never could have come this far.

Table of Contents

List of figures

Chapter 1

Introduction

1.1 Gene delivery and the development of delivery systems

1.1.1 Gene delivery

Gene delivery is a biological process that has been discovered and tested in research and industry for decades. This process is mainly exploited to introduce foreign genetic material into specific cells aiming to investigate the gene function through an overexpression of the genes, a knockdown of target proteins or an expression of mutant genes. The most notable contribution of gene delivery in biological research is its therapeutic application for treating or preventing diseases called gene therapy. Although the initial purpose of gene therapy was to apply on inherited genetic disorders, the approach has currently contributed a great impact on many diseases including cardiovascular diseases, certain viral infections, different forms of cancers, neurodegenerative disorders and many others. The therapy is generally utilised to compensate abnormal genes or express beneficial proteins required for the diseases [1, 2].

Basically, gene delivery consists of three main components; a delivery system which is able to protect the genetic material from unsuitable environment as well as specifically deliver it to the targets, a transgene which encodes a specific therapeutic protein and an expression system to control the transgene function within the target cells. To achieve a successful gene therapy, gene delivery needs to be designed based on the basis of the interaction between the delivery system and the target cells [3]. As a transgene carrier, several types of delivery systems have been developed and widely categorised into viral and non-viral vectors. The viral based vectors are derived from natural viruses while the non-viral based

vectors are generally a combination of genetic material and synthetic delivery vehicles such as cationic lipids or polymers. Each category of the vector possesses distinct advantages and drawbacks which are suitable for particular therapeutic approach.

1.1.2 Viral and non-viral based vectors

In the field of gene delivery, viral vectors had firstly emerged in 1984 when vaccinia virus was used against Hepatitis B in chimpanzees [4]. The viral vectors are biological vectors which adopt natural properties of viruses and are applied as gene delivery systems. The majority of viral vectors have been developed from adenovirus (Ad), adeno-associated virus (AAV) or lentivirus as they have been studied in great detail and are easy to manipulate *in vitro* [5]. In term of viral vector, they are well known of producing relatively high transduction efficiencies because most of the viruses have naturally evolved to infect hosts with various characteristics to avoid immune recognition, efficacy to invade the cells and ability to generate gene expression using the machinery within host cells [2, 5]. However, the efficacy of viral vectors comes with a price to pay. One main challenge of developing viral vectors is their native tropism or pathogenicity which are difficult to ablate. The first death of patient receiving adenovirus vector to correct a rare metabolic disease has raised many concerns of using viral vectors in gene therapy [6]. The other point to be aware of using viral vectors is their immunogenicity which limits the administration to just a single dose due to the secondary immune response [5]. Further, each viral vector has its own strengths and shortcomings which need to be concerned before designating each of them to a particular therapy.

Although the majority of gene delivery vectors in clinical trials are viral, many non-viral vectors have been developed and made notable progress in this research area [7]. Unlike the viral vectors, non-viral vectors are chemical or physical agents that combine with the genetic material to deliver to target cells. The chemical on-viral vectors are certain polymers and lipids while the physical non-viral vectors exploit physical properties and forces such as gene gun or

microinjection to encourage an uptake of the genetic material into cells. This vector type is considered less immunogenic and safer than the viral vectors. Also, the production of non-viral vectors is cost effective and amenable for large-scale. However, one main drawback of non-viral vector is its low gene transfer efficacy which is 10 to 1,000 less efficacious than the viral vector. Further, most of the non-viral gene transfer relies on injection-based methods which are invasive and limited to exposed tissues. Some non-viral methods also cause cellular stress. Thus, there is a trade-off between tissue damage and efficacy of the gene transfer. These make it challenging to perform systemic delivery of non-viral vector [7, 8]. Recently, some non-viral vectors have been modified to harness similar functions utilised by the viruses. Nonetheless, they have achieved very limited success in animal models and are much less studied than their viral archetypes [7, 9].

1.1.3 Conventional viral vector

According to their transducing efficacy, viral vectors have made great contribution in gene therapy. It is no doubt that most of the viral vectors are based on existing human viruses as they have evolved to efficiently infect mammalian cells. The majority of viral vectors tested in research and industry has been developed from adenovirus, adeno-associated virus (AAV) and lentivirus. These viral vectors are well characterised in the previous several decades and some of them have been tested in clinical trials

1.1.3.1 Adenovirus

Adenoviruses are non-enveloped viruses carrying approximately 36 kilobases (kbs) linear, double-stranded DNA genome. Adenoviral vectors are able to infect a broad range of human cells both dividing and non-dividing cells without integrating its genetic material into host cell genome. Thus, this vector type is considered safe from causing insertional mutagenesis. One of the most valuable assets of adenoviruses is they can accommodate large transgene inserts up to 30 kb. The production steps of adenoviral vectors are straightforward and can yield

very high titers with assistant of helper viral elements. However, there is a concern about the vector immunogenicity as adenoviruses naturally infect human whose immune system is quite capable of combating them. Therefore, adenoviral vectors could be recognized and cleared up by host immune response before reaching target cells. Moreover, it is very challenging to inject the vectors systemically due to their affinity for the hepatic tissue [10]. Despite the consideration of their immunogenicity, some of adenoviral vectors have been tested in cancer gene therapy trials especially for malignant glioma where therapeutic efficacy and clinical benefit were achieved after administration of adenoviral vector encoding the thymidine kinase of the Herpse Simplex Virus (HSV1-tk) suicide gene in combination with ganciclovir (GCV) [11, 12].

1.1.3.2 Adeno-associated virus

Adeno-associated viruses (AAV) are a small, non-enveloped DNA virus whose approximately 4.7 kb single-stranded DNA is encoded in icosahedral capsid. Both ends of AAV genome are flanked by inverted terminal repeat sequences (ITRs) that form a secondary hairpin structure to protect the genome and facilitate other function including replication. Wild type genome of AAV consists of two open reading frames called *rep* and *cap* that can be replaced by transgene sequences for AAV vector construction where the production steps are performed with helper viruses. Similar to adenoviruses, AAV is able to transduce a large range of cells including non-dividing cells. This vector type is non-pathogenic and found in a wide range of serotypes providing more options of vector usage in gene therapy. The gene expression profile of AAV vector is stable and persistent as the vector exists primarily in episomal form in host nuclei.

At present, AAV is a vector of choice in gene therapy. In 2017, the first FDA-approved AAV based product is LUXTURNA™ (voretigene neparvovec-rzyl) from Spark Therapeutics, Inc. targeting a disease caused by mutations in a single gene. This product is AAV2 serotype and administrated via sub-retinal injection to delivers a normal copy of *RPE65* gene to retinal cells in order to treat biallelic *RPE65* mutation-associated retinal dystrophy [13]. In addition, Glybera

(alipogene tiparvovec) from uniQure was granted European Medicines Agency (EMA) approval in 2012. The product is AAV1 vector expressing lipoprotein lipase in muscle for the treatment of lipoprotein lipase deficiency [14]. Apart from these, a wide range of AAV-based products have currently been under clinical trials [15] such as; SB-525 from Sangamo Therapeutics using AAV2/6 vector for long-term hepatic production of factor VIII in hemophilia A subjects (NCT03061201); AMT-060 from uniQure/St. Jude's Hospital which is AAV5 encoding factor IX gene for severe or moderately severe hemophilia B patients (NCT02396342); and AVXS-101 from AveXis using AAV9 to treat Spinal Muscular Atrophy Type 1 (SMA1) patients (NCT02122952).

There are a few concern of using AAV vector as they can accommodate a relatively small transgene and the vector production is costly [5, 16, 17]. Additionally, it has been controversial regarding the AAV integration property that can be site-specific into human chromosome 19 or random manner when *rep* is absent [18, 19]. However, both cases of AAV integration are unlikely to be oncogenic or pathogenic as observed with retroviral vectors.

1.1.3.3 Retrovirus

Retroviruses are enveloped viruses encoding around 7-11kb RNA in their genome. The common retroviral vectors used in gene therapy are gamma retrovirus (simple retrovirus) and lentivirus (complex retrovirus). The retroviral genome also contains viral reverse transcriptase and integrase which are essential enzymes to convert viral RNA to cDNA and integrate the cDNA into the host genome. According to their inability to infect non-dividing cells retroviruses are considered safe to use as majority of somatic cells are protected from accidental transduction. This vector type can accommodate up to 8 kb of exogenous sequence and mediates permanent gene expression due to its integration property. This integrating ability allows retroviruses to be used as single administration for long-term curative effect. However, this comes with a price to pay as vector integration via the integrase is random with the possibility to cause lethal or oncogenic issues if the foreign DNA is inserted into unpleasant

genome position of the host. Because of these safety concerns associated with retroviral use, alternative vectors for gene delivery have been developed to reduce or eliminate these specific safety risks [5, 20-22].

1.1.4 Bacteriophage based viral vector

Given the substantial concerns of conventional mammalian viruses, some alternative delivery tools such as prokaryotic viruses have started to draw attention in this field. The prokaryotic viruses e.g. bacteriophages (phages) are the viruses that have evolved to infect bacteria but not mammalian cells. There are various types of the bacteriophages with distinct physical forms and each of them is specific to certain bacterial species. Bacteriophages have been developed and primarily used as a biological control for bacteria where they were found clinically safe and efficient to apply *in vitro* and *in vivo* [23, 24]. After the discovery of antibiotics, the use of phage has shifted into food additives as well as nanocarriers of peptide and DNA vaccines [25-27]. Many scientific findings have shown their impact in several research fields including gene delivery where they have been further modified to infect mammalian cells through targeting strategy.

Among many bacteriophage types, filamentous bacteriophages have simple structures of major and minor coat proteins that assemble to a packaging signal encoding in their genome [28]. The most well-studied coat proteins of filamentous bacteriophages are pIII minor and pVIII major coat proteins. The pIII coat proteins are displayed around 3-5 copies on one terminal of phage particle while the pVIII major coat proteins are formed scale-like coat around the particle [29]. These coat proteins are generally modified to display peptide of interest such as targeting peptides for specific receptors. This modification allows the bacteriophage vector to specifically target mammalian cells, which can provide great benefits for gene therapy [30-32]. As bacterial viruses, bacteriophages lack native tropism on eukaryotic cells, they are considered safe for use in therapy in mammals. Another practical aspect of using the bacteriophages as gene delivery system is they can accommodate large transgene inserts which is an uncommon

feature in mammalian viruses. In term of production, bacteriophage based vectors are extremely economic to produce and purify making them more attractive in gene therapy.

Despite many advantages of bacteriophages, one main consideration when applied as gene delivery tool is they lack intrinsic ability to enter mammalian cells. Regarding this point, Hajitou and colleagues have developed a new direction in gene delivery by merging properties of bacteriophages and AAV. As such, the new delivery tool called Adeno-associated virus/phage (AAVP) is a hybrid vector in which inverted terminal repeat sequences (ITRs) from AAV were inserted into the bacteriophage genome (Figure 1.1). The AAVP vector inherits advantages of bacteriophage and AAV including very low immunogenicity of the phage capsid and gene expression efficiency profile of AAV. Also, the hybrid vectors have been modified to display a targeting peptide allowing them to home to their targets which are tumour cells for cancer gene therapy. The specific targeting aspect is through biding of the cyclic RGD4C ligand displayed on the vector pVIII coat proteins to $\alpha_v\beta_3$ integrin receptor overexpressed in tumour cells and tumour vasculature [31]. It has been well established that AAVP vector is an excellent delivery tool for treating cancer which shows great promising outcomes in various animal models including mice rats and pet dogs [31, 33-35]. The vector has been utilised with a number of therapeutic genes such as *HSV-tk* suicidal gene and *TNFα* to target a variety of tumour types including melanoma, pancreatic neuroendocrine tumour, sarcoma and glioma [32, 34-38]. The most interesting is the study in pet dogs that showed strong preclinical evidence of AAVP vector entity for repeated systemic administration without decreasing the vector efficacy or causing adverse side effects in large animals [34]. Furthermore, the vector ability to target both tumour cells and their angiogenic vasculature provides double benefit for treatment as angiogenesis is a hallmark for tumour growth.

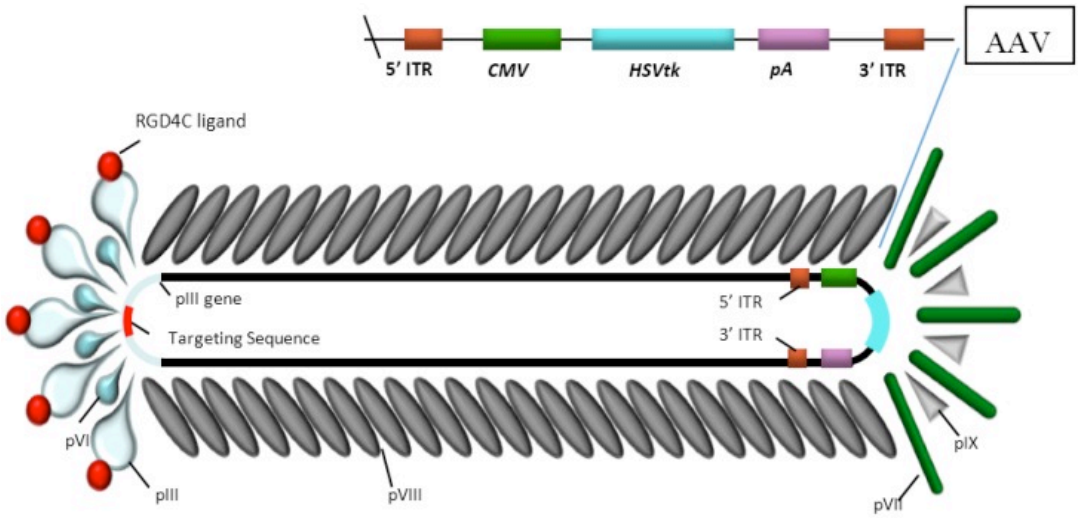

Figure 1.1. Structure of the hybrid vector AAV/phage (AAVP).

The particle contains a chimeric genome of a CMV-transgene cassette flanked by inverted terminal repeats (3' ITR and 5' ITR) of AAV-2 and M13 filamentous bacteriophage genome. The outer capsid belongs to the M13 phage and hence lacks tropism for mammalian cells. The capsid contains a major coat protein pVIII and four minor coat proteins pIII, pVI on one side and pVII pIX on the other. The αβ-integrin binding ligand, RGD4C, is expressed on the pIII minor coat protein of AAVP in order to allow ligand-directed targeting of the tumour cells and tumour vasculatures [39].

Recently, next generation of AAVP vector has been established in the Phage Therapy lab (Paladd Asavarut's PhD project) called Phagemid-AAV (PAAV). Unlike the phage vector system of AAVP, the new vector has been constructed using phagemid and helper phage system where ITRs sequence and therapeutic transgene are encoded in the phagemid genome while other structural coat proteins for the vector propagation are provided from the helper phage. As such, PAAV is much smaller in size which benefits its production and applications compared to the old vector. According to the investigation in our group, PAAV vector shows some advantages over AAVP vector including higher bacterial transforming efficiency resulting in higher yield production, capacity of accommodating larger DNA inserts due to its smaller genome and an enhanced therapeutic gene expression. The vector production is also cost-effective and amenable to large scale production. Furthermore, capsid modification capabilities of PAAV vector such as peptide displaying on pIII or pVIII coat proteins are retained with more convenient steps to conduct on the helper phage genome.

1.1.5 Biological barriers to gene delivery

A successful gene transfer of the vectors to their targets is challenging as the vector fate relies on many key factors. In particular, a systemic administration requires the travelling of the vectors from injected site to their destination. Firstly, the vectors have to overcome extracellular barriers such as degradation by host immune cells and the extracellular matrix that foreclose them from their targets. After overcoming the extracellular barriers, the vectors still have to confront challenges within the target cells. All these barriers can prevent the vectors to accomplish their biological function and result in a failure of the therapy. Thus, the design and construct of delivery tool should address these considerations [40, 41].

1.1.5.1 Extracellular barriers

As the genetic material is sensitive to environment condition such as pH or enzymes, the first difficulty of gene delivery is to pack the nucleic acid safely inside the vectors and prevent them from host enzyme degradation. According to this point, viral vectors show a superior ability to compact nucleic acids inside their particles as most of viruses have naturally evolved to protect and deliver their genome to host cells [3, 5].

The next extracellular barrier is intravascular degradation happening inside host circulation where the vectors encounter a complex environment of plasma proteins and immune cells [42]. Under these circumstances, the vector can be coated with phagocytosis-enhancing molecules through a process called opsonisation. The coated-vectors then become more immunologically visible to phagocytic cells (e.g. monocytes, macrophages, neutrophils, and dendritic cells) and subsequently get destroyed before reaching target site. Generally, the vectors can be opsonized within minutes after exposure to the circulating system. However, this depends on the vector surface characteristics such as charge and hydrophobicity [43].

Apart from being recognised and degraded by the immune system, the delivery particles can also be cleared out through host renal excretion which is a natural process to remove unpleasant particles from circulatory system of human. In this case, the small vector particles are sorted through glomerular filtration and rapidly excreted with urine [44, 45]. In contrast, macromolecules which are too large for the glomerular pores tend to accumulate in reticuloendothelial system (RES) in the liver, spleen, lung and bone marrow where they are degraded by activated monocytes and macrophages [42]. This includes a capture and elimination of delivery viral particles whose diameter sizes are between 10-20 nm [44].

After overcoming all intravascular degradation and host clearance, the vectors are expected to accumulate at target sites without nonspecific distribution in

other organs in order to achieve the greatest therapeutic effects and avoid adverse side effects [41]. However, once reaching their target site, semi-selective property of endothelial cells is another challenging mission that the vectors have to get through. In general, the leakage of intravascular substances into extravascular space (referred to as extravasation) relies on intercellular openings between the endothelial cells. These opening spaces have unique pore-size distribution to each microvasculature providing particular restricted permeation of macromolecules across capillary wall. Beneficially, tumour vasculature is more permeable to larger particles compared with normal capillaries [46-48]. However, each tumour type has its own range of vasculature pore-size that can prohibit extravasation of particular vectors. For example, brain tumour vasculature pore-size is around 7 nm while the pore-size of breast or pancreatic tumours ranges between 50-60 nm [49-52]. According to the pore-size heterogeneity, it is essential to consider this point when designing and delivery tools for biomedical applications. Furthermore, another barrier of concern in brain tumour targeting is the blood brain barriers (BBB) which is characterised by tight junction. The BBB remains as a key challenge for many therapeutic agents because it is very selective and tightly resistant to iron or small molecules exchanged between the brain and outside [53].

The last extracellular barrier for gene delivery is a dense network surrounding the cells called extracellular matrix (ECM). The ECM mainly composed of polysaccharides and fibrous proteins including collagen, laminin and fibronectin that act as a physical barrier preventing the transport of the vectors to the cell surfaces. Although the vectors are able to diffuse through the ECM, they are sometimes hindered by hydrodynamic, and electrostatic interactions between the particles and ECM components [54, 55]. Particularly in the tumour mass, the cells secrete more amounts of matrix molecules such as collagen and hyaluronic acid that can limit the distribution of therapeutic agents and result in unsuccessful therapy.

1.1.5.2 Intracellular barriers

Once overcoming all extracellular barriers and reaching the target cells, the vectors still have to confront intracellular barriers that can be their hardest hindrance. Firstly, the interaction between the vectors and cell membranes is a crucial step for vector internalisation. It is undoubted that viral vectors are more efficacious than the non-viral ones to attach themselves to host cell surfaces and enter the cells via various strategies. Some viruses bind to cell surface receptors and trigger endocytosis such as adenoviruses that use coxsakie- and adenovirus-receptor (CAR) on the host cell as a primary receptor followed by the interaction between Arg-Gly-Asp motif on the viral penton based protein and host αβ integrins for internalization [5, 56]. However, most of the enveloped viruses tend to use membrane fusion strategy to enter the cells. Also, it has been well studied that a targeting strategy that exploits particular ligands to bind to specific receptors on target cells can enhance the vector efficacy. Using targeting ligands mediates a specific cellular uptake which is faster than the non-specific one and therefore improves intracellular accumulation. The common targeting ligands used in gene therapy are transferrin and RGD4C peptide that is specific to integrin receptors on tumour cells and tumour vasculatures; lactose which binds to the asialoglycoprotein receptors (ASGRP-R) of the hepatocytes; mannose for mannose receptors (MR) of macrophages and dendritic cells; and folic acid for folate receptors on certain type of tumours [57-60]. This targeting strategy is expected to lower the injected dose of the vectors while maintaining a desirable efficacy.

In general, the aforementioned specific binding leads to receptor-mediated endocytosis of vectors where intracellular trafficking begins in early endosomal vesicles [61]. The endosomal maturation happens through a few natural processes to transform early endosomes to late endosomes and eventually fuse with lysosomes. Initially, intravesicular pH of early endosome is rapidly decreased because of cytosolic proton influx via ATPase proton-pump enzyme located on endosomal membranes. Then, late endosomes are fused with lysosomes where digestive enzymes are activated under acidic condition leading

to a degradation of the entrapped vectors [62, 63]. It is clearly shown that endosomal degradation forms an intracellular barrier which can foreclose a successful gene delivery especially for non-viral vectors.

The last intracellular task of the vectors is the way to enter nucleus of their target cells and mediate transgene expression. The genetic material of eukaryotic cells is separated from the cytosol by the nuclear envelope which functions as a physical barrier for nuclear import of macromolecules. The nuclear import is energy dependent and requires the nuclear localization signal (NLS) to allow nuclear translocation. As such, many NLS peptides, e.g. PKKKRKV signal peptide from tumour antigen of simian virus 40 (SV40), have been applied on the vectors to facilitate the vector genome into host nucleus to improve gene expression [64-66].

1.1.6 Endosomal escape strategy

According to the intracellular trafficking, it is undoubted that endosomal degradation is a bottleneck of gene delivery. Therefore, understanding the basis of the endosomal degradative pathway may lead to the development of endosomal escape strategy and improvement of gene transfer. Theoretically, the entrapped vectors have to handle the acidic environment inside endosomes and escape to cytosol in a time manner to carry out their biological function (Figure 1.2).

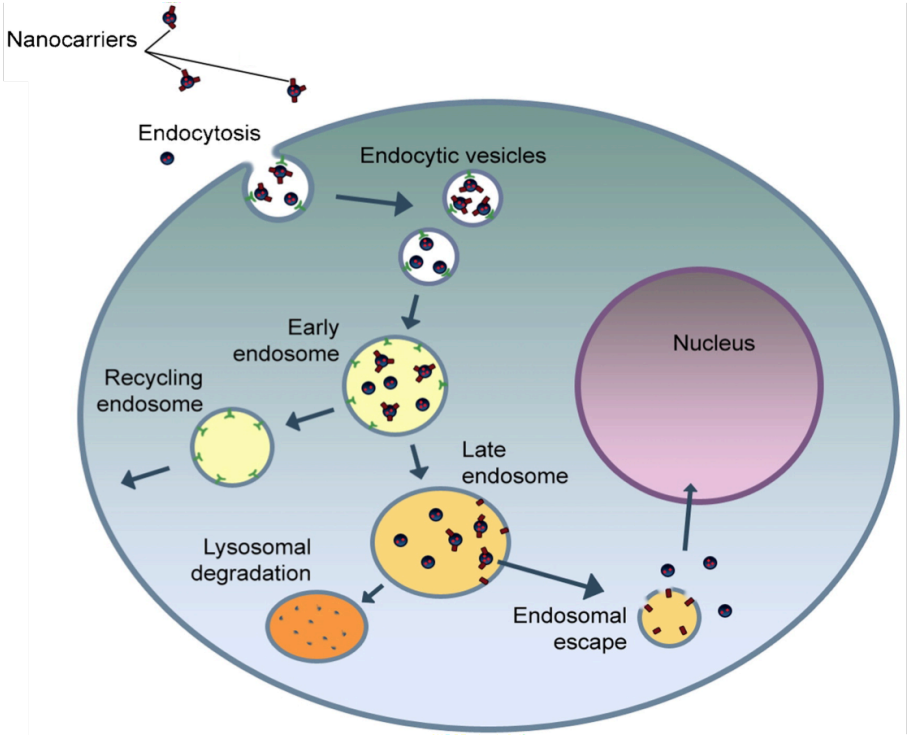

Figure 1.2. Conceptual illustration of intracellular transport pathways of nuclear targeting delivery system [64] .

1.1.6.1 Endosomal escape mechanisms

Many endosomal escape strategies integrated into delivery tools are inspired by viruses and bacteria which enter their hosts via endocytosis and utilise cleverly evolved strategies to escape toward cytosolic compartment [67, 68]. The mechanisms of these escaping processes have been intensely studied and found that they typically begin with endosomal membrane destabilisation following by the escape through either pore formation, membrane fusion or membrane rupture depending on the their characteristics. On one hand, most of enveloped viruses tend to fuse their viral peptide into endosomal membrane while non-enveloped viruses either lyse or generate a pore through the membrane to allow their escape. On the other hand, endosomal escape of the bacteria relies on pore formation mediated by bacterial exotoxins [69, 70].

Membrane destabilization is a by-product of the inherent acidification during endosomal maturation which can be manipulated for the vector escape. Based on biology of cell membrane, the outer layers of endosomal membrane are overall negatively charged phospholipids. During the acidification, some peptides of the vectors can undergo conformational change regarding to the ion influx inside the endosome and interact with the endosomal membrane causing a flip-flop mechanism where the cytosolic phospholipid leaflet flips into luminal side of the endosome (Figure 1.3). This mechanism results in non-lamellar phase changes and destabilization of endosomal membrane which benefits the vector escape [69, 71]. The Majority of membrane-destabilizing peptides applying on the vectors is inspired by natural viral entry peptides such as the HA-2 subunit of the influenza virus hemagglutinin [72]. However, some cationic agents such as poly (ethylene imine) (PEI), poly(l-lysine) (PLL) and chitosan were also reported their capability to induce the destabilization [71].

Once the endosomal membrane is destabilised, it is more convenient for the vector to escape. The first escaping strategy is pore formation based on an endosomal membrane tension to enlarge the opening spaces. Typically, the pore formation is a subsequent result of the membrane destabilization [69].

The second strategy is membrane fusion mediated by fusogenic peptides of the enveloped viruses. In theory, these peptides also undergo conformational changes during endosomal maturation and fuse into the phospholipids to allow the viruses escape toward cytosolic compartment. Haemagglutinin is a well-known fusogenic peptide that converts from a hydrophilic coil at pH 7.4 to a hydrophobic helical conformation at mild acidic condition [73]. The third strategy of endosomal escape is membrane rupture which relies on the well-studied mechanism called proton sponge effect. This mechanism is mediated by cationic agents which buffer the endosomal acidification by absorbing protons inside endosomal compartment. As the luminal pH remains neutral, V-type ATPases will keep pumping cytosolic protons into the endosome as same as an influx of counter-ions and water to balance membrane voltage and restore osmotic balance between inside the endosome and the cytosol. The intensive inflow of water results in an osmotic swelling of endosomal membrane and subsequently leads to endosomal rupture (Figure 1.4). The common agents that have buffering capacity and can cause proton sponge effect are PEI, poly-amido amines and imidazole-containing polymers [69, 71, 74, 75].

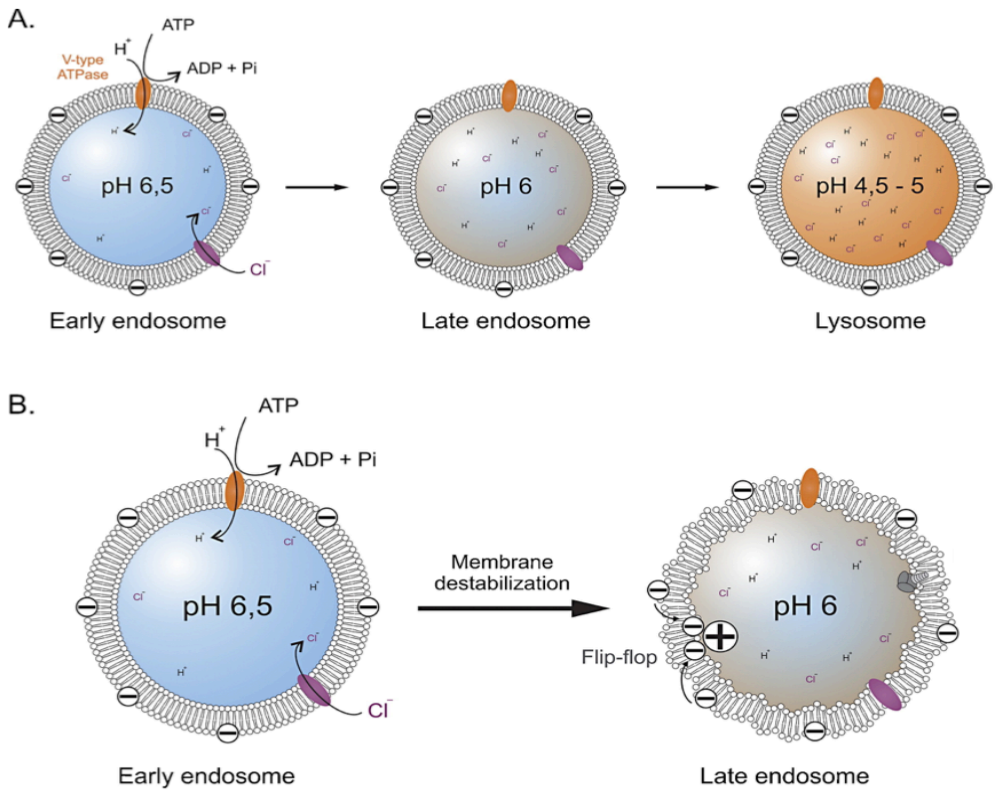

Figure 1.3. Illustration of endosomal acidification mechanisms.

(A) Normal acidification of the endosomes during maturation to late endosomes. (B) Upon acidification, cationic particles interact with negatively charged phospholipids and induce membrane destabilization [71].

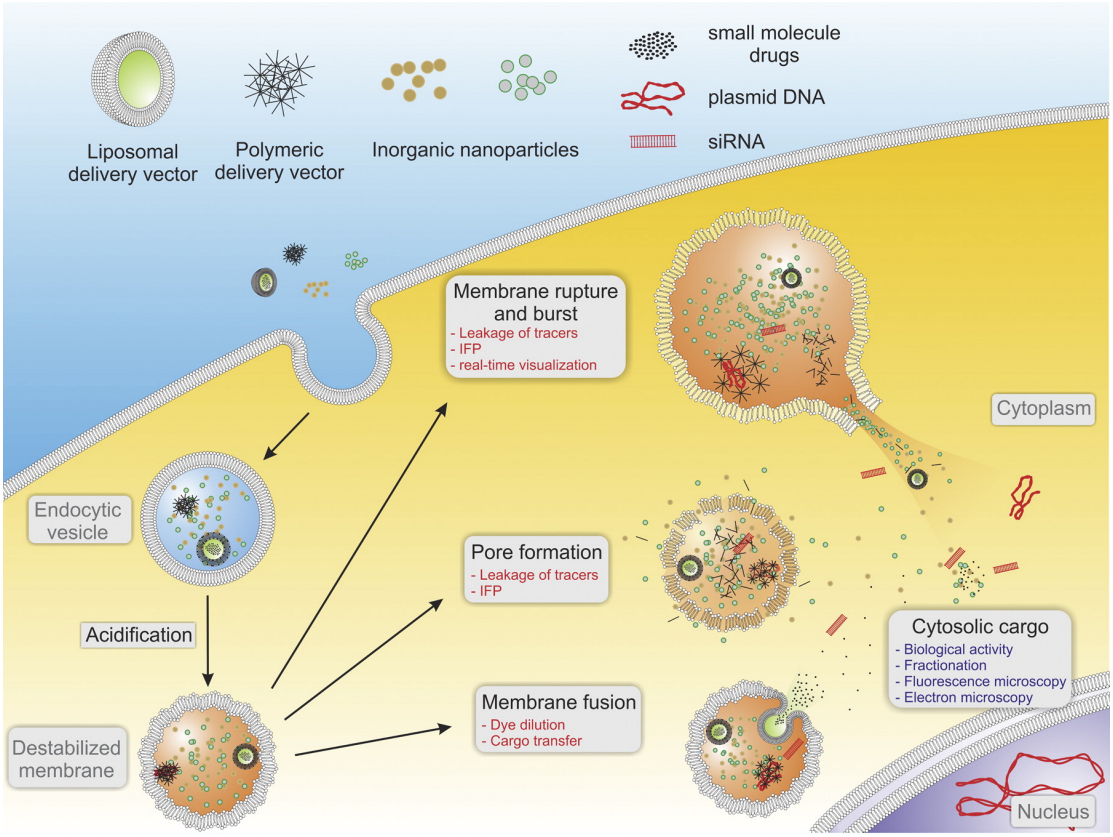

Figure 1.4. Different possible endosomal escape mechanisms after the endosomal membrane destabilisation.

These mechanisms consist of endosomal membrane rupture, pore formation through the endosomal membrane and fusion of the escape agents to endosomal membrane [71].

1.1.6.2 Endosomal escape agents

As a result of the intensive studies on endosomal escape strategies employed by viruses and bacteria, a wide range of endosomal escape agents have been purified or synthesized from different sources in order to apply on various vector types. These agents can be simply categorised into; 1) proteins and peptide based-agents and 2) chemical agents. The protein and peptide-based endosomal escape agents are generally derived from viruses, bacteria, plants, as well as synthetic peptides modified from those natural agents.

1.1.6.2.1 Viral derived endosomal escape agents

A variety of small peptides derived from viruses have been identified their crucial entity responsible for the endosomal escape. The most popular agent in this group is HA2 subunit of haemagglutinin (HA) protein from influenza viruses. Many scientific findings have confirmed that HA2 peptide undergoes conformational change under mild acidic condition that activates its 20 residues N-terminal fusogenic fragment and eventually induces endosomal membrane destabilization [72, 76]. Further, it was shown that conjugating with poly l-lysine can enhance the endosomal escape properties of the HA-2 peptide [77].

TAT protein from HIV is also well known for facilitating gene transfer via membrane destabilization. It is believed that arginine and lysine residues of this peptide are involved in lipid membrane penetration allowing TAT peptide to enhance the internalization of large molecules, such as dextran particles encapsulating magnetic beads [78]. Also, it has been reported that the presence of histidine and cysteine residues can enhance the endosomal escape properties as well as stabilise the TAT/DNA complexes [79].

Some viral peptides have shown a strong membrane-disrupting activity which is beneficial for endosomal escape such as L2 peptide from minor capsid protein of Papillomavirus. The peptide can mediate a strong membrane-disruption under acidic environment leading to the release of viral genome

into cytosol and also induce cytolysis of bacterial and eukaryotic cells [80]. Another example of the membrane-disrupting peptide is major envelope protein (E) of the West Nile viruses which show its maximum activity at pH 6.4 and below [81].

1.1.6.2.2 Bacterial derived endosomal escape agents

Similar to viruses, bacteria are considered as opportunistic microorganisms who manipulate host cells for their survival. They also sometimes destabilise host phagosomal membranes to avoid degradation and release themselves into the cytosol. For example, *Listeria monocytogenes* produces a cholesterol-dependent toxin called listeriolysin O that can induce pore formation in the cholesterol-containing lipid bilayers [82]. In many studies, listeriolysin O has been used in combination with lipid carriers and cationic polymers to enhance endosomal escape [83-86]. Pneumolysin from *Streptococcus pneumoniae* and streptolysin O from *Streptococcus pyogenes* are other pore-forming toxins that cause endosomal disruption [87]. In contrast, some bacterial protein acts as fusogenic peptide during endosomal acidification to enhance cytosolic uptake such as diphtheria toxin from *Corynebacterium diphtheria* [88, 89].

1.1.6.2.3 Plant derived endosomal escape agents

Some substances from plants also show endosomal escape property such as Ricin from *Ricinus communsis*. It is known as an anti-cancer agent which enters mammalian cells via endocytosis and has cytosolic targets. Thus, it is rational that Ricin has membrane-disruptive properties and able to facilitate large and small molecules escape from lipid vesicles [90, 91]. Similar to Ricin, Saporin is another member of plant ribosome-inactivating protein (RIP) family that has endosomal release properties. Particularly, Saporin does not require acidic pH to mediate membrane destabilization [92].

1.1.6.2.4 Animal/human derived endosomal escape agents

Several agents from human or animal sources are known to be effective in endosomal escape such as Penetratin, a peptide derived from Antennapedia homeodomain of *Drosphilia*, which shows a strong penetrating activity on lipid membranes of living cells through energy-independent mechanisms. The peptide has been used as an endosomal escape agent on many delivery tools and shown efficiency to facilitate cytosolic uptake in different cell lines [93, 94]. Another example is Melittin, a cationic peptide from bee venom, which shows capability to disrupt membranes. The peptide can form amphipathic α-helical structures in aqueous solution and insert into the phospholipid bilayers to induce destabilization [95, 96]. Human calcitonin derived peptide, hCT(9-32), also has a cell-penetrating activity. Although endosome disruptive mechanism of this peptide is still unclear, hCT(9-32) and its analogues show high efficiency to penetrate the membranes of various cell lines [97, 98].

1.1.6.2.5 Synthetic endosomal escape agents

At present, many artificial agents have been designed and synthesized in order to achieve better endosomal escape property. For example, EB1, a synthetic analog of penetratin, can form amphipathic alpha helix and destabilize the membrane at endosomal pH. EB1 is far more effective than penetratin to form complexes for siRNA delivery [99].

The most common fusogenic peptide HA2 of influenza has been used as a model to generate various new peptides with distinct entity. GALA is a cationic amphiphilic peptide inspired by HA2. The peptide is soluble at pH 7.5 and undergoes a pH-dependent conformational change and destabilises the endosomal membrane at a pH less than 6.0 [100, 101]. KALA is a cationic peptide modified from GALA. It is a fusogenic peptide which undergoes conformational change between pH 7.5 to 5 and effectively destabilises endosomal membranes [102, 103]. These two HA2 derived peptides show desirable endosomal escape properties in many studies [104-106]. Similarly, INF7 and E5WYG are anionic

amphiphilic peptides derived from HA2. These peptides contain glutamate residues and undergo conformational change from random coil to α-helix between pH 5.5-5. They can also improve endosomal escape capability of non-viral vectors [71, 107]. Furthermore, H5WYG is a histidine rich peptide modified by replacing histidyl residues to the parental HA2 subunit. The peptide is protonated and shows buffering capacity under mild acidic circumstance leading to endosomal membrane destabilization and rupture through proton sponge effect [71, 108].

1.1.6.2.6 Chemical endosomal escape agents

Several chemical agents have been reported for their endosome disruptive properties. According to their buffering capacity within a range of pH 7.5-5.0, PEI and imidazole-containing polymers can mediate endosomal rupture through proton sponge effect [75, 108, 109]. Additionally, poly (amidoamine)s (PAAs) possessing buffer capacities in the higher pH range (pH 7.4–5.1), may favourably contribute to the endosomal escape than PEI [74]. It also has been reported that poly(propylacrylic acid) (PPAA) can enhance endosomal escape capability and improve transfection efficiency of non-viral vectors [110]. Lastly, some agents such as ammonium chloride, chloroquine and methylamine have penetrating property on cellular and vesicular membranes and can act as proton sponge during endosomal acidification. However, they are less popular than other endosomolytic agents [111].

1.2. Gene delivery for cancer immunotherapy

1.2.1 Cancer immunotherapy

Cancer is one of the leading causes of death worldwide along with heart diseases [112]. Because it is a major public health problem, many researchers have been intensively focused on cancer treatments. Over the past decades, the fate of cancer patients generally relies on conventional treatments which are surgery, chemotherapy and radiotherapy. In some patients, the disease can be cured by these conventional strategies but in many cases cancer cells are not completely eliminated and cause recurrence. Among these strategies, surgery is the most effective treatment for localized primary tumours while chemotherapy and radiotherapy are usually applied as a combination on various cancers. However, chemotherapy which a hallmark of the treatments is not applicable for some cancer types or some individual patients and comes with unpleasant side effects because most of chemotherapeutic drugs are harmful to normal cells. Most recently, cancer therapy has been slightly shifted from conventional treatments to new strategies such as targeted therapy and immunotherapy [113].

After decades of extensive studies dedicated to the relationship between cancer and immunity, cancer immunotherapy has revolutionized oncological research and offered alternative options for treating many types of cancer [114]. Based on the fact that the immune system is able to spontaneously recognize tumour antigens and subsequently generates cytotoxic responses against the tumours, cancer immunotherapy mainly focuses on improving or generating a specific immunity through the generation of tumour specific cytotoxic T lymphocytes [115]. This new therapeutic strategy can be pursued in various approaches such as cancer vaccines, adoptive T-cell therapy and immune checkpoint inhibitors. Comparing to conventional treatments, cancer immunotherapy tends to be more attractive as it can be manipulated to effectively destroy cancer cells but spare the healthy tissues. At present, cancer immunotherapy field is growing tremendously and several clinical trials have investigated their potentials in cancer patients [116, 117].

1.2.2 Cancer immunosurveillance and immunoediting

In order to develop effective therapeutic strategies, a clear understanding in principal of tumour biology and immunology is required. Also, it has been suggested from preclinical and clinical research that an interaction between tumours and host immune system plays a key role for a successful cancer immunotherapy.

The concept of cancer immunosurveillance was initially hypothesised by Paul Ehrlich in 1909 that the immune system could repress cancer growth and emphasised by Macfarlane Burnet and Lewis Thomas in approximately 50 years later stating that the immune cells constantly surveyed and eliminated nascent transformed cells from host tissues. The hypothesis was expanded from further investigations that this inspecting action was an incorporation of both innate and adaptive immunity [118]. However, scientists have later recognised that the immunosurveillance may represent only one dimension of the cancer-immune system relationship because the host protecting aspect ultimately fails leading to clinical appearance of cancer. Based on the new findings that host immunity does not provide only protective duty against cancer but also promotes cancer development to escape the immune control, cancer immunoediting has been proposed as a conceptual framework of dynamic interactions between the immune system and developing cancers [119, 120].

In a complex interaction between cancer and host immune system, cancer immunoediting is a dynamic process consisting of three phases; elimination, equilibrium, and escape. In general, cancer outgrowth proceeds through these phases consecutively and can transit in a bidirectional manner. The elimination phase corresponds with classical concept of cancer immunosurveillance in which the transformed cells present some immunogenic elements that are recognised and destroyed by the immune cells. Many preclinical and human studies have confirmed that the elimination phase requires a contribution of several immune molecules and cells from both the innate and adaptive immunity including T cells, NK cells and macrophages. The anti-tumour immunity in this phase occurs

according to an expression of tumour antigens, MHC class I, Fas and TRAIL receptor on tumour cells as well as perforin, granzymes, interferons, interleukins and TNF-α in the tumour microenvironment. Sometimes the immune system is able to eradicate tumour cells completely therefore the elimination phase represents the full extent of the process otherwise the tumours remain dormant in equilibrium phase. Generally, equilibrium phase is a balance between anti-tumour and tumour promoting cytokines aiming to keep the tumour under control. To remain in this phase, adaptive immunity is required to conserve its action especially interleukin-12, interferon-γ, helper T cells and cytotoxic T cells. However, in most of the cases, tumour cells have become more heterogeneous under the constant immune pressure resulting in a diverse collection of cells harbouring distinct molecular signatures making the situation more challenging for the anti-tumour immunity. Further, the tumours often evolve several mechanisms to avoid the immune inspection paving their way to the last phase of cancer immunoediting. The escape phase occurs when anti-tumour immunity fails to restrict tumour outgrowth resulting in clinical appearance of the disease. The findings from extensive studies show that tumour cells in this phase establish direct and indirect mechanisms such as evading immune recognition or developing immunosuppressive tumour microenvironment to benefit their growth and metastases (Figure 1.5) [118-122].

According to immunoediting hypothesis, it is suggested that host immunity is capable of controlling cancer progress through their complex relationship. Thus, an improved understanding of the interaction between cancer and immune system may offer a shorten journey to reach a capstone of cancer immunotherapy to control or eliminate cancer cells.

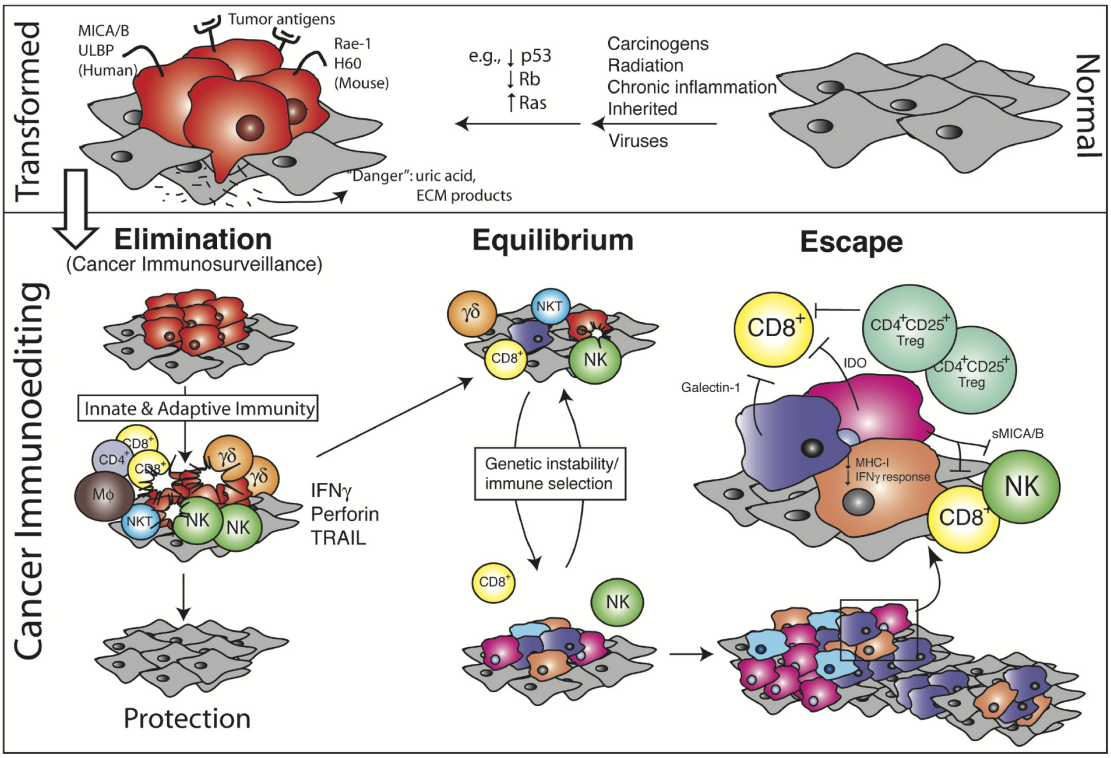

Figure 1.5. Three phases of cancer immunoediting.

Normal cells (gray) subject to oncogenic stimuli, undergo transformation and become tumour cells (red). At early stages of tumorigenesis, these cells may express distinct tumour-specific markers and generate "danger" signals to initiate the cancer immunoediting process. During elimination phase, cells and molecules of innate and adaptive immunity may eradicate the developing tumour cells and protect the host from tumour formation. If this process is not successful, the tumour cells may enter equilibrium phase where they can be either maintained chronically or immunologically sculpted to produce new populations of tumour variants. These variants may eventually evade the immune system by a variety of mechanisms and become clinically detectable in the escape phase [118].

1.2.3 Tumour microenvironment and immune escape mechanisms

According to the concept of cancer immunosurveillance, the immune system is able to retain cancer outgrowth and eradicate the cancer populations. However, it has been found that tumour cells can escape if the immunologic equilibrium is not effectively maintained. Also, many studies have shown the capability of the tumour cells to develop sophisticated mechanisms to avoid immune-mediated elimination. This emphasises the impact of tumour-immune cell relationship within tumour microenvironment that can lead to either tumour progression or rejection [123, 124].

Tumour microenvironment consists of heterogeneous group of tumour cells and diverse types of immune cells whose interplay can determine the tumour fate. Several cytokines secreted from those cells provide key signals to either keep the tumours survive quiescently in the equilibrium phase or let them outgrow [125]. It is undoubted that the presence of cytotoxic T cells, natural killer (NK) cells, mature dendritic cells (DCs) as well as IFN-γ, TNFα, IL-12 and IL-2 within tumour microenvironment play essential role to promote tumour cell death. In contrast, the population of regulatory T cells (T_{reg}), regulatory B cells (B_{reg}), myeloid-derived suppressor cells (MDSC) as well as the secretion of transforming growth factor β (TGFβ) and vascular endothelial growth factor (VEGF) tend to induce tumour-immunosuppressive microenvironment leading to tumour outgrowth. Also, some immune cells such as immature dendritic cells, T helper (Th_0) cells and macrophages seem to possess plasticity that can be exploited by tumour cells to promote their survival. VEGF secreted by tumour cells can inhibit DC maturation and tip the function of immature DCs to tumour progression [126]. Th_0 cells can differentiate into all T helper cells including type 1 T-helper (Th_1) cells, type 2 T-helper (Th_2) cells and regulatory T (T_{reg}) cells, depending upon cytokines they are exposed to. For example, Th_1 cells which promote tumour killing are differentiated from Th_0 exposed to IL-12. Conversely, when exposing to IL-4 and IL-13, Th_0 cells tend to differentiate into Th_2 cells which are associated with tumour progression. Last but not least, it has been found that the population of T_{reg} cells, which plays an important role in

preventing the immune response against tumours, is expanded in the presence of TGFβ and IL-10 [127, 128]. In term of macrophages, type 1 macrophages (M_1) promote anti-tumour activity via an induction of nitric oxide (NO) and ARG1 expression. In contrast, type 2 macrophages (M_2) or tumour-associated macrophages (TAMs) which support metastasis are induced by exposing to IL-4, IL-10 and TGF-β1 [129-131]. The functional network of these immune cells and the cytokines within tumour microenvironment is complex and many of them remain under investigation. Tipping the balance of these cells can induce immunosuppression leading to tumour growth, survival and invasion [132].

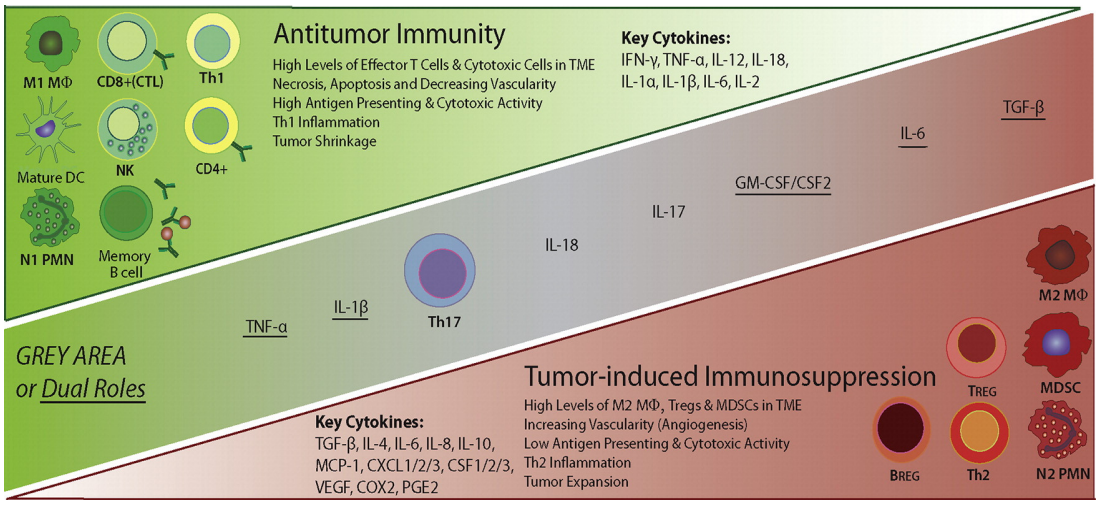

Figure 1.6. Cytokines and immune cells within tumour microenvironment.

Tumour microenvironment consists of heterogeneous group of tumour cells and diverse types of immune cells whose interplay can determine the tumour fate. Several immune cells and cytokines released from either the immune cells and/or tumour cells can either induce anti-tumour immunity or generate immunosuppressive environment [132].

It has been suggested that the immune pressure during elimination phase and their genomic instability can induce tumour cells to develop distinct mechanisms to escape the immune recognition and elimination [125, 132, 133]. This has been confirmed by many studies stating that tumour cells become invisible to the immune system by losing their antigenicity and/or immunogenicity through many tactics. For instant, the tumours can manage to acquire deficiencies in antigen presentation including the downregulation of major histocompatibility complex (MHC) class I, also known as human leucocyte antigen (HLA) class I, and the dysregulation of antigen processing machinery. This antigenic loss disturbs antigen presentation capacity in the context of a peptide-MHC complex and allows the tumours to escape the elimination mediated by tumour-specific T cells [134]. Most recently, the expression of MHC class I and II can be used as independent markers to predict the efficacy of immunotherapy and chemotherapy in some cancers [135-137]. In addition, the antigenic tumours can escape elimination by decreasing their immunogenicity. Due to their heterogeneous populations, the tumours harbour various molecular signatures with differential levels of immunogenicity. Mutational analysis of some solid tumours has shown a significant immunogenic variability among tumour types that can determine their response to immunotherapy. For example, melanoma express a number of immunogenic mutated antigens as a result from their high mutation rate while pancreatic ductal adenocarcinoma (PDAC) is considered as non-immunogenic according to their low mutation rate [138, 139]. However, it has been found that not all mutated antigens are strongly immunogenic and some non-mutated antigens show their capability as key targets for cancer immunotherapy [140]. Finally, tumours can up-regulate the expression of immunoinhibitory molecule such as PD-L1 to become non-immunogenic to tumour-specific T cells. The interaction between PD-L1 on tumour cells and PD-1 on cytotoxic T cells hinders T cell mediated cytotoxicity and leaves the tumours survive. Although the discovery of membranous PD-L1 and its function has encouraged many development of anti-PD-1 and anti-PD-L1 antibodies, it has been suggested that not every PD-L1^{+} tumour cells are associated with the infiltrated immune cells and some PD-L1^{+} tumours are unresponsive to anti-PD-1 immunotherapy [141, 142].

It is clearly shown that the complex interaction between the tumours and host immune system plays an important role to determine the death or survival of the tumours. These lead to the development of various cancer therapeutic approaches targeting immune cells or other elements within the tumour microenvironment [125].

1.2.4 Classes of cancer Immunotherapy

Since cancer immunotherapy has gained attention in the field of cancer, varieties of therapeutic approaches have been developed based on oncological and immunological knowledge. These approaches can be generally categorised into five classes as follow; immune checkpoint inhibitors, cytokine therapy, engineered T cells, agonistic antibodies against co-stimulatory receptors, and cancer vaccines. However, some of them can fit into one or more of these classes [143].

1.2.4.1 Immune checkpoint inhibitors

This approach has been proposed based on the ability of immune cells to keep healthy tissues safe through their checkpoint molecules such as PD-1 receptor expressed on activated T cells. However, tumour cells have evolved to express antagonistic elements called PD-L1 aiming to manipulate the immune recognition. The binding of PD-1 and PD-L1 inhibits T cell activity because the tumour cells are recognised as normal cells. Thus, monoclonal antibodies targeting either PD-1 or PD-L1 have been generated to block this interaction leading to tumour cell death [144-147]. In addition, anti CTLA4 antibody is another common checkpoint inhibitor to block the interaction between CTLA4 on T cells and its ligands, CD80 and CD86. Although a precise cellular mechanisms of CTLA4 blockade still remains under investigation, it has been shown that the blockade allows T cells to remain active and mediate anti-tumour activity [148, 149]. Over the past few years, clinical impact of the checkpoint inhibitor approach has grown intensively as five PD-1 or PD-L1 inhibitors and one CTLA4 inhibitor have been approved to treat various cancers. The inhibitors

have been reported to increase overall survival cancer patients and been applied in combination with chemotherapy or other targeted agents. However, it is worth to note that systemic administration of these inhibitors sometimes causes severe side effects and many patients do not respond to treatment with these checkpoint inhibitors [150-153].

1.2.4.2 Lymphocyte-promoting cytokines

Because anti-tumour immunity mainly relies on the function of particular immune cells such as T cells, some cytokines related to their activation and function have been proposed as another approach for cancer immunotherapy. This cytokine strategy principally focuses on three groups of cytokines; interleukins, interferons, and granulocyte–macrophage colony-stimulating factor (GM-CSF) [154]. It is undoubted that interleukins play major roles for $CD4^+$ and $CD8^+$ T cells proliferation and activation that lead to anti-tumour immunity. Therefore, many interleukins such as IL-2, IL-4, IL-12, IL-15 and IL-21 have been investigated and showed promising therapeutic outcomes in various tumour types [155-161]. Similarly, interferons have been reported for their activities to eliminate tumour cells and inhibit angiogenesis [162-165]. In addition, the first cytokine treatment approved by FDA in 1986 was a recombinant interferon-α (IFNα) for treating hairy cell leukaemia [166]. Finally, GM-CSF has been widely used in cancer immunotherapy regarding to its function to promote T cell homeostasis and to support dendritic cell differentiation which eventually benefit anti-tumour immunity [167-169]. Despite various advantages on anti-tumour immunity, this strategy generally requires relatively high dose of the cytokines due to their short half-life which can lead to serious adverse effects including cytokine release syndrome and vascular leak syndrome. Further, cytokine therapy can promote the survival of regulatory T cells that renders immunosuppressive situation [154, 170-172].

1.2.4.3 Engineered T cells

This strategy usually refers to chimeric antigen receptor (CAR) T and T cell receptor (TCR) T cells. Unlike others, this strategy requires T cell collection from patient for the genetic modification and re-administration of the modified T cells into the same patient. Therefore, it is preferably considered as personalised therapy. CAR T cells are MHC-independent as they can recognise the specific tumour antigens through CAR receptors whereas TCR T cells respond to the antigens presented by MHC. However, both of them induce tumour cell death via T cell-mediated cytotoxicity [173]. In addition, it has been suggested that CAR T cell strategy is typically a one-time therapy which the cells can continue their activity for over a decade after injection [174].

Regarding their clinical successes and FDA approvals, CAR T cells have currently gained much attention in the field of immunotherapy. The clinical success of CD19 CAR T cells, namely axicabtagene ciloleucel for diffuse large B cell lymphoma and tisagenlecleucel for acute lymphoblastic leukaemia and diffuse large B cell lymphoma, has encouraged great efforts to engineer CAR T cells for many different target antigens [175, 176]. However, the target antigens for TCR T cells are generally shared antigens, such as cancer–testis antigens, or patient-specific neoantigens derived from tumour mutations [177]. Although, many patients have achieved benefits from these therapeutic strategies, e.g. tumour elimination and prolonged overall survival, CAR T cells and TCR T cells can cause cytokine release syndrome and neurotoxicity [178, 179]. Also, the clinical successes of CAR T cells and TCR T cells are mainly on haematological tumours but are still limited for solid tumours.

1.2.4.4 Co-stimulatory receptor agonists

Majority of agonistic antibodies are designed to target T cell receptors such as co-stimulatory receptor (CD28) and tumour necrosis factor receptor (4-1BB and OX40) aiming to trigger intracellular signalling pathways that relate to T cell proliferation, survival and effective function against cancer cells [180]. At

present, two agonistic antibodies targeting 4-1BB (namely utomilumab and urelumab) and a number of antibodies targeting OX40 have been investigated under phase II clinical trials [181-183]. In addition, many studies have shown some shortcomings of the agonistic antibodies that need to be concerned such as the dose-limiting toxicities, the specificity on certain T cell subtype and the effect on regulatory T cell activity [180, 184].

1.2.4.5 Cancer vaccines

Vaccines have been the greatest triumphs of medicine to prevent numerous infectious diseases by training host immunity to rapidly and specifically destroy outraged pathogen. Taking this concept into cancer therapy, cancer vaccines have been proposed to enhance the potential of immune system against cancer. However, the cancer vaccines aim for therapeutic action rather than the protective aspect of the traditional vaccines. This strategy requires the knowledge and technology for two fundamentals; vaccine platform development and target antigen identification [185]. The vaccine platform generally categorised into cellular vaccines, peptide vaccines, nucleic acid vaccines and viral vector vaccines. It has been suggested from many studies that choosing the suitable vaccine platforms is essential for a successful therapy. According to vaccine technology, there are many considerations including adjuvants, doses, routes of administration and vaccine types need to be addressed to construct a potential vaccine platform [186-188]. Also, each type of the platform has different advantages and drawbacks that may require particular development and trouble-shooting. Despite many signs of success for the cancer vaccine strategy in clinical trials, the development of vaccine platforms still have a long journey to reach their final stage [185, 188].

In the mean times, there is a wide range of target antigens characterised for cancer vaccine strategy that can fit into two general classes; tumour-associated antigens (TAAs) and tumour-specific antigens (TSAs) (Figure 1.7). The TAAs are self-proteins that are abnormally expressed in tumour cells but probably expressed at some level in normal. MAGE-A3, NY-ESO-1, p53, MUC-1, gp100,

MART-1, HER-2, mesothelin, prostate-specific antigen (PSA), prostatic acid phosphatase (PAP) and prostate-specific membrane antigen (PSMA) are the common TAAs used in therapeutic cancer vaccines [187, 189-196]. Although many TAA-directed vaccines have been reported for their efficiency in the clinic, the immune response does not appear to be strong enough to achieve significant therapeutic impact. One possible reason for this insufficiency is that the TAAs are self-antigens which can generate immune tolerance [185]. Conversely, TSAs including oncoviral antigens derived from oncoviruses and neoantigens encoded by cancerous mutated genes, are truly tumour-specific and can be highly immunogenic. Among many types of cancer caused by viruses, there are only two preventive vaccines available, one for hepatitis B virus (HBV) and the other for human papillomavirus (HPV). The vaccines comprised of HBV surface antigens have been reported for their efficiency to prevent hepatocellular carcinoma (HCC), as well as, HPV-like particle vaccine have shown significant protection against HPV infection therefore preventing cervical carcinoma [197-199]. Regarding the immunogenicity and efficacy to stimulate the immune response, E6 and E7 oncoproteins from HPV have been currently tested in clinical trials and shown encouraging signs of efficacy [200-202]. Similar to oncoproteins, neoantigens are foreign antigens with capability to induce a strong immune response. The first breakthrough of the neoantigen potential was performed in B16 mouse melanoma model. In that study, the vaccine comprised of synthetic long peptide (SLP) against two mutant antigens showed a remarkable anti-tumour effect [203, 204]. These early results have encouraged further investigation of cancer vaccines targeting neoantigens. However, establishing this cancer vaccine strategy is challenging because the majority of neoantigens are unique to individual patients' tumours and required a personalized therapy [185, 205].

The first therapeutic cancer vaccine, sipuleucel-T, has been approved by FDA in 2010 for treating prostate cancer. The sipucleucel-T is a cellular cancer vaccine targeting the prostate differentiation antigen prostate acid phosphatase (PAP). It can prolong overall survival in patients with hormone-resistant prostate cancer by an average of 3 months. However, the exact action of sipucleucel-T still

remains unclear as it is generated from autologous peripheral blood monocytes (PBMCs) cultured with PAP linked to granulocyte-macrophage CSF (GM-CSF). As such, activated DCs and T cells in PBMCs can take action to mediate anti-tumour immunity [206]. In addition, many therapeutic vaccines have been clinically tested in patients with breast cancer, lung cancer, melanoma, pancreatic cancer, colorectal cancer and renal cancer. At some points, a survival advantage was achieved but no objective cancer regressions were noted yet [187].

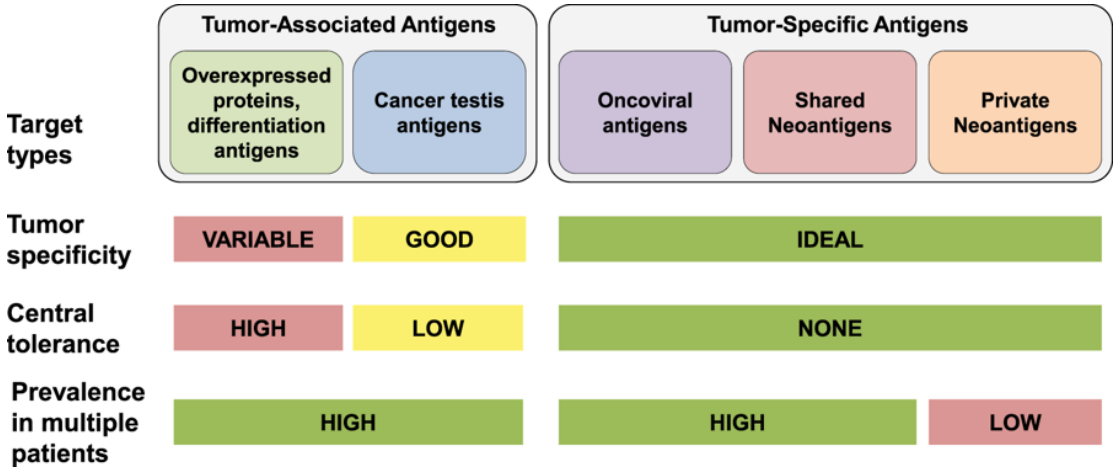

Figure 1.7. Target antigens for therapeutic cancer vaccine.

The antigens fall into two general classes: tumor-associated antigens (TAAs) and tumor-specific antigens (TSAs) [185].

1.3 Bacteriophage vector in cancer immunotherapy

After the first discovery by Frederick Twort and Felix d'Herelle, in 1915 and 1917 respectively [207, 208], bacteriophages have continuously been using in many potential applications in the modern biotechnology, for example, alternatives to antibiotics, tools for screening libraries of proteins, peptides or antibodies and delivery vehicles for gene therapy. Recently, an increasing number of these applications indicate the impact of bacteriophage particles as nanocarriers for a wide array of use in both research and industry [209, 210]. In term of cancer immunotherapy, the bacteriophages such as lambda and filamentous phages are considered immunogenic and able to stimulate immune response against their naive coat proteins as well as genomic elements [211, 212]. Their immunogenicity relies on innate immune receptors TRL9 and its downstream pathway, MyD88-dependent mechanism [213, 214]. This led to the development of several bacteriophage-based systems to activate innate immunity and consequently trigger adaptive immune response [209, 213, 215, 216]. The bacteriophages also contributed to overcome tumour-induced immunosuppression due to their ability to activate innate immune cells and promote pro-inflammatory activity within tumour microenvironment [217, 218].

The most common application of bacteriophages in cancer immunotherapy is phage display of antitumour peptides and antibody libraries [219]. In this case, bacteriophage coat proteins are fused to specific peptides or cancer therapeutic antibodies. Filamentous bacteriophages have been used to evaluate important immunogenic antigens including mammary oncogene int-2, pentraxin I, integrin β_5, p53, centromere protein F, cathepsin L2, and S3 ribosomal protein which involved in humoral immune responses in breast cancer patients [220]. The phage display technology is also applied in active immunotherapy evaluating many monoclonal antibodies for cancer therapy. For example, Fresolimumab (GC-1008) neutralizes three isoforms of TGF-β which is overexpressed in many tumour types, Mapatumumab (HGS-ETR1) and Lexatumumab (HGS-ETR2) specifically binds to tumour necrosis factor-related apoptosis-inducing ligand

receptor 1 (TRAIL-R1) and TRAIL-R2 respectively, then, subsequently induces apoptotic tumour cell death [221, 222].

Apart from the phage display technology, bacteriophages are also applied as vaccines which can be exploited in two distinct approaches; by displaying vaccine antigen on their coat proteins termed phage display vaccines; and by using the bacteriophages to deliver DNA vaccine expression cassette called phage DNA vaccines [209, 223]. Many studies have shown feasibility and efficacy of phage display vaccines in cancer immunotherapy. Lambda bacteriophage displaying GP2 peptide derived from HER2/neu pro-oncogene was use as a peptide vaccine against HER2/neu overexpressing tumours. The GP2-lambda vaccine showed a robust CTL response against TUBO tumour in BALB/c mice [224]. Similarly, bacteriophage particle displaying Δ16HER2 variant on coat protein was used as an anti-cancer vaccine and reported to break immune tolerance as well as trigger anti-Δ16HER2 humoral response against HER2-positive breast cancers [225]. Filamentous bacteriophage displaying tumour specific antigen epitope melanoma antigen $A1_{161–169}$ (MAGE-$A1_{161–169}$) on pVIII major coat proteins elicited antigen specific CTL responses and NK activity. The MAGE-$A1_{161–169}$ phage vaccine also showed effective protection from tumour growth and prolonged survival of tumour-bearing mice [226]. On the other hand, many bacteriophage-based vectors have been used as DNA vaccine delivery vehicles to treat various diseases including cancer [227]. Lambda phage encoding E7 gene of human papillomavirus type 16 (HPV-16 E7) showed therapeutic anti-tumour effects in C57BL/6 tumour mouse model. The mice vaccinated with lambda-HPV-16 E7 are able to generate potent therapeutic antitumour effects against E7-expressing TC-1 tumours [228]. These investigations suggest important features of bacteriophage-based vectors as efficient delivery tools and expression platforms for cancer vaccine strategy. In addition, the bacteriophages serve as strong adjuvants to enhance immune responses toward the antigens displaying on their surfaces and are able to avoid immunological tolerance against their self-proteins making them the ideal system to deliver cancer antigens [229].

Lastly, bacteriophages have also been exploited in targeted therapy as their capsids are able to protect DNA from degradation and capable of displaying foreign molecules for the targeting aspect [209, 230]. Filamentous bacteriophage displaying fibroblast growth factor (FGF2) showed effective targeting efficacy on COS-1 cells resulting in receptor-mediated transduction and expression of reporter gene [231, 232]. Moreover, MS2 bacteriophage displaying SP94 targeting peptide showed higher avidity for human hepatocellular carcinoma (HCC) than hepatocytes or endothelial cells. The MS2 particles delivered encapsidated therapeutic cargoes such as doxorubicin, cisplatin and siRNA cocktail to HCC cells resulting in cell death. Also, MS2-SP94 particles co-displaying H5WYG peptide and loading with ricin toxin A-chain (RTA) showed capability to destroy Hep3B cells without affecting the viability of control cells [233]. Bacteriophage HK97 nanoparticle displaying transferrin and fluorescent labels was targeted to different cancer cell lines via the transferrin receptor [234]. Displaying cyclic RGD (cRGD) peptides on pIII or pVIII capsids of filamentous bacteriophages can specifically target them to integrin receptors overexpressed on tumour cell surfaces and enhance vector internalisation into target cells [31, 235]. The targeting entity emphasises the bacteriophages as the outstanding delivery vehicles for many therapeutic applications including cancer immunotherapy.

According to their characteristics and applications, the bacteriophages are considered as the promising system that can be modified and applied in various aspects. As described before, Hajitou and colleagues developed filamentous bacteriophage vector named AAVP utilising phage display technology and targeting strategy through a binding of RGD4C ligands on AAVP vector and integrin receptors on tumour cell surfaces. AAVP vector made great contributions in the field of gene therapy demonstrated its efficacy as a targeted vector against cancer [31]. Recently, a next generation of AAVP vector called PAAV has been developed in our group and showed superior entity to mediate gene expression over its previous version (data in Phage therapy group). In this thesis, the PAAV vector was further modified to display endosomal escape peptide (H5WYG) on recombinant pVIII major coat proteins based on the

principal of phage display. This modification aimed to facilitate the vector to cytosolic compartment before getting destroyed through endosomal degradation. The vector was also applied in cancer immunotherapy. Firstly, PAAV vector was used as a delivery tool to mediate or enhance target antigen expression on tumour cells which subsequently made them more visible for the immune cells. This strategy is considered to be useful for CAR T cell therapy for solid tumours. Secondly, the vector was applied for cancer vaccination in combination with malaria vaccine (ME.TRAP). Malarial epitope sequences (Pb9) were encoded in PAAV genome and delivered to express on tumour cells. Pb9 served as a target antigen for specific immune cells stimulated by the ME.TRAP vaccine. These applications are based on tumour-targeting efficacy of PAAV vector to generate the antigen expression on tumour cells. According to its specificity, PAAV vector may contribute for the development of universal target antigen for cancer immunotherapy in the future.

1.4 Hypothesis

Hypothesis 1: Displaying H5WYG peptide on PAAV recombinant pVIII capsids could enhance the vector capacity to escape endosomal degradative pathway leading to an augmentation of transgene expression.

Hypothesis 2: Applying PAAV as a delivery vector to express tumour-associated antigens (MUC1 and PSMA), could enhance the antigen expression that might be useful for CAR T cell therapy in solid tumours.

Hypothesis 3: Combining PAAV as a delivery system with malaria vaccine could establish a feasible and efficient therapeutic vaccine strategy for treating cancer.

1.5 Aims of thesis

All works in this thesis are categorized into two main subjects, a further modification of PAAV vector and an application of PAAV vector in cancer immunotherapy. The aims of this thesis are to:

1. Display H5WYG endosomal escape peptide on recombinant pVIII capsids of PAAV vector and investigate endosomal escape capability of the modified PAAV vector.

2. Augment tumour-associated antigens (MUC1 and PSMA) expression on solid tumours using PAAV encoding MUC1 and PSMA vector and a delivery system.

3. Investigate the feasibility and efficiency of the new cancer vaccine strategy which combing phage vector delivery system with malaria vaccine.

Chapter 2

Materials and methods

2.1 Materials

2.1.1 Chemical reagents

Name	Source
DEAE-Dextran hydrochloride	Sigma
FuGENE® 6 Transfection Reagent	Promega
Bafilomycin A1 from *Streptomyces griseus*	Sigma
Puromycin dihydrochloride from *Streptomyces alboniger*	Sigma
QUANTI-Luc coelenterazine substrate	Invivogen
Recombinant Mouse Interleukin-2 (IL-2)	Thermo Fisher scientific
Clear Back (Human Fc receptor blocking reagent)	MBL
Human TruStain FcX™ (Fc Receptor Blocking Solution)	Biolegend
Restriction endonuclease	New England Biolabs
TRIZOL	Ambion life technologies
Cell Dissociation Buffer	Gibco
UltraPure™ DEPC-Treated Water	Invitrogen
D-luciferin	Gold Biotechnology
Fixable viability dye eFluor780	Invitrogen

2.1.2 Kits

Name	Source
QIAprep Spin Miniprep Kit	Qiagen
HiSpeed Plasmid Maxi Kit	Qiagen
QIAquick Gel Extraction Kit	Qiagen
QIAquick Nucleotide Removal Kit	Qiagen
QIAquick PCR Purification Kit	Qiagen
PureLink™ RNA Mini Kit	Invitrogen
GeneAmp® RNA PCR Core Kit	Thermo Fisher scientific
Limulus Amebocyte Lysate (LAL) PYROGENT™ Plus Single Test Vials	Lonza
High Capacity Endotoxin Removal kit	Novus Biologicals
Mouse Interferon gamma (IFNγ) ELISPOT Kit	Abcam
CytoTox 96® Non-Radioactive Cytotoxicity Assay	Promega
Mouse Granzyme b Uncoated ELISA kit	Invitrogen
Cell Titer-Glo® Luminescent Cell Viability Assay	Promega
MycoAlert™ mycoplasma detection kit	Lonza

2.1.3 Antibodies

Primary antibodies	Conjugation	Species raised	Application	Source
Anti-α_v integrin	-	Mouse	IF	Abcam
Anti-β_3 integrin	-	Mouse	IF	Abcam
Anti-β_5 integrin	-	Rabbit	IF	Abcam
Anti-MUC1	-	Mouse	FC	Dr. John Maher (King's College London, UK)
Anti-PSMA	-	Mouse	FC	MBL
Anti-H-2K^d	Alexa Fluor-488	Mouse	FC	Bio Legend
Anti-MHC II	APC	Rat	FC	Myltenyi Biotec
Anti-CD3	PerCP-Cy5.5	Mouse	FC	eBioscience
Anti-CD4	FITC	Rat	FC	eBioscience
Anti-CD8	PE	Rat	FC	eBioscience
Anti-cleaved Caspase3	-	Rabbit	IHC-F	Cell signaling

Secondary antibodies	Conjugation	Species raised	Application	Source
Anti-mouse	Alexa Fluor-488	Goat	IF, FC	Invitrogen
Anti-rabbit	Alexa Fluor-488	Goat	FC	Invitrogen

IF = Immunofluorescence, FC = Flow cytometry,

IHC-F = Immunohistochemistry (Frozen)

2.1.4 Cell lines

Name	Tissue origin	Source
HEK293	Human Embryonic Kidney	American Type Culture Collection (ATCC)
M21	Human melanoma	Professor David Cheresh (University of California, San Diego, USA)
U87	Human glioblastoma	American Type Culture Collection (ATCC)
A549	Human lung carcinoma	Professor Ian M. Adcock (Imperial College London, UK)
Suit2	Human pancreatic cancer	Professor Eric O. Aboagye (Imperial College London, UK)
UW228	Human medulloblastoma	Dr. Jonathan Ham (University College London, UK)
EF43.*fgf4*	Mouse mammary tumour	Established by Dr.Amin Hajitou (Imperial College London)

2.1.5 Plasmids

Name	Purpose	Source
f88-4	Recombinant pVIII	Dr. George Smith (University of Missouri)
pUNO1-hTNFα	Soluble TNFα	Invivogen
pMOD-LucSH	luciferase	Invivogen
pDRIVE-rGRP78	rGRP78 promoter	Invivogen
pUC57.TIP.Pb9.Kan	TIP.Pb9 gene	GENEWIZ
pUC57.ubi.Pb9.Kan	Ubiquitin.Pb9 gene	GENEWIZ
pGL4.20 [luc2 Puro]	Puromycin resistant gene	Promega
pUC57.MUC1.IL-4	MUC1 gene	Dr. John Maher (King's College London, UK)
pUC57.PSMA	PSMA gene	Dr. John Maher (King's College London, UK)

2.1.6 Synthetic DNA fragments

Name	Sequence
HindIII.H5WYG.PstI sense	5’ atcgAAGCTTcGGCTTGTTCCACGCCATCGCGCA CTTCATTCATGGGGGTTGGCACGGTCTCATCCA TGGTTGGTACGGGaCTGCAGatgc 3’
PstI.H5WYG.HindIII antisense	5’ gcatCTGCAGtCCCGTACCAACCATGGATGAGAC CGTGCCAACCCCCATGAATGAAGTGCGCGATGG CGTGGAACAAGCCgAAGCTTcgat 3’
BamHI.IL-2 signal peptide.EcoRI sense	5’ atcgaGGATCCATGTACAGAATGCAACTCCTGTC TTGTATTGCACTAAGTCTCGCACTTGTCACAAA CAGTGAATTCatcga 3’
EcoRI.IL-2 signal peptide.BamHI antisense	5’ tcgatGAATTCACTGTTTGTGACAAGTGCGAGAC TTAGTGCAATACAAGACAGGAGTTGCATTCTG TACATGGATCCtcgat 3’

2.1.7 Oligonucleotides

<u>For molecular cloning</u>

Primers	Sequence
Rec.pVIII.SacII.forward	5’ attatCCGCGGtccccgtcaagctctaaatcg 3’
Rec.pVIII.SacII.reverse	5’ atctgCCGCGGccagccattgagtaagtttttaagc 3’
sTNFα.EcoRI.forward	5’ atcgGAATTCGTCAGATCATCTTCTCGAACCCCGA 3’
sTNFα.EcoRI.reverse	5’ CGCTAGTCGACGTCTGGCCAGCTAGCTCACAG 3’
LucSh.EcoRI.forward	5’ atcgGAATTCCCATGGAGGATGCCAAGAAT 3’
LucSh.SalI.reverse	5’ atcgatGTCGACTATCCTCAGTCCTGCTCCTCT 3’
PSMA.XbaI.forward	5’ ACTCGTCTAGAtagatGCGGCCGCTCca 3’

PSMA.SalI.reverse	5’ actcgGTCGACggatccgatGGATCCTcagg 3’
Grp78.MluI forward	5’ CGACGCGTGCAGGGCCCACTAGTCGGGA 3’
Grp78.BsaBI reverse	5’ CGCGATCCGCATCCTGTCCACCAGTCATGCTAGCC 3’
Puromycin.RsrII.forward	5’ atcgCGGWCCGctgatctgcgcagca 3’
Puromycin.RsrII.reverse	5’ ctgtcgaccgatgccCGGWCCGcgat 3’

For sequencing

Primers	**Sequence**
Rec.pVIII.seq	5’ cgtcaagctctaaatcgg 3’
MUC1.PSMA.seq	5’ CCATCACTTTGGCAAAGAAT 3’
Grp78.seq	5’ ACTTCTTCCGAGTGAGAGACa 3’
Pb9.seq	5’ TGGATCCGATATCTAGACAGA 3’
Puromycin.seq	5’ CTGGTCTCCAACTCCTAATCTC 3’

For qPCR

Primers	**Sequence**
qPCR.MUC1.forward	5’ GCACCATCATCCACGTGAAGG 3’
qPCR.MUC1.reverse	5’ GATGATGAAGGCCACGGTCAC 3’
qPCR.PSMA.forward	5’ CCACTACGATGTCCTGCTGAG 3’
qPCR.PSMA.reverse	5’ ACGATGTCGCTCACGTTCTC 3’
qPCR.TIP.Pb9.forward	5’ TCTTACCTCTGAGCTACCCGG 3’
qPCR.TIP.Pb9.reverse	5’ CTGCGCTCGGGATGTATGA 3’
qPCR.ubi.Pb9.forward	5’ AAGACAAGGAGGGCATACCAC 3’
qPCR.ubi.Pb9.reverse	5’ CTTCTCTGCGCTCGGTATGTA 3’
qPCR.GAPDH.forward	5′ CCCCTTCATTGACCTCAACTAC 3’
qPCR.GAPDH.reverse	5′ GATGACAAGCTTCCCGTTCTC 3’

2.2 Methods

2.2.1 Construction of helper phage plasmid and PAAV plasmid carrying gene of interest

All molecular cloning strategy was performed according to standard protocol described below. Molecular cloning steps of each PAAV vector are shown in figure 2.1-2.10.

Restriction Enzyme digestion

All restriction enzymes was purchased from NEB. Plasmid digestion was conducted according to manufacturer's instructions. The digestion reaction consisted of 1ug DNA, 3 units of each restriction enzyme, 1x reaction buffer and appropriate volume of DEPC water. The mixture was incubated and heat-inactivated according to the manufacturer's protocol. The digested DNA was then visualised on 1% agarose gel.

Standard Polymerase Chain Reaction

The PCR was conducted using Q5 High-Fidelity DNA Polymerase. The reaction mixture was prepared up to 50ul final volume consisting of 10µl of 5x Q5 reaction buffer, 1µl of 10mM dNTPs, 2.5µl of 10µM of each forward and reverse primers, 1-10ng of template DNA plasmid, 0.5µl of Q5 High-Fidelity DNA polymerase, 10µl of 5X Q5 High GC Enhancer and nuclease-free water up to 50µl. The mixture was placed in PCR machine and set under the conditions as described in the commercial protocol. PCR products were then verified using gel electrophoresis.

Gradient oligonucleotide alignment

5ug DNA of top and bottom complimentary single stranded nucleotides were dissolved in 100ul of DEPC water and aligned at decreasing gradient

temperature in PCR machine. The mixture was incubated for1 minute in each step where the temperature was changed 5 degree decrement from 95°C to 4°C.

Dephosphorylation of DNA fragments

The digested DNA fragment was dephosphorylated its 5' and 3' ends by recombinant shrimp alkaline phosphatase (rSAP, NEB). The reaction were digested DNA fragment, 2 units of rSAP, 1x Cut Smart buffer and appropriate volume of DEPC water. The mixture was incubated at 37°C for 2 hours and heat-inactivated at 65°C for 20 minutes.

Agarose gel electrophoresis

1% agarose gel was prepared in 1X TAE buffer with 1X SYBR safe DNA stain. The gel solution was poured into a casting tray and allowed to solidify at room temperature. The DNA samples were prepared by adding 1X loading dye, loaded in each lane of the gel and run in 1X TAE buffer at 90-120V for about 50-90 minutes. DNA ladder was loaded in one lane along with the samples to determine the DNA fragment size. The DNA bands were then visualised under the UV using the UVP Bio Doc-It imaging system. If purification of the DNA fragment was required, the bands were visualised using Pearl Blue Light Transilluminator and the DNA bands of the required molecular weight were cut. The DNA was then extracted from the gel using QIAquick gel extraction kit.

DNA ligation

The ligation reaction was performed by either Quick ligase or T4 DNA ligase. Backbone to insert ratio was 1:3 for sticky end ligation and 1:5 for blunt end ligation. The reaction with quick ligase consisted of 50ng of the backbone, appropriate amount of the insert, 1µl of Quick ligase, 2X Quick ligase buffer and DEPC water. The mixture was incubated at room temperature for 5 minutes. Similar to quick ligase reaction, the reaction with T4 DNA ligase consisted of 50ng of the backbone, appropriate amount of the insert, 1µl of Quick ligase, 10X

T4 DNA ligase buffer and DEPC water. The mixture was incubated at 16°C overnight and heat-inactivated at 65°C for 20 minutes. The ligated plasmid was then transformed to competent bacteria.

Transformation of competent bacteria

DH5-alpha competent *E.coli* cells were thawed on ice for 30 minutes. The plasmid DNA was then added to the bacterial solution. The mixture was incubated on ice for 30 minutes, heat shocked at 42°C for 90 seconds and immediately placed back on ice for 3 minutes. After that, 300µl of SOC medium was added to the mixture and shaken at 180 rpm for 45 minutes at 37°C. The bacteria were then pelleted at low speed spinning, 200µl of supernatant was removed and the bacteria solution was finally spread on 2XYT agar plate containing appropriate antibiotics. The plates were incubated overnight at 37°C.

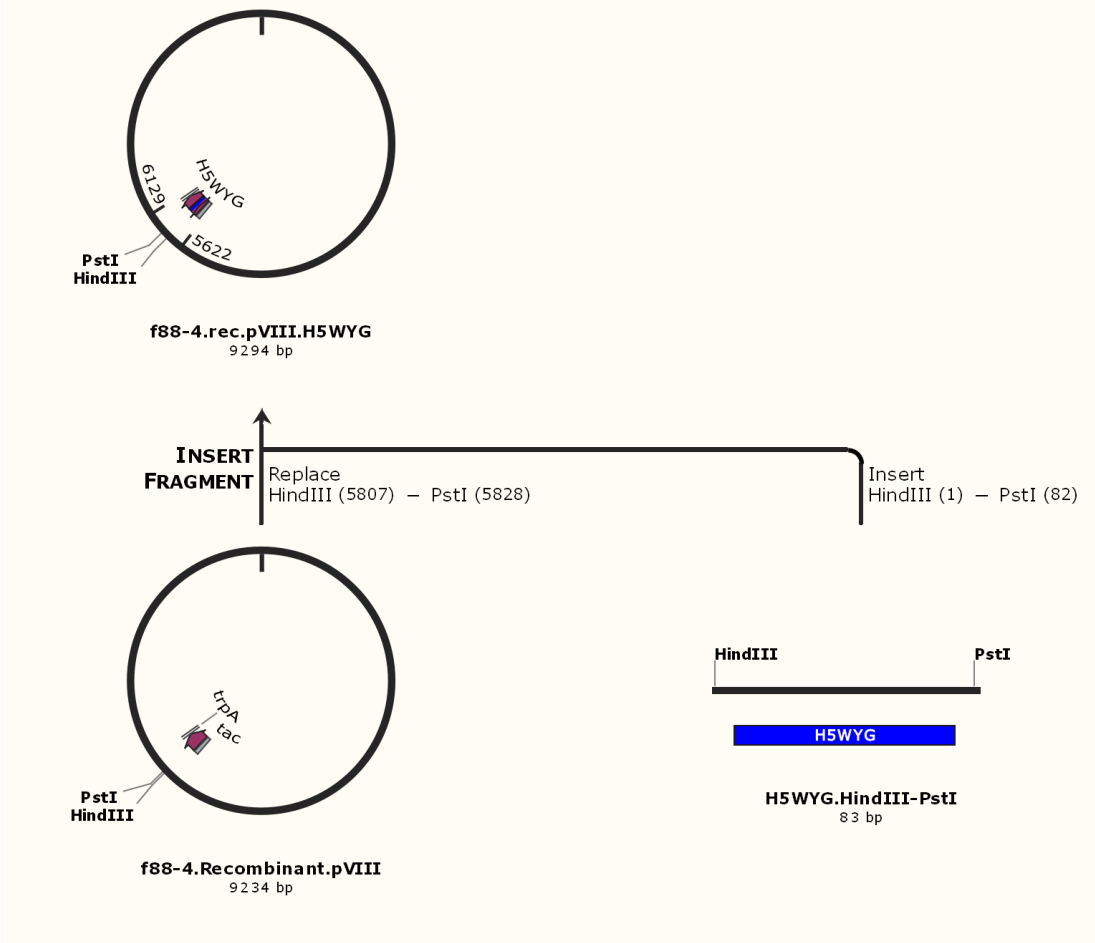

Figure 2.1. Schematic chart illustrating the constrcution of f88-4 plasmid carrying H5WYG sequence (f88-4.H5WYG).

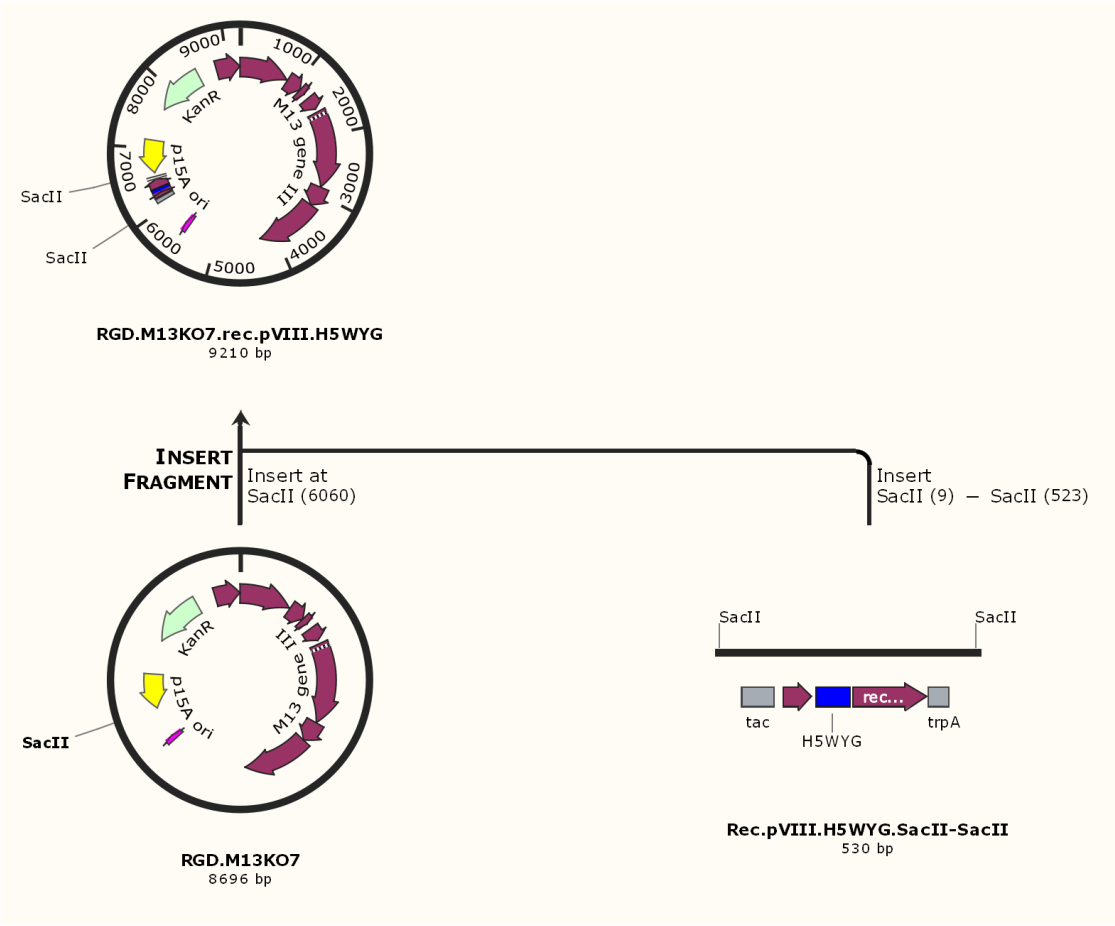

Figure 2.2. Schematic chart illustrating the construction of targeted helper phage plasmid carrying H5WYG sequence (RGD.M13KO7.H5WYG).

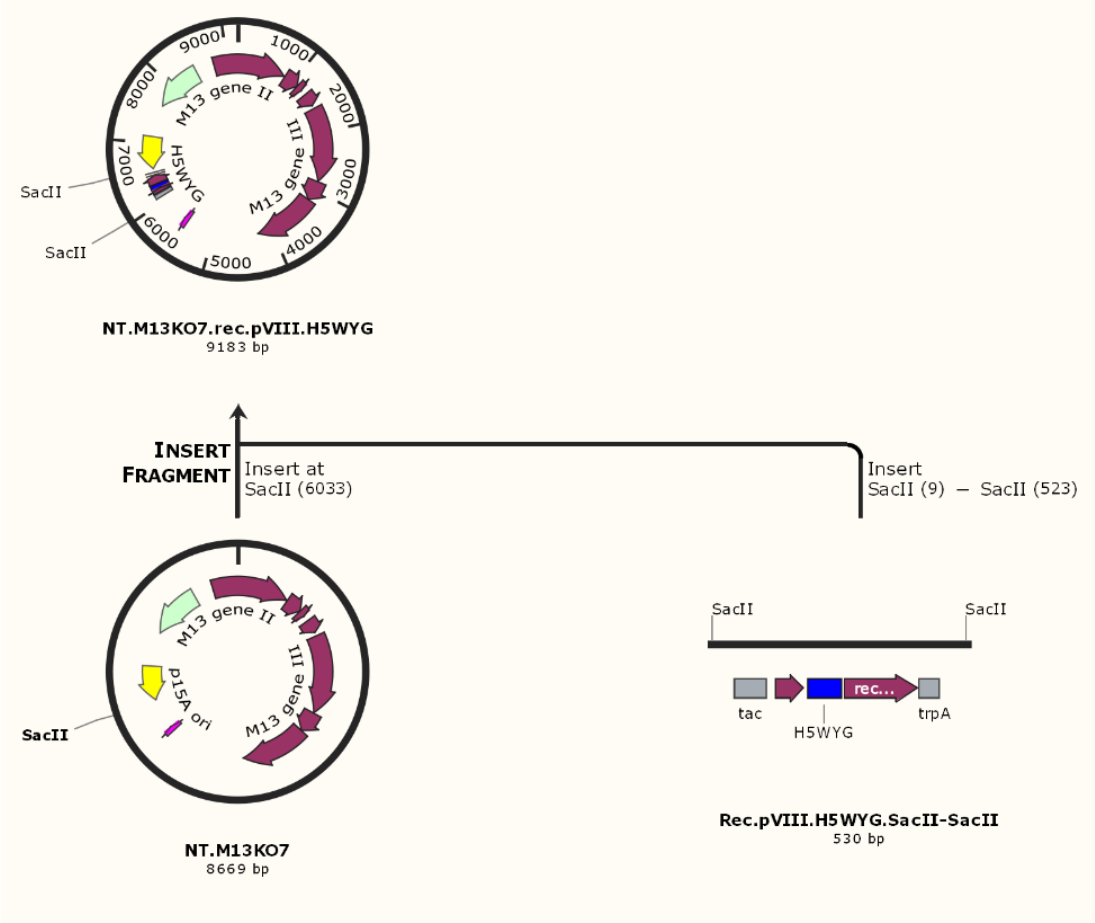

Figure 2.3. Schematic chart illustrating the construction of non-targeted helper phage plasmid carrying H5WYG sequence (M13.KO7.H5WYG).

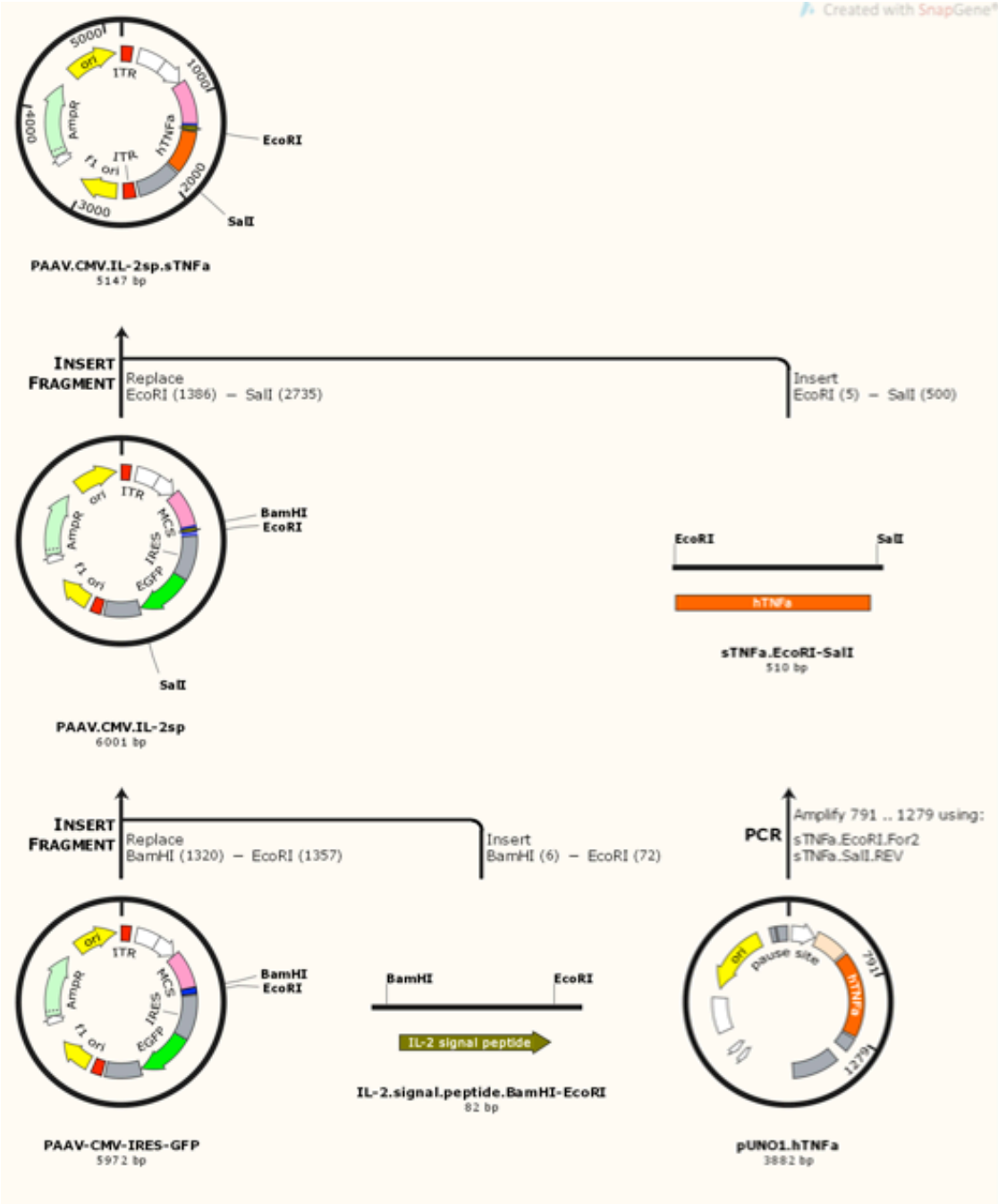

Figure 2.4. Schematic chart illustrating the construction of PAAV vector encoding secreted TNFα gene (PAAV.*IL-2.sTNFα*).

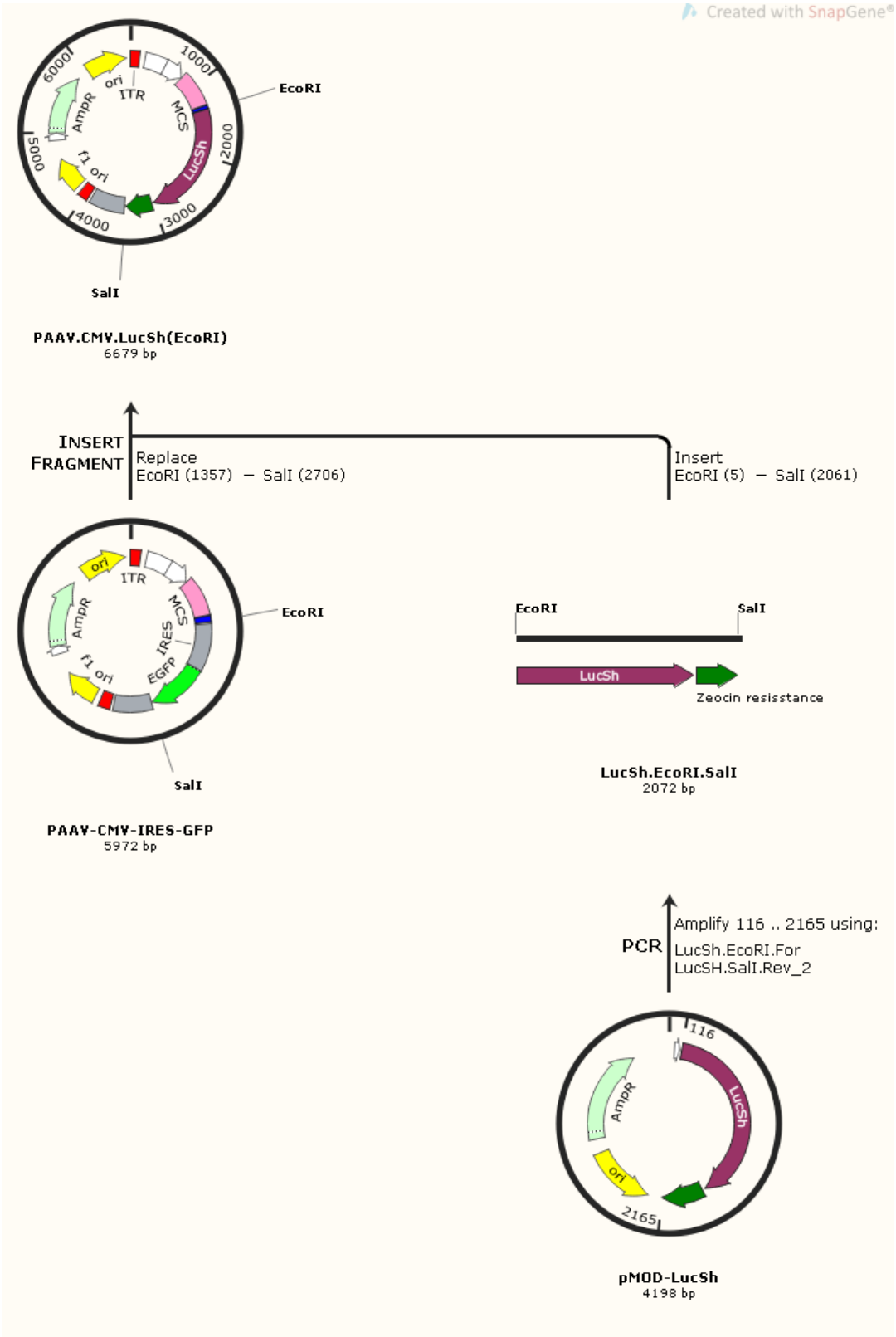

Figure 2.5. Schematic chart illustrating the construction of PAAV vector encoding luciferase gene (PAAV.CMV.*LucSh*).

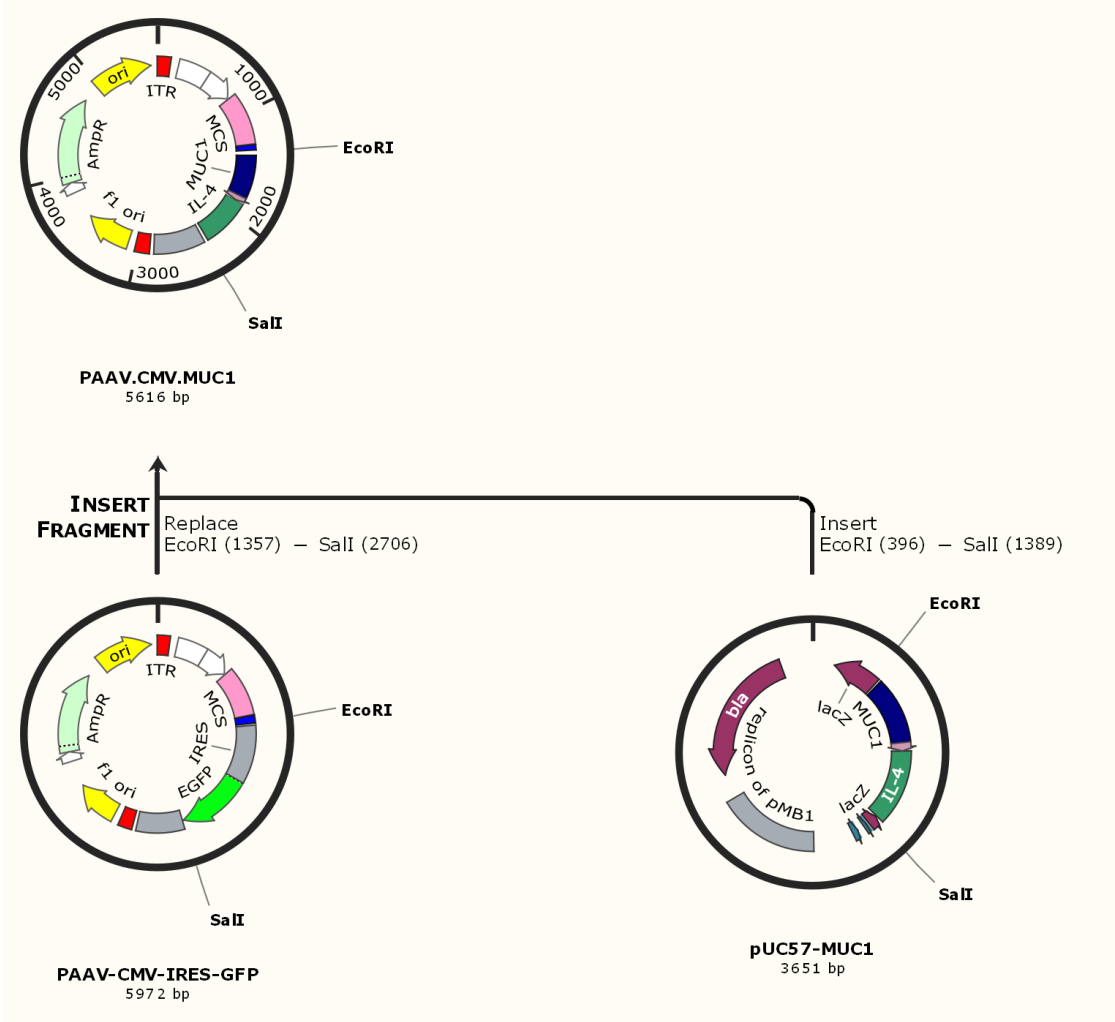

Figure 2.6. Schematic chart illustrating the construction of PAAV vector encoding MUC1 gene (PAAV.*MUC1*).

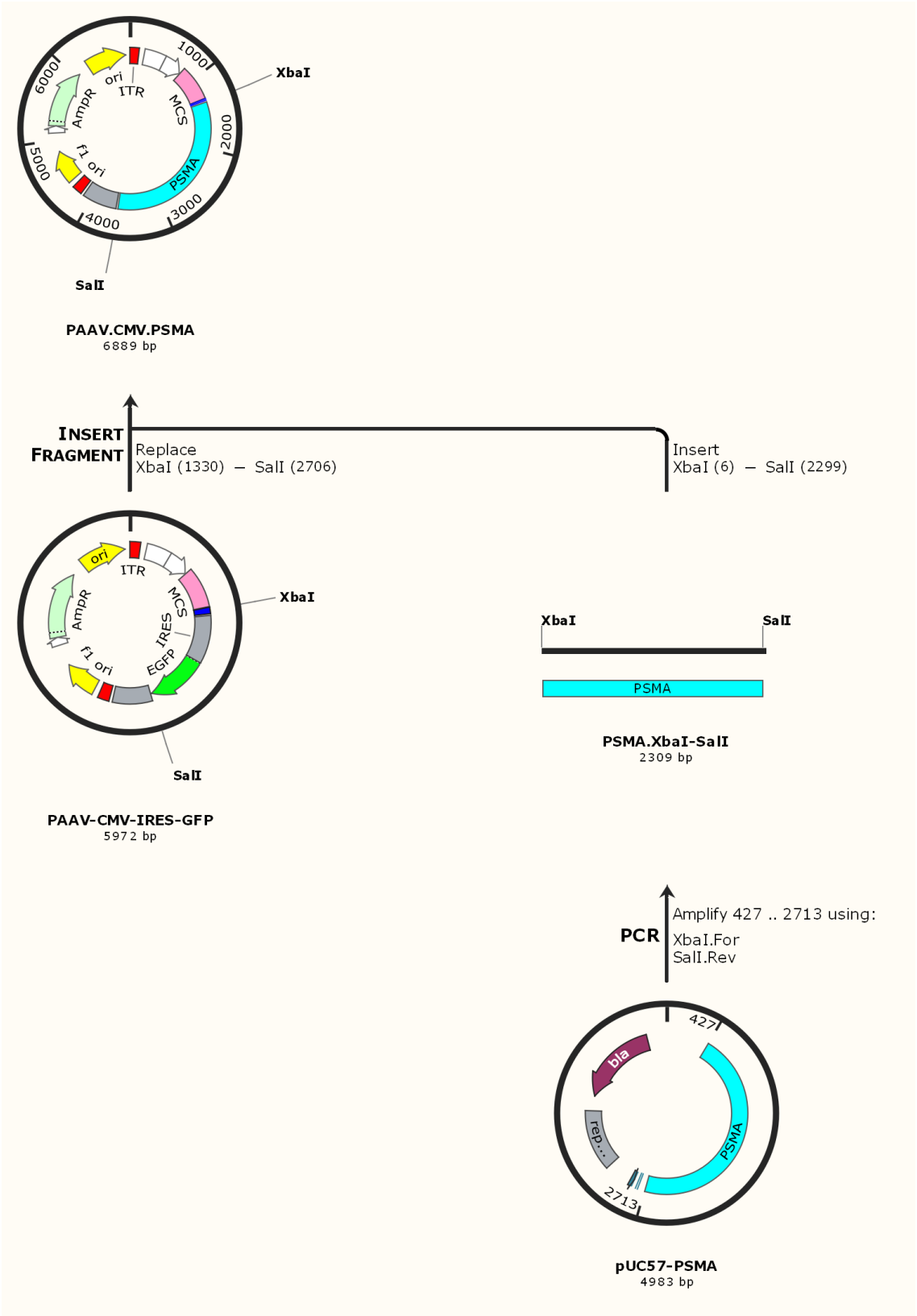

Figure 2.7. Schematic chart illustrating the construction of PAAV vector encoding PSMA gene (PAAV.*PSMA*).

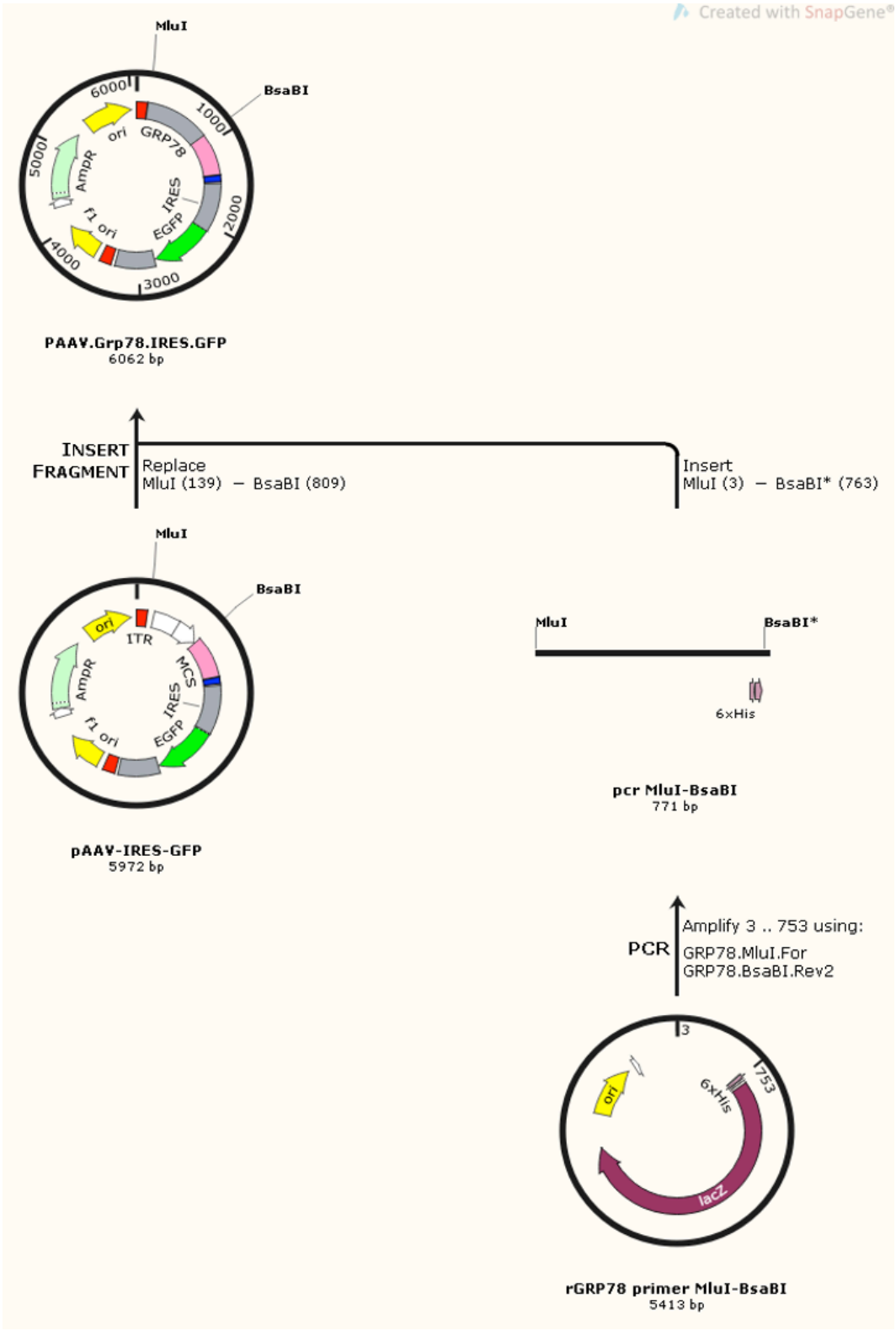

Figure 2.8. Schematic chart illustrating the construction of PAAV vector with Grp78 promoter (PAAV.Grp78).

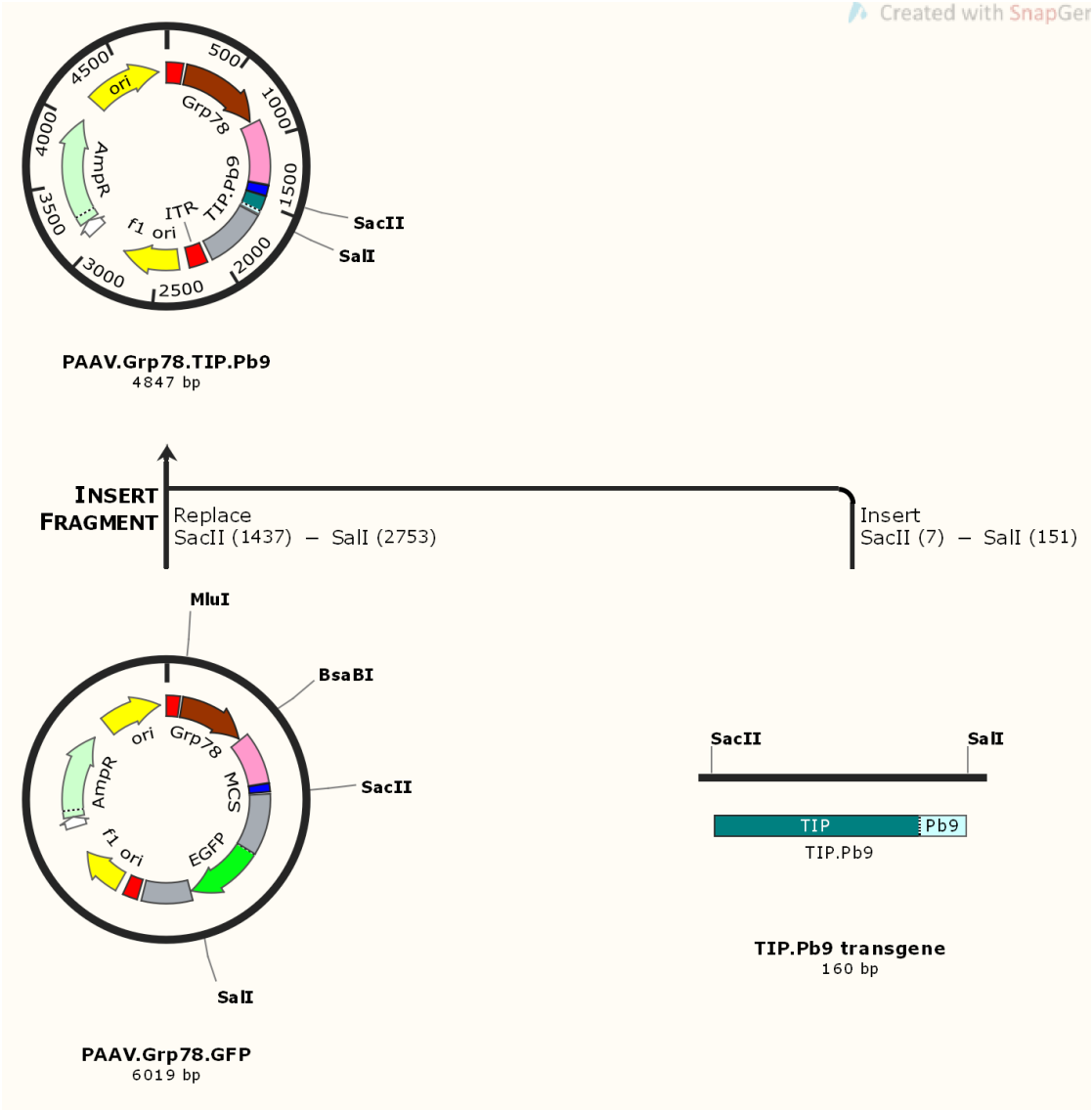

Figure 2.9. Schematic chart illustrating the construction of PAAV vector encoding TIP.Pb9 gene (PAAV.*TIP.Pb9*).

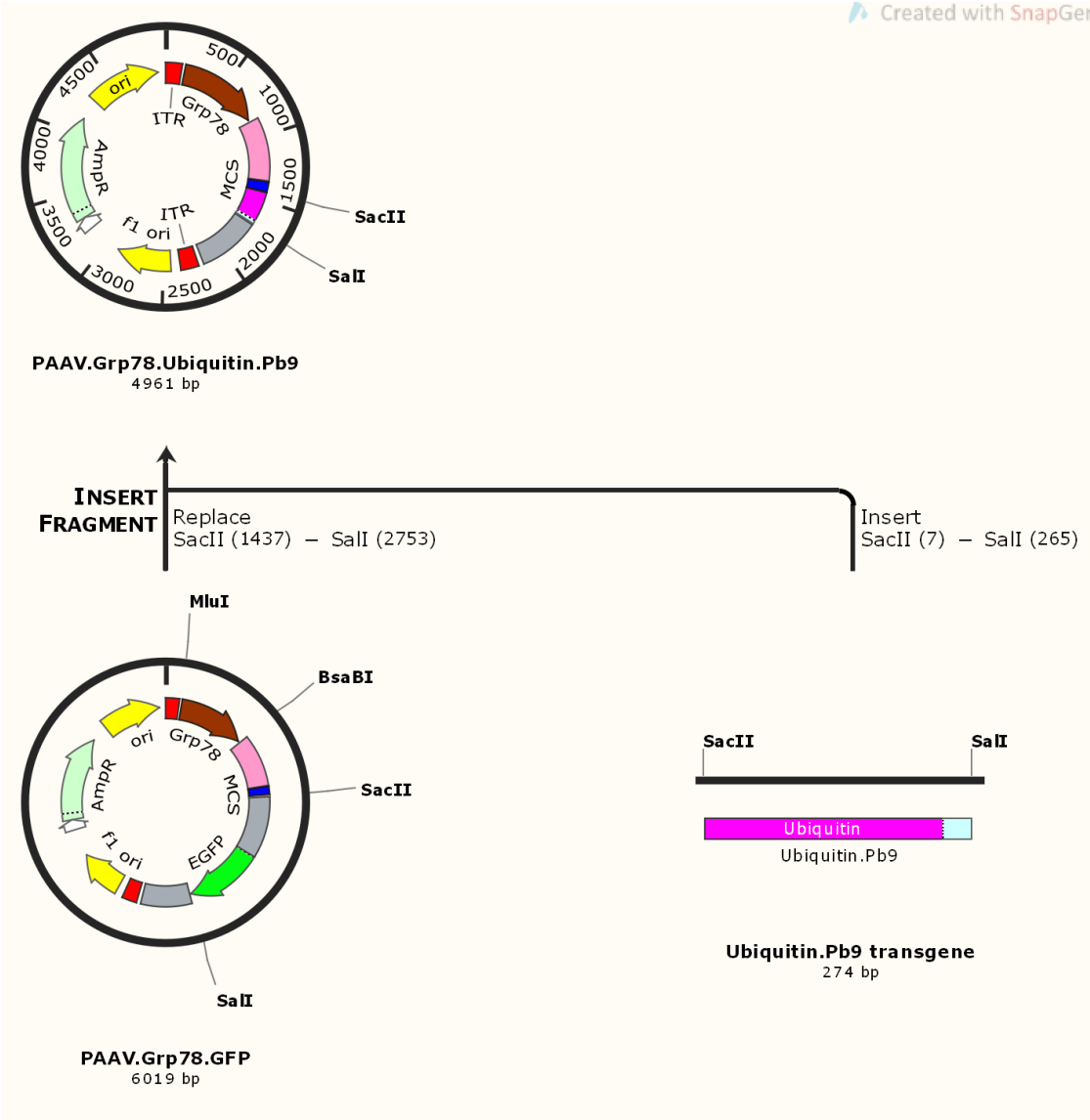

Figure 2.10. Schematic chart illustrating the construction of PAAV vector encoding ubiquitin.Pb9 gene (PAAV.*ubi.Pb9*).

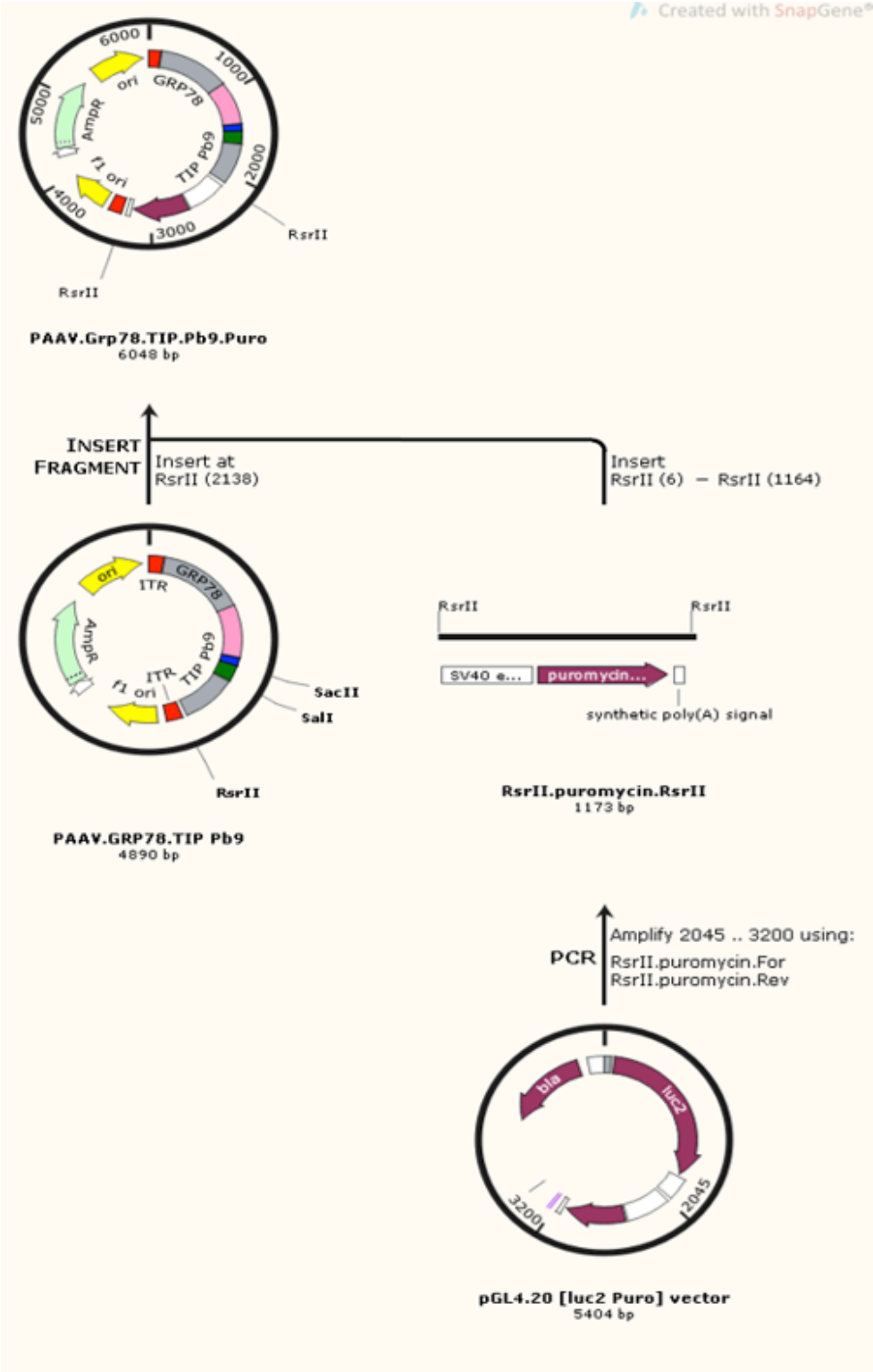

Figure 2.11. Schematic chart illustrating the construction of PAAV.*TIP.Pb9* vector with puromycin resistant gene (PAAV.*TIP.Pb9.Puro*).

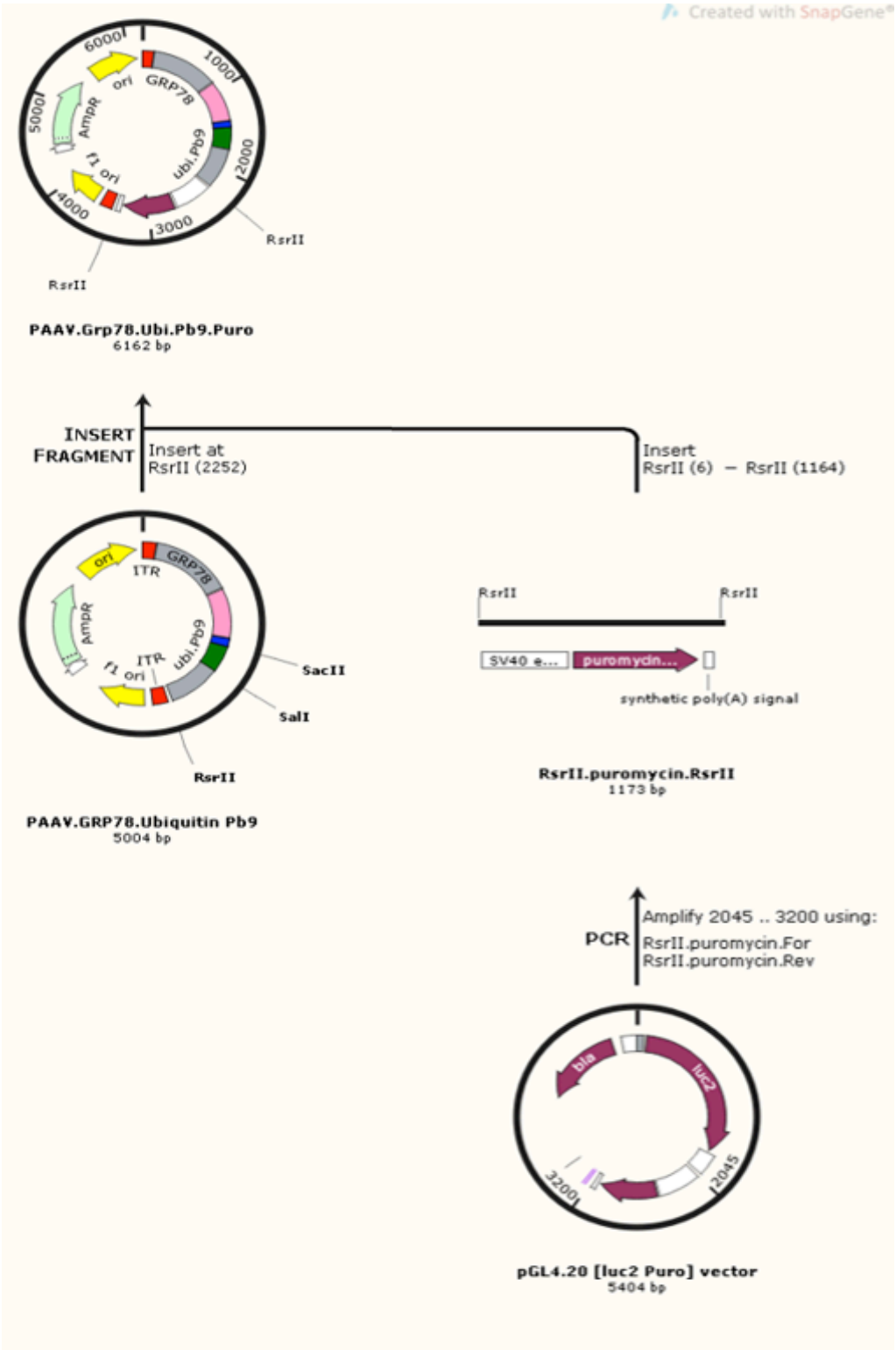

Figure 2.12. Schematic chart illustrating the construction of PAAV.*ubi.Pb9* vector with puromycin resistant gene (PAAV.*ubi.Pb9.Puro*).

2.2.2 Vector production

PAAV vector production

The PAAV plasmid carrying gene of interest was transformed into mix and go TG1 as described in the commercial protocol and allowed to grow overnight in 2xYT medium containing 100µg/ml of ampicillin at 37°C with shaking at 250 rpm. Next day, the 1 ml of the overnight culture was sub-cultured in 100ml 2xYT with ampicillin until optical density reaches mid log phase (600 is between 0.4-0.8). Then 10-15 ul of helper phage were added into the culture and incubate at 37°C without shaking for 30 minutes following by shaking at 180 rpm for 45 minutes. All the culture was transferred to 2 litre flask and topped up to 500 ml with 2xYT medium containing 100µg/ml of ampicillin and 50µg/ml of kanamycin. The cultured was incubated for 18 hours in shaking incubator at 37°C and 250 rpm. After that, the overnight culture was centrifuged at 4,000-6,000g for 15-30 minutes at 4°C to harvest the vector. The bacterial pellet was discarded while the supernatant was kept at 4°C in sterile bottle for subsequent precipitation.

PAAV vector purification

Cold PEG/NaCl solution at 25-30% v/v was added to the supernatant and mixed properly. The mixture was then kept at 4°C overnight for the first precipitation. Next day, the mixture was centrifuged at 4,000g for 30 minutes at 4°C. The supernatant was discarded while the pellet was re-suspended in PBS. Then, 25-30% v/v of cold PEG/NaCl solution was added to the vector-PBS mixture and left at 4°C for 2 hours for the second precipitation. After the incubation the mixture was centrifuged again at 4,000g for 30 minutes at 4°C. The pellet was re-suspended in appropriate volume of sterile PBS and allowed to gradually dissolve at 4°C overnight. The solution was spun using a bench top centrifuge at 13,000rpm for 10 minutes and the pellet was discarded to remove debris residues. Finally, the supernatant containing PAAV vector was filtered through

0.45µm low protein binding PVDF filter, removed endotoxin contamination using High Capacity Endotoxin Removal kit and kept at 4°C.

PAAV vector quantification

The purified PAAV solution from previous step was serially diluted in sterile 1xPBS by factor of 10. The host bacteria, naïve TG1, were grown in 2xYT media until reached 0.4-0.8 OD_{600}. Then 5ul of each PAAV dilution was added to 500ul of TG1 and incubated at 37°C for 30 minutes. After the incubation, 100ul of infected TG1 was plated on 2xYT agar plate containing 100µg/ml ampicillin. Also, 100ul of infected TG1 was plated on 2xYT agar plate containing 50µg/ml kanamycin to quantify the helper phage contamination. The negative controls containing ampicillin or kanamycin and plating with 100ul of naïve TG1 were included. All the agar plates were incubated at 37°C for 18-20 hours. The colonies were counted and calculated back to determine the vector transduction units per microliter (TU/ul) of PAAV stock solution. The titer of helper phage should be less than 10% of the PAAV titer. The protein concentration of the PAAV stock can be measured using nanodrop and represented as mg/mL unit.

The helper phage displaying H5WYG peptide production

The helper phage plasmid carrying *recombinant pVIII* and *H5WYG* gene was transformed into mix and go TG1 as described in the commercial protocol and allowed to grow until reached 0.4-0.8 OD_{600} in 15-20ml of 2xYT medium containing 50µg/ml of kanamycin at 37°C with shaking at 250 rpm. The starter culture was then expanded in 500ml of 2xYT containing 50µg/ml of kanamycin and 1mM Isopropyl-beta-D-thiogalactopyranoside (IPTG) to induce *tac* promoter of *recombinant pVIII* gene. The culture was grown for 18 hours in shaking incubator at 37°C and 250 rpm. Next day, the overnight culture was centrifuged at 4,000-6,000g for 15-30 minutes at 4°C. The bacterial pellet was discarded while the supernatant was kept at 4°C in sterile bottle for subsequent precipitation, purification and quantification as previously described.

2.2.3 *In vitro* and *ex vivo* experiments

Maintenance of cell stocks

HEK293, A549, M21, UW228, EF43.fgf4, Suit2 and U87 cell lines were cultured in D-MEM supplemented with 10% Foetal Bovine Serum (FBS), L-glutamine (2mM), Penicillin (100 units/ml) and streptomycin (100µg/ml). The FBS was heat inactivated at 56°C for 30 minutes before use. The cells were cultured in T-75 flasks, maintained in a 5% CO_2 humidified cell culture incubator at 37°C and passaged once they reached 80-90% confluence. To keep them under mycoplasma-free condition, the cells were regularly checked for mycoplasma contamination using the Myco Alert Mycoplasma detection kit.

When passaging the cells, firstly, culture medium was aspirated and the cells were gently washed with 1X sterile PBS. Secondly, 2ml of trypsin-ethylenediaminetetraacetic acid (Trypsin-EDTA) was added into the flask and incubated at 37°C for 1-4 minutes to detach the cells. Thirdly, 8ml of sterile culture medium was added into to flask to inactivate trypsin. Fourthly, cell solution was transferred into sterile falcon tube and centrifuged at 900rpm for 5 minutes to pellet the cells. Finally, the cell pellet was resuspended in 10ml sterile culture medium and 1ml of aliquot was transferred into a new flask containing 13ml of sterile complete medium.

Generation of stable cells

In order established EF43.fgf4 cells stably expressing Pb9 peptide on cell surface, the cells were transfected with either PAAV.Grp78.*TIP.Pb9.Puro* or PAAV.Grp78.*ubi.Pb9.Puro* plasmids. Then, the Pb9 peptide stably expressed cells were selected with puromycin antibiotic.

Initially, EF43.fgf4 cells were seeded in 6-well plate and allowed to reach 80% confluent. Before transfecting, the cells were incubated in Opti-MEM transfection medium for 1 hour in cell culture incubator. The transfection mixture was

prepared by mixing 1µg of plasmid DNA per well and 6µl of FuGENE® 6 in 100µl Opti-MEM per well (Ratio of FuGENE® 6 Transfection Reagent to DNA is 3:1), then, added to each well. The cells were incubated with the transfection mixture for 6 hours at 37°C in a 5% CO2 humidified cell culture incubator. After 6 hours, culture medium in each well was replaced by DMEM supplemented with 10% FBS, Penicillin (100 units/ml), streptomycin (100µg/ml), and L-glutamine (2mM). On day2 post transfection, the culture medium was replaced again with DMEM complete medium supplemented with 1µg/ml of puromycin. Non-transfected cells were used as a control. The puromycin-containing medium was replaced every three days for few weeks until all control cells were dead. The puromycin-resistant cells were selected and monitored under the microscope to form clones, which were pooled and expanded.

Integrin Immunostaining

The cells were seeded on poly-lysine coated coverslips in 12-well plate and allowed to reach 70-80% confluent. The cell were washed with PBS twice, fixed with 4% PFA for 15 minutes at room temperature and washed three times with PBS. Then, the cells were treated with 50 mmol/L of ammonium chloride for 5 minutes and washed three times with PBS before blocking with 2% BSA in 0.1% TWEEN20 PBS for 1 hour at room temperature. After that, the cells were incubated with the primary antibodies; mouse anti-α_v, anti-β_3 or rabbit anti-β_5 integrins diluted 1:50 in the blocking reagent overnight at 4°C. Next day, the cells were washed three times with 0.1% TWEEN20 PBS and incubated with the appropriate secondary AlexaFluor- conjugated antibodies (diluted 1:750) and 0.5µg/ml of 4',6-diamidino-2-phenylindole (DAPI) for one hour in the dark at room temperature. Finally, The coverslips were washed three times with 0.1% TWEEN20 PBS, mounted with prolong gold anti-fade reagent and allowed to dry in the dark overnight before subjecting to fluorescent microscope or being kept at -20°C.

PAAV plasmid transfection in adherent cells

The cells were seeded in appropriate well plate and allowed to grow in complete DMEM until reached 90-95% confluent. Before transfecting, the culture medium in each well was changed to opti-MEM and incubated for at least 45 minutes. The transfecting reagent containing PAAV plasmid was prepared according to FuGene6 protocol, added into each well and incubated for 6 hours. After the incubation, the medium was replaced by DMEM containing 10% FBS and 2mM L-glutamine.

PAAV vector transduction in adherent cells

The cells were seeded in appropriate well plate and allowed to grow in complete DMEM until reached 75-80% confluent. On the day of transduction, the transducing medium was prepared by adding PAAV solution into opti-MEM and incubated at 37°C for 15 minutes. Then, the culture medium in each well was replaced by the transducing medium and incubated for 24 hours at 37°C in 5% CO_2. Finally, the medium was changed to complete DMEM.

Acidic-based titration for endosome buffering capacity

The acid-base titration method was used to determine the endosome buffering capacities of PAAV vector displaying H5WYG peptide. The vectors prepared to their optimised ratios in de-ionized water (DI water). The final volume of vector-DI water solution is 10ml. The solution pH was adjusted to 10 by 0.1M NaOH. The titration was carried out with 2ul increment of 0.1M HCl to lower the solution pH down to 3. Changes in pH were recorded using a pH meter. The titration of DI water was used a control.

QUANTI-Luc luminescence assay

Cells at 70% confluent in 96-well plate were transduced with PAAV vector encoding *Lucia* (PAAV.*Lucia*). The transduced cells secrete a specific

coelenterazine-utilising luciferase into culture medium. The Lucia protein was monitored daily by pipetting 10µl of culture medium from each well and transferring into white opaque 96-well plate. Quanti-Luc, a coelenterazine-based substrate was prepared according to the manufacturer's protocol. 25ul of the substrate was added into each well containing the medium. The luminescence was immediately measured using Promega GloMax Navigator Luminometer. The medium was changed daily after Lucia measurement.

Cell viability assay

The cells were seeded in 96-well plate, allowed to grow at 70% confluent and transduced with PAAV vector encoding *secreted TNFα* (PAAV. *sTNFα*). Cell death was microscopically observed daily. Once it was noticeable, the plate was carried out for Cell Titer-Glo® assay or Sulphorodamine B (SRB) assay to quantify cell viability.

Cell Titer-Glo® assay

The cells in 96-well plate were washed twice with 1x PBS. 100ul of 1x Glo lysis buffer was added to each well and incubated for 10 minutes or until the cells were completely lysed. Then, 50ul of the cell solution was transferred to white opaque 96-well plate where 50ul of Steady-Glo® luciferase substrate was added into each well and incubated for 10 minutes. Finally, the plate was read using Promega GloMax Navigator Luminometer.

Sulphorodamine B (SRB) assay

The cells in 96-well plate were washed twice with 1x PBS and fixed overnight at 4°C with a final concentration of 10% TCA in serum free medium. The plate was washed in slow running tap water and left to dry at room temperature. The cells in each well were stained with 100µl of 0.4% SRB for 30 minutes with orbital shaking. The unbound SRB was removed by washing with 1% acetic acid, then, the plate was allowed to dry at room temperature. The SRB-stained cells in each

well were dissolved in 150µl of 10mM Tris pH 10.5 under shaking condition. The absorbance of completely dissolved solution was read at 490nm.

Quantitative Real-Time PCR (qRT-PCR)

The cells were collected in TRIZOL reagent and total RNA was isolated using Pure Link RNA mini kit. 2ug of RNA was diluted in DEPC water to a final volume 16ul and treated with DNase I at room temperature for 12 minutes. Then EDTA was added to the sample and heat-inactivated at 65°C for 10 minutes to stop the DNase activity. After that the samples were used as a template for reverse transcription and cDNA was synthesised using Gene Amp RNA PCR core kit. QRT-PCR was performed with appropriate primers, SYBR green universal PCR master mix and subjected to an ABI 7900 real-time PCR instrument. GAPDH was applied as a reference gene. Relative gene expression was quantified with comparative Ct method (ΔCt). ΔΔCt value was calculated against reference sample (RNA extracted from non-transduced cells/ transduced with the non-targeted vector). The expression was calculated as $2^{-\Delta\Delta Ct}$.

Flow cytometry analysis

For MUC1 and PSMA staining, the cells were harvested by removing the culture medium, washing with 1x PBS and incubating in cell dissociation buffer until they were completely detached from the well. After that, the cells were washed three times in 2%FBS 1xPBS (washing buffer) and re-suspended at 1,000,000 cells/ml/tube in the washing buffer. The cell solution was spun down at 500g for 1 minute and the supernatant was discarded. The cell pellet was re-suspended in 100ul of washing buffer and incubated with 5ul of Clear Back or Human TruStain FcX™ Fc receptor blocking solution for 5-10 minutes. Then, the cells were washed once in washing buffer and incubated in appropriate dilution of primary antibody (20ul of anti-MUC1 or 10ug/ml of anti-PSMA per sample) for 45-60 minutes at room temperature. The cells were washed three times in washing buffer and incubated in the dark with anti-mouse Alexa Fluor 488 secondary antibody (1:500) for 25 minutes at room temperature. After that, the cells were

washed three times in washing buffer and fixed in 100ul of 4% paraformaldehyde for 10-15 minutes at room temperature. Finally, the cells were washed twice with 1x PBS and subjected to flow cytometry. The results were analysed using FlowJo version 10.5 software.

For H2-K^d MHC I and MHC II staining, EF43.fgf4 cells were washed with 1x PBS and detached from the flask by incubating in in cell dissociation buffer. The cells were washed twice in 1xPBS containing 0.5%BSA (washing buffer), re-suspended at 1,000,000 cells/100ul/tube and blocked with 1xPBS containing 10% goat serum and 0.3M glycine for 20 minutes at room temperature. Then the cells were incubated in the dark with 0.15ug anti-MHC II-APC and 0.25ug anti-H2-K^d-Alexa Fluor 488 antibodies diluted in 100ul washing buffer for 15 minutes at 4°C. After the incubation, the cells were washed three times in washing buffer (500g, 5 minutes), fixed with 4% paraformaldehyde for 10-15 minutes at room temperature, washed twice with 1xPBS and subjected to flow cytometry.

For CD3, CD4 and CD8 staining, mouse splenocytes were washed twice and re-suspended in 1xPBS at 1,000,000 cells/ml/tube. 1ul of fixable viability dye eFluor 780 was added to each tube, vortexed immediately and incubated in the dark for 30 minutes at 4°C. Then, the cells were washed twice with 100ul PBS, and incubated with appropriate concentration of antibody mixture (1ug anti-CD3, 0.25ug anti-CD4 and 0.25ug anti-CD8 antibodies in 100ul 1x PBS per tube) for 15 minutes at 4°C. After the incubation, the cells were washed twice with 1xPBS, fixed with 4% paraformaldehyde for 10-15 minutes at room temperature. Finally, the cells were washed twice with 1xPBS and subjected to flow cytometry.

Murine splenocyte isolation

Spleens were collected from euthanized mice, quickly rinsed through normal saline and kept on ice in eppendorf containing RPMI-washed medium (RPMI medium supplemented with 2% Foetal Bovine Serum (FBS), Penicillin (100 units/ml), streptomycin (100µg/ml) and 1% Antibiotic-Antimycotic agent). The spleens were cut into small pieces and passed through 70µm cell strainer.

The splenocyte solution was spun at 500 g for 5minutes at 4°C to pellet the cells and re-suspended with RPMI-washed medium. The washing steps were repeated 3 times. After the last spinning, the cell pellet was re-suspended in 5ml of ACK lysis solution for 2 minutes at room temperature to lyse red blood cells, then, 5ml of 1xPBS was immediately added to stop the cell lysis. The cells solution was pelleted at 500 g for 5minutes at 4°C and re-suspended in RPMI complete medium (RPMI medium supplemented with 10% FBS, Penicillin (100 units/ml), streptomycin (100µg/ml), 1% Antibiotic-Antimycotic agent, L-glutamine (2mM) and 50µM 2-mercaptoethanol. The splenocytes were finally cultured in RPMI complete medium and maintained in a 5% CO_2 humidified cell culture incubator at 37°C.

Effector immune cell activation and function

The effector cell activation was assessed from IFNγ secretion by IFNγ ELISpot assay while their function was measured from granzyme b by ELISA assay. Murine splenocytes were seeded to anti-IFNγ coated PVDF bottomed 96-well plate and incubated for 1 hours at 37°C in a 5% CO_2 humidified cell culture incubator. Then, EF43.fgf4 cells which are stably expressing Pb9 antigen were added to each well in the ratio 10:1 of splenocytes to tumour cells. The plate was incubated for 16 hours in the cell culture incubator. The wells of splenocytes or EF43.fgf4 alone were included as control. After incubating, the culture medium from each well was taken to measure granzyme b using mouse granzyme b uncoated ELISA kits while the plate was carried out to detect IFNγ secretion using mouse IFNγ ELISPOT kit.

Tumour cell killing

Tumour cell killing was investigated from a release of lactase dehydrogenase (LDH) by non-radioactive cytotoxicity assay. Initially, splenocytes were cultured with tumour cells in various ratios (1:1, 5:1, 10:1, 20:1 and 50:1) and defined as experimental wells. Splenocytes were included for effector cell spontaneous LDH release. Two sets of wells containing tumour cells alone were kept for target cell

spontaneous LDH release and target cell maximum LDH release. The plate was incubated for 6 hours at 37°C in a 5% CO_2 humidified cell culture incubator. After the incubation, lysis solution was added to one set of wells containing tumour cells alone to get target cell maximum LDH release. The culture medium from each well was then taken and carried on for the cytotoxicity assay. The percentage of cytotoxicity was calculated from the follow formula.

$$\%\text{Cytotoxicity} = \frac{\text{experimental-effector spontaneous-target spontaneous}}{\text{target maximum-target spontaneous}} \times 100$$

2.2.4 *In vivo* experiments

Generation of stable tumour cells expressing GFP-Luc

EF43.fgf4 cells were seeded in 24-wells plate in complete DMEM and allowed to reach 60-70% confluent. When transfecting, the culture medium was replaced with 500µl of DMEM containing 8µg/µl polybrene and lentivirus vector (*CMV-GFP-T2A-Luciferase*) at ≈10 MOI (Multiplicity of Infection). Then, the plate was centrifuged at 2000rpm for 90 minutes and incubated overnight at 37°C in a 5% CO_2 humidified cell culture incubator. Next day, the cells were washed three times with complete DMEM and kept at 37°C in cell culture incubator. The infected cells were monitored from GFP expression under fluorescent microscope and expanded until reached 90% confluent of T75 flask for cell sorting. Then, the cells were trypsinised and resuspended in 1x PBS containing 1mM EDTA, 25mM HEPES pH7.0 and 1% FCS. After that, the GFP positive cells were sorted by MRC-BRC-IC Flow Cytometry. Finally, the sorted cells were maintained in complete DMEM containing 1x Antibiotic- Antimycotic agent as the sorting step was not performed under sterile condition.

Subcutaneous inoculation of tumour cells

The tumour cells were prepared at appropriate cellular density in DMEM media without additives. Then 50-100 ul of the tumour cell solution was subcutaneously injected to the mice.

Bioluminescence Imaging (BLI)

Mice were anesthetised with isoflurane and subcutaneously injected with 100mg/kg of d-luciferin. Luciferase expression was monitored by Vivo Imaging System (IVIS 100, Caliper Life Sciences). The luciferase activity was calculated from region of interest (ROI) defined over the tumour using Live Image software version 4.3.1 and interpreted as total photon counts per second per cm^2.

Haematoxylin and Eosin staining

Tumours were collected from each mouse, mounted in optimal cutting temperature compound (O.C.T compound), snap frozen in dry ice-ethanol bath and immediately kept at −80°C. The frozen tissues were sectioned at 5μm thick, placed on slides and kept at -20°C.

The tissue sections were fixed in 95% ethanol for 10 minutes, then, dipped in tap water and distilled water until all O.C.T compound was cleared out. The sections were stained with hematoxylin for 5 minutes, washed in running tap water and blued in lukewarm tap water. After that, the sections were counterstained with eosin for 1-2 minutes and washed in running tap water until eosin stopped streaking. Finally, the sections were dehydrated respectively in 70% ethanol, 80% ethanol, 90% ethanol, 100% ethanol, cleared through two changes of xylene and mounted in DPX mounting medium.

Fluorescent staining of frozen sections (cleaved Caspase-3)

The sections were warmed at room temperature for 2-3 minutes, fixed in 3% formaldehyde in 1x PBS at room temperature for 30 minutes and washed three times in 1x PBS for 5 minutes each. Then, the sections were blocked in 1x PBS containing 5% goat serum and 0.3% Triton™ X -100 for 60 minutes. While blocking, cleaved Caspase-3 primary antibody was prepared in 1x PBS containing 1% BSA and 0.3% Triton™ X -100 (dilution 1:400). The sections were incubated overnight in the primary antibody solution at 4°C. Next day, the sections were washed three times in 1x PBS for 5 minutes each and incubated in diluted anti-rabbit Alexa Fluor 488 secondary antibody (1:800) as well as DAPI (1:3000) in 1x PBS containing 1% BSA and 0.3% Triton™ X -100 at room temperature for 45 minutes in the dark. After the incubation, the sectinos were washed three times in 1x PBS for 5 minutes and subsequently and mounted with prolong gold antifade reagent. The slides were dried overnight at room temperature in the dark before subjecting to fluorescent microscope or being kept at -20°C.

2.2.5 Statistical analysis

Statistical analysis was performed using IBM SPSS statistics software version 23. The data presented in this thesis are mean value ± standard error of the mean (SEM). *P* value was generated by the student t-test and one-way ANOVA with Tukey's honestly significant difference (HSD) post hoc test for normally distributed data. Mann-Whitney and Kruskal-Wallis test was used as a non-parametric test. The P values were considered significant at $p<0.05$and represented as follows: *$p<0.05$, **$p\leq0.01$.

2.2.6 Bioinformatics

Bioinformatic analysis was performed using SnapGene software version 4.2.5 which includes the design and construction of plasmids, determination of bands with restriction enzyme digestion and analysis of sequencing results.

Chapter 3

H5WYG peptide capability to enhance endosomal escape of PAAV vector

3.1 Introduction

Gene delivery is a biological technology aimed to transfer a gene into cells of interest with an ultimate goal to drive a stably functional expression of the transferred gene. The development of gene delivery contributes to great benefits in many biomedical fields including gene therapy. In order to deliver the gene to the target site, a sufficient delivery system is required. Thus, many delivery tools, widely categorized into viral and non-viral vectors, have been developed and exploited for gene delivery. Each of these vector categories has their advantages and drawbacks. Viral vectors are considered more efficacious than the non-viral ones due to their high transduction efficacy. However, non-viral vectors tend to be safer to use because they are lack of native tropism and pathogenicity [8, 22]. Apart from their advantages and disadvantages, both viral and non-viral vectors confront similar difficulties to mediate gene transfer. Stable vector manufacture, efficient targeting strategy, capability of cellular internalization, sufficient intracellular trafficking, nuclear uptake and functional gene expression are crucially required to achieve a successful gene delivery [5, 40, 41]. Additionally, the vectors have to traverse multiple barriers from administered site to their destination. Intracellular trafficking is one of the barriers that the vectors need to overcome [71].

Because a cellular uptake of foreign vectors usually relies on endocytosis, the vectors are initially internalised and resided in endocytic vesicles. Most of viral vectors are taken up via clathrin-mediated endocytosis [236]. The intracellular

vesicle generally undergoes early endosome formation and maturation to become late endosomes. During the maturation, cytosolic H^+ ions are pump into endosome resulting in a decrease of intravesicular pH. Late endosomes are destined to fuse with lysosomes where digestive enzymes are activated under acidic condition. As a result of all these steps, the sequestered vectors are frequently degraded by active enzymes. According to this intracellular trafficking, the vectors are needed to escape from endosome in a time manner to carry out their biological function [62, 71].

Although a wide variety of strategies have been developed to release the vectors from endosomes before getting degraded in the lysosomes, endosomal escape is still recognised as a bottleneck of gene transfer. Based on the principal of intracellular trafficking, one strategy to overcome endosomal degradative pathway is to employ endosomal escape agents. These agents are derived from various sources, for example, haemagglutinin (HA2) from influenza [72], listeriolysin O (LLO) from bacteria [82], human calcitonin derived peptide [98] and Ricin from plants [91]. While some agents are purified from natural source, the others are synthesized in analogous to the parental models such as EB1[99], KALA and GALA peptides [100, 102]. Also, several chemical agents such as polyethylenimine (PEI) and Poly(amidoamine)s (PAAs) have been reported for their contribution to endosomal escape [74, 75].

It is well known that viral vectors are more efficacious than non-viral vectors both *in vitro* and *in vivo*. Understanding mechanisms that viruses utilise to escape from their host's barriers is beneficial for the intracellular delivery. These mechanisms are basically related to endosomal membrane destabilisation followed by pore formation, membrane rupture or fusion peptide depending on their characteristics. The enveloped viruses tend to fuse their envelopes with endosomal membranes while the non-enveloped ones usually make a pore through the membrane and escape to cytosol [69]. In many studies, small viral peptide domains were reported for their crucial capability for endosomal escape. Therefore many viral-based endosomal escape agents have been developed and applied in gene transfer. According to the previous studies in our group, three

endosomal escape peptides; H5WYG, INF-7 or PC1; were displayed on recombinant pVIII of AVVP vector and assessed for their endosomal escape capability. Among these peptides, H5WYG is considered as a promising one because the targeted vector displaying H5WYG resulted in substantially more gene expression compared to the vector displaying INF-7 or PC1 peptides (accepted manuscript PNAS 2019). Thus, H5WYG was chosen over the other two peptides to display on recombinant pVIII of PAAV vector in this chapter.

H5WYG (GLFHAIAHFIHGGWHGLIHGWYG) peptide was designed in analogous to the N-terminal segment of haemagglutinin (HA2) subunit from Influenza virus. The parental HA2 subunit (GLFGAIAGFIEGGWTGMIDGWYG) was modified by replacing G-4, G-8, E-11, T-15, and D-19 with histidyl residues. M-17 was also replaced by a leucyl residue [237]. H5WYG is a histidine-rich peptide which is weakly soluble at neutral pH. However, it undergoes conformation change under mildly acidic conditions as all histidines are protonated. The histidines are considered as key elements of this peptide to facilitate the vectors out of endosomes through a mechanism called proton sponge effect. According to many studies, proton sponge effect is usually mediated by agents with high buffering capacity. The mechanism generally begins with endosomal membrane destabilisation followed by endosomal rupture [69, 71, 238-240].

H5WYG peptide contains five histidyl residues which are capable of getting protonated during endosomal acidification. This protonation process causes a conformational change of the peptide following by its interaction with endosomal membrane. The interaction is believed to induce a flip of cytosolic membrane leaflet into endosomal lumen which consequently destabilises endosomal membrane. Moreover, the buffering capacity of H5WYG peptide makes it more difficult to lower endosomal pH during the maturation as all histidines are protonated. Thus, excessive cytosolic proton is required. When the protons are pumped in, there is also an intensive inflow of counter-ions and water to balance membrane voltage and restore osmotic balance between endosomal compartment and the cytosol. The osmotic swelling caused by water inflow together with already destabilised membrane results in endosomal

rupture and a release of entrapped materials. Relevant to its capability, H5WYG peptide has been reported for its contribution to enhance gene expression in many studies. The peptide was applied in many types of delivery systems such as antisense oligonucleotide, polyethylene glycol-based vehicle and peptide-based nanocarriers [107, 239, 241].

The aim of this chapter is to investigate the capability of H5WYG peptide to facilitate endosomal escape that leads to an augmentation of PAAV-mediated gene expression. In a series of experiments, firstly, PAAV vector has been further modified to display H5WYG peptide on its recombinant pVIII major coat protein. Secondly, the modified vector was characterised for its morphological change by transmission electron microscopy and assessed its buffering capability by acidic-based titration. All experiments in this chapter were primarily optimised in HEK293 cells and translated to a panel of tumour cell lines. Three different tumour cell lines namely A549 (lung adenocarcinoma), M21 (melanoma) and UW228 (medulloblastoma) were chosen as preliminary models to test the H5WYG endosomal escape capability. Therefore, thirdly, the tumour cells were characterised for their expression of α_v, β_3 and β_5 integrins, receptor of PAAV. Next, the vector transduction efficacy on A549, M21 and UW228 tumours was optimised from *Lucia* reporter gene expression. Fourthly, the capability of H5WYG peptide to enhance gene expression was assessed by comparing differences in *Lucia* gene expression mediated by PAAV displaying H5WYG to the one mediated by the vector lacking the peptide. Fifthly, bafilomycin A1, a specific inhibitor of a vascuolar ATPase proton pump, was applied to PAAV transduction in order to investigate mechanism by which H5WYG facilitates the vector escape from endosomes. Sixthly, the modified vector was applied in gene therapy by delivering a transgene encoding for secreted *TNFα* (*sTNFα*). The efficiency of H5WYG peptide was investigated for tumour cell death mediated by PAAV vector encoding *sTNFα* gene. Seventhly, preliminary *in vivo* experiment was performed on CD1 nu/nu mice in order to show a proof of concept that H5WYG peptide is able to augment vector-mediated gene expression *in vivo*.

3.2 Results

3.2.1. Construction of M13.KO7 helper phage displaying the H5WYG peptide

To construct helper phage displaying the peptide, firstly, *H5WYG* DNA sequence (GGCTTGTTCCACGCCATCGCGCACTTCATTCATGGGGGTTGGCACGGTCTCATCCAT GGTTGGTACGGG) flanked by *HindIII* and *PstI* restriction sites was inserted in to recombinant pVIII of f88-4 plasmid (GenBank Accession AF218363). The plasmid with *H5WYG* sequence was confirmed by DNA sequencing (figure 3.1). Secondly, the plasmid from a previous step was used as a PCR template to amplify recombinant *pVIII* with *H5WYG* sequence. The PCR product was then ligated to RGD.M13.KO7 and M13.KO7 helper phage plasmid.

The constructs with insert were verified by restriction enzyme digestion and confirmed by DNA sequencing (figure 3.2 and 3.3). The construct with the corrected DNA sequencing result was chosen and proceeded for helper phage production. After the production, there were two helper phage displaying H5WYG peptide. One was a targeted helper phage called RGD.M13.KO7.H5W. The other was non-targeted helper phage called M13.KO7.H5W. The helper phages without H5WYG peptide, RGD.M13.KO7 and M13.KO7, were also produced and included in the experiments in this chapter. The helper phage figures demonstrating capsid proteins and displaying peptides are shown in figure 3.4.

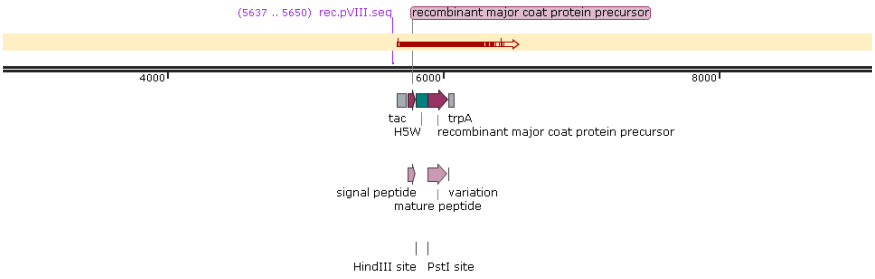

Figure 3.1. DNA sequence of recombinant pVIII with H5WYG in f88-4 plasmid.

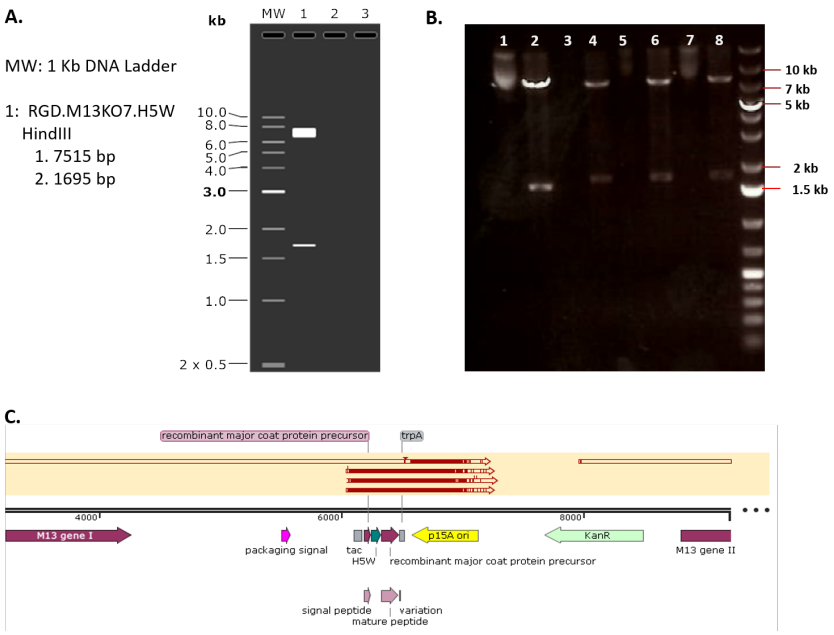

Figure 3.2. Construction of targeted helper phage plasmid with H5WYG peptide (RGD.M13.KO7.H5WYG).

The plasmid was digested with *HindIII* restricted-enzyme which cuts at two restriction sites, inside the insert and on the backbone. **A** *In silico* digested bands from Snap Gene software. **B** The helper phage plasmids were digested and run on 1% agarose gel to identify correct DNA fragments. Lanes with odd number are undigested plasmids while the ones with even number are the plasmid undergone *HindIII* restricted-digestion. **C** DNA sequencing results of RGD.M13.KO7.H5WYG plasmid.

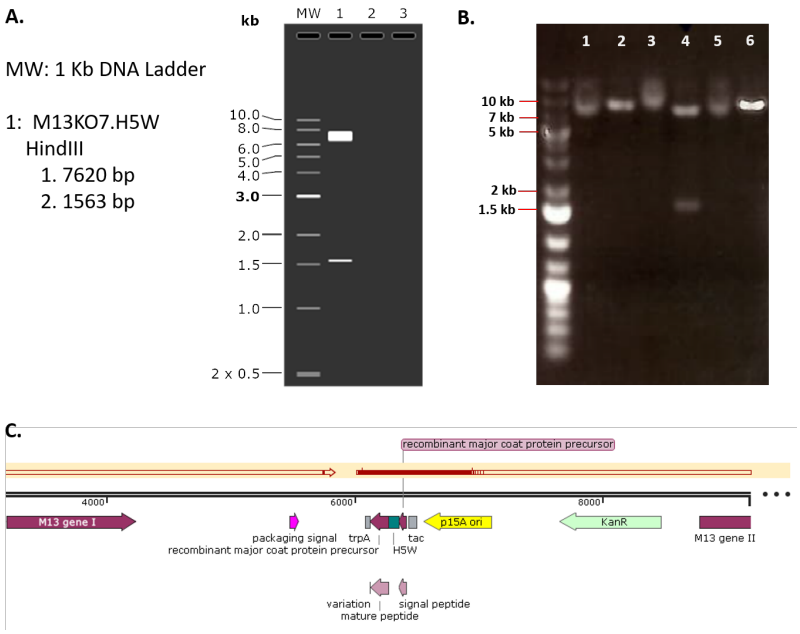

Figure 3.3. Construction of non-targeted helper phage plasmid with H5WYG peptide (M13.KO7.H5WYG).

The plasmid was digested with *HindIII* restricted-enzyme which cuts at two restriction sites, inside the insert and in the backbone. **A** *In silico* digested bands from Snap Gene software. **B** The helper phage plasmids were digested and run on 1% agarose gel to identify correct DNA fragments. Lanes with odd number are undigested plasmids while the ones with even number are plasmid undergone *HindIII* restricted-digestion. **C** DNA sequencing result of M13.KO7.H5WYG plasmid.

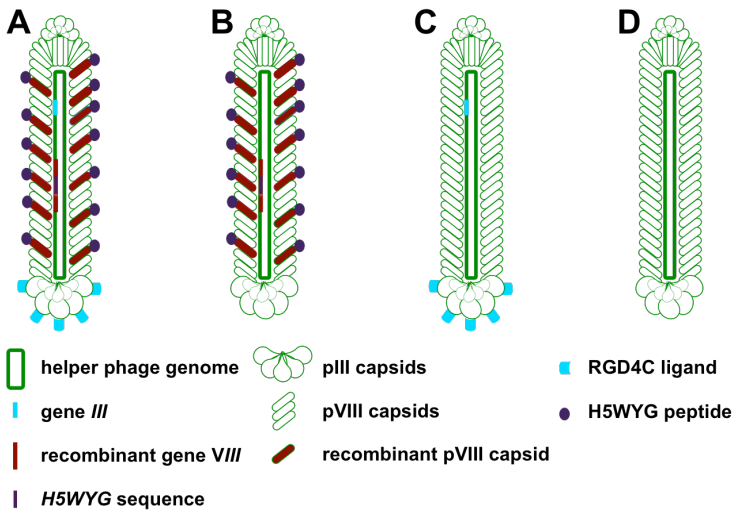

Figure 3.4. Schematic illustartion of helper phages.

A represents a targeted helper phage displaying H5WYG peptide (RGD.M13.KO7.H5W). **B** represents a non-targeted helper phage displaying H5WYG peptide (M13.KO7.H5W). **C** represents a targeted helper phage without H5WYG peptide (RGD.M13.KO7). **D** represents a non-targeted helper phage without H5WYG peptide (M13.KO7)

3.2.2. Construction of PAAV vector encoding secreted *TNFα*

According to endosomal escape capability of H5WYG peptide, it is challenging to apply the modified vector to gene therapy. In doing so, *secreted tumour necrosis factor alpha* (*sTNFα*) gene was chosen to assess an enhanced therapeutic effect mediated by PAAV vector displaying H5WYG peptide. It is well-known that TNFα is an inflammatory cytokine possessing anti-tumour activity and has been utilized in different strategies to induce anti-tumour responses [242, 243]. Many preclinical studies have proved TNFα efficiency for targeted gene therapy. Also, this therapeutic gene was applied on the previous version bacteriophage vector (AAVP) and shown efficacy to treat naturally occurring cancers in pet dogs [34]. At present, two forms of TNFα; transmembrane (tmTNFα) and secreted (sTNFα); were genetically constructed into PAAV vector. The two forms were compared their efficiency in a number of tumour cell lines where sTNFα showed superior anti-tumour response over tmTNFα (unpublished data in Phage therapy group).

To investigate the efficacy of H5WYG peptide on enhancing therapeutic gene expression, PAAV vector encoding secreted *TNFα* was genetically constructed. Signal peptide sequence of interleukin IL-2 was fused to the DNA sequence of *TNFα* in order to generate secreted *TNFα* (*IL-2sp.sTNFα)*. Then *IL-2sp.sTNFα* sequences flanked by *BamHI* and *SalI* restriction sites was ligated to PAAV backbone. Finally, the corrected construct was confirmed by restriction enzyme digestion and DNA sequencing (figure 3.5).

In order to produce 4 different PAAV vectors encoding secreted *TNFα* transgene, PAAV.*IL-2sp.sTNFα* plasmid was transformed into competent TG1 *Escherichia coli* and co-infected with one of RGD.M13.KO7, M13.KO7, RGD.M13.KO7.H5W or M13.KO7.H5W helper phage. Thus, there are 4 different PAAV vectors RGD.PAAV.*IL-2sp.sTNFα*.H5W, RGD.PAAV.*IL-2sp.sTNFα*, PAAV.*IL-2sp.sTNFα*.H5W and PAAV.*IL-2sp.sTNFα*. The first and the third one are displaying H5WYG peptide on the recombinant pVIII major coat proteins (figure 3.6).

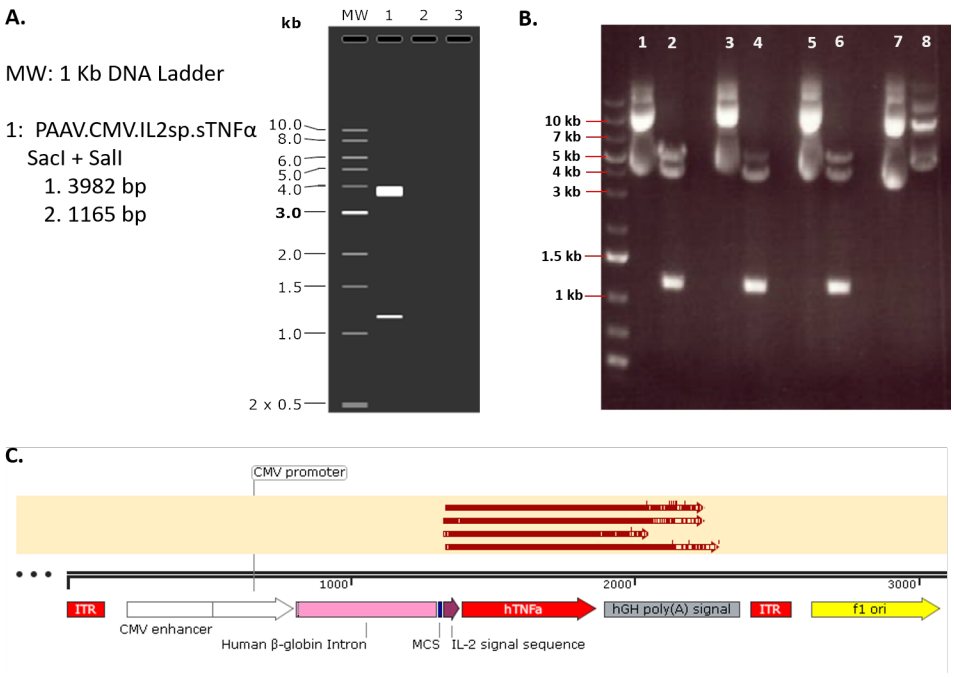

Figure 3.5. Construction of PAAV vector encoding secreted TNFα (PAAV.*IL-2sp.sTNFα*).

The plasmid was digested with *SacI* and *SalI* restricted-enzymes. A.) *In silico* digested bands from Snap Gene software. B.) The plasmids were digested and run on 1% agarose gel to identify correct DNA fragments. Lanes with odd number are undigested plasmids while the ones with even number are the plasmids undergone restriction enzyme double digestion. C.) DNA sequencing results of PAAV.*IL-2sp.sTNFα* plasmid.

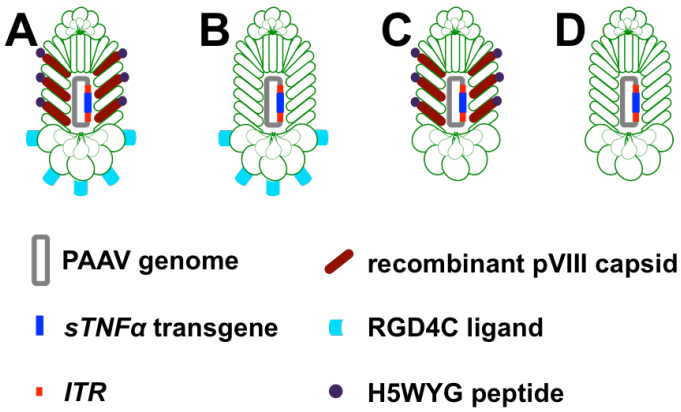

Figure 3.6. Schematic illustration of PAAV vectors encoding TNFα (PAAV.*IL-2sp.sTNFα*).

A represents a targeted vector displaying H5WYG peptide (RGD.PAAV.*IL-2sp.sTNFα*.H5W). **B** represents a targeted vector without H5WYG peptide RGD.PAAV.*IL-2sp.sTNFα*). **C** represents a non-targeted vector displaying H5WYG peptide (M13.PAAV.*IL-2sp.sTNFα*.H5W). **D** represents a non-targeted vector phage without H5WYG peptide (M13.PAAV.*IL-2sp.sTNFα*)

3.2.3. Characterisation of M13.KO7 helper phage by Transmission Electron Microscopy

To determine the size difference between unmodified helper phage and helper phage displaying H5WYG peptide, RGD.M13.KO7 and RGD.M13.KO7.H5W were produced, stained and subjected to transmission electron microscopy (TEM). The production steps were conducted at Imperial College London (UK) while TEM related methods were performed at Chiang Mai University (Thailand) by collaborators. A commercial helper phage (M13.KO7) was included as a control. As shown in figure 3.7, all helper phage particles observed under the microscope were long filamentous rod-like shape. Dark spots found in RGD.M13KO7.H5W were bacteria debris from the vector production when IPTG was added to induce tac promoter driving an expression of H5WYG peptide. To compare length of each helper phage particles, the particle size was measured by ImageJ software andshowed that RGD.M13.KO7 particle was slightly longer than the commercial M13.KO7 particle, in length of 1186.46 and 1218.82 nm respectively. As theoretically expected, RGD.M13.KO7.H5W particle was averagely 1277.61 nm in length which is significantly longer than the other two particles.

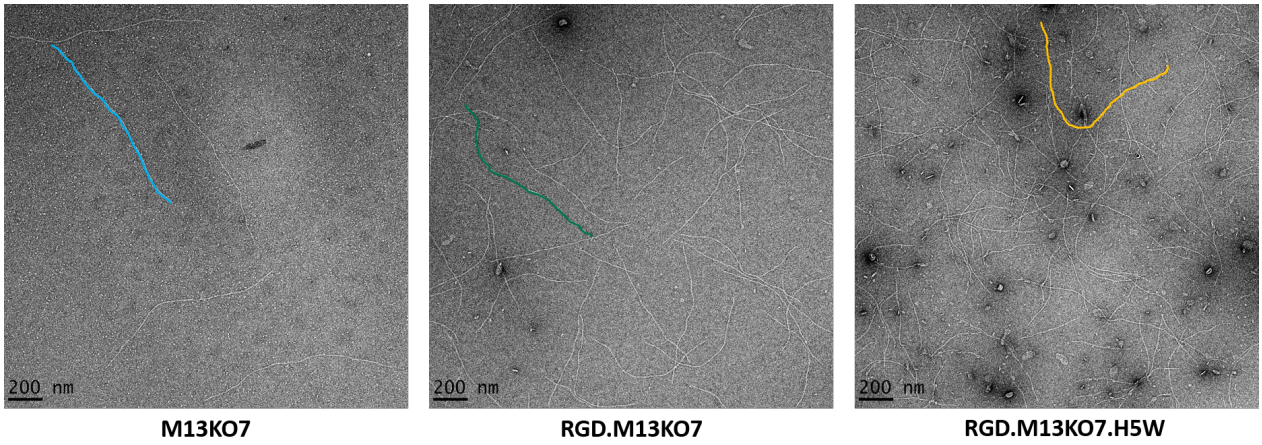

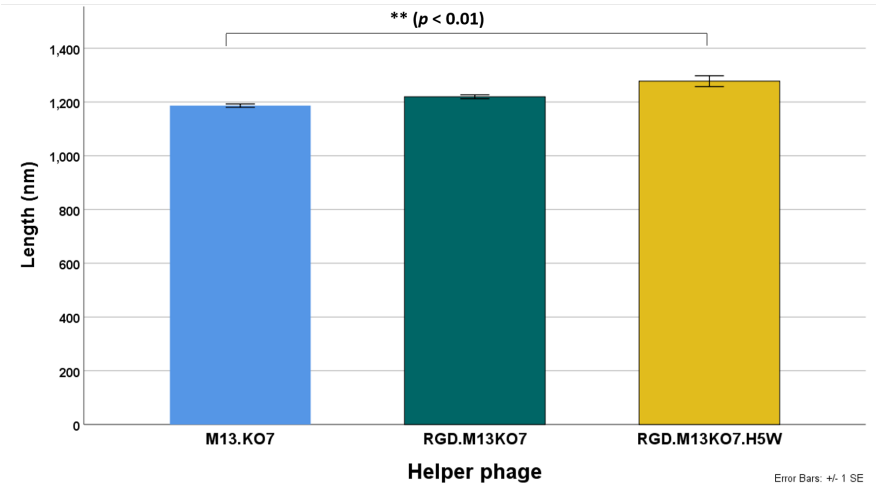

Figure 3.7. Characterisation of helper phages by transmission electron microscopy (TEM).

RGD.M13.KO7 and RGD.M13.KO7.H5W helper phage were produced and subjected to TEM. All helper phage particles observed under the microscope were long filamentous rod-like shape. The commercial M13.KO7 (n = 26), RGD.M13.KO7 (n = 7) and RGD.M13.KO7.H5W (n = 20) are represented by blue, green and yellow free-shaped line, respectively. Dark spots in RGD.M13.KO7.H5W were bacteria debris which is a byproduct from the vector production with IPTG. The particle size was measured using ImagJ software. Data are shown as mean±SEM. Statistical significance was determined by one-way ANOVA with Tukey's honestly significant difference (HSD) post hoc test.

3.2.4. Characterisation of PAAV vector displaying H5WYG peptide

3.2.4.1. PAAV particle size determined by transmission electron microscopy

In order to characterise morphological changes of the PAAV vector displaying H5WYG peptide on recombinant pVIII capsid proteins, RGD.PAAV and RGD.PAAV.H5W were produced and subjected to transmission electron microscopy. All PAAV particles observed under the microscope were long filamentous rod-like shape. Dark spots found in RGD.PAAV.H5W were bacteria debris from the vector production when IPTG was added to induce tac promoter driving an expression of H5WYG peptide. The PAAV particle displaying H5WYG peptide was significantly shorter as compared to the particle without the peptide, in length 734.37 and 856.85 nm, respectively (figure 3.8). The helper phage particles were also found in the sample. They were distinguished from the size which approximately 400-500 nm longer than PAAV particles.

3.2.4.2. Buffering capacity mediated by PAAV particle displaying H5WYG peptide

As endosomal escape is a crucial step to enhance vector-mediated gene expression. Displaying H5WYG peptide on the vector capsid proteins is considered to enhance the endosomal escape by inducing osmotic swelling and disruption of endosomal membrane. In order to assess the endosomal escape efficacy of PAAV vector, its buffering capacity within pH range from 10 to 3 was measured by acidic-based titration. Initially, the vectors were prepared at 3 mg protein dissolved in de-ionized water and 0.1M HCl was added in 2 µl increment. Titration of de-ionized water was conducted in parallel as control. As shown in figure 3.9A, PAAV vector showed a slight buffering capacity compared to control while PAAV.H5W elicited more buffering capacity than PAAV alone. The experiment was repeated with an increase of vector protein to 5 mg and a lower increment of 0.1M HCl. Comparing within natural endosome pH range 6.8- 5.1, PAAV.H5W required 32 ul of 0.1M HCl to lower the pH from 10 to 6.8 while PAAV

alone needed only 15 ul of the solution. Also, PAAV.H5W required 48 ul of 0.1M HCl to reach pH 5 while PAAV alone needed 22 ul of 0.1M HCl to reach the same pH (figure 3.9B). The results indicate that PAAV.H5W has around 2-fold higher buffering capacity than PAAV alone.

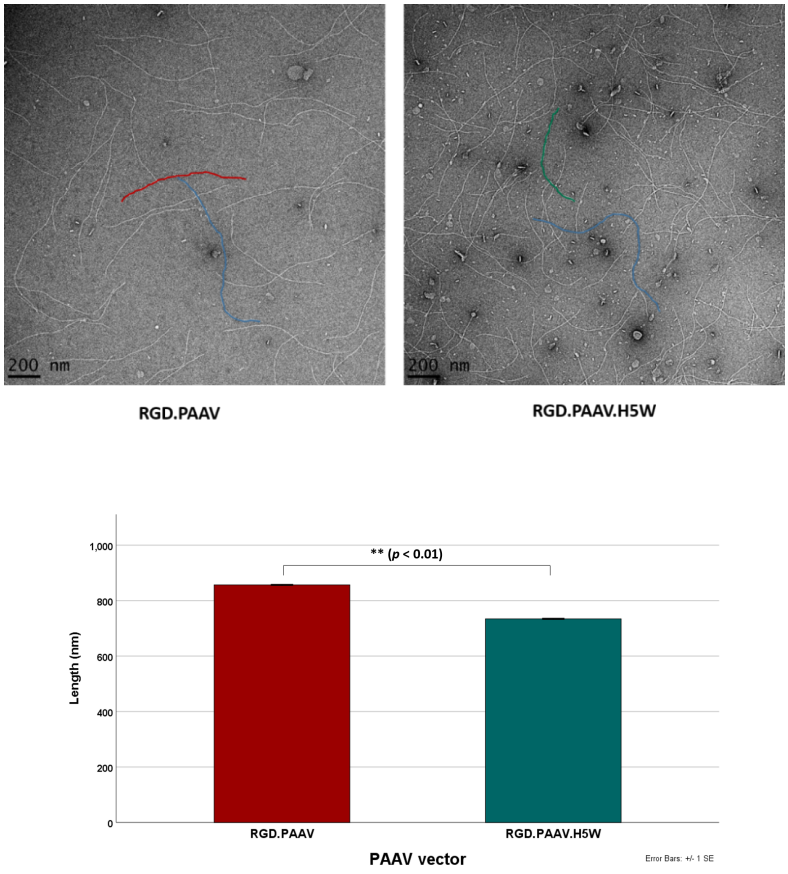

Figure 3.8. Characterisation of PAAV particles by transmission electron microscopy (TEM).

RGD.PAAV and RGD.PAAV.H5W vectors were produced and subjected to TEM. All PAAV particles were long filamentous rod-like shape. Red and green free-shaped line represents RGD.PAAV (n = 107) and RGD.PAAV.H5W particle (n = 70), respectively. The helper phage particles (longer blue free-shaped line) were found in the sample and identified from their longer size. Dark spots in RGD.PAAV.H5W were bacteria debris which is a byproduct from the vector production with IPTG. The particle size was measured using ImagJ software. Data are represented as mean±SEM. Statistical significance was determined by student t-test.

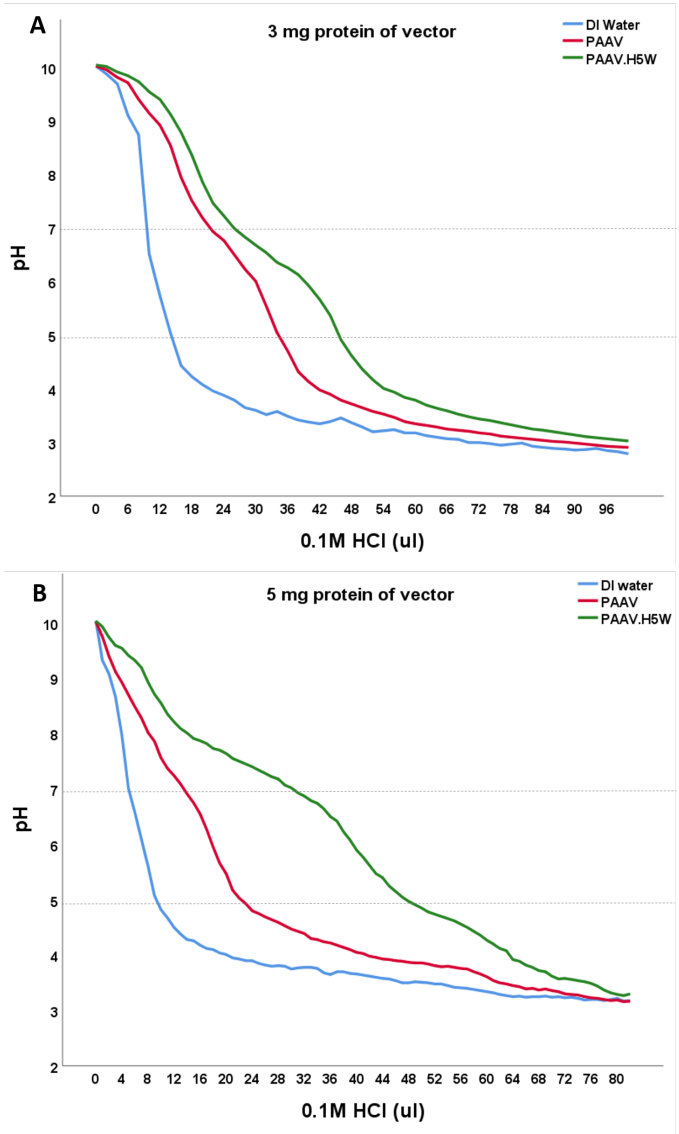

Figure 3.9. Buffering capacity of PAAV vector.

PAAV and PAAV.H5W vector were separately dissolved in de-ionized water and adjusted to pH10 by adding 0.1M NaOH. The titration was carried on by adding 0.1M HCl until reach pH3. The pH was measured by the pH metre. Titration curve of de-ionized water was added as a control. Dashed lines represent the typical pH range in endosome (pH 6.8-5.1). **A** The titration was performed with 3 mg protein of each PAAV vector and 0.1M HCl was added in 2 µl increment. **B** The titration was performed with 5 mg protein of PAAV vector and 0.1M HCl was added in 1 µl increment.

3.2.5. Characterisation of A549, M21 and UW228 cell lines

3.2.5.1. Integrin expression

As PAAV vector is targeted to tumour cell through binding of the RGD4C ligands to $\alpha_v\beta_3$ and/or $\alpha_v\beta_5$ heterodimeric receptors. Tumour cell models (A549, M21 and UW228) were checked for α_v, β_3 and β_5 expression by immunofluorescent staining in order to test their suitability for being targeted by RGD.PAAV vector. As shown in figure 3.10, A549 and UW228 cells expressed all three integrin subunits. On the other hand, M21 showed a good expression of α_v and β_5 integrins but a slight expression of β_3 integrins.

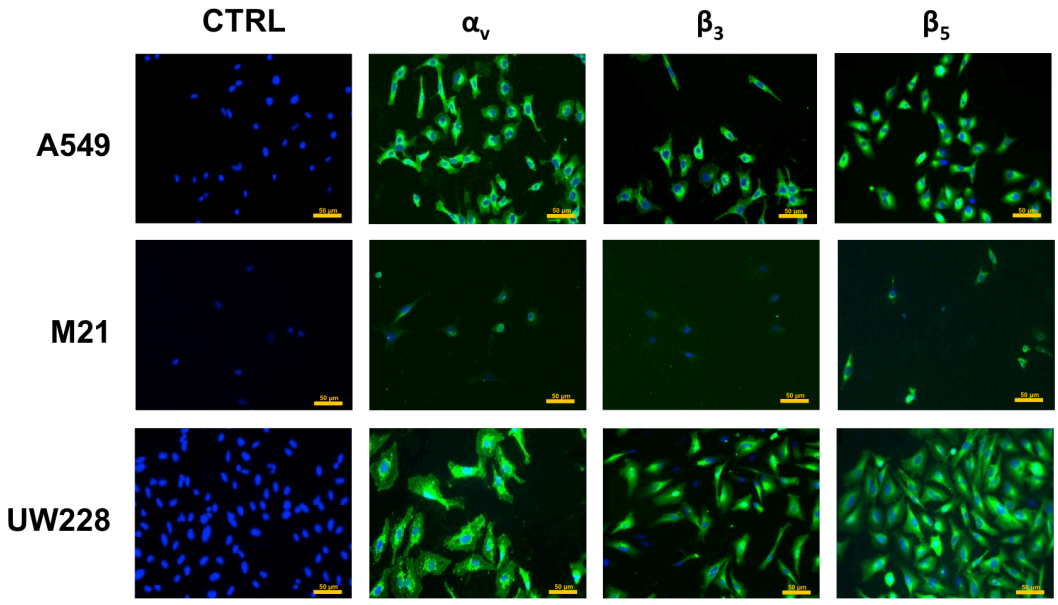

Figure 3.10. Immunofluorescent staining of A549, M21 and UW228 for α_v, β_3 and β_5 integrin receptor expression.

The cells were seeded on coverslips, fixed and stained with the primary anti- α_v, β_3, or β_5 antibodies (diluted 1:50 in 2% BSA/PBS) overnight. Cells were then washed and stained with AlexaFluor-488 conjugated secondary antibody (diluted 1: 750 in 2% BSA/PBS) and DAPI (diluted 1: 3000 in 2% BSA/PBS). The control was stained with only secondary antibody and DAPI. Scale bar= 50µm

3.2.5.2. Luciferase expression mediated by PAAV vector transduction

The efficiency of targeted vector (RGD.PAAV) as a delivery vehicle was investigated from the expression of secreted luciferase reporter gene (*Lucia*). In order to optimise the vector efficiency, firstly, HEK293 cells were transduced with PAAV encoding the reporter gene (PAAV.*Luc*) at four different transducing units (TU)/cell (100,000; 500,000; 1,000,000 and 2,000,000 TU/Cell). The secreted Lucia in the cell culture medium was measured daily starting from day 1 post-transduction. The highest expression was detected on day 4 post-transduction in dose-dependent manner (figure 3.11A). Non-targeted vector (M13.PAAV) was used as a control. Lucia expression was also detected on the cells transduced with non-targeted vector due to non-specific uptake.

Similar experiments were conducted on A549, M21 and UW228 tumour cells. The highest Lucia expression was found on day 5 post-transduction for A549 cells and on day 4 post-transduction for M21 and UW228. The expression was also detected in dose-dependent manner (figure 3.11B, 3.11C and 3.11D). However, there was a slightly non-specific uptake found on UW228 cells transduced with 500,000; 1,000,000 and 2,000,000 TU/cell of the control non-targeted PAAV.*Lucia*. These data indicate that RGD.PAAV is capable of selectively delivering the reporter gene to A549, M21 and UW228 cells with high transduction efficacy *in vitro.*

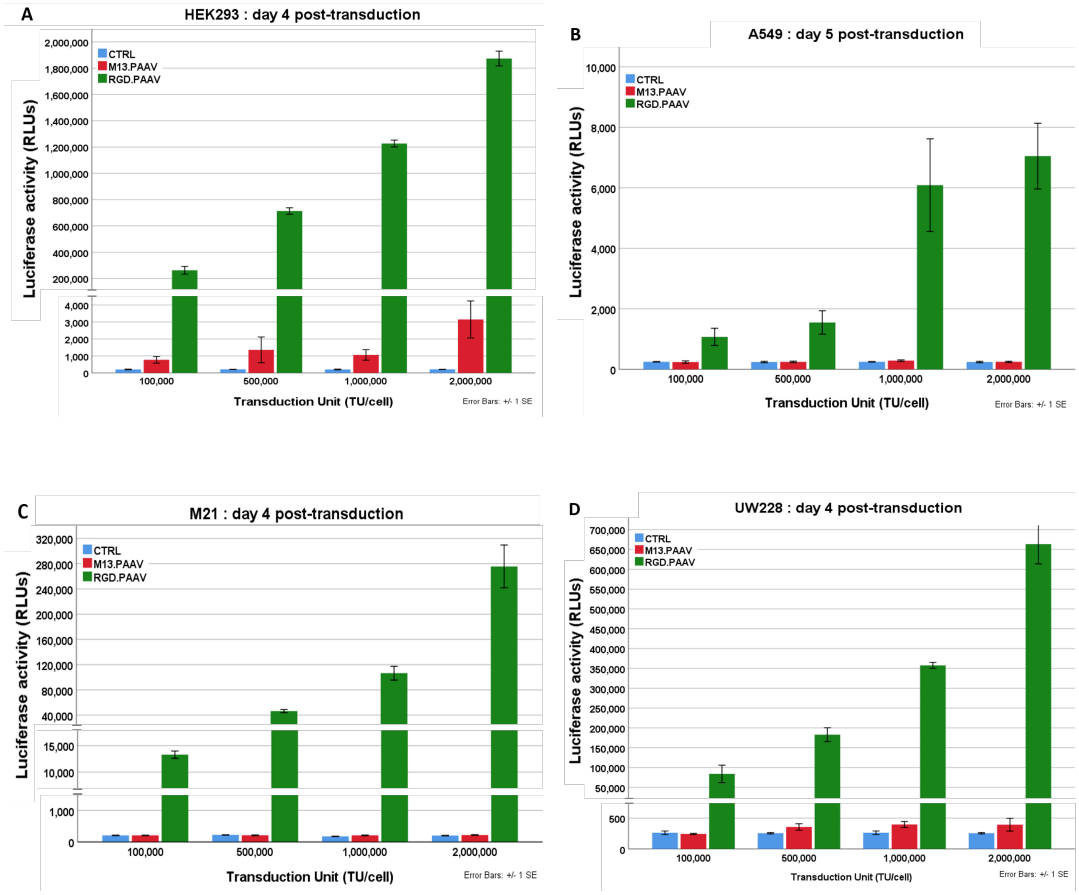

Figure 3.11. Transduction of HEK293, A549, M21 and UW228 cells by PAAV vector.

The cells were in 96- well plate and grown to 60-70% confluence then transduced with targeted PAAV encoding *Lucia* reporter gene (RGD.PAAV) or non-targeted vector (M13.PAAV) at four different vector doses of 100,000; 500,000; 1,000,000 or 2,000,000 TU/cell. Results are shown as mean ± SEM of triplicate wells of one representative experiment. All experiments were repeated twice.

3.2.5.3. Specificity of PAAV vector and its transduction efficacy on normal cells

As safety issue is very crucial for cancer gene therapy, the delivery systems are expected to maintain their specificity on the tumour cells without any side effects on normal cells. In this chapter, three normal cell models; lung fibroblasts, skin fibroblasts and astrocytes; were chosen in related to A549, M21 and UW228 tumours to investigate the safety of PAAV vector on normal cells. The cells were transduced with various transducing units between 500,000 and 3,000,000 TU/cell of targeted or non-targeted PAAV vector encoding *Lucia* reporter gene. The Lucia expression was monitored from day 2 to day 7 post transduction and no expression was detected on any of them. The luciferase signal shown in the figures was a medium background detected from all wells including the control (figure 3.12). This indicates the specificity of the vector for cancer cells.

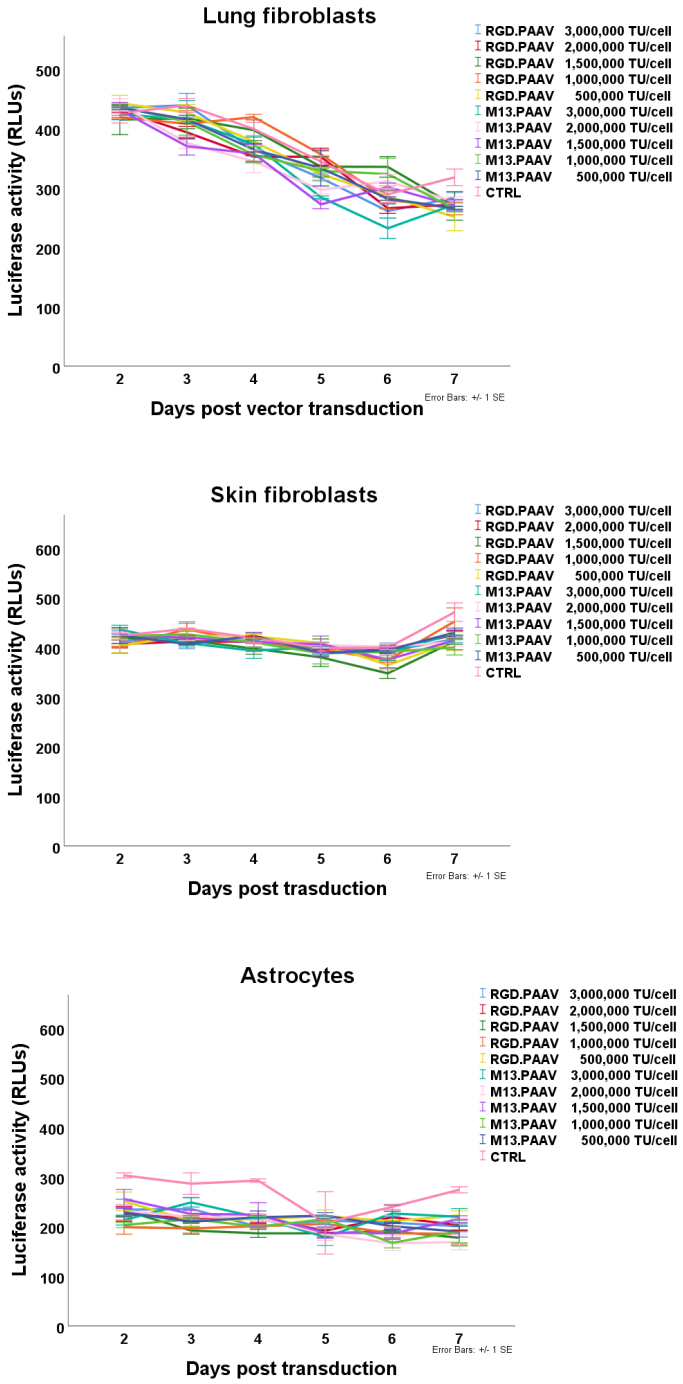

Figure 3.12. PAAV transduction in normal cells (lung fibroblasts, skin fibroblasts and astrocytes).

The cells were seeded in 96- well plate and grown to 60-70% confluence then transduced with targeted PAAV encoding *Lucia* reporter gene (RGD.PAAV) or non-targeted vector (M13.PAAV) at various transduction units. Results are shown as mean ± SEM of triplicate wells of one representative experiment. All experiments were repeated twice.

3.2.6. Efficacy of H5WYG peptide on increasing reporter gene expression

To investigate the efficiency of the peptide on driving a higher gene expression, PAAV.*Lucia* vectors displaying H5WYG peptide on capsid proteins were produced with a co-infection of either RGD.M13.KO7.H5W or M13.KO7.H5W. Then four different vectors (RGD.PAAV.*Lucia*, PAAV.*Lucia*, RGD.PAAV.*Lucia*.H5W and PAAV.*Lucia*.H5W) were applied on HEK293 cell transduction. The cells were transduced with 25,000; 50,000; 75,000 or 100,000 TU/cell of each vector. The expression was quantitatively measured from culture medium of transduced cells on day 4 post-transduction. As shown in figure 3.13A, RGD.PAAV vector displaying the H5WYG peptide showed more efficacious at transduction resulting in a 3.9, 1.4, 1.9 and 3 fold increase in Lucia expression compared to RGD.PAAV vector without H5WYG peptide. There was a non-specific uptake found on the cells transduced with M13.PAAV.H5W vector at 75,000 and 100,000 TU/cells.

Similar experiments at the same TU/cell of PAAV vector were performed on M21 and UW228 tumour cells while the experiments on A549 cells were done with 250,000; 500,000; 750,000 and 1,000,000 TU/cell of the vector. The results on these three cell lines seemed to be repeated as the ones found on HEK293 cells. As shown in figure 3.13B, C and D, Lucia expression from cells transduced with RGD.PAAV.H5W was significantly higher than the expression from the cells transduced with RGD.PAAV vector. The expression showed in dose-dependent trend in all A549, M21 and UW228 cells. The highest expression was found on day 4 in M21 and UW228. However, Lucia expression detected in A549 cells was slightly lower than the ones from M21 and UW228. The highest expression from A549 was detected on day 5 post vector transduction. From all experiments performed in this thesis, it shown that A549 cells were more difficult to transduce and mediated gene expression in a delayed time manner compared to other cell lines. Additionally, there was a Lucia expression found on M21 and UW228 cells transduced with 50,000; 75,000 and 100,000 TU/cell of PAAV.H5W due to a non-specific uptake of the vector.

The specificity of PAAV vector displaying H5WYG peptide was also assessed on normal cells. Lung fibroblasts, skin fibroblasts and astrocytes were transduced with targeted or non-targeted PAAV vector encoding *Lucia* reporter gene and displaying H5WYG peptide. The transduction unit was varied from 50,000 to 1,000,000 TU/cell. The reporter gene expression was monitored everyday between day2 and day 7 post transduction and no expression was detected from any of them. The luciferase signal shown in the figures was a medium background detected from all wells including the control (figure 3.14). This indicates that H5WYG peptide does not affect the vector specificity for cancer cells.

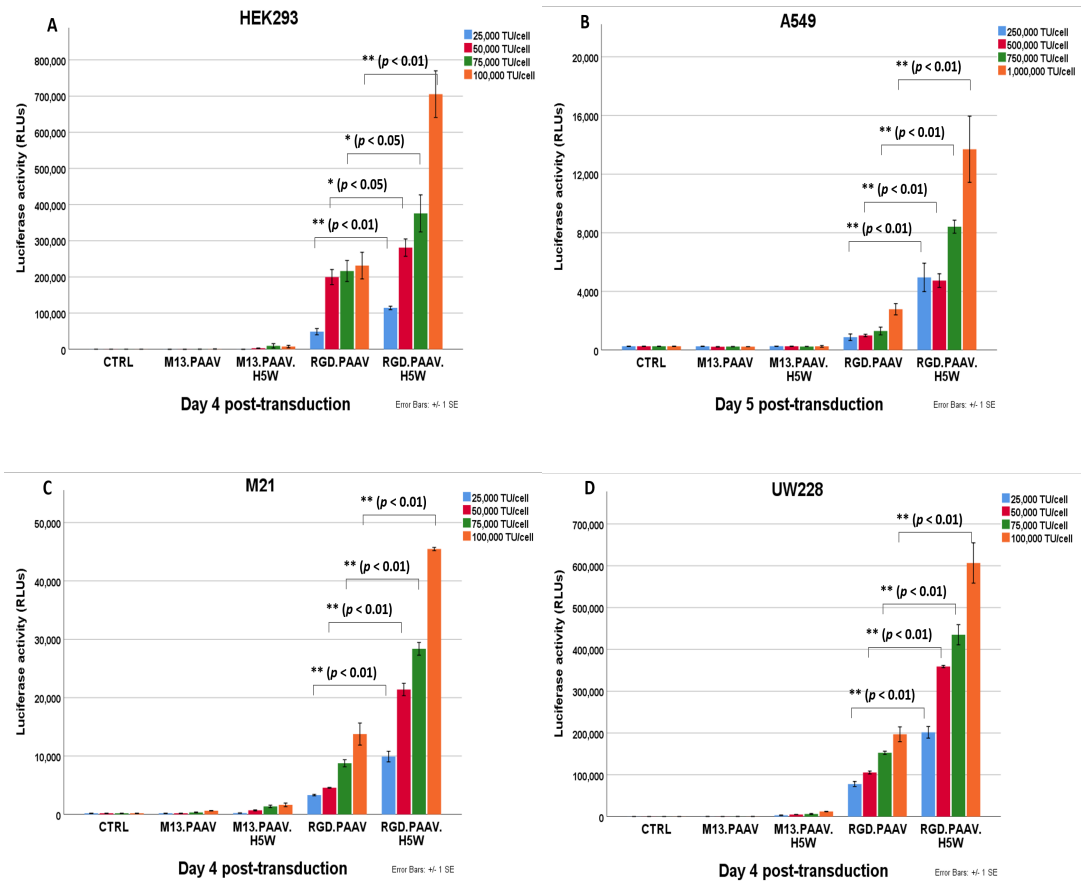

Figure 3.13. Transduction of HEK293, A549, M21 and UW228 by PAAV vector displaying H5WYG peptide.

Cells were plated in 96- well plates and grown to 60-70% confluence then transduced with targeted PAAV encoding *Lucia* reporter gene and displaying H5WYG peptide (RGD.PAAV.*Lucia*.H5W) or targeted PAAV without the peptide (RGD.PAAV.*Lucia*) at four different vector doses. Non-targeted PAAV displaying peptide (M13.PAAV.*Lucia*.H5W) and non-targeted vector without the peptide (M13.PAAV.*Lucia*) were also included as controls. Results are shown as mean ± SEM of triplicate wells of one representative experiment. All experiments were repeated three times. Statistical significance was determined by one-way ANOVA with Tukey's honestly significant difference (HSD) post hoc test.

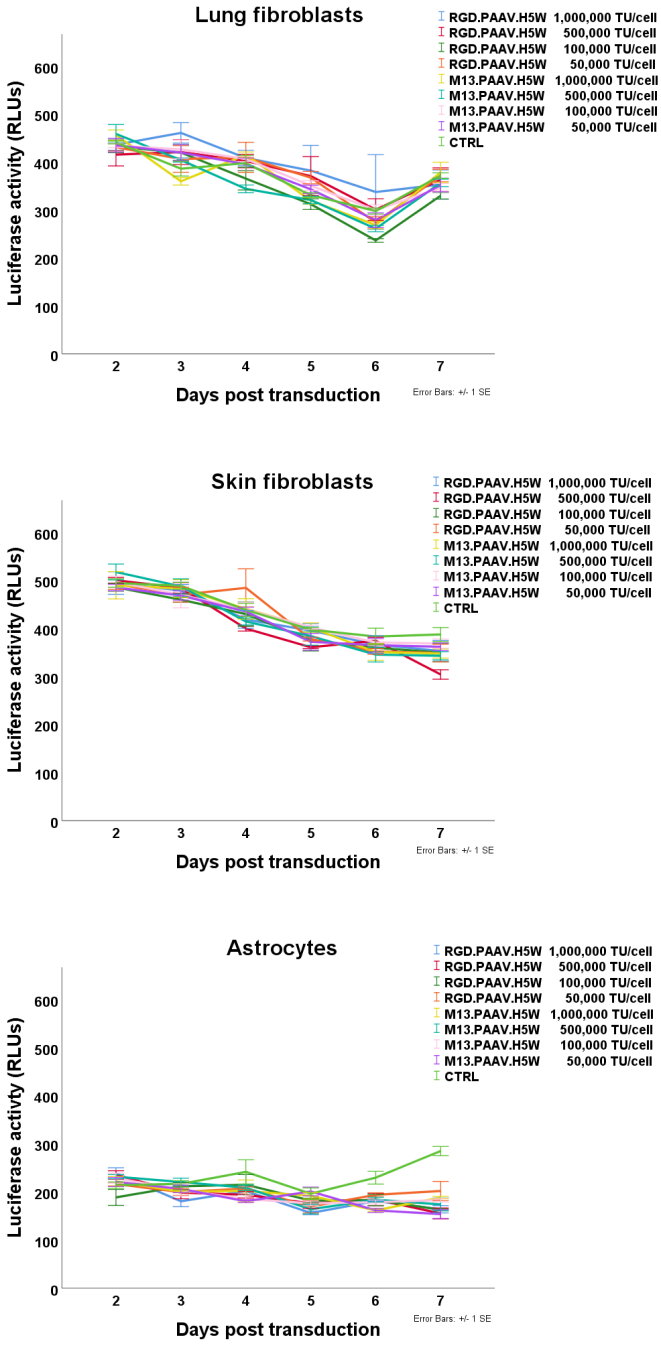

Figure 3.14. Transduction of normal cells (lung fibroblasts, skin fibroblasts and astrocytes) by PAAV vector displaying H5WYG peptide.

The cells were plated in 96-well plate and grown to 60-70% confluence then transduced with targeted PAAV encoding *Lucia* reporter gene and displaying H5WYG peptide (RGD.PAAV.*Lucia*.H5W) or non-targeted PAAV displaying peptide (M13.PAAV.*Lucia*.H5W). Results are shown as mean ± SEM of triplicate wells.

3.2.7. Proton buffer capacity of PAAV vector displaying H5WYG peptide

Proton sponge effect is one of the endosomal escape mechanisms mediated by a protonable agents with high buffering capacity. In previous results, H5WYG peptide showed buffering capacity within natural endosome pH between 6.8-5.1. The peptide is considerately able to induce the proton sponge effect.

To investigate this hypothesis, bafilomycin A1 was applied on PAAV transduction. Bafilomycin A1 is known to inhibit proton sponge mechanism by blocking vacuolar ATPase activity. The transductions were performed at two doses of the vector TU/cell for each cell line. As shown in figure 3.15, Lucia expression mediated by RGD.PAAV.H5W transduction decreased in the presence of bafilomycin A1 on all cell lines (A549, M21 and UW228). The decrease was dependent on the concentration of bafilomycin A1 applied on the transduction. These results suggested that H5WYG peptide mediates endosomal escape of an entrapped vector via proton sponge effect.

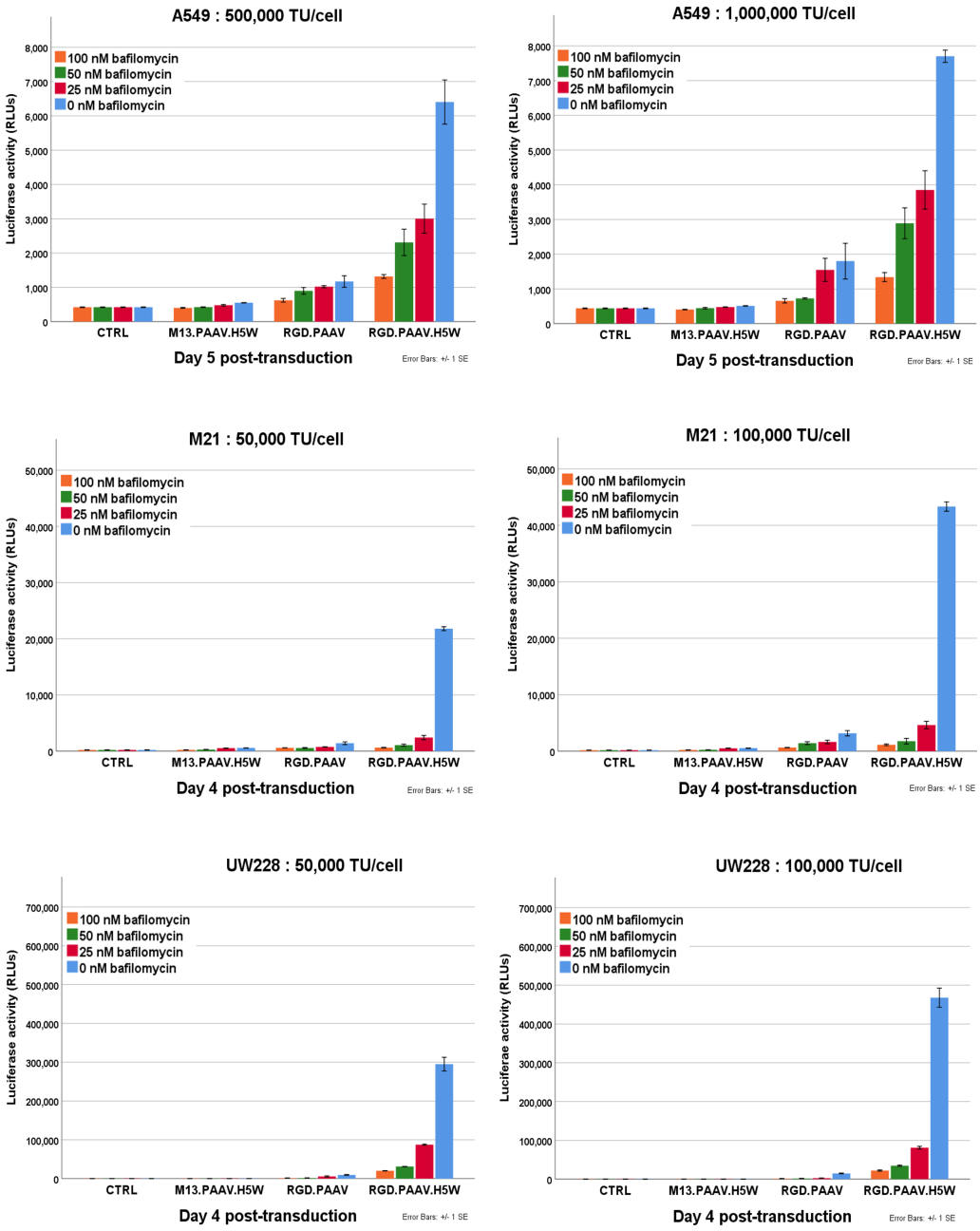

Figure 3.15. Bafilomycin A1 effect on PAAV transduction efficacy.

A549, M21 and UW228 cells were seeded in 96- well plate and grown to 60-70% confluence. The cells were incubated with different concentrations of bafilomycin A1 for 1hr before transducing with RGD.PAAV.*Lucia*.H5W or RGD.PAAV.*Lucia* vector at two different TU/cell. Non-targeted vectors (M13.PAAV.*Lucia*.H5W and M13.PAAV.*Lucia*) were also used as a control. Results are shown as mean ± SEM of triplicate wells of one representative experiment. All experiments were repeated twice.

3.2.8. Enhancement of secreted TNFα expression by H5WYG peptide

To apply the modified PAAV vector in gene therapy, PAAV vector encoding secreted *TNFα* (*sTNFα*) in the genome and displaying H5WYG peptide on major capsid protein was produced with the combination of H5WYG helper phage (RGD.M13.KO7.H5W or M13.KO7.H5W).

A549, M21 and UW228 cells were transduced with targeted PAAV vector encoding *sTNFα* and displaying H5WYG peptide (RGD.PAAV.*sTNFα*.H5W) or targeted vector encoding *sTNFα* without the peptide (RGD.PAAV.*sTNFα*). The cells transduced with non-targeted vectors (M13.PAAV.*sTNFα*.H5W and M13.PAAV.*sTNFα*) and untreated cells were also used as a controls. Cell death was observed under the microscope on day 5 post-transduction for A549 and day 4 post-transduction for M21 and UW228. As shown in figure 3.16, RGD.PAAV.CMV.*sTNFα*.H5W seemed to induce more cell death compared to RGD.PAAV.CMV.*sTNFα* on all three cell lines.

The cell death was then confirmed using a cell viability assay. Firstly, Cell Titer-Glo® assay was applied to measured cell viability based on a quantitation of ATP. Through this assay, RGD.PAAV.CMV.*sTNFα*.H5W showed more efficacious on inducing cell death than RGD.PAAV.CMV.*sTNFα*. There were 0.88, 0.84 and 0.53 fold decrease of cell viability on A549, M21 and UW228, respectively (figure 3.17). Secondly, the cell viability based on cellular protein content was measured by sulphorodamine B assay. The results were found in the same trend as previous results. The cell viability of all three cell lines transduced with PAAV vector displaying H5WYG peptide was significantly lower than the one from the cells transduced with PAAV vector without the peptide (figure 3.18).

These results show that H5WGY peptide is able to enhance secreted TNFα expression leading to an increase of tumour cell death on A549, M21 and UW228 cell line.

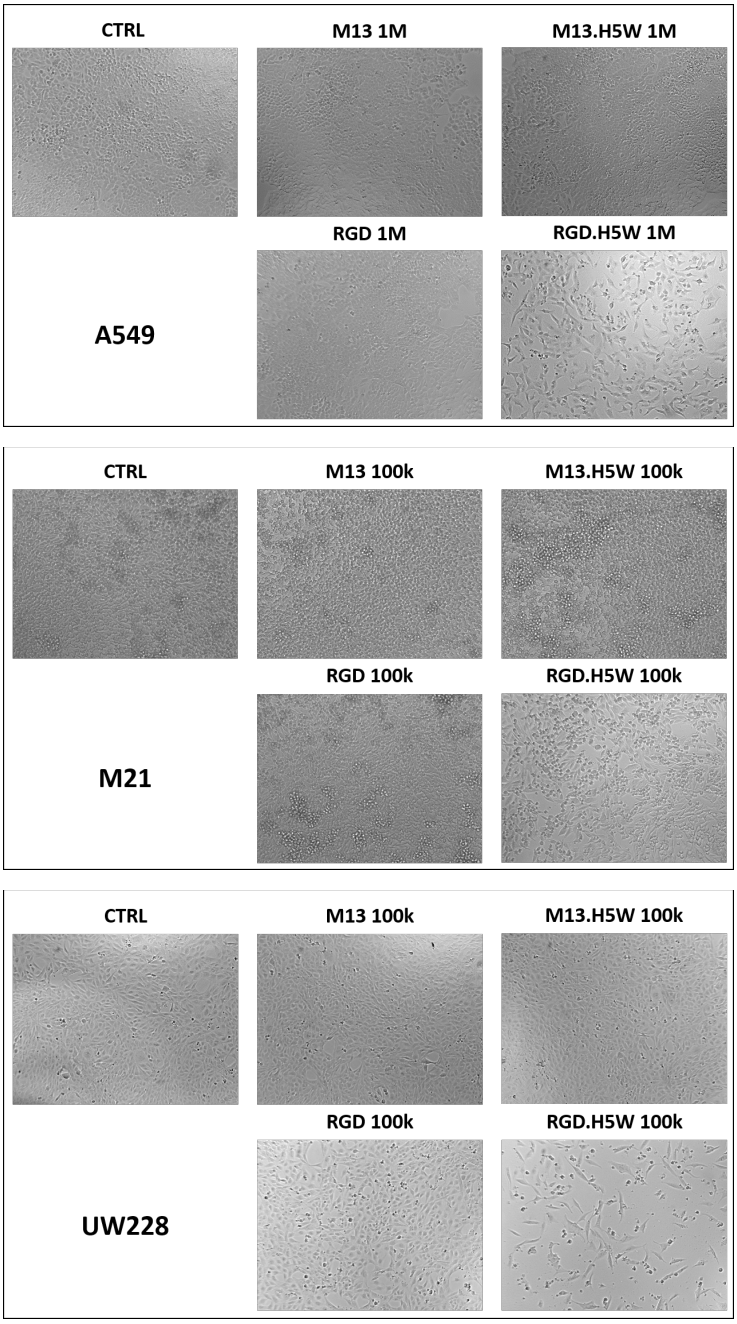

Figure 3.16. Cell death mediated by PAAV vector encoding secreted TNFα.

A549, M21 and UW228 cells were seeded in 96-well plate and allowed to reach 80-90 % confluence. The cells were then transduced with targeted PAAV vector encoding secreted *TNFα* and displaying H5WYG peptide (RGD.PAAV.*sTNFα*.H5W) or targeted vector encoding *sTNFα* without the peptide (RGD.PAAV.*sTNFα*). Non-targeted vectors (M13.PAAV.*sTNFα*.H5W and M13.PAAV.*sTNFα*) were also used as a control. Cell death was observed under live microscope. Images were taken using 10x objective lens.

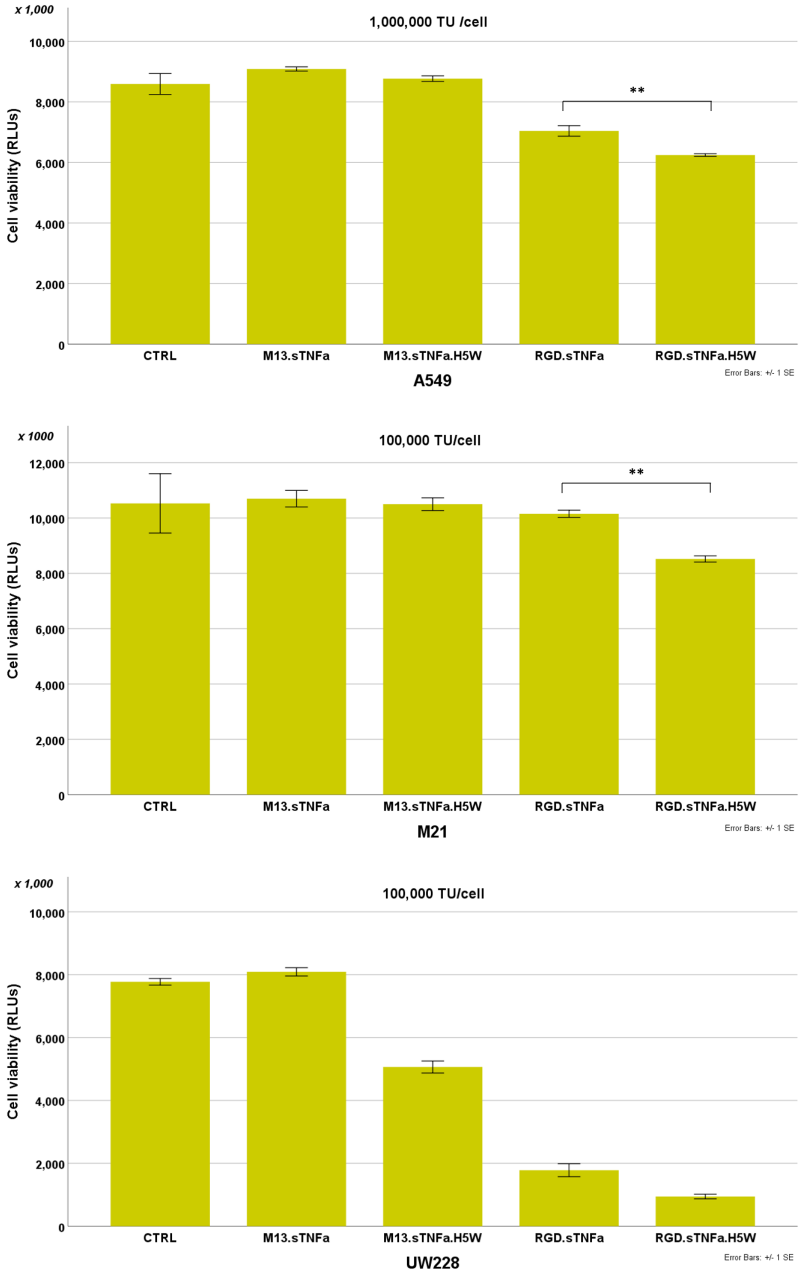

Figure 3.17. Cell viability of A549, M21 and UW228 cells based on ATP quantification.

The cells were plated in 96-well plate at 80-90 % confluence and transduced with RGD.PAAV.CMV.*sTNFα*.H5W, PAAV.CMV.*sTNFα*.H5W, RGD.PAAV.CMV.*sTNFα* or PAAV.CMV.*sTNFα*. Cell viability was assessed by Cell Titer-Glo® assay on day 6 post-transduction. Results were shown as mean ± SEM of triplicate wells of one representative experiment. All experiments were repeated twice. Statistical significance was determined by one-way ANOVA with Tukey's honestly significant difference (HSD) post hoc test. $^{**}p \leq 0.01$.

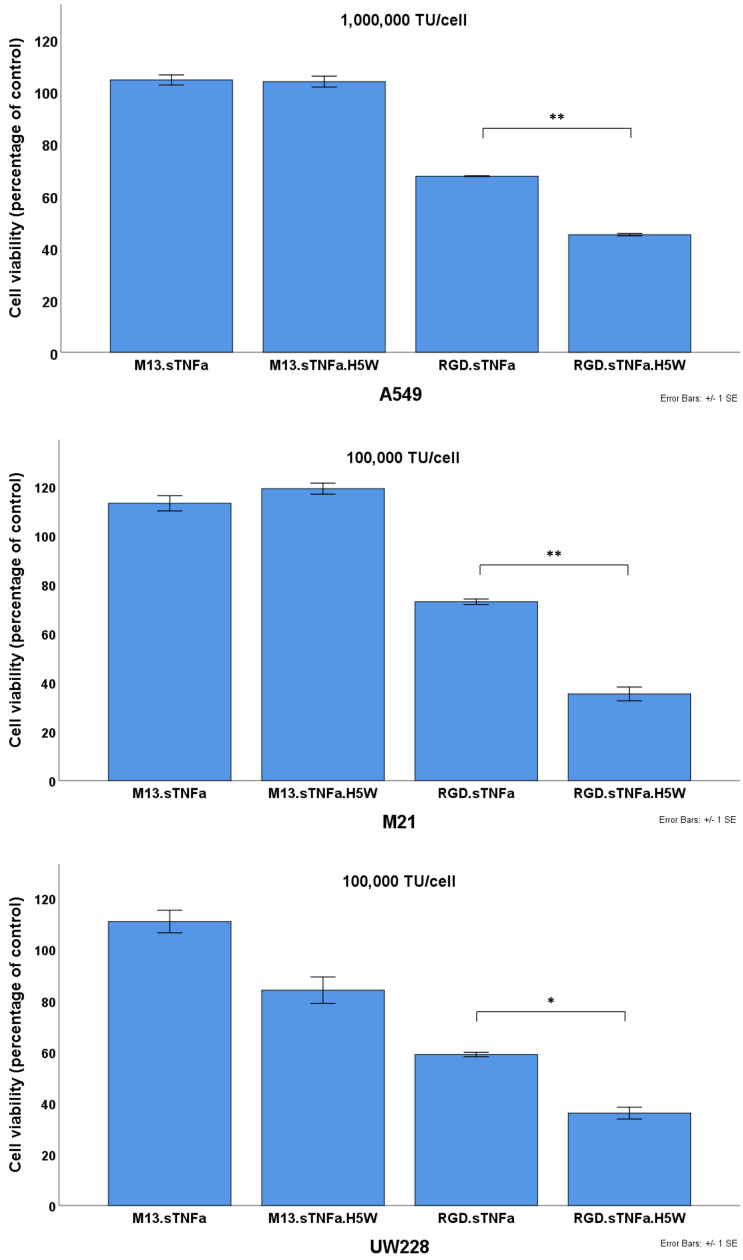

Figure 3.18. Cell viability of A549, M21 and UW228 cells based on cellular protein content.

The cells were in 96-well plate at 80-90 % confluence and transduced with RGD.PAAV.CMV.*sTNFα*.H5W, PAAV.CMV.*sTNFα*.H5W, RGD.PAAV.CMV.*sTNFα* or PAAV.CMV.*sTNFα*. Cell viability was measured by sulphorodamine B assay on day 6 post-transduction. Results are shown as mean ± SEM of triplicate wells of one representative experiment. All experiments were repeated twice. Statistical significance was determined by one-way ANOVA with Tukey's honestly significant difference (HSD) post hoc test. *$p \leq 0.05$, **$p \leq 0.01$.

3.2.9. Preliminary *in vivo* experiment

As reported in previous results, H5WYG peptide proved its potential to enhance gene transfer *in vitro*. Further experiments were designed to investigate the peptide's ability to enhance gene delivery in an animal model. The concept of this experiment is to target the vector encoding a reporter gene to solid tumours. The vector-transduced tumour cells, then, produce reporter proteins that interact with specific substrate and subsequently provide a detectable signal. The capability of H5WYG peptide is investigated by comparing the reporter gene expression mediated by PAAV vector displaying the peptide to the one mediated by PAAV alone.

This experiment was conducted in consistency with the *in vitro* ones using *lucia* reporter gene to assess the vector efficacy. Redi Ject Coelenterazine H bioluminescent substrate (Perkin Elmer) was chosen to monitor PAAV-mediated gene expression by bioluminescence imaging. M21 cells were subcutaneously implanted to immunodeficient CD1 nu/nu mice. Then targeted PAAV vectors with or without H5WYG peptide (RGD.PAAV.*lucia*.H5W or RGD.PAAV.*lucia*) were systemically injected to tumour-bearing mice. The expression was assessed on day 6 post vector injection by subcutaneously received Redi Ject Coelenterazine H substrate and subjected to bioluminescence imaging. The paradigm of the experiment is shown in figure 3.19.

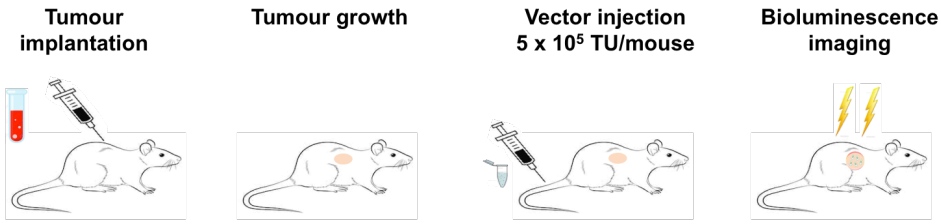

Figure 3.19. *In vivo* experimental plan.

CD1 nu/nu mice were subcutaneously implanted with M21 cells. Tumour-bearing mice were randomly assigned to control group (normal saline), targeted vector (RGD.AAVP.*luciferase*) or targeted vector displaying H5WYG peptide (RGD.AAVP.*luciferase*.H5W). The vectors were systemically injected to each mouse. Luciferase activity was monitored by bioluminescence imaging on day 6 post vector injection.

Unexpectedly, the reporter gene expression was not detected only at the tumour environment but also found from the control mice that did not received PAAV vector. This may cause by the substrate nonspecific background that strongly showed wherever it was injected (figure 3.20A). To confirm this background issue, tumour and organs were collected from the mice, soaked in Redi Ject Coelenterazine H substrate and subsequently subjected to bioluminescence imaging. As shown in figure 3.20B, the signal was found on almost every piece of the tissues including the ones collected from the control mice. On the other hand, another set of tumour and organs were soaked in Quanti-Luc substrate (Invivogen) which is routinely used to monitor lucia expression *in vitro* in our group. There was no signal detected on this set of tissues. These results indicate that neither Redi Ject Coelenterazine H nor Quanti-Luc was a suitable substrate for Lucia reporter gene on this experiment due to its high nonspecific background and not giving a signal, respectively.

To continue on the *in vivo* experiment, the vector encoding luciferase reporter gene is needed. Unfortunately, we did not have PAAV vector with the reporter gene at that moment. In order to construct a vector with new gene, several

cloning steps are required. Due to time constraint, the *in vivo* experiment is set to be performed in the future.

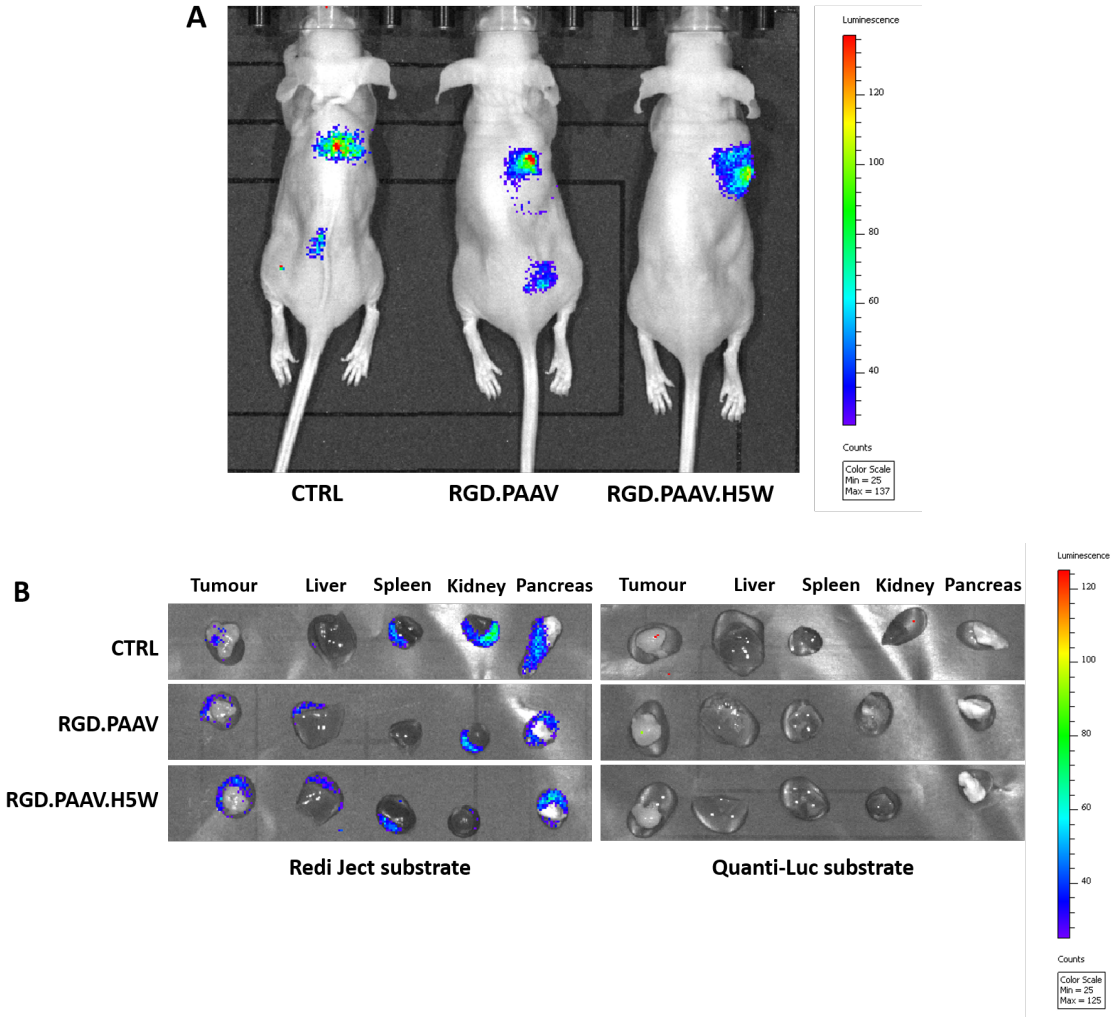

Figure 3.20. *In vivo* bioluminescent imaging of Lucia expression.

The animals were subcutaneously inoculated with M21 cells. Targeted vector encoding *Lucia* reporter gene and displaying H5WYG peptide (RGD.PAAV.*Lucia*.H5W) or targeted vector encoding the reporter gene without the peptide (RGD.PAAV.*Lucia*) were intravenously injected to the mice when the tumour was noticable. The reporter gene expression was assessed on day 6 post vector injection. **A** The mice were subcutaneously injected with Redi Ject Coelenterazine H bioluminescent substrate and subjected to bioluminescence imaging. **B** The mouse tumour and organs were collected and soaked in Redi Ject Coelenterazine H or Quanti-Luc substrate. The expression was assessed by bioluminescence imaging.

3.3 Discussion

PAAV is a hybrid bacteriophage vector constructed by adding AAV sequence into filamentous bacteriophage genome. The vector was modified to display RGD4C ligand on pIII capsid protein allowing it to specifically target to tumour cells through a binding of the ligand and $\alpha_v\beta_3$ and/or $\alpha_v\beta_5$ integrin receptor on the tumour cell surface. Although PAAV has already proved its efficacy on driving a desirable gene expression, the vector can be further modified. Considering endosomal degradation issue that almost all of the vectors encounter, it would be very helpful to pay more attention on facilitating the vector escape out of endosomes. Therefore, PAAV was additionally engineered to display endosomal escape peptide called H5WYG on recombinant pVIII capsid protein.

Because PAAV vector is designed as a phagemid-based hybrid system, genetic elements for structural proteins were decoupled from the vector genome. All the capsid proteins for vector propagation are provided from filamentous helper phage. Thus, *H5WYG* sequence was genetically inserted into the helper phage genome instead of PAAV vector genome. The modification resulted in a longer genome of the new helper phage encoding *H5WYG* sequence together with *recombinant pVIII* sequence compared to the non-modified helper. The helper phage was subsequently characterised for its morphology by TEM. The results were found consistent to the genome length as the modified helper particle displaying H5WYG peptide was slightly longer in size than the particle without the peptide. This is a consequence of the longer genome of the modified helper that elongates its particle. However, an incompatible outcome was found when characterising PAAV vector morphology. In spite of having the same genome, PAAV particle displaying H5WYG peptide was shorter in size compare to the original PAAV particle. According to phage display system [244], the filamentous bacteriophage vector displaying two types of pVIII capsid protein contains two sets of gene VIII in its genome. One is recombinant gene capable of bearing a foreign sequence and another one is wild type gene. As recombinant gene *VIII* is synthetic and differs from wild type gene, this might result in slight differences between the recombinant and wild type pVIII molecules. Considering molecular

weight of each type of pVIII, one subunit of recombinant pVIII consisting of 69 amino acid residues weighs 7.25 kilodaltons while each wild type pVIII with 73 residues weighs 7.63 kilodaltons. These two types of pVIII capsids are displayed in a mosaic manner on the vector in which recombinant pVIII capsids are around 12% of all pVIII subunits. Those 12% recombinant pVIII subunits which are smaller in size than the wild type ones may shorten the PAAV particles displaying H5WYG peptide.

It has been suggested that the hybrid vectors internalise via clathrin-mediated endocytosis and resides in endosomes where it is subsequently degraded by digestive enzymes. Incorporating H5WYG peptide to PAAV vector is considered to facilitate it escape from endosomal degradative pathway. To confirm the theory, an acidic-based titration was set in relevant to the situation during endosome maturation when endosomal pH is gradually decreased by an influx of cytosolic protons. A relatively promising outcome was found from this experiment as PAAV vector displaying H5WYG peptide showed greater buffering capacity than the vector without the peptide. The buffering capacity is believed to be a key point of endosomal escape through proton sponge mechanism mediated by a protonation of histidyl residues. As histidines have pK_a between 5.6-6, they are protonated at slightly acidic condition during endosomal acidification. The protonation leads to conformational change of the peptide and its specific interaction to destabilise endosomal membrane. This conformational change was confirmed by Alipour *et al.* whose peptide-based vector fused with H5WYG peptide showed a drastic change of secondary structure from non-structural to helical conformation at low pH [241].

PAAV vector is modified to target tumour cells via a binding of RGD4C ligands with $\alpha_v\beta_3$ and/or $\alpha_v\beta_5$ integrin receptors on tumour cell surface. Therefore, three chosen tumour cell lines (A549, M21 and UW228) were assessed their suitability for being targeted by the vector. The cells were initially checked α_v, β_3 and β_5 integrin expression. All three integrin receptors are highly expressed on A549 and UW228 cell surface confirming that they are suitable for PAAV vector targeting. To serve as a target receptor for RGD4C ligand, $\alpha_v\beta_3$ and/or $\alpha_v\beta_5$

heterodimeric receptors are formed by the obligation of the α- and β-subunits [245]. Tumour cells expressing either $\alpha_v\beta_3$ or $\alpha_v\beta_5$ receptors on their cell surface are specifically targeted by RGD4C-PAAV. Thus, M21 expressing high level of α_v and β_5 but slightly low level of β_3 integrin receptor are still considered as a suitable target for the vector.

The suitability was confirmed by the transduction of PAAV encoding *Lucia* reporter gene at various transduction units. The Lucia expression was firstly detected on day 2 post vector transduction, reached the highest expression around day 4-5 depending on the cell line and fell down after day 5 as the cells were over confluent and started to die. Among all cell lines, HEK293 cells showed the greatest transduction efficacy of PAAV vector whereas non-specific transducing was also detected. It is very well known that HEK293 cells are permissive for transfection and capable of processing post-translational modification of both mammalian and non-mammalian nucleic acids. These make it very convenient to detect an effective transduction and high protein yields on this cell line [246, 247]. Within three tumour cell lines, A549 seem to be the most difficult one to be transduced as they showed a relatively low expression of PAAV-mediated Lucia compare to M21 and UW228 cell lines. As an alveolar type II derived cell line, A549 is considered to produce surfactant proteins which are primarily essential for maintenance and protection of lung alveoli. [248]. Unfortunately, the surfactants turn to be a major physical barrier because nanoparticles are coated with the surfactants [249]. This is believed to reduce PAAV transduction efficacy on this cell line.

In term of safety issue, nanoparticles are expected to remain specificity on their targets only. In this case, PAAV vector is considered to specifically target tumour cells via RGD4C ligand and integrin complex without harming healthy tissues. To ensure that, the vector was transduced to lung fibroblasts, skin fibroblasts and astrocytes which were chosen as normal cell models related to A549, M21 and UW228 tumour models. Although the normal cells were reported for their minimal expression of α_v, β_3 and β_5 integrin receptors [36], they were not able to be transduced successfully by PAAV vector. The transduction was performed up

to 3 million transduction units but no expression of PAAV-mediated Lucia was detected between day 1 and day 7 post-transduction. This genuinely confirms the vector specificity on tumour cells but not normal cells.

H5WYG peptide enhanced transduction efficacy of the vector at different levels depending on the cell lines. The peptide seemed to have an effect on the vector specificity when the transduction was performed at very high dose. Therefore, lower transduction unit, below 100,000 TU/cell, would be recommended when working on permissive cell lines such as UW228. Although H5WYG peptide insignificantly decreased the PAAV specificity on some permissive tumour cells, the peptide did not affect the safety issue on normal cells. The transduction of PAAV vector displaying the peptide did not mediated any gene expression on the chosen normal cells. Thus, displaying the peptide on PAAV vector is able to enhance the vector transduction efficacy on tumour cells but remain safe on normal cells.

The capacity of H5WYG peptide relies on proton sponge mechanism to facilitate the vector out of endosome. As mentioned before, all histidyl residues of the peptide are protonated resulting in conformational change of the peptide and subsequently destabilises endosomal membrane. The protonated histidyl residues also relate to an excessive influx of cytosolic proton, counter-ions and water which induce endosomal membrane swelling. These processes eventually cause membrane rupture and release the entrapped PAAV vector into cytosol. Thus, PAAV vector can carry out its function and enhance gene expression. The transduction experiment in the presence of bafilomycin A1 confirmed that H5WYG peptide is able to mediate proton sponge effect. As a specific inhibitor of vascuolar ATPase, bafilomycin A1 stops an inflow of cytosolic proton by blocking V-ATPase activity during endosomal maturation. According to that, histidyl residues of the peptide are not protonated keeping the peptide in non-structural conformation and not interact with endosomal membrane. As the membrane remains intact, the vectors are entrapped inside endosome and not able to complete their biological function. Thus, a decrease of PAAV-mediated gene expression was found in dose dependent of bafilomycin A1 concentration.

H5WYG peptide shows a promising capacity on enhancing gene transfer in many studies. Polyethylene glycol-based vehicles conjugated with H5WYG peptide showed pH-dependent membrane lytic activity at mild acidic condition and transfection efficiency of the vehicles increased when coupled with the peptide [107]. Asseline *et al.* conjugated H5WYG to antisense oligonucleotides and found an increase of the fluorescein-labelled oligonucleotides in cytosol and nuclease [239]. The oligonucleotide-mediated luciferase activity at mRNA and protein level increased at 6.6 and 2 folds when H5WYG was applied. H5WYG peptide was also conjugated to peptide-based nanocarrier and significantly enhanced its transfection efficiency [241]. According to the literatures and all results mentioned before, it is challenging to apply the peptide to therapy. In this chapter, sTNFα was chosen to investigate H5WYG peptide capacity on augmenting sTNFα-mediated cell death. PAAV encoding sTNFα and displaying the peptide was produced and tested on A549, M21 and UW228 cell lines. The results were found in consistency with previous experiments as more cell death was detected in cells transduced with vector displaying H5WYG peptide. Relatively to Lucia expression, UW228 showed more cell death than A549 and M21 as they are more permissive than the others.

Because of the luciferase substrate issue stated before, we have not completed an *in vivo* investigation of the new vector yet. However, there was a similar experiment performing with the old version of the hybrid vector called AAVP. The old vector is encoding the reporter gene in its genome and displaying H5WYG peptide on recombinant pVIII coat protein, in the same pattern as PAAV is. Although AAVP is considered less efficient in gene delivery than PAAV, it is capable of mediating a detectable luciferase expression. Comparing to the vector without the peptide, AAVP displaying H5WYG mediated higher gene expression and maintained the expression level for a longer period of time (unpublished data). This proved the peptide capability on enhancing gene delivery. However, similar *in vivo* experiment with targeted PAAV.*luciferase* will be performed to show a proof of concept that PAAV vector displaying H5WYG peptide can augment gene transfer in animal models.

All results in this chapter confirm that the vector displaying H5WYG peptide appears to be a promising gene delivery tool with higher transducing efficacious but remains safe in normal cells. The modified vector can be useful in a number of applications in the field of gene transfer. Additionally, our hybrid vector is designed as a targeted delivery system against cancer cells. The previous version vector, AAVP, is successfully targeted to various pre-clinical human tumour models such as melanoma, pancreatic cancer and brain tumours [32-35, 37, 38]. Altogether the bacteriophage hybrid vector with H5WYG peptide is considered a powerful tool with high specificity for targeted gene delivery on both *in vitro* and *in vivo*. The vector can be beneficial for cancer gene therapy as it is already shown in this chapter that it enhances tumour cell death mediated by secreted TNFα.

In summary, H5WYG peptide shows its buffering capacity at slight acidic condition. When displaying the peptide on recombinant pVIII capsid protein of PAAV, it increases vector-mediated gene expression. Due to its protonated histidines, H5WYG peptide facilitates the vector escape from endosomal degradation via proton sponge effect which causes endosomal membrane destabilisation and rupture. The peptide also enhances therapeutic effect of *sTNFα* which is beneficial for cancer therapy and shows a promising outcome in *in vitro* experiments.

Chapter 4

Augmentation of tumour-associated antigen expression by a hybrid bacteriophage vector

4.1 Introduction

CAR T cell therapy is one approach of cancer immunotherapy that relies on the efficiency of the specific T lymphocytes (T cells). The T cells are collected from the patients and genetically modified to express chimeric antigen receptors (CAR) on their cell surface. The receptors allow the modified T cells to target a specific extracellular antigen of tumours after re-administrating into the same patients. Unlike other adaptive cell transfer strategies, CAR T cell therapy does not require a peptide-MHC matched manner. The modified T cells can recognise the specific target antigen on the tumour cell surface and eventually destroy tumour cell through cytotoxic T cell mediated process. Although, CAR T cell therapy is considered as a one-time treatment that are able to maintain the therapeutic effect for a decade after the modified T cell injection, further research is required to investigate long-term effect of the therapy. Moreover, stable expression of the target antigen is essential for the therapeutic impact [173, 250].

CAR T cells are able to recognise a broad types of antigens expressed on tumour cell surface, ranking from proteins, carbohydrates to glycolipids [251, 252] Identification of a suitable antigen is a crucial step for this therapy. The ideal antigen is expected to be specifically expressed on tumour cells but not on normal cells. To gain more therapeutic benefit, the antigen should be indispensable for tumour cell survival [253] Recently, several tumour-associated antigens have been identified and undergone clinical trials, for example, CD19 and CD20 for hematological malignancies, CEA for metastatic colorectal cancer,

EGFRvIII for glioblastoma [254], ERBB2 for colon cancer metastasized to the lung and liver, GD2 for relapsed neuroblastoma, GPC3 for gastrointestinal cancer, Mesothelin for metastatic pancreatic cancer, MUC1 for metastatic seminal vesicle cancer, and PSMA for metastatic or recurrent prostate cancer [253]. Despite a number of identified tumour-associated antigens, the current research mainly focuses on the antigens that preferentially expressed on certain types of tumours. There is no such a universal antigen capable to serve as a target for all tumour types yet [253].

CAR T cell strategy has been developing over decades and is now being clinically tested on diverse tumour types [255]. Although it is proposed as a treatment for various types of liquid and solid tumours, the breakthrough in this field of study was yet achieved in only B cell hematologic tumours. There are two FDA approved CAR T cell products, KYMRIAH (tisagenlecleucel) [256] and YESCARTA (axicabtagene ciloleucel). These two strategies are based on anti-CD19 modified T cells for B-cell precursor acute lymphoblastic leukemia (B-ALL) and certain type of large B-cell lymphoma, respectively [257]. Despite the current success in haematological tumours, the full effectiveness of CAR T cell therapy in solid tumours is challenging. Some antigens such as ERBB2, Mesothelin and CEA have been clinically tested on a number of subjects. Unfortunately, none of evaluable outcome from any of them have been reported yet [258].

There are several major considerations for the CAR T cell therapy such as CAR T cell architecture which requires complex techniques and intensive time, the modified T cell efficiency on each tumour types, as well as, the natural barriers at tumour microenvironment. Beside those challenges, the availability of target antigen with sufficient expression and the loss of tumour-associated antigen on tumour cell surface are ones of the obstacles in this field [258]. As mentioned before CAR T cells are currently engineered against particular antigens expressed on certain types of tumour. Some antigens are expressed on many tumour types but at different expression levels. For example, MUC1 is highly expressed on breast and lung cancer cells but a lesser extent is found in hematopoietic cells [259]. Although, CAR T cells are claimed to efficiently

recognise the specific antigen at a marginal expression, the therapeutic impact could be augmented by increasing the antigen expression level. In addition, regarding the safety and efficacy concerns of CAR T cells, new generation of these cells are currently under investigation focusing on the selective targeting. T cells are engineered to express two CARs to ensure a double recognition of two specific antigens expresses on the same tumour cells [258, 260]. Despite achieving a better specificity, a range of target tumour cells expressing two antigens at the same time is narrowing down. In this case, it would be very helpful if the two specific antigens are artificially expressed on the same tumour cells. Beyond the lack of targetable antigen issue, the antigen loss within the tumours is another concern for CAR T cell therapy. Due to their genomic instability, tumour cells are generally heterogeneous resulting in a diverse collection of cells harbouring different molecule signatures. The cells might express new distinct molecules and/or lose other molecules including CAR-targeted antigen [133, 261]. By losing the antigen, tumour cells become invisible to CAR T cells. According to this, there is a need to retrieve the antigen expression on tumour cells.

The aim of this chapter is to overcome the antigen-loss and the lack of targetable antigen issues mentioned above. PAAV vector is applied as a delivery tool to maximise an expression level of selected antigens on tumour cells. Mucin1 (MUC1) and prostate-specific membrane antigen (PSMA) are chosen as targeted antigens. Either *MUC1* or *PSMA* gene is encoded in the genome of PAAV vector and being delivered to be expressed on tumour cells. According to the National Cancer Institute, MUC1 and PSMA were ranked as the second and the eleventh promising antigen of 75 tumour associated antigen [262]. MUC1 represents as an ideal target for CAR T cell therapy because of these following three factors. First, it is overexpressed on most solid tumours. Second, the form of MUC1 expressed on tumour cells is different from the one expressed on normal cells. This prevents off target on the normal cells expressing MUC1. Third, the polarity of tumour associated MUC1 is lost allowing the tumour cells to be more accessible to CAR T cells. PSMA is selected as a target antigen because of its large extracellular domain that serves as an excellent target for the therapy, as well as,

its overexpression on the neo-vasculature of most solid tumours. Additionally, these two antigens are the common target antigens for CAR T cell therapy with positive preclinical outcome.

Although CAR T cells were not applied in this chapter, this strategy is considered useful for the applications with CAR T cell therapy. Technically, T cells are harvested from patient and genetically modified to express CAR on their cell surface. While expanding the modified T cells expressing CAR, the patient can receive PAAV vectors encoding target antigen compatible to the CAR T cells. The vector will target to tumours in the patient and generate or enhance the antigen expression on tumours making them more visible for CAR T cells. After that the patient will be re-infused with CAR T cells which recognise and destroy the tumours expressing PAAV-mediated specific antigen. Furthermore, this strategy is able to applied in any tumour types expressing αβ integrin receptors and also used with dual CAR T cells which recognise two specific antigens expressing on the same tumour cells.

With the aim to augment the expression of target antigen for CAR T cell therapy, a series of experiments were conducted as follow. Firstly, *MUC1* and *PSMA* sequences were genetically inserted into the PAAV genome. Secondly, the transduction efficacy of PAAV encoding *MUC1* or *PSMA* gene was optimised on HEK293 and U87 cells to investigate the optimal time of MUC1 and PSMA expression after vector transduction. Thirdly, cationic derivative (DEAE-dextran) was applied to PAAV transduction to enhance the PAAV-mediated MUC1 or PSMA expression. Fourthly, three different tumour cell types were chosen, namely A549, a common model of non-small cell lung cancer usually being reported for chemoresistance; Suit-2, a pancreatic cancer with high metastatic capability and UW228, a common paediatric brain tumour originated in the cerebellum. The PAAV-mediated MUC1 and PSMA expression on tumour cells was assessed both at mRNA and protein level.

4.2 Results

4.2.1. Optimisation of MUC1 and PSMA expression delivered by PAAV vectors encoding *MUC1* or *PSMA* genes

HEK293 cells were cultured in 48-well plate and allowed to grow until reaching 70% confluency. The transduction was performed with 1 million transduction unit per cell (TU/cell) of either targeted vector (RGD4C.PAAV.*MUC1*) or non-targeted vector (M13.PAAV. *MUC1*) carrying *MUC1* gene. The expression was measured on day 4 and day 6 post transduction by fluorescence-activated cell sorting (FACs). As shown in figure 4.1A, the expression of MUC1 was marginally detected on day 4 and slightly increased on day 6 post transduction (figure 4.1B). There was no MUC1 expression detected on the cells treated with non-targeted vectors.

To optimise PAAV-mediated PSMA expression, HEK293 cells were transduced with either 1 million TU/cell of targeted vectors (RGD4C.PAAV.*PSMA*) or non-targeted vectors (M13.PAAV.*PSMA*) carrying *PSMA* gene. Although there was no PSMA expression detected on day 4 post vector transduction (figure 4.1C), the expression increased significantly on day 6 post transduction (figure 4.1D).

Similar experiments were also performed on human glioblastoma (U87). MUC1 and PSMA expression was detected in relevant to those found in HEK293 cells. MUC1 expression was barely detected on day 4 (figure 4.2A) and slightly increased on day 6 post vector transduction (figure 4.2B). There was a slight expression of MUC1 on the cells treated with non-targeted vectors. Despite no PSMA expression detected on day 4 post transduction (figure 4.2C), the slight expression was found on day 6 as shown in figure 4.2D.

These data indicate specificity and efficacy of RGD4C.PAAV vector to mediate MUC1 and PSAM expression to the target cells. The expression of both antigens was appropriately detected on day 6 post vector transduction.

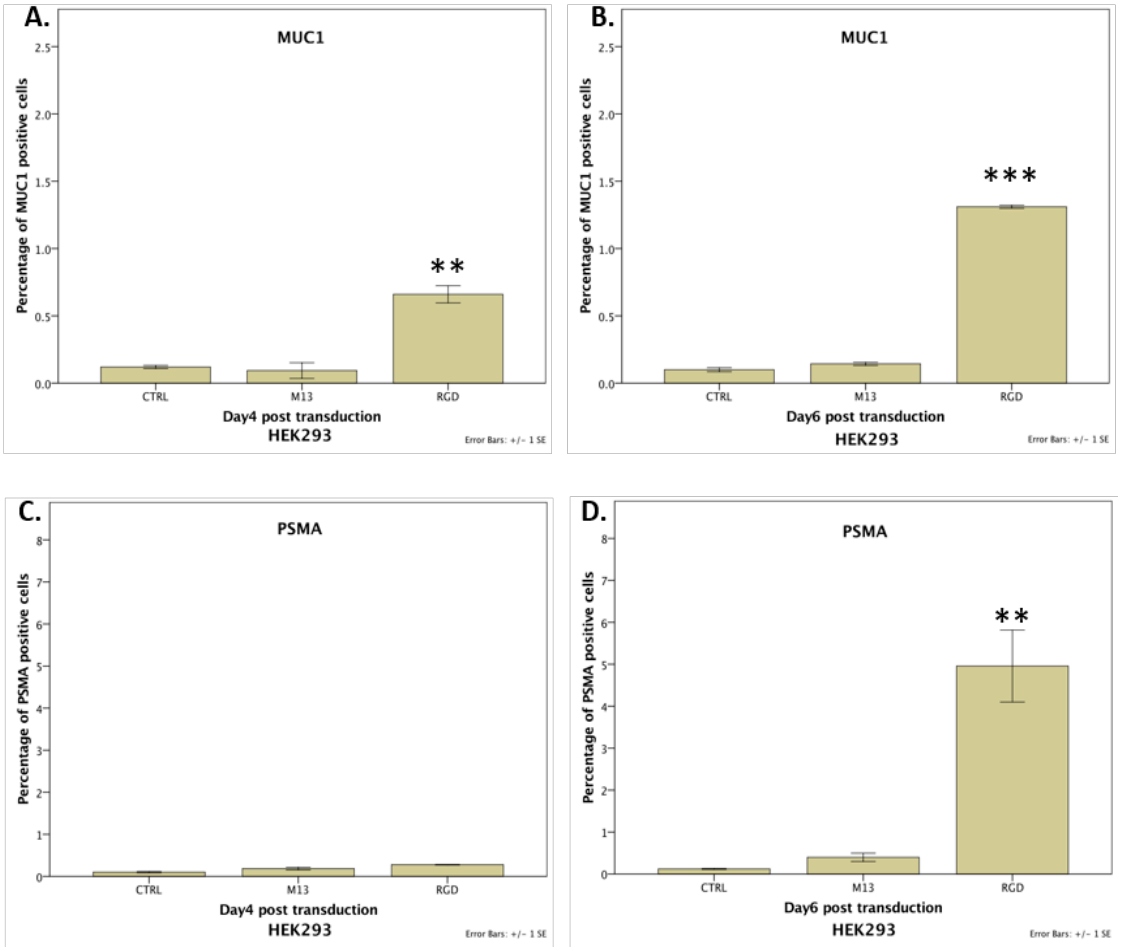

Figure 4.1. Optimisation of MUC1 and PSMA expression in HEK293 cells.

HEK293 were seeded in 48-well plate and transduced with 1 million TU/cell of either RGD4C.PAAV.*MUC1*, M13.PAAV. *MUC1*, RGD4C.PAAV.*PSMA* or M13.PAAV.*PSMA*. The cells were collected on day 4 and 6 post-transduction. The expression was measured by flow cytometry and analysed by FlowJo software. Data are represented as mean ± SEM of triplicate wells. The experiment was repeated twice.

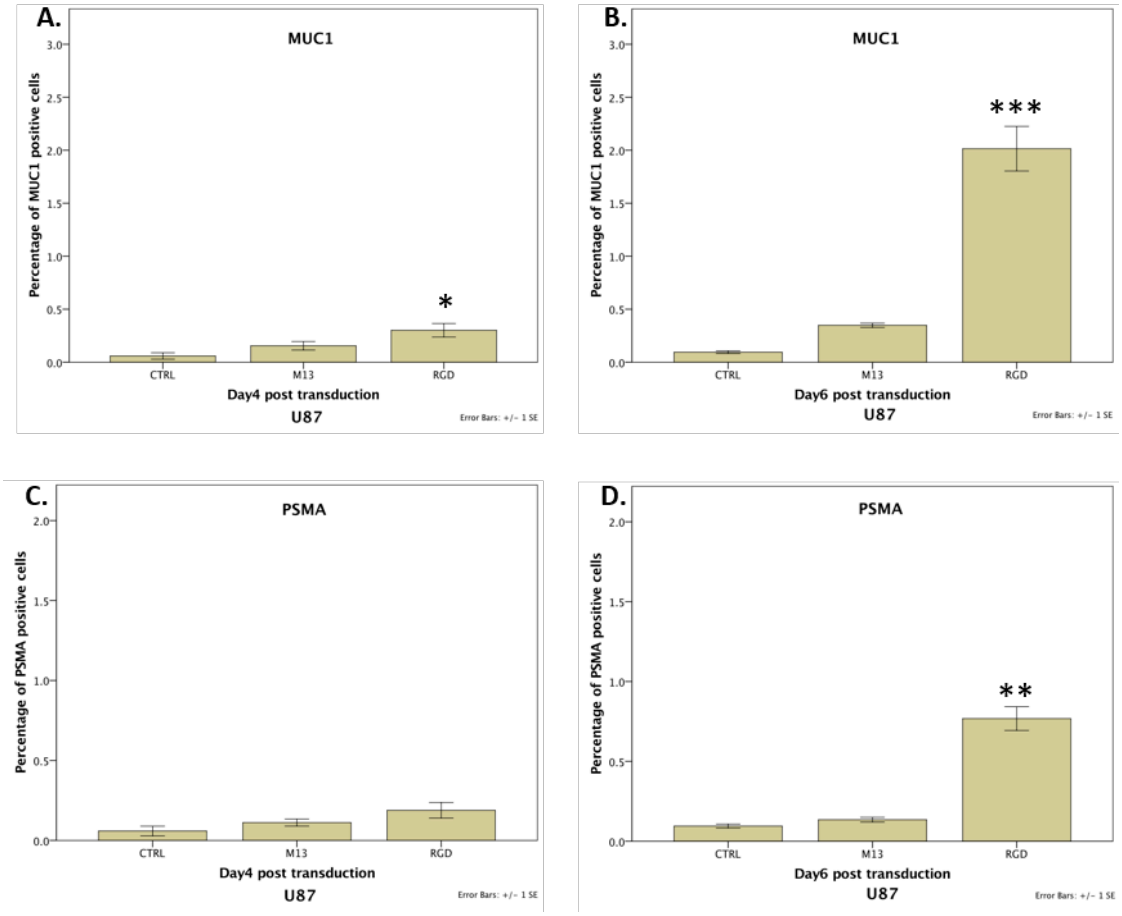

Figure 4.2. Optimisation of MUC1 and PSMA expression in U87 cells.

U87 were seeded in 48-well plate and treated with 1 million TU/cell of either RGD4C.PAAV.*MUC1*, M13.PAAV. *MUC1*, RGD4C.PAAV.*PSMA* or M13.PAAV.*PSMA*. The cells were collected on days 4 and 6 post-transduction. The expression was measured by flow cytometry and analysed by FlowJo software. Data are represented as mean ± SEM of triplicate wells. The experiment was repeated twice.

4.2.2. Enhancement of MUC1 and PSMA expression by DEAE-dextran

To enhance expression of MUC1 and PSMA, DEAE-dextran was applied at 60 ng/ug protein of the vectors when performing PAAV transduction.

HEK293 cells at 70% confluent in 48-well plate were transduced with 1 million TU/cell of either RGD4C.PAAV.*MUC1*, M13.PAAV.*MUC1*, RGD4C.PAAV.*PSMA* or M13.PAAV.*PSMA*. As shown in figure 4.3A and 4.3B, PAAV-mediated MUC1 expression when using DEAE-dextran was significantly higher than the one without DEAE-dextran on both day 4 and day 6 post vector transduction. Expression of PSMA was found in a similar trend to MUC1 expression. An increase of PAAV-mediated PSMA expression was achieved when applying DEAE-dextran to the vector transduction. However, it is important to note that a significant non-specific uptake mediated by non-targeted vector was found on both days 4 and day 6 post transduction when using DEAE-dextran.

Similar investigation was done on M21 cells, there was no expression of either MUC1 or PSMA shown when transduction was performed without DEAE-dextran. The expression of both antigens increased significantly when DEAE-dextran was applied without any non-specific uptake of non-targeted vectors detected (figure 4.3E and 4.3F).

The data indicate that DEAE-dextran is able to enhance the transduction efficiency with a concern of non-specific uptake in particular cell lines.

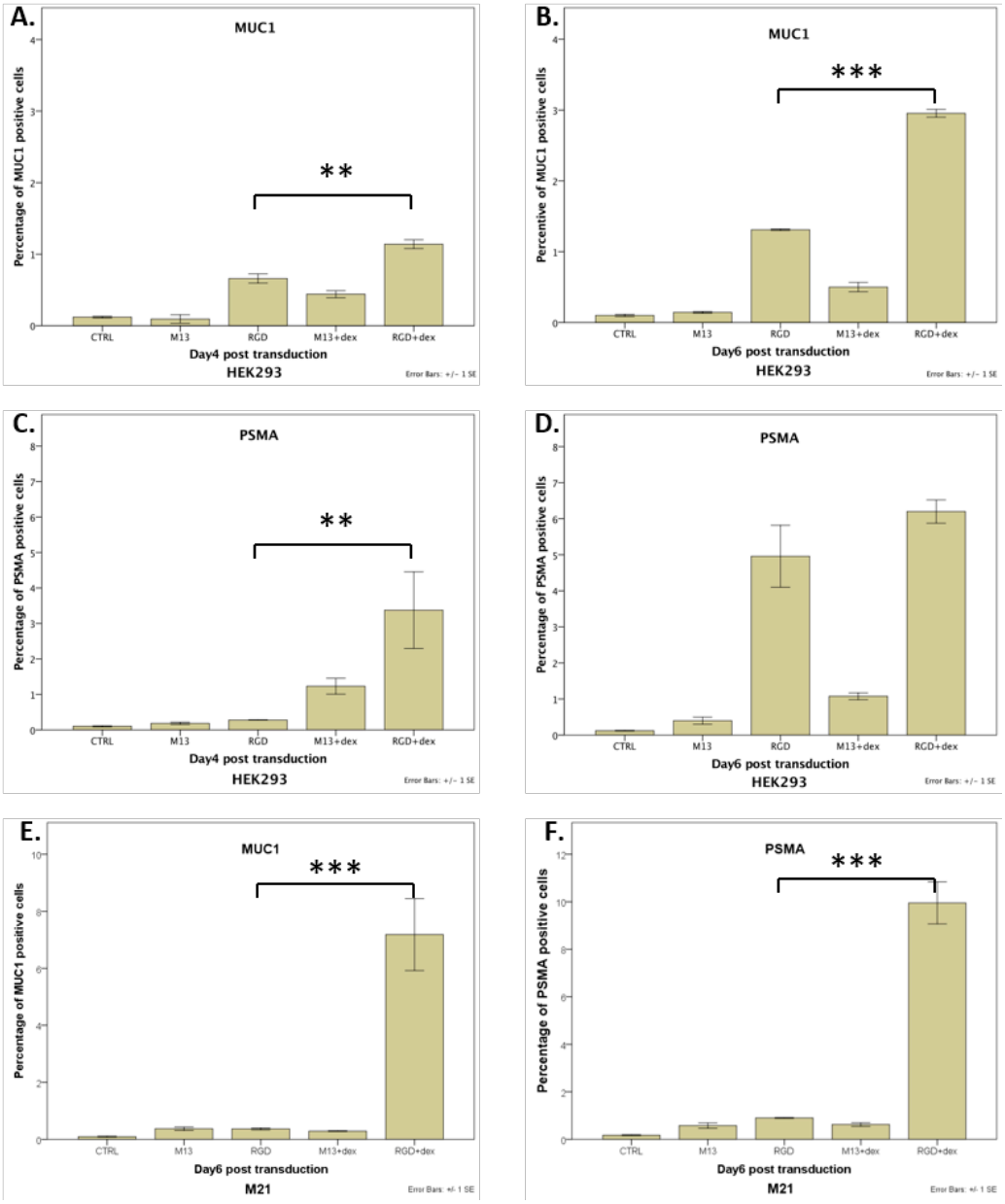

Figure 4.3. Enhancement of MUC1 and PSMA expression by DEAE-dextran.

HEK293 and M21 cells were seeded in 48-well plate and transduced with 1 million TU/cell of either RGD4C.PAAV.*MUC1*, M13.PAAV. *MUC1*, RGD4C.PAAV.*PSMA* or M13.PAAV.*PSMA*. DEAE-dextran was applied at concentration of 60 ng/ug protein of the vectors. The HEK293 cells were collected on days 4 and 6 post-transduction. M21 were collected on day 6 post-transduction. The expression was measured by flow cytometry and analysed by flowjo. Data are represented as mean ± SEM of triplicate wells. The experiment was repeated twice.

4.2.3. MUC1 and PSMA expression mediated by PAAV plasmid transfection

In this chapter, A549, Suit2 and UW228 cells were chosen as representative models of lung, pancreatic and brain tumours, respectively. Before performing PAAV vector transduction, the cells were transfected with either PAAV.*MUC1* or PAAV.PSMA plasmids to confirm the plasmid functionality in these three cell lines.

To assess *MUC1* and *PSMA* expression at mRNA level, the cells seeded in 6-well plate were transfected with PAAV plasmids. mRNA from the cells was collected on day 1 post transfection. *GAPDH* mRNA expression was measured as internal control. As shown in figure 4.4, *MUC1* and *PSMA* expression at mRNA level were significantly detected in A549, Suit2 and UW228 cells.

To confirm expression at the protein level, the cells were seeded in 48-well plate and transfected with either PAAV.*MUC1* or PAAV.PSMA plasmids. The expression was measured on day 3 post-transfection. Non-transfected cells were included to represent endogenous expression of MUC1 or PSMA. Higher levels of MUC1 and PSMA expression were detected in cells transfected by PAAV plasmid compared to their endogenous expression. The augmented expression of MUC1 and PSMA was found on the three cell lines except MUC1 expression in Suit2 detected at the same expression level of endogenous expression (figure 4.5).

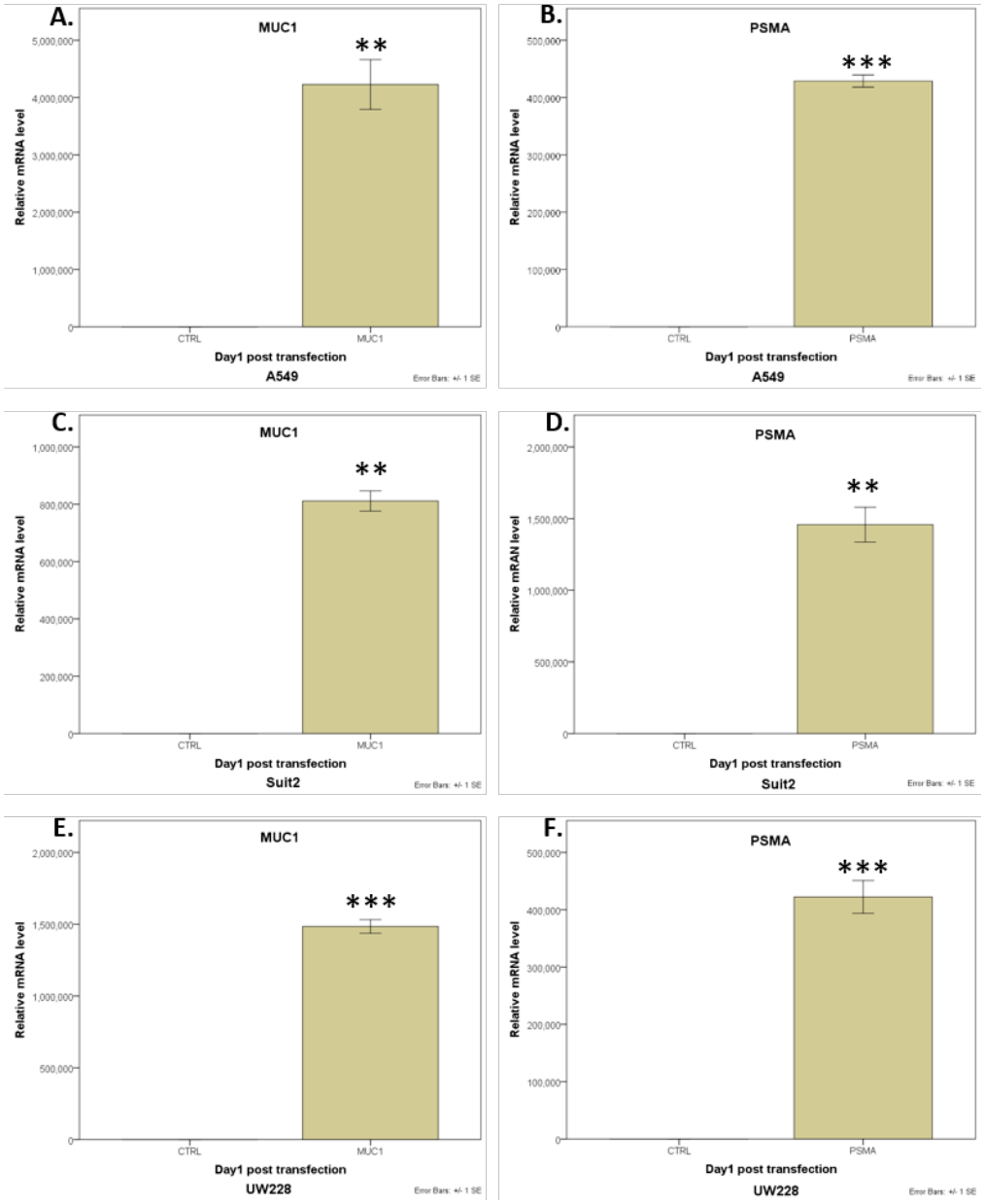

Figure 4.4. MUC1 and PSMA mRNA expression mediated by PAAV plasmid.

The cells were seeded in 6-well plate and transfected with either PAAV.*MUC1* or PAAV.PSMA plasmids. The mRNA was collected on day 1 post-transfection. *GAPDH* mRNA expression was measured as internal control. Data are represented as mean ± SEM of triplicate wells. The experiment was repeated twice.

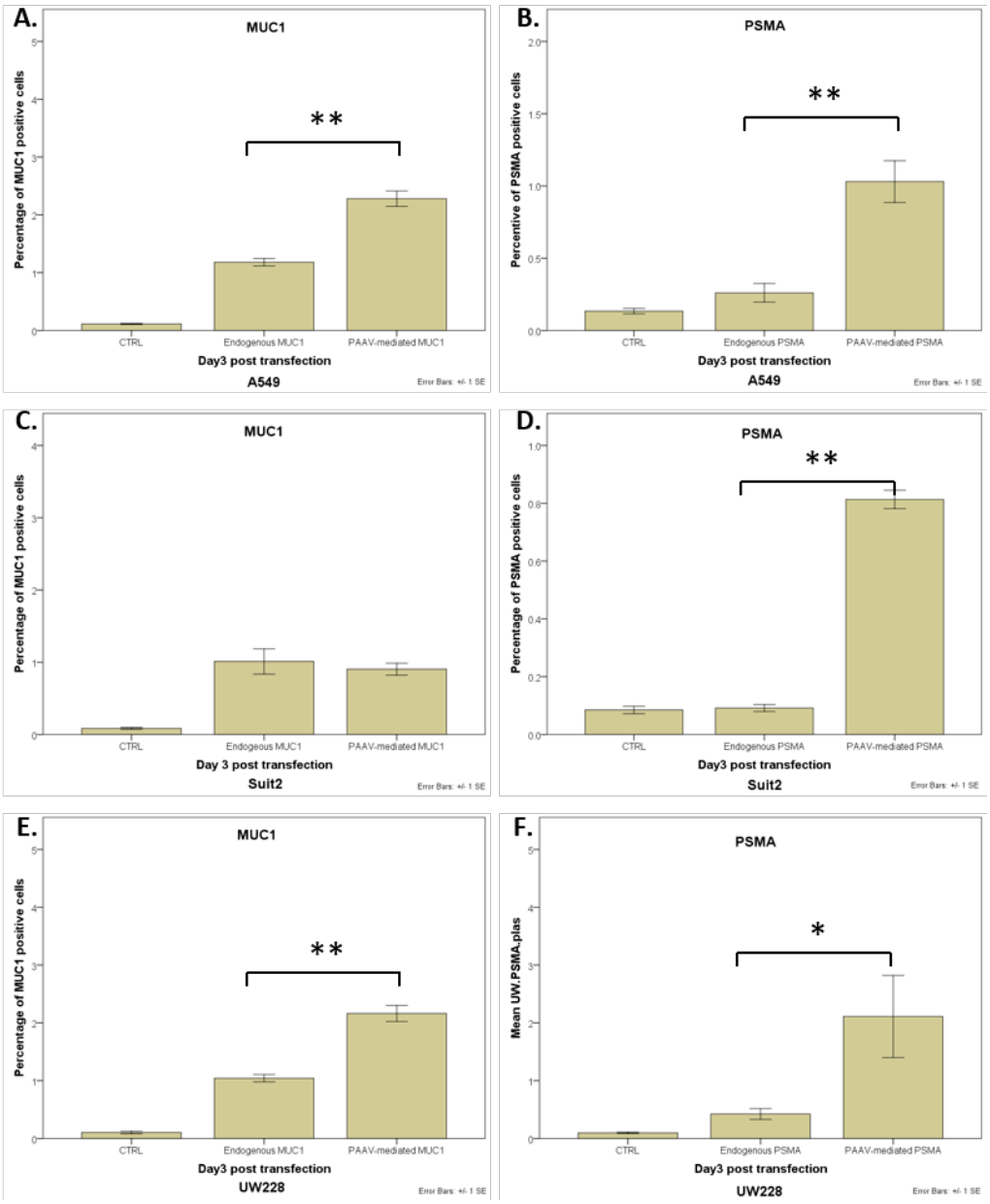

Figure 4.5. Protein expression of MUC1 and PSMA mediated by PAAV plasmid transfection.

The cells were seeded in 48-well plate and transfected with either PAAV.*MUC1* or PAAV.*PSMA* plasmid. The cells were collected on day 3 post-transfection. Non-transduced cells were included to show endogenous expression. The expression was measured by flow cytometry. The results were analysed by FlowJo software. Data are represented as mean ± SEM of triplicate wells. The experiment was repeated twice.

4.2.4. mRNA expression of MUC1 and PSMA mediated by PAAV vector transduction

To assess MUC1 and PSMA expression at mRNA level, the cells seeded in 6-well plates were transduced with 1 million TU/cell of either RGD4C.PAAV.*MUC1*, M13.PAAV.*MUC1*, RGD4C.PAAV.*PSMA* or M13.PAAV.*PSMA*. mRNA from cells were collected on day 3 post-transduction. *GAPDH* mRNA expression was measured as internal control.

Similar results were found on the three chosen cell lines, A549, Suit2 and UW228. *MUC1* and *PSMA* expression was significantly detected in cells transduced with RGD4C.PAAV.*MUC1* or RGD4C.PAAV.*PSMA*. The slight expression was found in cells transduced with M13.PAAV. *MUC1* or M13.PAAV.*PSMA* due to non-specific uptake (figure 4.6).

4.2.5. Protein expression of MUC1 and PSMA mediated by PAAV vector transduction

In addition to mRNA expression analyses, MUC1 and PSMA expression at protein level was confirmed by flow cytometry. The cells were transduced with 1 million TU/cell of either RGD4C.PAAV.*MUC1*, M13.PAAV. *MUC1*, RGD4C.PAAV.*PSMA* or M13.PAAV.*PSMA*. The expression was measured on day 6 post vector transduction. Non-transduced cells were included to show MUC1 or PSMA endogenous expression.

On A549, as shown in figure 4.7A, PAAV-mediated MUC1 expression was detected at the same level of endogenous MUC1 expression while PSMA expression mediated by PAAV was detected at 2.7 times higher than its endogenous expression (figure 4.7B). There was no MUC1 or PSMA expression detected in cells transduced with non-targeted vectors.

In UW228 cells, MUC1 and PSMA expression mediated by PAAV was detected at 2.4- and 2.25-fold higher compared to its endogenous expression, respectively.

There was no expression of MUC1 or PSMA detected in cells transduced with non-targeted vectors (figure 4.7C and 4.7D).

On Suit2, MUC1 expression mediated by PAAV was slightly higher than its endogenous expression (figure 4.8A). In contrast, PAAV-mediated PSMA expression was barely detected (figure 4.8B). However, it was still higher than the endogenous PSMA expression. To achieve higher expression of MUC1 and PSMA, DEAE-dextran was applied at 60 ng/ug protein of the vectors when performing transduction. As shown in figure 4.8C and 4.8D, this enhanced both MUC1 and PSMA expression with a slight non-specific MUC1 expression detected in cells transduced with non-targeted vectors.

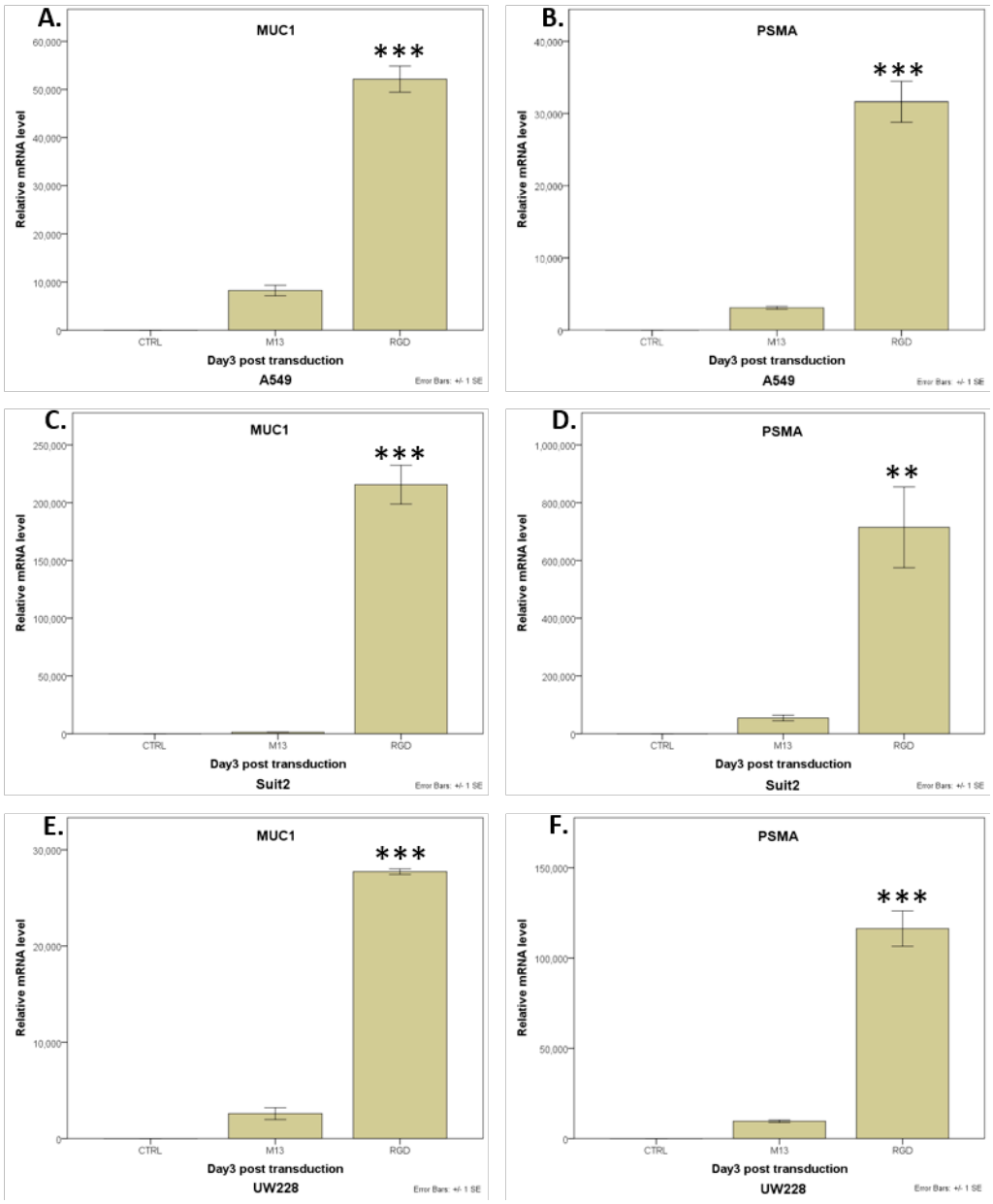

Figure 4.6. mRNA expression of MUC1 and PSMA in A549, Suit2 and UW228 cells.

The cells were seeded in 6-well plate and transduced with 1 million TU/cell of either RGD4C.PAAV.*MUC1*, M13.PAAV.*MUC1*, RGD4C.PAAV.*PSMA* or M13.PAAV.*PSMA*. The mRNA from cells was collected on day 3 post-transduction. *GAPDH* mRNA expression was measured as internal control. Data are represented as mean ± SEM of triplicate wells. The experiment was repeated twice.

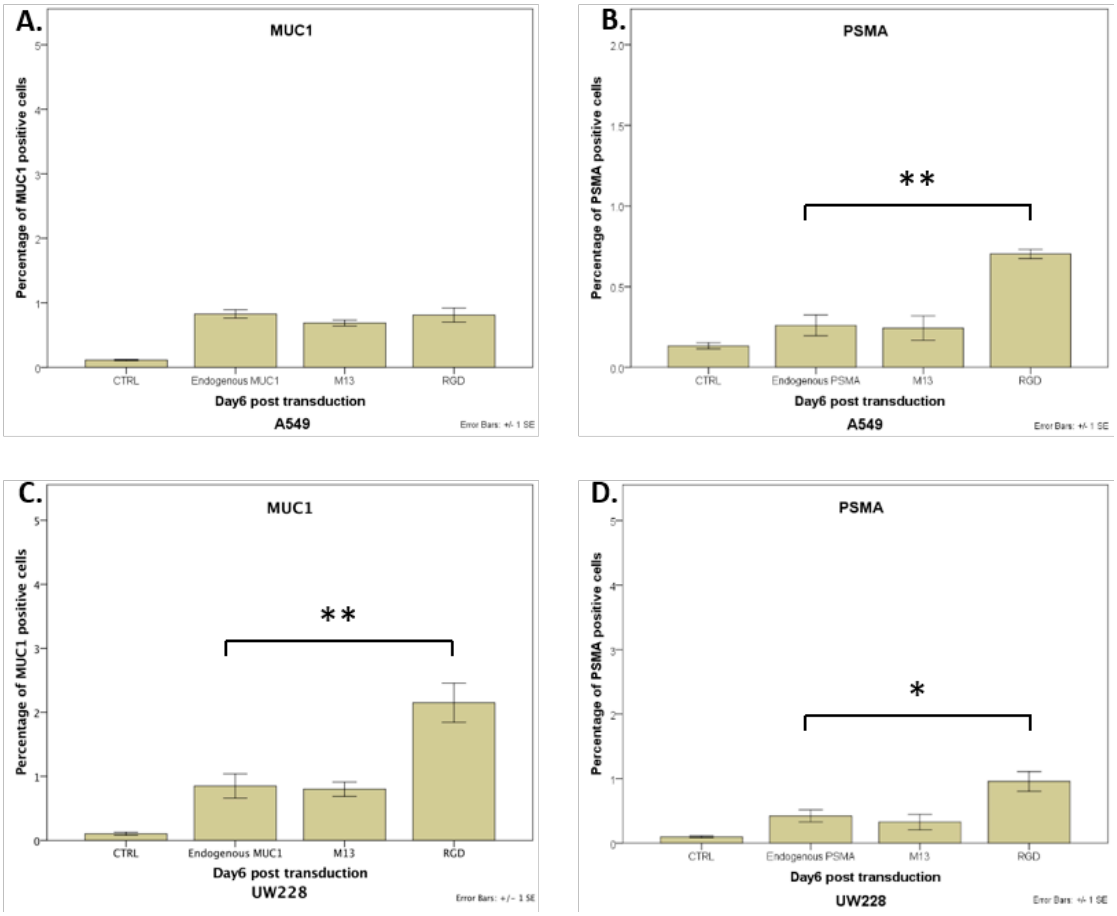

Figure 4.7. Protein expression of MUC1 and PSMA in A549 and UW228 cells.

The cells were seeded in 48-well plate and transduced with 1 million TU/cell of either RGD4C.PAAV.*MUC1*, M13.PAAV. *MUC1*, RGD4C.PAAV.*PSMA* or M13.PAAV.*PSMA*. The cells were collected on 6 post-transduction. Non-transduced cells were included to show endogenous expression. The expression was measured by flow cytometry. The results were analysed by FlowJo software. Data are represented as mean ± SEM of triplicate wells. The experiment was repeated twice.

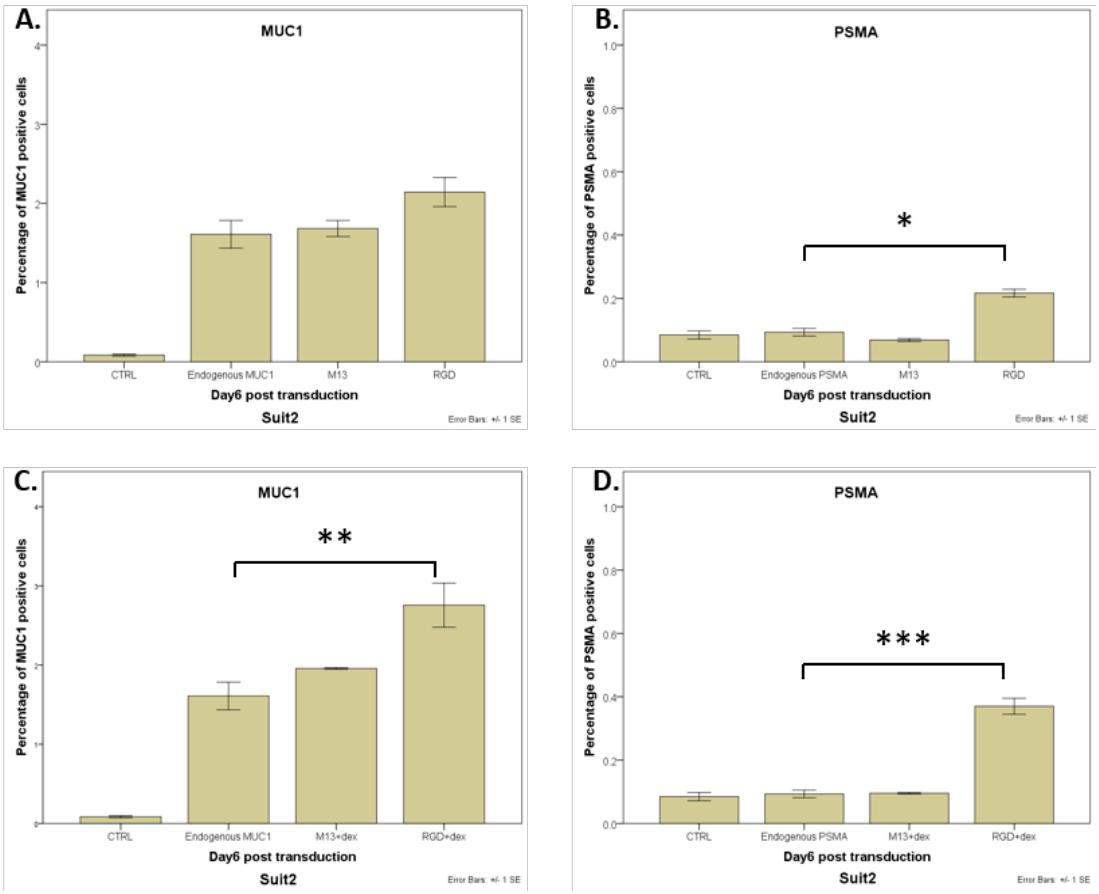

Figure 4.8. Protein expression of MUC1 and PSMA in Suit2 cells.

The cells were seeded in 48-well plate and transduced with 1 million TU/cell of either RGD4C.PAAV.*MUC1*, M13.PAAV. *MUC1*, RGD4C.PAAV.*PSMA* or M13.PAAV.*PSMA*. The cells were collected on day 6 post-transduction. Non-transduced cells were included to show endogenous expression. The expression was measured by flow cytometry. The results were analysed by FlowJo software. Data are represented as mean±SEM of triplicate wells. The experiment was repeated twice.

4.2.6. PAAV-mediated stable MUC1 and PSMA expression with puromycin selection.

Although a high mRNA expression of MUC1 and PSMA were detected in all three cell lines, the protein expression of both antigens were not appropriately achieved did not reach a desired level. Thus, an experiment with puromycin selection was set to confirm that PAAV vectors are able to mediate MUC1 and PSMA expression. In order to select the cells that are stably expressing MUC1 or PSMA, puromycin resistant gene was genetically inserted in to PAAV.*MUC1* or PAAV.*PSMA* plasmids. The new plasmids were called PAAV.*MUC1.Puro* and PAAV.*PSMA.Puro*. The cells were then transduced with 1 million TU/cell of either RGD.PAAV.*MUC1.Puro* or PAAV.*PSMA.Puro*. Puromycin was added to the cell culture to select the PAAV-transduced cells.

With puromycin selection, MUC1 and PSMA expression increased in all three chosen cell lines. In A549 cells, PAAV-mediated MUC1 expression was found at 3-fold higher compared to endogenous MUC1 expression (figure 4.9A). Similarly, PAAV-mediated PSMA expression was 3.5-fold higher than its endogenous expression as shown in figure 4.9B. In Suit2, PAAV-mediated MUC1 expression was slightly 1.5 higher (figure 4.9C) while PAAV-mediated PSMA expression was significantly detected at 4 times higher than its endogenous expression (figure 4.9D). Lastly, in UW228, the expression of MUC1 and PSMA mediated by PAAV was significantly detected in the cells. PAAV-mediated MUC1 and PSMA expression was 3.9- and 85-fold, higher than its endogenous expression, respectively (figure 4.9E and 4.9F).

These data indicate that PAAV vector is capable to mediate MUC1 and PSMA expression in A549, Suit2 and UW228 cells.

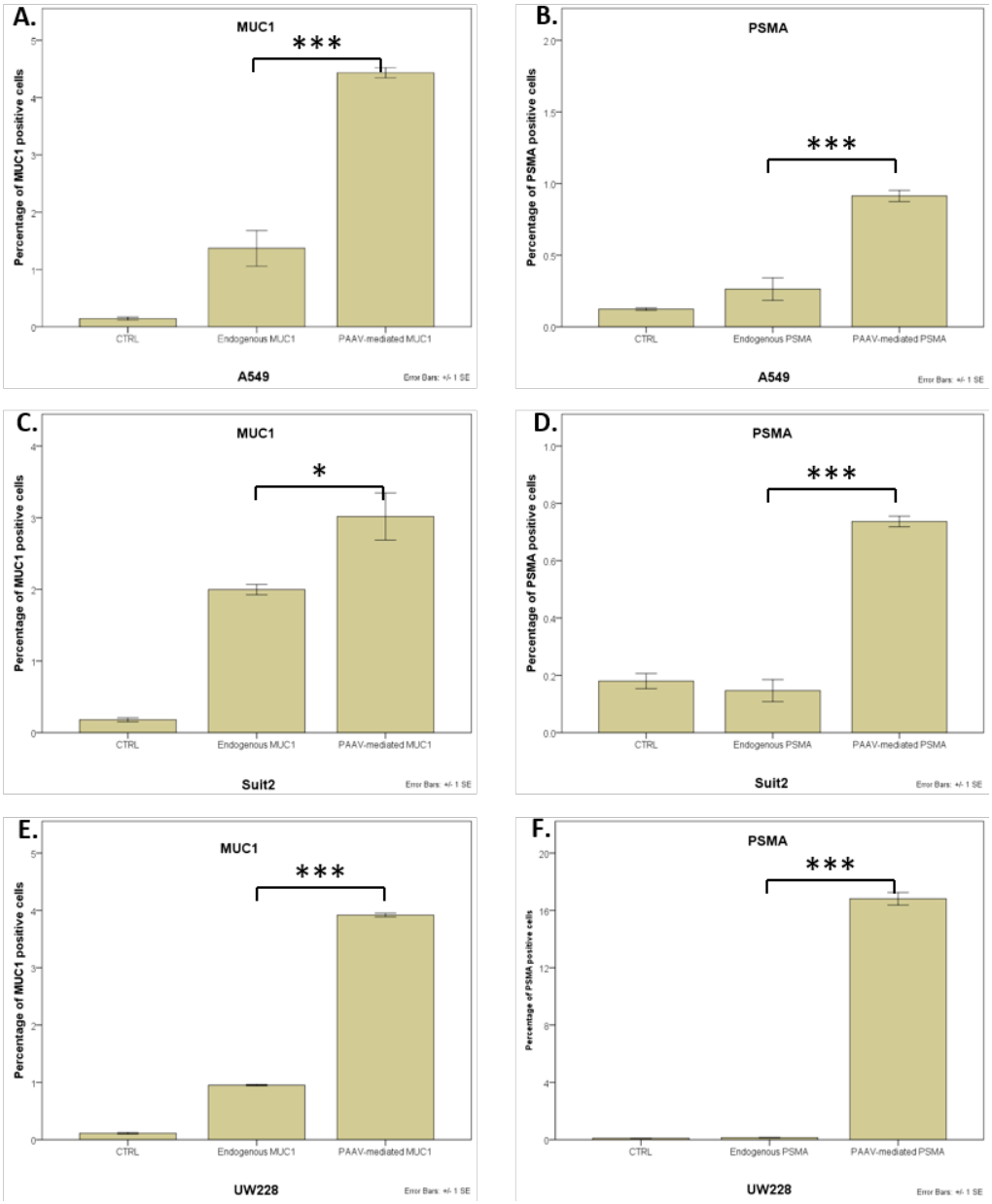

Figure 4.9. Stable expression of MUC1 and PSMA in A549, Suit2 and UW228 cells.

The cells were transduced with 1 million TU/cell of either RGD.PAAV.*MUC1.Puro* or PAAV.*PSMA.Puro*. The stably MUC1 or PSMA expressed cells were selected by applying puromycin. The expression was measured by flow cytometry. Non-transduced cells were included to represent endogenous expression. The results were analysed by FlowJo software. Data are represented as mean ± SEM of triplicate wells. The experiment was repeated twice.

4.3 Discussion

As mentioned in previous chapter, PAAV-mediated luciferase expression mostly reached the peak on days 4 or day 5 then started to drop on day 6 post vector transduction. With slightly different, the expression of MUC1 and PSMA was barely detected on day 4 but significantly higher on day 6 post-transduction.
The efficiency of the detecting method could be the reason behind these differences. By adding a specific substrate, coelenterazines, even a marginal luciferase expression level on early days of the transduction can be sensitively detected and provides intense signals. In contrast, in order to detect MUC1 and PSMA expression, their optimal expression levels and specific antibodies are required. In this study, two anti-MUC1 and anti-PSMA antibodies were used, and almost three months of time were spent to optimise the protocol. Although HMFG2, anti-MUC1 antibodies produced in John Maher group, and anti-PSMA monoclonal antibody from MBL showed better efficiency to detect MUC1 and PSMA expression, the satisfactory expression level of both antigens on tumour cells was not achieved. MUC1 and PSMA expression on day 8 post-transduction was also investigated in HEK293 and U87 cells (data not shown), unfortunately, the cells were over confluent and started to die. Thus, there was too much debris but very low number of cells with MUC1 and PSMA expression detected when applied to flow cytometry. Splitting the cells on days 5 or 6 before apply to the machine on day 8 post-transduction might solve this problem.

Adding cationic polymers, DEAE-dextran, can enhance vector-mediated MUC1 and PSMA expression. These positively charged polymers act as linkers between the negative charges on phage capsids and tumour cell membrane. When DEAE-dextran is applied during the transduction, a complex of PAAV-vector and DEAE-dextran, which can be observed under the microscope, is formed. The complex provides a stronger binding between cell membrane and the vectors, as well as, facilitates vector escape from the endosomal-lysosomal degradation in the cells leading to a better transduction efficiency. Despite the enhancement of gene expression, it is worth to note that DEAE-dextran slightly decreased the vector

specificity. Optimisation for different concentrations of DEAE-dextran would be performed on individual cell line [263]

CAR T cell therapy relies on the activity of the modified T cells through recognition of extracellular antigen expressing on tumour cells. Although the identification of target antigens is an essential step for CAR T cell therapy, their optimal expression level on tumour cells contributes to the success of the therapy. As shown in the results section, MUC1 and PSMA expression mediated by PAAV vector are higher than their endogenous expression. This would enhance the therapeutic impact. Also, PAAV genome is capable of accommodating more than one gene of interest. The vector is able to deliver two target antigens to be expressed on the same tumour cells. This would be very helpful for the dual targeting of CAR T cell approach. Regarding other problems of CAR T cell therapy, the antigen-loss might be responsible for the failure in this field of study, and should not be ignored. Some target antigen such as a splice variant of epidermal growth factor receptor (EGFRvIII) is identified as an ideal target antigen for glioma cells due to its specific expression and vital role for the cell survival. However, EGFRvIII loss within the tumours was reported in some treated subjects [264]. PAAV as an antigen delivery tool is expected to overcome antigen-loss issue caused by tumour heterogeneity. The vector specifically mediate antigen expression in tumour cells, as long as, the cells express αβ heterodimer integrins. The desire expression level can be maintained by a repeatable administration of the vector. To gain more therapeutic benefits, PAAV is also targeted to angiogenic blood vessels which are one central factor for tumour progression. With the dual targeting, the vector-mediated antigens are expressed both on tumour cells and angiogenic blood vessels and serve as dual targets for CAR T cells. This would provide a synergistic killing effect and enhance the therapeutic impact. Moreover, by using PAAV vector as a delivery tool, the most promising target antigen can be delivered to be expressed in a broad range of tumour types without any requirement of endogenous expression. This raises a hope on a universal antigen which can be artificially expressed on all tumour types and serves as a target for universal CAR T cell therapy.

It is significantly shown in this chapter that PAAV-mediated antigen expression is higher than its endogenous expression. However MUC1 and PSMA protein expression are still considered as low level. An increasing expression is detected when puromycin selection was used; unfortunately, this strategy can not apply in an actual therapy. An alternative strategy would be considered to increase PAAV-mediated antigen expression. To achieve a better result, PAAV-vector can be further modified by displaying endosomal escape peptide, H5WYG, on its capsids. It is believed that the modification would augment an antigen expression on tumour cells. Although this strategy has not been performed in this chapter, it is considered as a practical approach which should be beneficial of CAR T cell therapy.

This chapter was initially planned for three main experimental parts, to assess antigen expression mediated by PAAV vectors, to produce anti-MUC1 and anti-PSMA CAR T cells and to compare CAR T cell-mediated tumour regression between PAAV-transduced tumour cells and the non-transduced ones. To produce CAR T cells, Non-Clinical Issue (NCI) application for human T cells purchasing was submitted to NHS Blood & Transplant (NHSBT) committee. According to the Human Tissue Authority's Codes of Practice, a Research Ethics Committee (REC) approval for the use of human tissue is required in order to get human T cells. Unfortunately, our group does not have the ethical approval and it generally takes time to get an approval. Thus the experiments have not continued for further investigations. However, we have shown proof of concept that PAAV vector serves as a good system for antigen delivery and can augment antigen expression in various solid tumour types. This would be useful for CAR T cell therapy.

In conclusion, it is illustrated in this chapter that PAAV vector can mediate antigen expression in HEK293, U87, M21, A549, suit2 and UW228. This could light shade for CAR T cell therapy in treating solid tumours.

Chapter 5

New strategy of bacteriophage-guided cancer vaccination in combination with malaria vaccine

5.1 Introduction

Since principal knowledge of cancer and the immune system has been linked together in the past decades, cancer immunotherapy has undoubtedly become a powerful strategy for treating cancer. Unlike other treatments, this new therapy focuses on natural mechanisms of immune cells against tumours. Also cancer immunotherapy is considered less adverse side effects compared to the traditional treatments such as chemotherapy and has potentials in extending overall survival of cancer patients [265]. Majority of this strategy is based on the principal of cell-mediated immunity. The process starts when a tumour antigen is taken and processed by antigen presenting cells (APCs). The APCs migrate to lymphoid organs and present the processed antigen to naïve T cells. Then, the naïve T cells undergo maturation to become effector T cells and travel to tumour site where the tumour cells are recognised by the specific tumour antigen and eliminated through T cell mediated cytotoxicity. After the tumour clearance, population of tumour specific memory T cells is generated for a long-term anti-tumour protective aspect [266]. Cancer immunotherapy can be divided into five classes as follow: immune checkpoint inhibitors, lymphocyte-promoting cytokines, engineered T cells, agonistic antibodies and cancer vaccines [143]. All of them are facing several challenges related to efficacy and safety.

As one approach of cancer immunotherapy, cancer vaccination has recently gained much interest in both preclinical and clinical research. After the first

therapeutic cancer vaccine (sipuleucel-T) has been approved by FDA in 2010, a wide range of vaccine types have been developed to enhance the potential of the immune system against cancer [206]. It is no doubt that cancer vaccine strategies aim for therapeutic aspect rather than protection. The strategy mainly focuses on the activation of tumour specific immune cells for tumour killing. However, the generation of tumour specific memory T cells after tumour clearance is also a key point to prevent tumour relapse. Although the concept of cancer vaccine is simple and straightforward, the strategies remain challenging in clinical trials [267, 268]. One of the difficult issues is the immune escape tactics exploited by tumours to avoid immune-mediated elimination. The immune escape mechanisms are generally found in two categories. On one hand, the tumours down-regulate the expression of antigenic or immunogenic elements such as MHC molecules, antigen processing machinery and target antigens. On the other hand, the tumours develop immunosuppressive properties such as PD-L1, CTLA-4, IL-10 and TGFβ to inhibit the anti-tumour activity of the immune system [124]. Regarding the immune escape mechanisms, it is important to take this point into account when applying cancer vaccine to any cancer treatments.

Based on the principal of molecular immunology, the majority of cancer vaccine approaches consist of two fundamental concepts which are target antigens and vaccine platforms to complete the therapy [185]. Considering the choice of antigen, there are three considerations to identify the ideal target antigen for cancer vaccine strategy. Firstly, the antigen should be expressed on tumour cells but not on normal cells to prevent off target side effect. Secondly, the antigen should be highly immunogenic to stimulate the specific immune response. Thirdly, the antigens should be an essential element for tumour survival to minimise the chance of tumour immune escape through antigen down-regulation. In the past decades, most of cancer vaccine approaches are based on each of the following antigens; 1.) tumour-associated antigens (TAAs) which are abnormally expressed on tumour cells 2.) oncogenic viral antigens derived from cancer-causing viruses, 3.) neoantigens that arose from cancer mutation [185]. Each type of these antigens is facing different challenges. Most of TAAs are

overexpressed on many tumour types and can be compatibly applied on multiple cancer patients. However, some of these antigens are slightly expressed on normal cells which can lead to normal cell toxicity during the treatment [269]. Also, TAAs are still considered as self-antigens and sometimes become tolerant to the immune response [270]. Unlike TAAs, oncogenic viral antigens and neoantigens are tumour-specific antigens and can be high immunogenic. However, oncogenic viral antigens seem to limit the treatment for viral-associated cancer such as hepatocellular carcinoma caused by hepatitis B virus [271]. Moreover, the majority of neoantigens are unique to each patient and require the development of personalised therapy [185]. Thus, selecting the suitable antigen is crucial for this strategy. The most preferred antigen should induce effective response of the treatment against tumour cells but harmless to normal cells, as well as, generalise to multiple patients to extend to a range of cancer patients that could benefit from the treatment [272].

To carry out cancer vaccine treatment, the development of a therapeutic vaccine platform is needed in parallel with the antigen identification. The vaccine should be compatible with the selected antigen and strongly stimulate a tumour specific immune response for tumour clearance. As most of tumour antigens are derived from intracellular proteins, the development of a vaccine platform is based on T cell-mediated anti-tumour activity rather than B cell responses. The vaccine platforms can generally be designed in four types; cellular vaccines, peptide vaccines, nucleic acid vaccines and viral vector vaccines [185, 273]. Each of these vaccine platforms has strengths and weaknesses which can be further improved. The cellular vaccines are usually utilised with either killed cancer cells or autologous APCs pulsed with cancer antigens. The well-known cellular vaccine is sipuleucel-T which is dendritic cell-based cancer vaccine for prostate cancer [206]. Generally, this vaccine type does not require cancer antigen isolation [185]. However, the efficacy of most cellular vaccines is still limited in clinical trials although they show a promising impact in murine models [274-277]. Additionally, the production of these vaccines requires particular techniques and intensive budget. The peptide vaccines can be produced as single antigen-based short peptides up to 15 amino acids and usually require adjuvants or immune

modulators [268, 278, 279]. However, the short peptide vaccines sometimes lose efficacy as tumours evolve to down-regulate the antigen expression and develop immunosuppressive tactics [280]. Applying synthetic long peptides consisting of multi-epitopes could improve the peptide vaccine efficacy [281]. Nucleic acid vaccines can be either DNA or RNA vaccines. Although these cancer vaccine types are simple and cost-effective production, one of their limitations is the efficiency to enter target cells. In general, nucleic acid vaccines require delivery formulations or techniques such as nanoparticles, gene gun and microneedle arrays to improve intracellular uptake. Thus, DNA or RNA vaccines are usually applied together with other platforms such as viral vectors [185, 282]. A wide range of viral vector vaccines has currently been tested and showed promising outcome in clinical trials. Each virus has distinct pros and cons according to its native properties. Many viral vector vaccines can also accommodate multiple therapeutic genes to enhance the therapy effect [283]. However, these vaccine types are sometimes neutralised by host antibodies due to anti-viral immunity that limits the multiple vaccination. As mentioned above, each vaccine platform has advantages and disadvantages which can determine the feasibility of particular therapeutic setting. Therefore, choosing the suitable platform which is compatible to the target antigen is necessary for a successful cancer immunotherapy.

In this chapter, a new strategy of cancer vaccine was proposed in combination with malaria vaccine. According to its efficacy to induce T cell response in the field of malaria [284], a simian adenoviral vector encoding conserved malarial antigen was used as a vaccine. The vaccine is comprised of thrombospondin-related adhesion protein (TRAP) from *Plasmodium falciparum* fused to a multi-epitope (ME) string of malarial epitopes. The ME.TRAP vaccine is considered highly immunogenic and safe to apply on humans [285, 286]. As one epitope in ME string, Pb9 epitope from *Plasmodium berghei* was chosen as a target antigen. The epitope can be used compatibly with ME.TRAP vaccine [287]. Additionally, the epitope was fused in frame with either TIP or ubiquitin sequence to assure that Pb9 was properly generated, processed and presented on tumour cell surface [288]. Using PAAV vector as a delivery system, Pb9 was specifically

delivered to express on the tumour cell surface through binding of the cyclic RGD4C (CDCRGDCFC) ligand on its capsids, and, the $\alpha_V\beta_3$ and/or $\alpha_V\beta_5$ integrin receptor on tumour cell surface and tumour blood vessels. As a foreign antigen, Pb9 is considered safe from adverse side effects and immunogenic to host immune response. Together with the tumour-targeting specificity of PAAV vector, the new vaccine strategy is considered feasible to apply on any tumour type.

The aim of this chapter is to investigate the feasibility and efficacy of the new cancer vaccine strategy using Pb9 as a target antigen and adenovirus encoding ME.TRAP sequence as a vaccine. In a series of experiments, firstly *Pb9* sequence was inserted into PAAV vector under Grp78 promoter. Secondly, the preliminary tumour model, EF43.fgf4 mouse breast tumour, was checked for their suitability for this therapeutic strategy. Thirdly, PAAV-mediated Pb9 expression was assessed by qPCR. Fourthly, therapeutic impact of this strategy was initially investigated *ex vivo* as follow: efficiency of ME.TRAP vaccine on inducing cytotoxic T cell proliferation, activation of Pb9-specific immune cells and tumour cell killing. Fifthly, EF43.fgf4 cells were established in Balb/c mice. Sixthly, *in vivo* experiments were performed in Balb/c mice using targeted PAAV encoding *Pb9* sequence. Seventhly, EF43.fgf4 cells stably expressing luciferase reporter gene were generated to monitor tumour growth in live animals which responds to therapy. Eighthly, therapeutic impact of the cancer vaccine strategy was investigated in Balb/c mice.

5.2 Results

5.2.1. Construction of PAAV vector encoding *Pb9* sequence

There were two molecular cloning steps to construct PAAV.Grp78.*TIP.Pb9* and PAAV.Grp78.*Ubiquitin.Pb9*. Firstly, CMV promoter in PAAV phagemid was replaced by Grp78 promoter. To do so, *Grp78* sequence was amplified from pDRIVE-rGRP78 plasmid using *Grp78.MluI* forward and *Grp78.BsaBI* reverse primers by PCR. *Grp78* sequence flanked by *MluI* and *BsaBI* was ligated to the PAAV backbone. PAAV.Grp78 plasmid was verified by restriction enzyme digestion and DNA sequencing using *Grp78.seq* primer (figure 5.1). Secondly, *TIP.Pb9* or *Ubiquitin.Pb9* sequences flanked by *SacII* and *SalI* were ligated into the PAAV.Grp78 backbone. The *TIP.Pb9* and *Ubiquitin.Pb9* sequences were provided from Dr. Simon Draper, Oxford University. The final constructs were verified by restriction enzyme digestion and DNA sequencing using *Pb9.seq* primer (figure 5.2 and 5.3). Then the corrected constructs were used for PAAV vector production. There were four PAAV constructs used in this chapter as shown in figure 5.4.

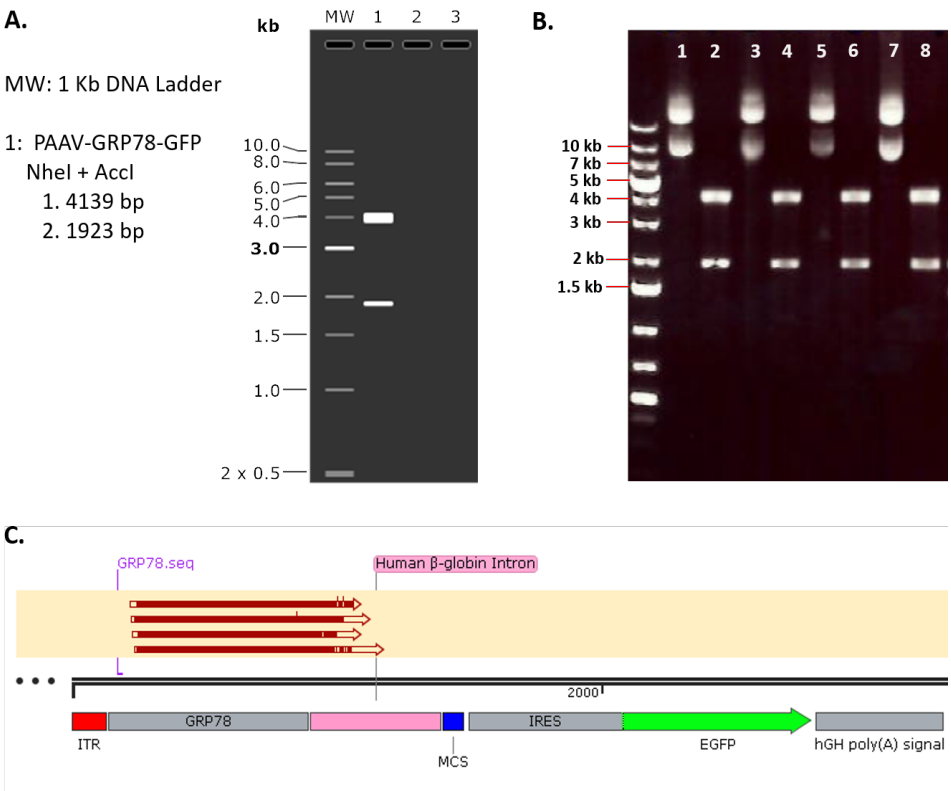

Figure 5.1. Construction of PAAV vector with Grp78 promoter (PAAV.Grp78).

PAAV.Grp78 plasmid was digested with *NheI* and *AccI* restricted-enzymes. **A** *In silico* digested bands from Snap Gene software. **B** PAAV.Grp78 plasmids were digested and run on 1% agarose gel to identify correct DNA fragments. Lanes with odd numbers are undigested plasmids while the ones with even number are plasmid undergone *NheI* and *AccI* restricted-digestion. **C** DNA sequencing results of the PAAV.Grp78 plasmid.

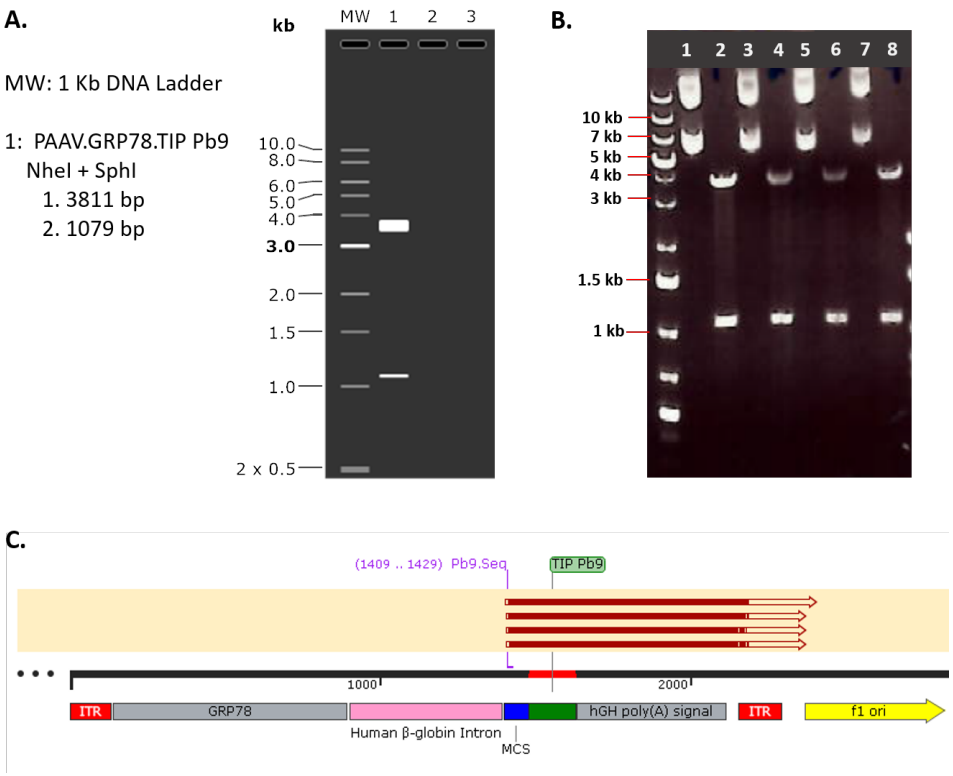

Figure 5.2. Construction of PAAV vector encoding *TIP.Pb9* (PAAV.Grp78.*TIP.Pb9*).

PAAV.Grp78.*TIP.Pb9* plasmid was digested with *NheI* and *SphI* restricted-enzymes. **A** *In silico* digested bands from Snap Gene software. **B** PAAV.Grp78.*TIP.Pb9* plasmids were digested and run on 1% agarose gel to identify correct DNA fragments. Lanes with odd numbers are undigested plasmids while the ones with even number are plasmids that undergone *NheI* and *SphI* restricted-digestion. **C** DNA sequencing results of PAAV.Grp78.*TIP.Pb9* plasmid.

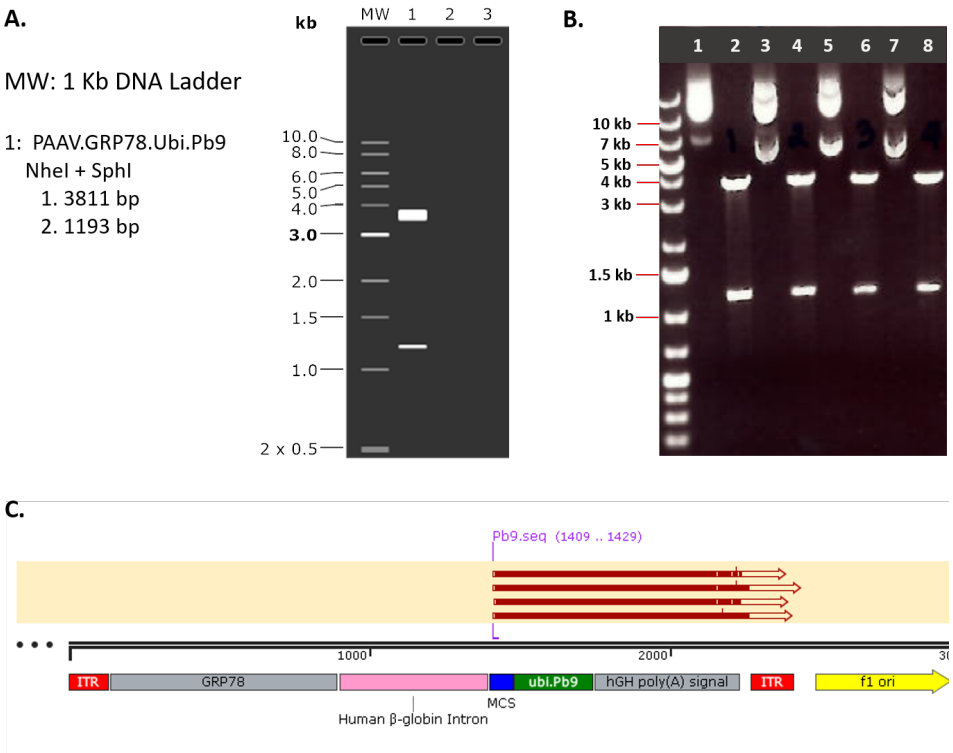

Figure 5.3. Construction of PAAV vector encoding *ubiquitin.Pb9* (PAAV.Grp78.*ubi.Pb9*).

PAAV.Grp78.*ubi.Pb9* plasmid was digested with *NheI* and *SphI* restricted-enzymes. **A** *In silico* digested bands from Snap Gene software. **B** PAAV.Grp78.*ubi.Pb9* plasmids were digested and run on 1% agarose gel to identify correct DNA fragments. Lanes with odd number are undigested plasmids while the ones with even number are plasmid that undergone *NheI* and *SphI* restricted-digestion. **C** DNA sequencing results of PAAV.Grp78.*ubi.Pb9* plasmid.

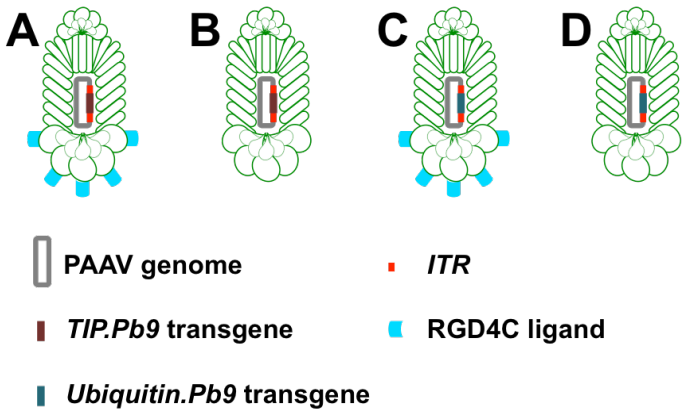

Figure 5. 4. Schematic illustration of PAAV vectors encoding Pb9.

A represents a targeted vector encoding *TIP.Pb9* (RGD.PAAV.Grp78.*TIP.Pb9*). **B** represents a non-targeted vector encoding *TIP.Pb9* (M13.PAAV.Grp78.*TIP.Pb9*). **C** represents a targeted vector encoding *ubiquitin.Pb9* (RGD.PAAV.Grp78.*ubi.Pb9*). **D** represents a non-targeted vector encoding *ubi.Pb9* (M13.PAAV.Grp78.*ubi.Pb9*).

5.2.2. Characterization of EF43.fgf4 cells

EF43.fgf4 cells, Balb/c derived breast cancer, were chosen as an initial *in vivo* tumour model. The cells were initially assessed their suitability for PAAV transduction by measuring α_v, β_3 and β_5 expression. As shown in figure 5.5A, EF43.fgf4 cells express all three integrin subunits. The cells were then transduced by PAAV vector encoding a secreted luciferase reporter gene (*Lucia*) to optimise the vector efficacy. The transduction was conducted at various doses as follow; 100,000; 500,000; 1,000,000 and 2,000,000 TU/Cell to identify an appropriate transduction unit regarding the vector efficacy and specificity. The Lucia expression was detected in a dose-dependent manner. A slight expression mediated by non-targeted vector was also found on the cells transduced with 2,000,000 TU/cell. The highest expression was detected on day 4 post vector transduction (figure 5.5B). Therefore, all experiments in this chapter were performed with 1,000,000 TU/cell of the vector and the results were assessed on day 4 post transduction, unless otherwise indicated. Finally, EF43.fgf4 cells were

checked for MHC class I and class II expression by flow cytometry. As expected, the cells showed a good expression of MHC class I molecules whereas none of MHC class II expression was detected (figure 5.5C).

These data indicate that the cells can be specifically targeted by PAAV vector with the optimised transduction units. Also, the cells are more suitable for presenting endogenous antigen than exogenous antigen as they highly express MHC class I molecules.

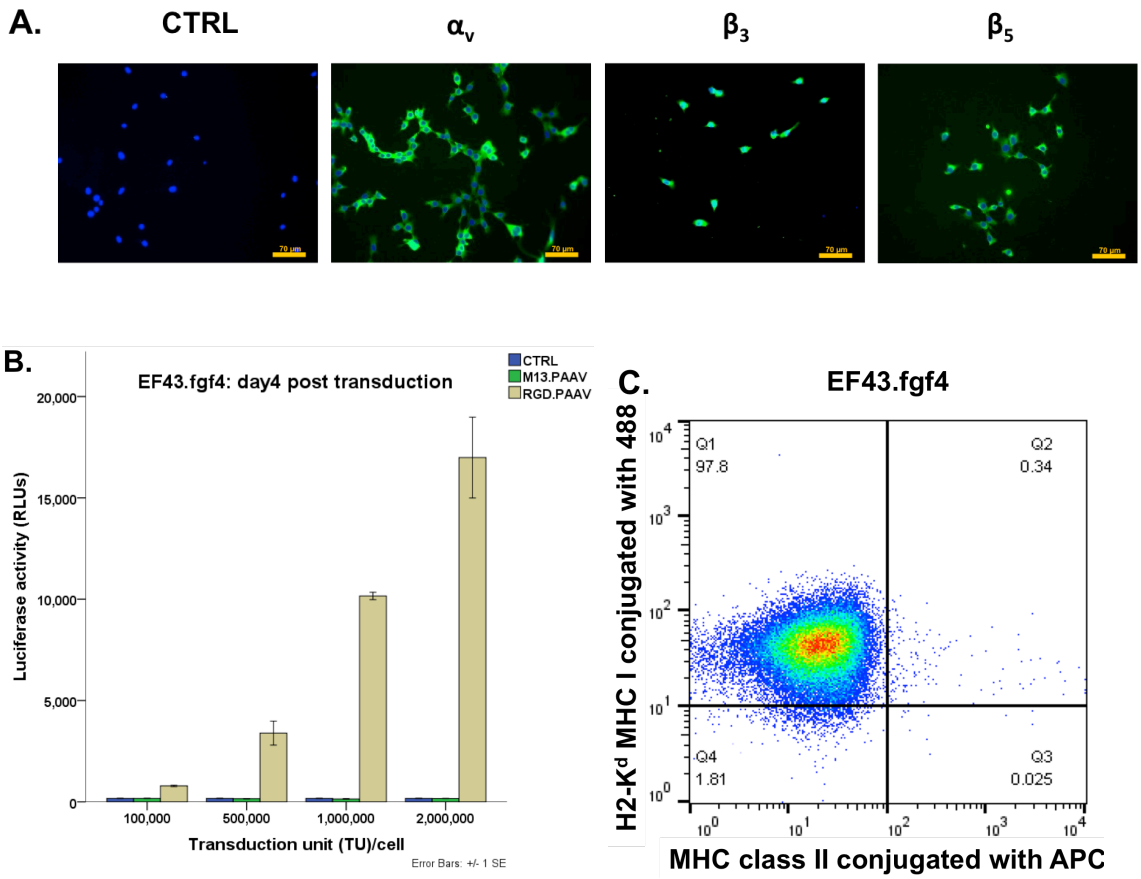

Figure 5.5. Characterisation of EF43.fgf4 cells.

EF43 fgf4 cells were chosen as a preliminary tumour model and assessed their suitability. **A** Immunofluorescent staining of α_v, β_3 and β_5 integrin receptor expression. **B** Optimisation of PAAV transduction at various transduction units. **C** MHC class I and MHC class II expression.

5.2.3. Pb9 expression mediated by PAAV vector

Pb9 expression mediated by PAAV was assessed only at mRNA level by quantitative RT-PCR because there is no existing antibody against the Pb9 epitope. The expression was initially assessed from PAAV plasmid transfection on HEK293 cells to ensure that the plasmids contained Pb9 sequences correctly. HEK293 cells seeded in 6-well plate were transfected with either PAAV.Grp78.*TIP.Pb9* or PAAV.Grp78.*ubi.Pb9* plasmids. mRNA from the cells was collected on day 1 post transfection. *GAPDH* mRNA expression was measured as internal control. As shown in figure 5.6), *Pb9* expression mediated by PAAV plasmid was detected.

PAAV vector transduction was then performed on HEK293 and EF43.fgf4 cells. The cells were transduced with 1,000,000 TU/cell of PAAV vector encoding either *TIP.Pb9* or *ubiquitin.Pb9* sequence (RGD.PAAV.Grp78.*TIP.Pb9* or RGD.PAAV.Grp78.*ubi.Pb9*). Non-targeted vectors, M13.PAAV.Grp78.*TIP.Pb9* and M13.PAAV.Grp78.*ubi.Pb9*, were used as controls. mRNA from the cells were collected on day 3 post transduction. *GAPDH* mRNA expression was measured as internal control. *TIP.Pb9* and *ubi.Pb9* mRNA expression was highly detected from the cells transduced with RGD.PAAV (figure 5.7). A slight expression of Pb9 was also found from the cells transduced with non-targeted PAAV. The results indicate that PAAV vector is able to mediate *Pb9* expression at mRNA level in EF43.fgf4 cells.

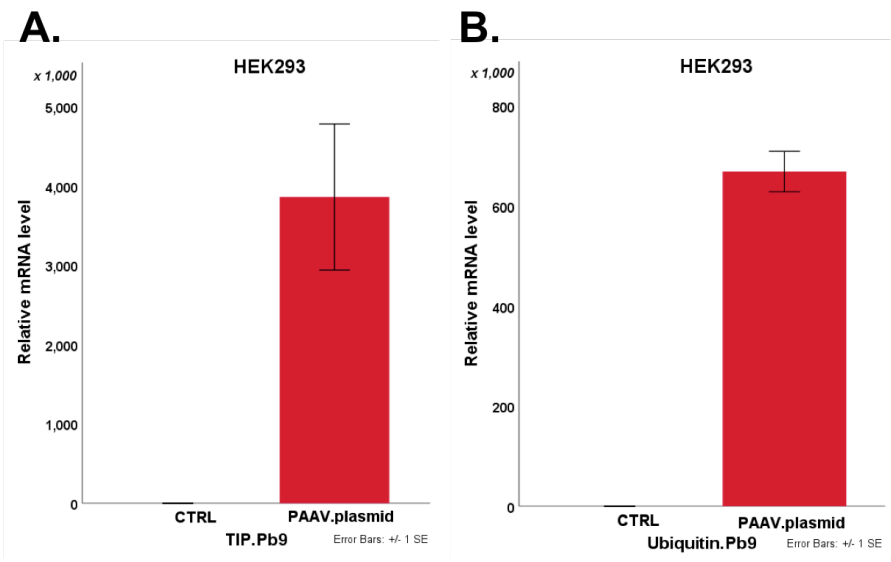

Figure 5.6. mRNA expression of TIP.Pb9 and ubiquitin.Pb9 mediated by PAAV plasmid transfection.

HEK293 cells were transfected with PAAV.*TIP.Pb9* or PAAV.*ubi.Pb9* plasmids. Total RNA was collected on day 1 post transfection. *GAPDH* mRNA expression was measured as an internal control. Results are shown as mean ± SEM of triplicate wells.

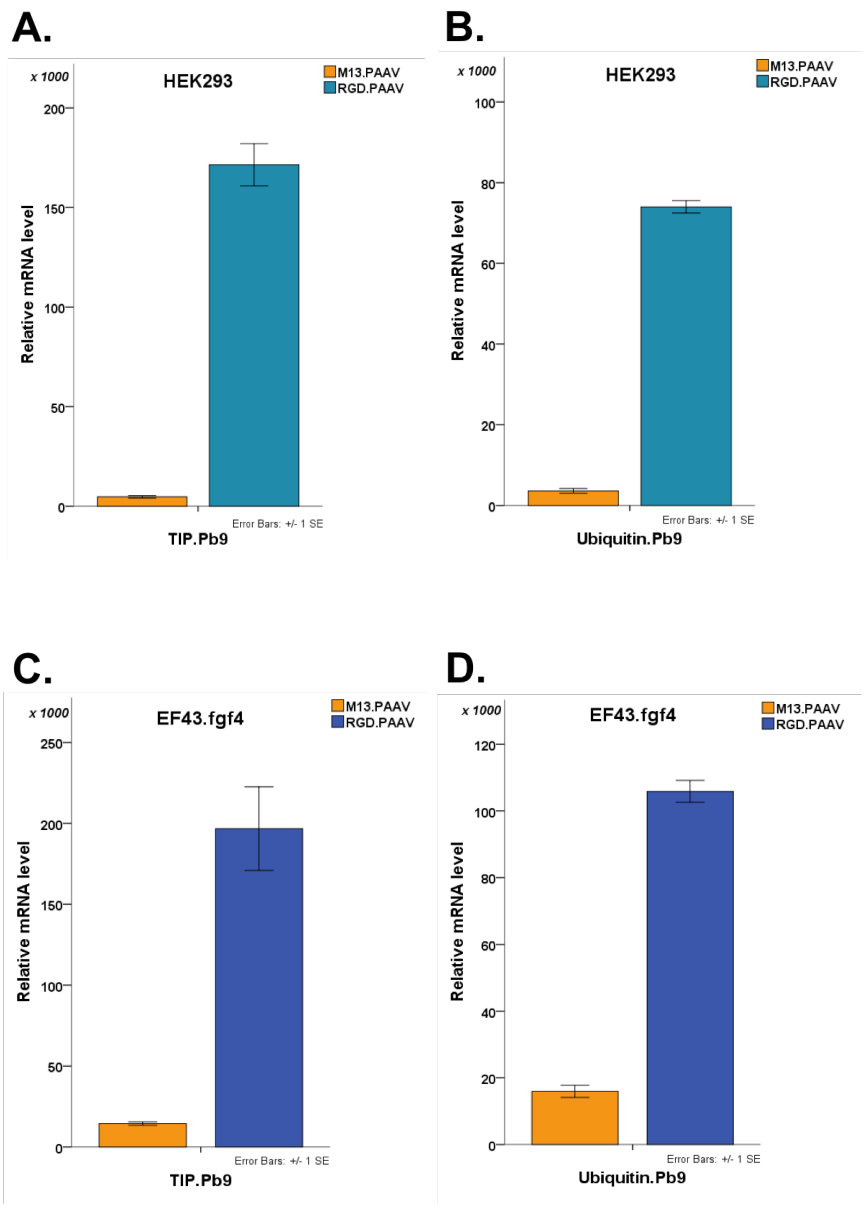

Figure 5.7. mRNA expression of TIP.Pb9 and ubiquitin.Pb9 mediated by PAAV vector transduction.

The HEK293 and EF43.fgf4 cells were transduced with 1,000,000 TU/cell of targeted or non-targeted PAAV vectors. Total RNA was collected on day 3 post vector transduction. *GAPDH* mRNA expression was measured as an internal control. Results are shown as mean ± SEM of triplicate wells. **A** represents mRNA expression of *TIP.Pb9* on HEK293 cells. **B** represents mRNA expression of *ubi.Pb9* on HEK293 cells. **C** represents mRNA expression of *TIP.Pb9* on EF43.fgf4 cells. **D** represents mRNA expression of *ubi.Pb9* on EF43.fgf4 cells.

5.2.4. *Ex vivo* anti-tumour immunity investigations

According to the concept of this chapter, specific immune cells are activated by the vaccination and play their role on specific tumour killing. As such, Balb/c mice were intramuscularly vaccinated with Adeno.ME.TRAP. The mice were sacrificed and splenocytes of each mouse were collected on day 14 post vaccination. A series of *ex vivo* experiments were set as follow. ME.TRAP vaccine efficiency on stimulating T cell proliferation was initially investigated by flow cytometry. Then, activation of Pb9-specific immune cells was assessed through IFN-γ secretion by ELISpot assay. The specific immune cell function was assured from granzyme B release by ELISA assay. Finally, Pb9-specific immune cell-mediated tumour killing was measured from the release of LDH and confirmed by SRB assay. The splenocytes from non-vaccinated mice were also collected and used as control.

5.2.4.1. ME.TRAP vaccine efficiency

Efficiency of Adeno.ME.TRAP vaccine was assessed from the number of $CD3^+$ $CD8^+$ cells and $CD3^+$ $CD4^+$ cells by flow cytometry. As shown in figure 5.8, a significant increase of $CD3^+$ $CD8^+$ cell population was detected on splenocytes from vaccinated mice. This confirms that ME.TRAP vaccine is able to induce proliferation of cytotoxic T cells which are needed for anti-tumour activity. It is worth to note that there was an increase of $CD3^+$ CD4 cells which are believed to promote T cell survival.

5.2.4.2. Antigen specific immune cell activation and function

Next step, the specific immune cell activation was investigated through IFN-γ secretion. EF43.fgf4 cells stably expressing Pb9 were used as a stimulant. To generate Pb9-expressing EF43.fgf4, the cells were transfected with PAAV plasmid encoding *Pb9* and *puromycin* sequences, then selected by puromycin antibiotic. The splenocytes and Pb9-expressing EF43.fgf4 cells (ratio 10:1) were co-cultured in anti-IFN-γ pre-coated wells and incubated for 16 hours.

Splenocytes or EF43.fgf4 cells alone were included as controls. IFN-γ secretion was measured from spots developed on each well and interpreted as spot forming unit per 1 million splenocytes. The IFN-γ secreting spots were observed only from the wells consisting of vaccinated mouse splenocytes and Pb9-expressing EF43.fgf4 cells. The co-cultured wells showed a significant number of activated immune cells compared to others (figure 5.9A and 5.9B). Apart from the immune cell activation, their functionality was assured from granzyme b which is released from activated immune cells to induce tumour cell killing. Granzyme b concentration was measured from co-culturing medium by ELISA assay. The results were found in relevant to IFN-γ secretion as granzyme b was significantly detected when vaccinated mouse splenocytes were cultured with Pb9-expressing EF43.fgf4 cells. A slight increase of granzyme b was found when culturing vaccinated mouse splenocytes with original EF43.fgf4 cells (figure 5.9C).

These results indicate that specific immune cells such as cytotoxic T cells and NK cells are activated and carried out their biological function when culturing them with Pb9-expressing EF43.fgf4 tumour cells. This paves the way for a potential anti-tumour immunity.

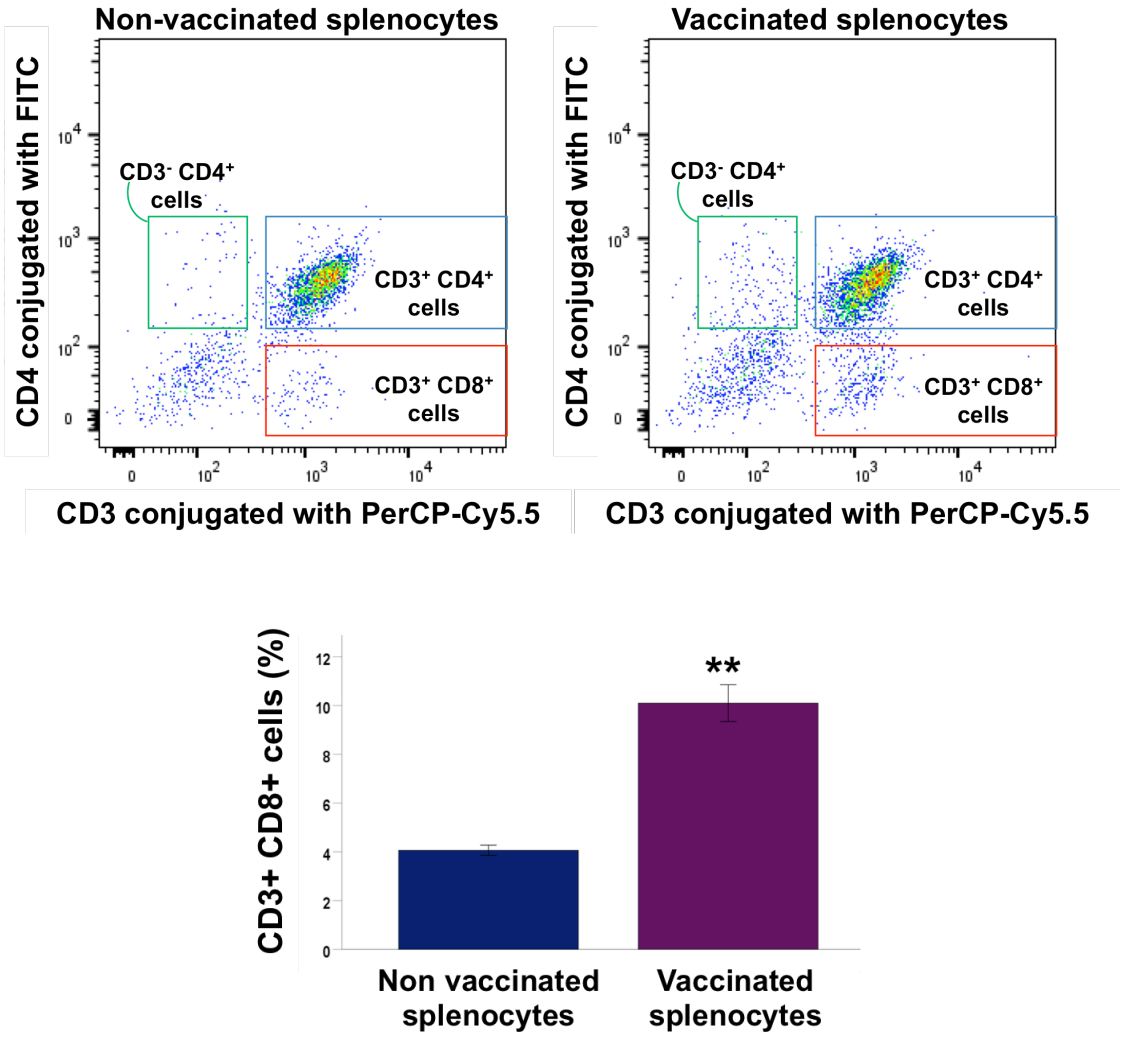

Figure 5.8. Proportion of CD4⁺ and CD8⁺ cells after ME.TRAP. adenovirus vaccination.

Balb/c mice (n=5) were received vaccination with Adeno.ME.TRAP. Splenocytes were collected from each mouse on day 14 post vaccination, stained with anti-CD3 conjugated with PerCP-Cy5.5, anti-CD4conjugated with FITC and anti-CD8 conjugated with PE antibodies and subjected to flow cytometry. Splenocyted of non-vaccinated mice were included as control. Percentage of positive cells was gated using FlowJo software (v10.5). $CD3^{+}CD8^{+}$ positive cells were shown in bar graphs. The data are represented as mean ± SEM. Statistical significance was determined by student's t-test.

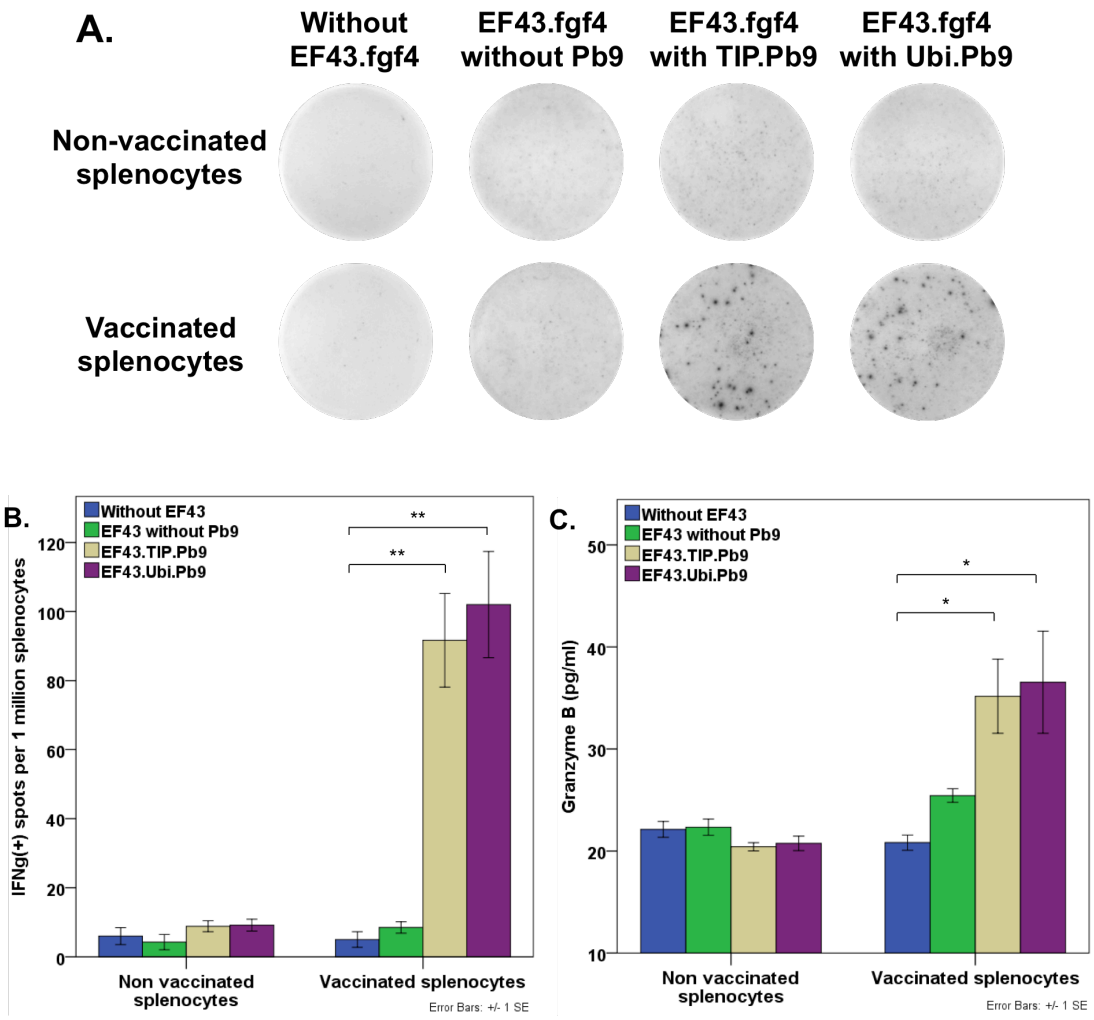

Figure 5.9. Pb9 specific immune cells activation and function mediated by ME.TRAP vaccine

Splenocytes of Balb/c mice (n=5) were cultured with Pb9-expressing EF43.fgf4 cells. **A** ELISpot assay for Pb9-specific immune cell activation. Spots of IFN-γ secreting immune cells were automatically counted by ELISpot plate reader. **B** The number of IFN-γ secreting cells was interpreted as spot forming unit per 1 million splenocytes in bar graphs. **C** Granzyme b concentration was measured by ELISA assay for Pb9-specific immune cells functionality. Splenocytes or EF43.fgf4 cells alone were included as control. The data are represented as mean ± SEM. Statistical significance was determined by one-way ANOVA with Tukey's honestly significant difference (HSD) post hoc test.

5.2.4.3. Tumour cell killing

According to previous *ex vivo* finding, anti-tumour activity was assessed by culturing mouse splenocytes with Pb9-expressing EF43.fgf4 cells or original EF43.fgf4 cells in various ratios (1:1, 5:1, 10:1, 20:1 and 50:1). Splenocytes or EF43.fgf4 cells alone were included as control.

Tumour cell killing was quantified from lactase dehydrogenase (LDH) released from the damaged cells. The culture media were taken from each well after 10 hours incubation and measured LDH release according to manufacture protocol. Percentage of cell killing was calculated in direct proportional to the amount of LDH in the culture media. Cell death was detected when Pb9-expressing EF43.fgf4 cells were cultured with vaccinated splenocytes. The cell killing increased correlatively to splenocyte ratios added into the co-cultured wells. (figure 5.10A).

Although cell killing determined by LDH was detected after 10 hours of co-culturing, it took 3 days to observe cell death under the microscope. As shown in figure 5.10B, more cell death was found when vaccinated mouse splenocytes were cultured with Pb9-expressing EF43.fgf4 cells compared to control wells. The anti-tumour activity of splenocytes was confirmed by tumour cell viability on day 5 of the experiment using SRB assay. The result showed a decrease of tumour cell viability when culturing with vaccinated mouse splenocytes. The cell viability varied indirectly to the ratio of splenocytes added to the culture. Also, there was a slight decrease of cell viability when the original EF43.fgf4 cells were cultured with vaccinated mouse splenocytes (figure 5.10C). These findings emphasize the synergistic effect of ME.TRAP vaccination and PAAV-mediated Pb9 expression on mediating anti-tumour immunity.

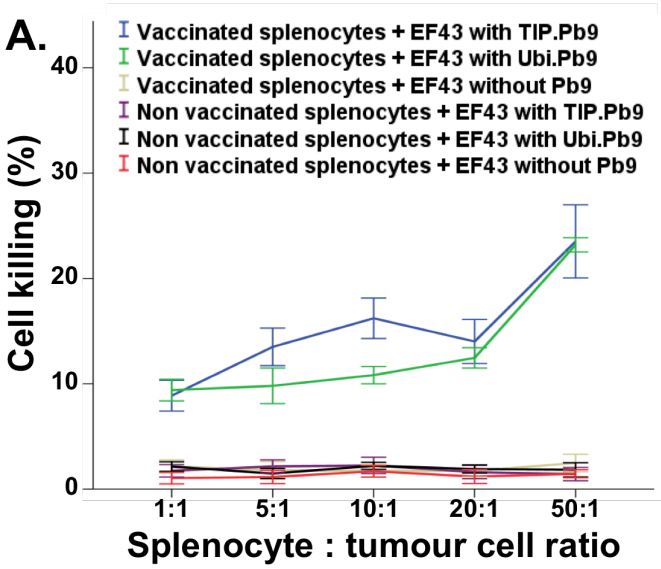
A.
Vaccinated splenocytes + EF43 with TIP.Pb9
Vaccinated splenocytes + EF43 with Ubi.Pb9
Vaccinated splenocytes + EF43 without Pb9
Non vaccinated splenocytes + EF43 with TIP.Pb9
Non vaccinated splenocytes + EF43 with Ubi.Pb9
Non vaccinated splenocytes + EF43 without Pb9
Cell killing (%)
40
30
20
10
0
1:1
5:1
10:1
20:1
50:1
Splenocyte : tumour cell ratio

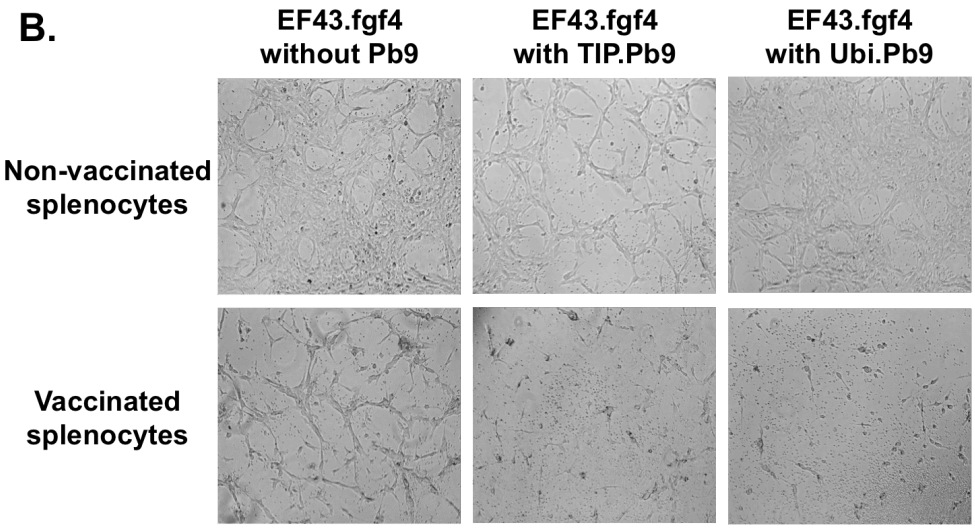
B.
EF43.fgf4 without Pb9
EF43.fgf4 with TIP.Pb9
EF43.fgf4 with Ubi.Pb9
Non-vaccinated splenocytes
Vaccinated splenocytes

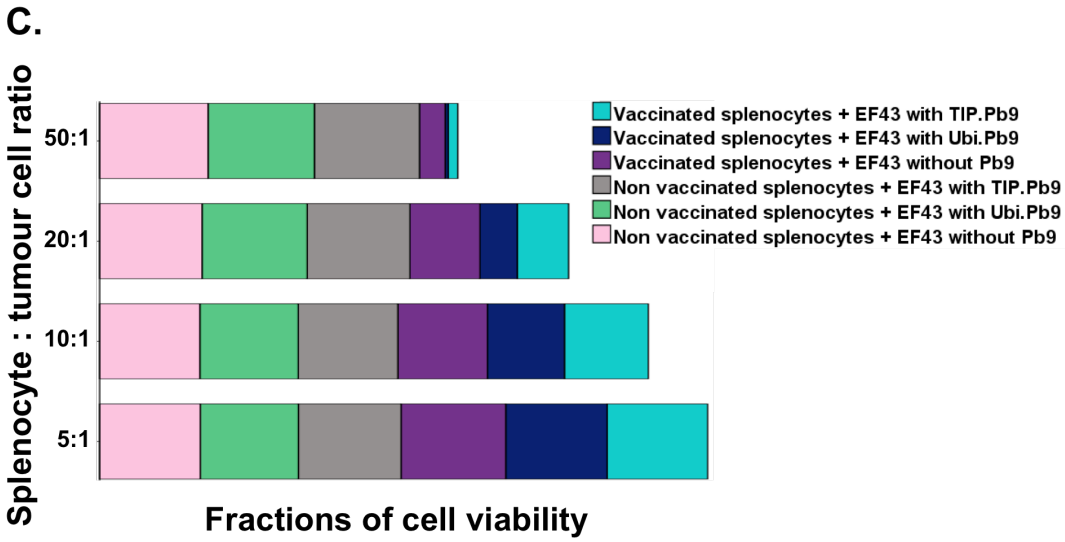
C.
Splenocyte : tumour cell ratio
50:1
20:1
10:1
5:1
Vaccinated splenocytes + EF43 with TIP.Pb9
Vaccinated splenocytes + EF43 with Ubi.Pb9
Vaccinated splenocytes + EF43 without Pb9
Non vaccinated splenocytes + EF43 with TIP.Pb9
Non vaccinated splenocytes + EF43 with Ubi.Pb9
Non vaccinated splenocytes + EF43 without Pb9
Fractions of cell viability

Figure 5.10. Anti-tumour immunity against Pb9-expressing EF43.fgf4 cells.

Splenocytes of Balb/c mice (n=5) were cultured with Pb9-expressing EF43.fgf4 cells or original EF43.fgf4 cells in various ratios (1:1, 5:1, 10:1, 20:1 and 50:1). Splenocytes or EF43.fgf4 cells alone were included as control. **A** Lactate dehydrogenase was measured after 10 hours of incubation. The results were calculated and interpreted as percentage of tumour cell killing. The data are represented as mean ± SEM. **B** Tumour cell death was observed under microscope on day 3 of the experiment. **C** Cell viability of EF43.fgf4 was measured on day 5 of the experiment using SRB assay. The data are represented as mean ± SEM.

5.2.5. EF43.fgf4 establishment in Balb/c mice

As Pb9 epitope is restricted to H2-K^d MHC class I, Balb/c mice are required for animal investigation related to this epitope. EF43.fgf4 cells derived from Balb/c mice were chosen as a model and assessed their growth rate in mice before performing the therapeutic experiment. The cells (160,000 per mouse) were subcutaneously injected to Balb/c mice (n=3) and tumour growth was measured by calipers. The tumour mass was noticeable on day 14 post injection, then grew very fast. The animals reached endpoint as noted in the Project Licence and were sacrificed on day 20 of the experiment (figure 5.11A). The mice were also monitored for their wellbeing and showed no weight loss throughout this experiment (figure 5.11B).

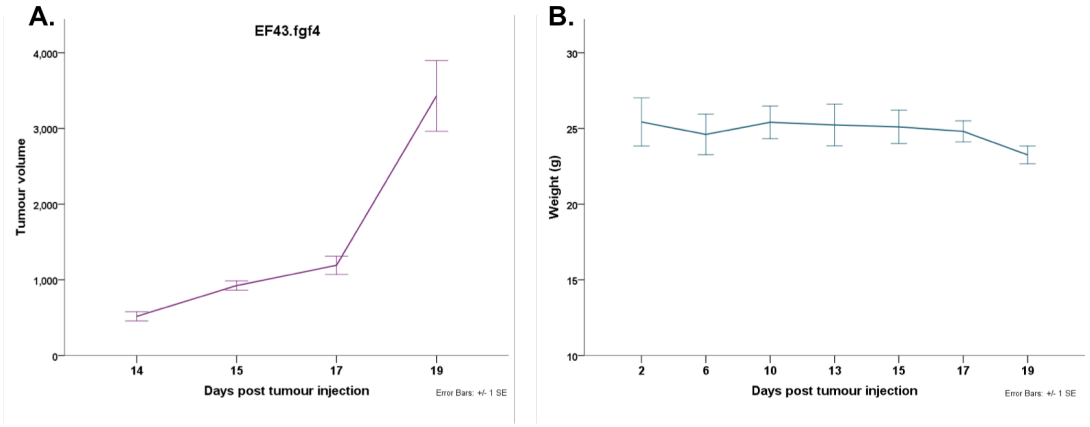

Figure 5.11. Establishment of EF43.fgf4 tumours in Balb/c mice.

The cells were subcutaneously injected to Balb/c mice (n=3). **A** Tumour growth was measured by caliper. **B** Weight of the mice during the experiment are shown as mean ± SEM.

5.2.6. Preliminary *in vivo* experiment

An initial therapeutic experiment was conducted in Balb/c mice. The mice were assigned into three groups; control (n=3), TIP.Pb9 (n=4) and ubi.Pb9 (n=4). TIP.Pb9 and ubi.Pb9 groups received intramuscular vaccination of $1x10^{10}$ ME.TRAP adenoviral particles. All mice were subcutaneously implanted with 160,000 cells of EF43.fgf cells on day 7 post vaccination. The mice in TIP.Pb9 and ubi.Pb9 group were systemically injected with targeted PAAV encoding *TIP.Pb9* (RGD.PAAV.*TIP.Pb9*) and targeted PAAV encoding *ubi.Pb9* (RGD.PAAV.*ubi.Pb9*), respectively, when tumours were established (day 10 post vaccination). The control group received vehicle saline intravenously. As shown in figure 5.12A, the mice in TIP.Pb9 and ubi.Pb9 group developed smaller solid tumour compared to the control mice. Interestingly, tumour shrinkage was seen in a couple of mice from ubi.Pb9 group. The mice were monitored and showed no weight loss throughout this experiment (figure 5.12B). As the mice of ubi.Pb9 group showed slightly slower tumour growth compared to the mice of TIP.Pb9 group, RGD.PAAV.*ubi.Pb9* vector was chosen for further *in vivo* therapeutic experiment.

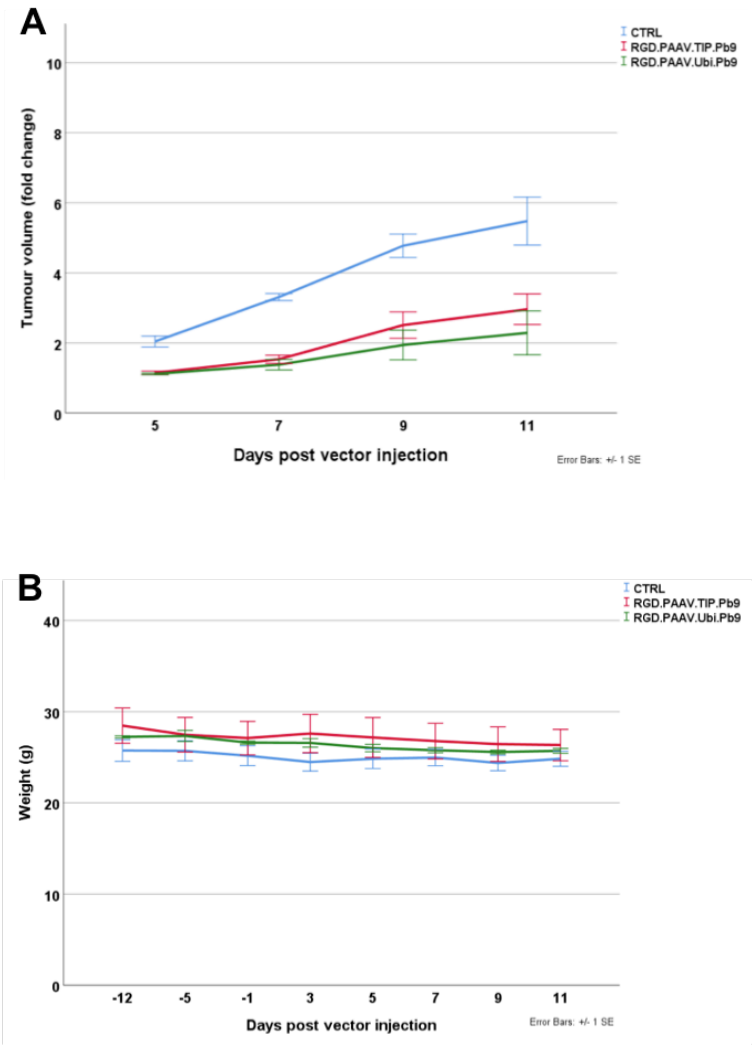

Figure 5.12. Preliminary *in vivo* therapy.

Balb/c mice were assigned into three groups; control (n=3), TIP.Pb9 (n=4) and ubi.Pb9 (n=4). The mice in TIP.Pb9 and ubi.Pb9 group were vaccinated with $1x10^{10}$ viral particles of ME.TRAP vaccine. EF43.fgf cells were subcutaneously implanted to all mice on day 7 post vaccination. Tumour-bearing mice in in TIP.Pb9 and ubi.Pb9 group systemically received RGD.PAAV.*TIP.Pb9* or RGD.PAAV.*ubi.Pb9* respectively while control mice received vehicle saline. **A** Tumour growth measured by calipers. **B** Weight of the mice throughout the therapy shown as mean ± SEM.

5.2.7. Generation of EF43.*fgf4.GFP.luciferase* stable cells

In order to monitor tumour growth and therapeutic response *in vivo*, EF43.*fgf4* cells stably expressing GFP and luciferase reporter genes were generated by infecting with a lentiviral vector encoding GFP and luciferase reporter genes. The cells were observed under fluorescent microscopy for GFP expression. The infected cells were expanded and sorted for GFP positive cells by fluorescence-activated cell sorter. The sorted cells were further confirmed for their luciferase expression through a luciferase assay (figure 5.13).

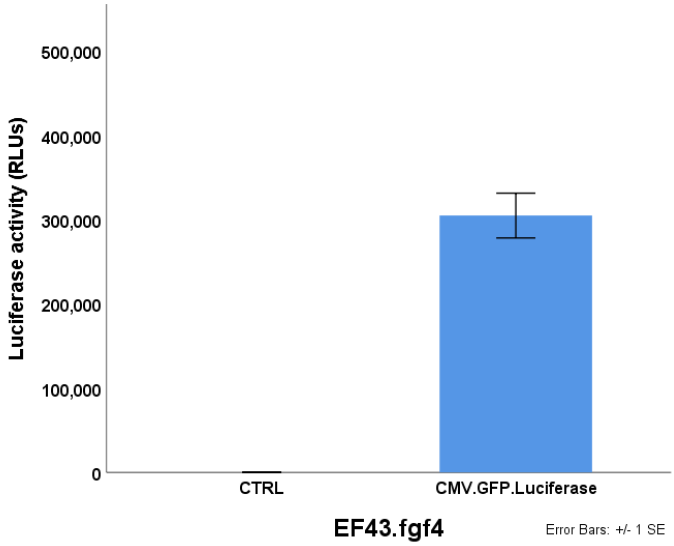

Figure 5.13. Generation of stable EF43.fgf4 cells expressing GFP and luciferase for long term non-invasive *in vivo* imaging.

The cells were transfected with a lentivirus vector encoding GFP and luciferase at a multiplicity of infection (MOI) =10, then sorted for GFP positive cells by fluorescence- activated cell sorter. Luciferase activity of the sorted cells was measured by luciferase assay.

5.2.8. Therapeutic experiment in Balb/c mice

To evaluate the efficiency of this therapeutic strategy *in vivo*, Balb/c mice were randomly assigned into 7 groups (n=5) and each group was defined as shown in figure 5.14. We describe the design of randomized animal experiments to test our vector for the treatment of tumour-bearing mice and follow the tumour size progression. We need a certain number of animals to detect statistically significant differences between the group means at the 5% significance level with a statistical power of at least ~80%. An 80% power may be sufficient to catch large effects while fewer animals are needed, as we abide by applying the principles of the 3Rs (Replacement, Reduction and Refinement). This number should be 5 animals per group. Moreover, we will use 7 animals per group for the future experiment, which should increase the statistical power above 80%.

Three groups of mice were intramuscularly vaccinated with $1x10^{10}$ viral particles of ME.TRAP adenovirus while the other four groups were kept along without vaccination. All mice were then implanted with luciferase-expressing EF43.fgf cells on day 7 post vaccination. Three days later, the mice were systemically injected with $5x10^{10}$ TU of appropriate PAAV vector through tail vein. The control group was injected with the vehicle saline intravenously. The plan of *in vivo* study is shown in figure 5.15. The mouse wellbeing was routinely checked by their behaviour and weight.

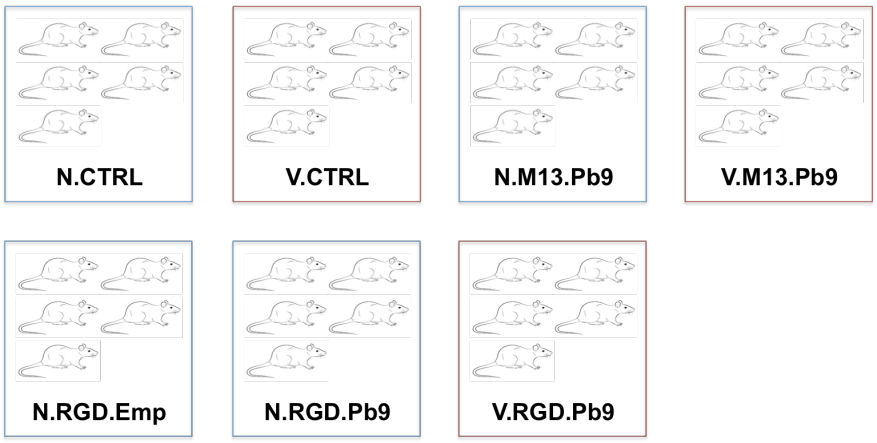

Figure 5.14. Groups of Balb/c mice for *in vivo* therapy.

N refers to non-vaccinated mice and V refers to vaccinated mice. Each group of animals was defined as follow; N.CTRL was a group of mice that did not receive METRAP vaccine or any treatment, V.CTRL group received the ME.TRAP vaccine only, N.M13.Pb9 group received non-targeted PAAV encoding *ubi.Pb9*, V.M13.Pb9 group received ME.TRAP vaccine and non-targeted PAAV encoding *ubi.Pb9*, N.RGD.Emp group received only targeted PAAV without therapeutic gene, N.RGD.Pb9 group received only targeted PAAV encoding *ubi.Pb9* and V.RGD.Pb9 group received ME.TRAP vaccine and targeted PAAV encoding *ubi.Pb9*.

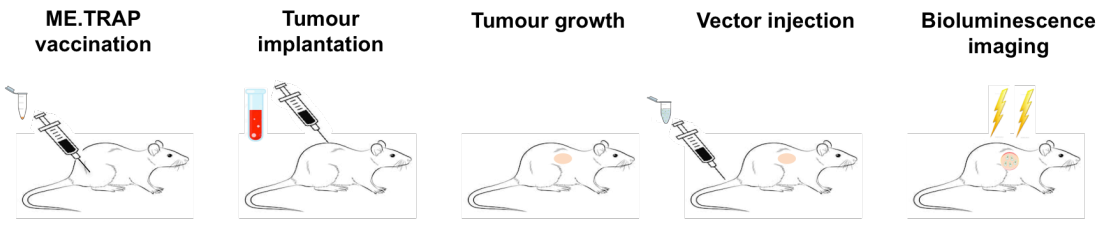

Figure 5.15. *In vivo* experimental plan.

Balb/c mice in vaccinated groups were intramuscularly injected with $1x10^{10}$ viral particles of ME.TRAP adenovirus. Then all mice were subcutaneously implanted with luciferase-expressing EF43.fgf cells. After that, tumour-bearing mice were systemically injected with $5x10^{10}$ TU of appropriate PAAV vectors. Tumour viability was monitored by bioluminescence imaging on day 4 and 9 post vector injection.

Regarding the hypothesis of this therapeutic strategy, ME.TRAP vaccine would stimulate specific immune responses including cytotoxic T cells against tumour cells expressing PAAV-mediated Pb9 epitope. Tumour growth and therapeutic effect were monitored by bioluminescence imaging (BLI) on day 4 and 9 post vector injection. Luciferase signal from the tumours showed a delay of tumour growth in mice receiving both ME.TRAP vaccine and targeted PAAV encoding *Pb9* (figure 5.16A and 5.16B). The tumour volume was also measured by calipers throughout the experiment and showed a consistent result with the tumour activity assessed by BLI (data not shown). Although the mice were culled on day 16 post vector injection as they had reached endpoint noted in the Project Licence, the therapy seemed to prolong overall survival of the mice that received ME.TRAP vaccine and targeted PAAV vector encoding Pb9 compared to others (figure 5.17A). Additionally, the animals did not show any weight loss during the experiment (figure 5.17B).

After the animals reached an endpoint, solid tumours were collected from each mouse and performed histological analysis. The tumour sections stained with haematoxylin and eosin (H&E) revealed damage in tumour of mice that received the ME.TRAP vaccine. The mice received targeted vector also showed lower tumour density than the controls. An enhance therapeutic effect was found in mice that received both ME.TRAP vaccine and targeted PAAV encoding *Pb9* as the tumour sections in this group showed the lowest density of tumour cells compared to the others. Tumour sections from control mice (N.CTRL) and from mice that received non-targeted PAAV vector alone (N.M13.Pb9), showed very high tumour cell density (figure 5.18A). However, tumour cell death shown here was subjective preliminary observation and further quantitative assessment will be needed to confirm the finding. Immunofluorescent staining of cleaved Caspase-3 was also performed to confirm apoptotic cell death. The cleaved Caspase-3 positive cells were obviously seen on the tumour sections from mice that received ME.TRAP vaccine and targeted PAAV encoding *Pb9*. A slight expression of cleaved Caspase-3 was also observed in the tumour sections of ME.TRAP vaccinated mice (figure 5.18B).

In summary, PAAV vector mediated desirable expression of the malaria target antigen (Pb9) on EF43.fgf4 breast tumor cells. The therapeutic strategy showed a promising efficiency on stimulating specific immune cells response which eventually led to tumor cell killing. *In vivo*, the delay of tumour progress and extended survival of tumour-bearing mice were also achieved. Altogether, these data prove feasibility and efficacy of the combination of tumor-targeting phage vector and malaria vaccine in cancer immunotherapy.

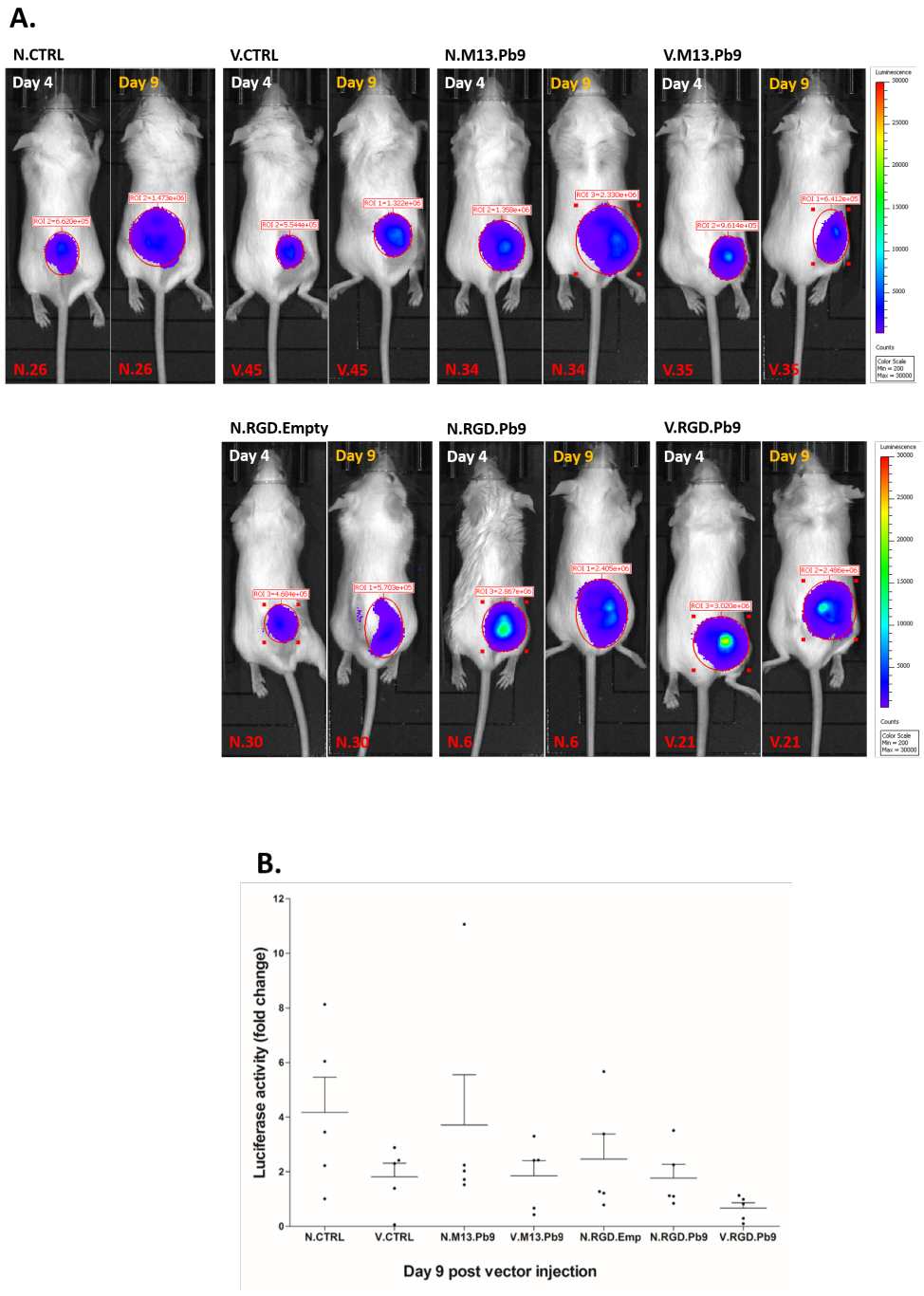

Figure 5.16. Visualisation of subcutaneous tumour growth throughout immunotherapy.

A *In vivo* bioluminescent imaging of luciferase expression on day 4 and day 9 post vector injection. **B** Tumour viability measured by bioluminescent imaging.

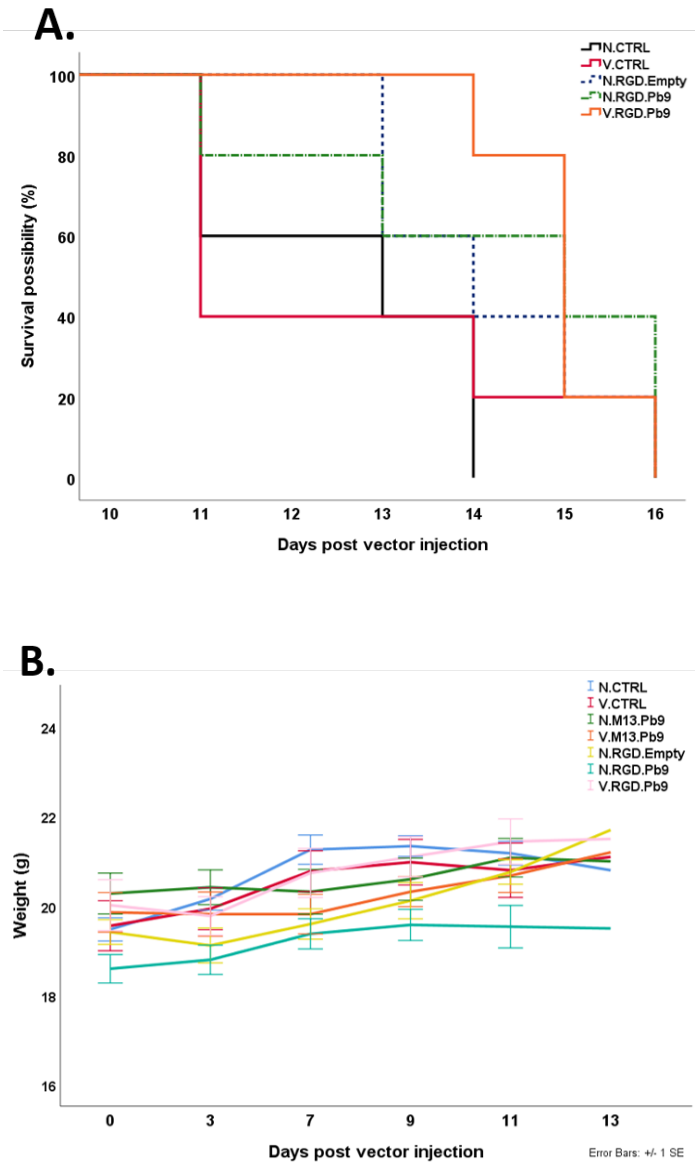

Figure 5.17. Overall survival of the animals throughout the therapy.

A Overall survival of Balb/c mice. **B** Weight of the mice during the experiment are shown as mean ± SEM.

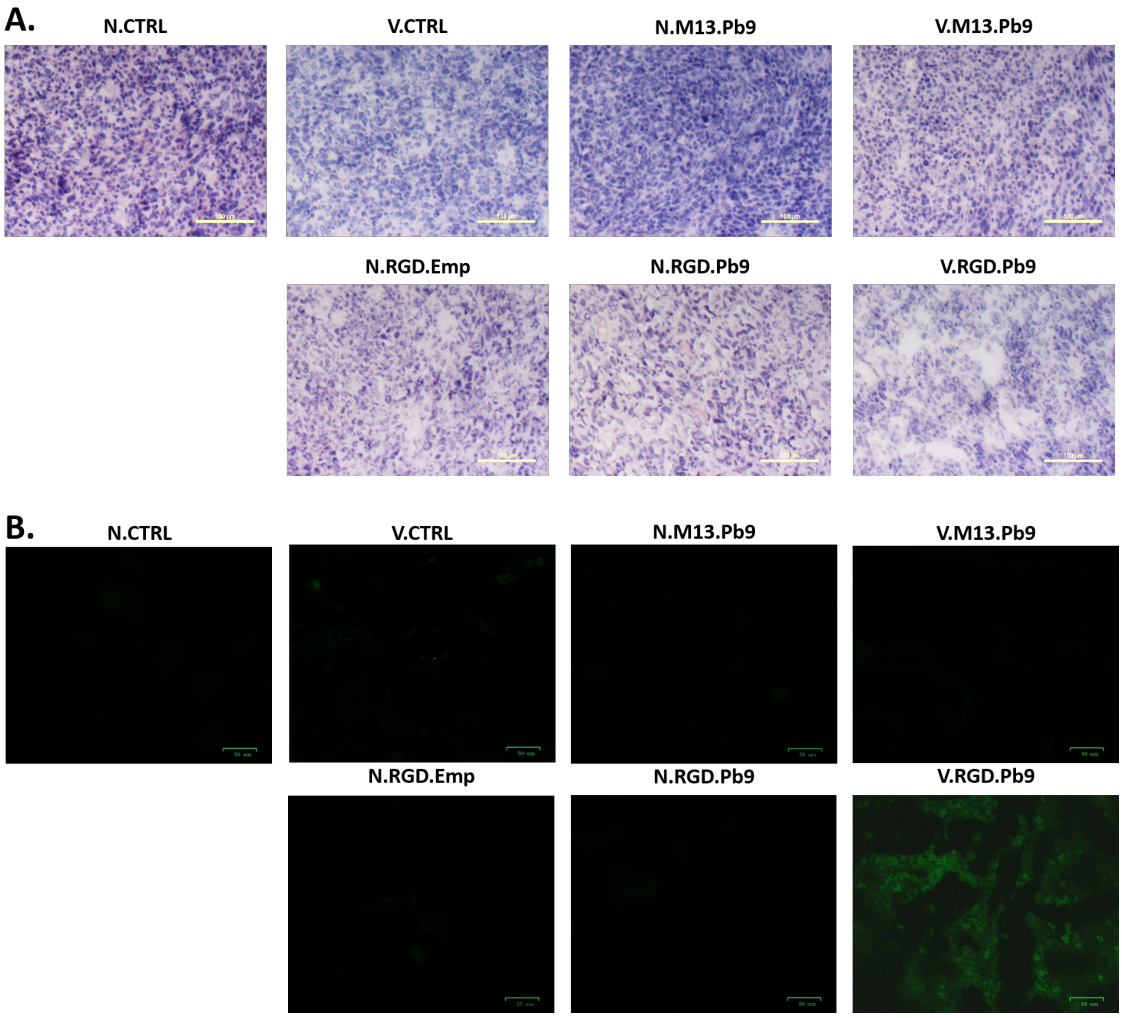

Figure 5.18. Histological analysis of solid tumours.

Tumours were collected from each mouse and 5 μm sections were produced. **A** Tumour sections stained with haematoxylin and eosin (H&E). **B** Tumour sections stained with rabbit primary antidody against cleaved Caspase-3 (1:800) followed by anti rabbit IgG Alexa Fluor-488 secondary antibody.

5.3 Discussion

As gene therapy has become an intensive research focusing on many diseases including cancer, a wild range of viral and non-viral vectors have been developed and applied to this field of study. The decades of experimental work dedicated to gene therapy has confirmed its contribution to cancer treatment in both research and clinical trials. With the ultimate goal on efficiency and selectivity of the approach, various strategies have been applied to cancer gene therapy aiming for a better therapeutic impact. One such strategy is transcriptional targeting to tumour cells using tumour-specific promoters [39, 289]. Among many promoters, Grp78 promoter is considered attractive for the transcriptional control. As a stress-induced promoter, Grp78 is highly activated under glucose and oxygen depletion as well as acidic circumstances within the tumour microenvironment. Applying this promoter into the treatment can enhance suicidal gene expression and increase tumour cell death [290, 291]. Grp78 promoter is also activated when used in combination with chemotherapeutic drugs such as temozolomide [36] and cisplatin (unpublished data in Phage therapy group). In addition, grp78 promoter is upregulated in various cancer types especially in hypoxic areas of solid tumours but remains at low levels in normal tissues. This allows additional safety of tumour cell targeting. Therefore, the promoter was applied in PAAV constructs to drive Pb9 expression within tumours.

Apart from the tumour specific promoter, choosing a target antigen is a crucial step for a successful therapy. An ideal antigen should be highly expressed on tumour cells but completely inactive in normal cells to avoid serious side effects. Additionally, in a context of antigen presentation, antigenic peptides are accommodated in peptide-binding grooves of MHC molecules. Amino acid residues of the peptides contribute to the biding in different manners and determine specificity of the peptide to different MHC alleles [292-294]. Thus, matching the peptides to specific MHC alleles is needed for the therapy relying on the immune system. In this chapter, Pb9 epitope (SYIPSAEKI) from *Plasmodium berghei* was chosen as a target antigen because it is a foreign antigen

and can be used in combination with malarial vaccine (ME.TRAP). The epitope is compatible to H-2K^d MHC of Balb/c mice allowing an efficient presentation of the epitope on the tumour cell surface [295]. It is worth to note that MHC molecules can accommodate only a short peptide within the range of 8-10 amino acid residues. To assure that Pb9 epitope is generated correctly, the epitope was fused in frame with either TIP epitope or ubiquitin. TIP as Tuberculosis, Immunodeficiency virus and *Plasmodium* epitope string is also considered as a helping epitope and believed to accelerate the immune responses against tumour cells when the epitopes are processed and presented on the tumour cell surface [288, 296]. The two constructs of Pb9 with TIP or ubiquitin were compared their function as a target antigen *in vitro* and one of them was chosen for *in vivo* investigation.

As mentioned before, PAAV vector is targeted to tumour cells through a binding of RGD4C ligands to $\alpha_v\beta_3$ and/or $\alpha_v\beta_5$ integrin receptors. EF43.fgf4 cells show their suitability as a preclinical tumour model for PAAV as they highly express all integrin subunits required for the binding. The cells can be targeted by PAAV and generate desirable levels of Lucia reporter gene expression when transduced with a targeted vector. The suitability of EF43.fgf4 cells also ensures by their MHC class I expression. Because Pb9 epitope is delivered to EF43.fgf4 cells as a transgene inserted in PAAV genome, *Pb9* sequence is transcribed and processed via endogenous pathway and finally presented through the specific H2-K^d MHC class I molecule. Although MHC class I is expressed on all nucleated cells, some tumour cells are reported for the MHC class I down-regulation to avoid immunosurveillance [124]. Thus, it is more promising for the therapy if the tumour cells strongly express antigen specific presenting molecules. In particular, EF43.fgf4 cells highly express H2-K^d MHC class I molecules which are restricted for Pb9 epitope. Taking this into account, the epitope should be efficiently presented as a target antigen and should provide a great benefit for the therapeutic strategy.

Pb9 expression detected from PAAV plasmid transfection and PAAV vector transduction confirms the transducing efficacy of the vector. The expression was

assessed only at the mRNA level because there is no antibody against Pb9 epitope. PAAV-mediated Pb9 expression at the protein level was attempted to achieve using protein tag (V5 tag). The *V5 tag* DNA sequence was fused in frame at the C-terminal of *Pb9* epitope. However, no expression was detected by neither western blotting nor fluorescent staining. Although Pb9 expression at protein level was not successfully assessed, *ex vivo* findings indirectly suggested the presentation of Pb9 epitope on the tumour cell surface via an activation of splenocytes obtained from vaccinated mice when culturing them with EF43fgf4 cells expressing PAAV-mediated Pb9. In addition, there is a Pb9 H2-K^d tetramer commonly used to detect Pb9-specific cytotoxic T cells [297]. The tetramer could be applied to investigate the Pb9 epitope expressed on the EF43.fgf4 cell surface. This assay is added in a future plan and will be performed later.

The *ex vivo* experiments were set to investigate the impact of the therapeutic strategy before performing preclinical experiments on animals. As cytotoxic T cells ($CD8^+$ T cells) are known to play a key role in anti-tumour immunity, their population and activity are necessary for a successful therapy. In a field of malaria, ME.TRAP is widely used as a vaccine to induce protective immunity against liver stage parasites. The vaccine showed protective capability on H2-K^d -expressing Balb/c mice from *Plasmodium* challenging [298]. The protection of ME.TRAP vaccine is based on cellular response rather than humoral immunity as the vaccine strongly stimulates cytotoxic T cells [299]. In this chapter, *ME.TRAP* sequence carried by an adenoviral vector showed similar results as reported in previous literatures. The increase of $CD3^+CD8^+$ cell population detected on splenocytes of ME.TRAP-vaccinated mice represented a stimulation of cellular immunity which is needed for anti-tumour activity. The vaccine itself is considered to generate immune response against many infectious diseases as well as cancer [295]. Although the ME.TRAP efficiency is known to rely on $CD8^+$ T cell activity, it is worth noting that a small population of $CD3^-CD4^+$ cells was detected from the vaccinated splenocytes in this *ex vivo* investigation. This cell population is believed to promote T cell survival and support helper T cells for memory antibody responses [300]. In term of memory B cells, they can rapidly generate a specific response when re-exposed to small amount of antigen. The

population of $CD3^{-}CD4^{+}$ cells could offer a basis protective approach when the tumour relapses. However more investigation are required in order to confirm their contribution in cancer therapy.

The activation of specific immune cells was confirmed by IFN-γ secretion. IFN-γ is a soluble cytokine released from both innate and adaptive immune cells such as NK cells and cytotoxic T cells. However, IFN-γ secreting cells found in this *ex vivo* experiment is believed to be cytotoxic T cells rather than NK cells as ME.TRAP vaccine mainly stimulates adaptive immune response based on $CD8^{+}$ T cell activity [299]. Also, Pb9 epitope is restricted to H2-K^{d} MHC class I molecules which are compatible with Balb/c $CD8^{+}$ T cells [295]. A release of IFN-γ affects many immune cells within the tumour environment that benefits the therapy as it is related to an activation of anti-tumour immunity and also an inhibition of immunosuppressive immune cell activity [301]. In addition, the IFN-γ secreting spots solely detected when vaccinated splenocytes were cultured with EF43.fgf4 cells expressing Pb9 indicate the antigen specific activation of $CD8^{+}$ T cells. An attenuated fowlpox virus (FPV) vaccine encoding *Plasmodium berghei* circumsporozoite (PbCS) strongly stimulated IFN-γ secreting Balb/c splenocytes against Pb9 epitope where the frequency of the Pb9 specific IFN-γ secreting cells was correlated with the protection against malarial sporozoite challenge in mice [302].

Apart from the activation of the antigen specific $CD8^{+}$ T cells, their function against tumours is truly needed for the cell killing. The biological function of activated tumour specific immune cells can be investigated through many indicators including granzymes. As cell-death inducing enzymes, granzymes are stored in granules inside $CD8^{+}$ T cells and NK cells, then released into target cells together with perforin molecules whose expression are induced during T cell activation. Despite their intracellular cytotoxic function inside tumour cells, low concentration of granzymes is also detected in serum [303]. Among their several types, granzyme b is the most well studied one and known to activate cell death through caspase-3 cascade apoptotic pathway [304, 305]. The concentration of granzyme b detected from the co-culture media of vaccinated splenocytes and

EF43.fgf4 expressing Pb9 epitope indicates the anti-tumour activity of Pb9 specific $CD8^+$ T cells. Although Pb9 epitope is served as a specific antigen to stimulate specific immune responses, a marginal increase of granzyme b concentration was detected from the co-culture media of vaccinated splenocytes and EF43.fgf4 cells without Pb9 expression. This could be related to innate anti-tumour activity of NK cells as they recognise their targets in MHC unrestricted manner and do not require specific antigen to stimulate their cytotoxic activity [306]. Also, the granzyme b circulation was found increased in *Plasmodium falciparum* infection patients [303].

Ex vivo anti-tumour activity of the vaccinated splenocytes in killing EF43.fgf4 cells not only gave a hope for the successful therapy but also indicated the possibility of applying malaria vaccine and tumour-targeted PAAV vector encoding malarial antigen for cancer treatment. The vaccination with Ty virus like particles encoding a string of malarial antigens elicited cytotoxic T cells responses against Pb9 epitope in Balb/c mice. The immunised murine splenocytes mediated 18-23% specific cell lysis in Pb9 peptide-prepulsed P815 H2-K^d cells between 10:1 and 40:1 of effector:target ratio. The cytotoxicity was detected by ^{51}Cr releasing assay [287]. According to cell-mediated cytotoxicity mechanism, it is believed that Pb9-expressing EF43.fgf4 cells are recognised by specific cytotoxic T cells through an interaction of TCR-CD3 and Pb9-H2-K^d MHC I complexes as well as co-stimulatory signals (CD8 and CD28). The tumour cell killing is mediated via two main mechanisms; 1) granule exocytosis of pore forming protein and granzymes, and, 2) death ligands such as FasL, TNFα and TRAIL. Both mechanisms are known to induce apoptotic cell death through Caspase 3-dependent and cytochrome c releasing pathway [307, 308]. Interestingly, the tumour killing was found through SRB assay when vaccinated splenocytes were cultured with non-Pb9 expressing EF43.fgf4 cells at the high ratio of the effector cells. It is believed to be an innate immune response of NK cells as they show spontaneous cytolytic activity against tumours under MHC unrestricted manner [309]. Moreover, it has been proposed that NK cells could limit the early stage of asexual parasite replication in malaria challenge rodent model [310].

In vivo experiment to investigate the success of the therapeutic strategy were performed in Bal/c mice. Initially, EF43.fgf4 cells were subcutaneously inoculated to the mice to estimate tumour growth rate on the animals. The preliminary therapy was conducted with targeted PAAV encoding *TIP.Pb9* or *ubiquitin.Pb9* sequence (RGD.PAAV.*TIP.Pb9* or RGD.PAAV. *ubi.Pb9*). Both PAAV vector showed the capability to delay tumour growth in equal efficiency which is correlated to *ex vivo* findings mentioned before. Interestingly, a couple of mice in the group receiving RGD.PAAV.*ubi.Pb9* were found drying out and developing scab which seemed to be a good sign of the therapy. However, the mice lost the scab in few days later, which could be from scratching, and the tumours were defined as broken with bleeding. The mice were finally culled as the broken tumour is counted as an endpoint of the animals noted in our animal Project Licence (PPL), even the mice were still active and did not show any suffering signs or weight loss. Based on *in vivo* and *ex vivo* findings, PAAV vector encoding *ubiquitin.Pb9* sequence was chosen for the next therapeutic experiments.

To make it more convenient to monitor tumour growth as well as the therapeutic response, EF43.fgf4 cells stably expressing luciferase reporter gene were used in this experiment. Although the mice were injected with less number of luciferase-expressing EF43.fgf4 cells (80,000 cells/mouse) than the previous experiment, attempting to slow down tumour growth rate, all the mice were culled within 16 days post vector injection as the tumours had reached the maximum tumour size allowed under our PPL. The tumour activity assessed by bioluminescent imaging indicated a promising impact of the therapeutic strategy in combination with malaria vaccine and the tumour-targeting PAAV vector encoding malarial antigen. Histological analyses of the tumours after endpoint of the *in vivo* experiment showed the related outcomes to the tumour cell bioactivity measured by bioluminescent imaging. The lowest density of tumour cells and the highest cleaved Caspase-3 activity were observed on the tumour section from the mice that received ME.TRAP vaccine and targeted PAAV encoding *Pb9*. According to the cell-mediated cytotoxicity, the main mechanism of cell death is Caspase-3 dependent pathway. The activation of cleaved Caspase-3 and its further cascades leads to tumour apoptotic cell death [307]. These findings

indicated that the specific anti-tumour immunity against Pb9 epitope leads to tumour cell death.

However, the vaccinated animals received targeted vector without *Pb9* also showed a delayed tumour growth monitoring by bioluminescent imaging. This could be an effect of RGD4C-targeting peptides which have a marginal anti-tumour activity [245, 311]. The vector itself is also considered to induce anti-viral immune response restricted to viral replication and assembly through innate immunity [312]. This might contribute to a synergistic effect on anti-tumour immunity. Moreover, the malaria vaccine tends to accelerate anti-tumour immunity through helper T cells which link to innate immunity [310, 313]. Together with damaged-associated molecular patterns (DAMPs) generated and served as danger signals for the immune cells within the tumour microenvironment [314], these could cause moderate tumour cell death without the malarial antigen presented on the tumour cell surface. However, further investigation is suggested in order to confirm these points.

In the field of malaria, it has been reported that various types of malarial vaccines such as DNA vaccines, Ty-virus-like particles and recombinant viruses stimulated desirable $CD8^+$ T cell responses against malarial antigens in rodent models. However, a significant anti-malaria activity was not achieved when performing single or repeated homologous immunizations [284, 315-320]. This could be the reason of a fair achievement of the *in vivo* outcomes where EF43.fgf4 cells were not completely eliminated by this therapeutic strategy. Furthermore, multiple immunizations with the same viral vaccine platform reduced the vaccine efficiency against malaria because of pre-existing immune response toward the viral epitope [321]. As such, a combination of heterologous vaccine platforms; for example DNA/adenovirus, DNA/MVA, adenovirus/MVA and fowlpox/MVA vaccine encoding the same antigenic sequences has been applied in many studies [295, 299, 302, 321, 322]. Among those, adenovirus/MVA prime-boost regimen shows a promising efficiency on stimulating strong immune responses and its safety in rodents and human [322, 323]. The combination of prime-boost Ad/MVA immunisation provides the

strongest response against Pb9 dominant epitope stimulated by Ad and broader modest responses toward the sub dominant epitopes mediated by MVA in Balb/c mice [324]. Therefore, this heterologous vaccine regimen has been applied in a wild range of diseases including malaria, tuberculosis, human immunodeficiency virus, influenza and hepatitis C [325-331]. According to all bases of effective immune responses and safety in human, prime-boost Ad/MVA vaccination is considered to be useful for treating cancers in combination with tumour-targeting PAAV vector.

In summary, the *ex vivo* and *in vivo* results in this chapter truly indicate an impact of the therapeutic strategy for treating cancer. Although the tumours were not completely eliminated from the Balb/c mice, a delay of tumour progress and extended survival of the animals were achieved. The tumour density and cleaved Caspase-3 activity also confirmed the specific anti-tumour immunity leading to tumour cell death. However, it is suggested to confirm the therapeutic impact in other Balb/c derived tumour models such as 4T1 breast tumour or CT26 colon carcinoma. Also, prime-boost Ad/MVA vaccination will be applied into the further experiment regarding their efficiency on inducing the immune response. Finally, it is worth to investigate immune cell profiles and checkpoint inhibitors within the tumour microenvironment in order to understand certain situation and enhance the therapeutic impact.

Chapter 6

General discussion and conclusion

It is no doubt that targeting gene delivery has become a powerful tool for treating many diseases. A wide range of delivery systems, simply categorised into viral and non-viral vectors, has been developed and applied in both research and clinical translation. According to the transduction efficacy, viral vectors are considered more efficacious than non-viral vectors. However, viral vectors often possess natural pathogenicity that can be lethally harmful [6]. This raises more attention in the field of vector development to focus on safety of the vectors in parallel with their efficacy. As each vector has distinct strength and weakness relating to its native properties, choosing the most suitable one for the particular therapy is crucial.

A hybrid bacteriophage vector called adeno-associated virus/phage (AAVP) was first-even characterised by Hajitou and colleagues in 2006 [31]. The vector was constructed by integrating adeno-associated virus (AAV) into filamentous phage genome. By doing so, the new vector is able to overcome the limitation of AAV native tropism and adopt the advantages of bacteriophage. To confer tumour specificity, AAVP vector displayed the RGD4C ligand on the pIII capsid protein allowing it to target $\alpha_v\beta_3$ and $\alpha_v\beta_5$ integrins which are overexpressed on tumour cells and angiogenic blood vessels of solid tumours. Although AAVP vector has been applied and proved it efficacy in several *in vitro* and *in vivo* investigations, it can be further modified to achieve better properties. Thus, next generation of hybrid bacteriophage vector called phagemid/ adeno-associated virus (PAAV) has been developed from the basis of AAVP vector in Hajitou group. The new vector is constructed based on a phagemid system which therapeutic genes are encoded in its genome while all structural capsids are provided from the helper

phage. PAAV vector is shorter in size allowing the new vector to be more efficacious in production and application compared to AAVP vector.

It is found that most of the vectors are taken to target cells via clathrin-mediated endocytosis resulting in their entrapment inside the endosomes. Regarding this issue, PAAV vector has been further modified to display the endosomal escape peptide (H5WYG) on recombinant pVIII capsid protein aiming for endosomal escape aspect and enhancement of therapeutic gene expression. The PAAV displaying H5WYG peptide showed great buffering capacity at mild acidic pH relating to the situation during endosomal maturation. The modified vector also enhanced luciferase reporter gene expression in lung carcinoma (A549), melanoma (M21) and meduloblastoma (UW228). There are a number of studies which H5WYG peptide is conjugated to nanocarries and enhanced the vector efficacy. Lee *et al*. conjugated H5WYG and IFN7 peptide to PEG-tetraacrylate (PEG-TA) via a Michael-type addition. The vehicles with either H5WYG or IFN7 peptide showed the highest pH-dependent membrane lytic activity at pH 5.5 and 5, respectively. However the vehicle coupling with INF7 peptide seemed to have greater transfection efficiency than the one with H5WYG peptide [107]. The peptide was also conjugated at the 5'-end of the RNase H-incompetent antisense 2'-O-methyl-phosphodiester oligonucleotide (2'-Ome RNA705) to target aberrant splicing of luciferase pre-mRNA in HeLa pLuc705 cells. The antisense oligonucleotides were also conjugated with fluorescein at 3'-end. After 4 h and overnight of transfection, H5WYG peptide enhanced the presence of fluorescein-labelled 2'-Ome-RNA705 in the cytosol and nucleus. Further, the peptide increased luciferase activity and luciferase mRNA levels in HeLa pLuc705 cells at 6.6- and 2-fold higher, respectively [239]. In this thesis, it is suggested that the efficacy of H5WYG peptide relies on proton sponge effect which destabilise and burst the endosome. This hypothesis confirmed by a decrease of the PAAV-mediated gene expression when applying vascuolar ATPase inhibitor (bafilomycin A1) to the vector transduction. Also, Far-UV circular dichroism analysis performed by Alipour *et al.* evaluated the influence of pH between 7.4-5.4 on the secondary structure of their peptide-based vector conjugated with H5WYG peptide. The vector with H5WYG underwent conformation change from

non-structured to helical conformation at low pH [241]. This suggested a conformational change of the peptide during endosomal maturation which eventually led to proton sponge effect and endosomal rupture. In addition, H5WYG peptide can enhance vector-mediated gene expression in tumour cells but did not mediate any gene expression in lung fibroblasts, skin fibroblasts and astrocytes which are normal cells related to the chosen tumour models. This confirmed efficacy and specificity of the modified PAAV in tumour cells. Furthermore, displaying H5WYG peptide on PAAV capsids augmented the secreted TNFα gene expression resulting in a greater cell death of A549, M21 and UW228 cells. Based on the findings in this thesis, it is suggested that displaying the H5WYG peptide can enhance the vector efficacy which could be beneficial in many applications. Last but not least, the capability of H5WYG peptide is unaffected by the presence of serum providing an added advantage for in vivo gene delivery [237].

Despite many characterisations of PAAV vector conducted in our group, more investigation especially its application remains to be done. Recently, PAAV vector has been applied in AAV production to replace the plasmid transfection methods which are not appropriate for large-scale production. Also the vector has been used either alone or in combination with other therapeutic agents in pre-clinical cancer immunotherapy. Current applications of PAAV tested in our group are to express cytokines such as TNFα and various interleukins at the tumour site and to deliver target antigens to tumour cells. The results in chapters 4 and 5 of this thesis represented some parts of the PAAV application for CAR T cells and cancer vaccine strategy where the vector was applied as a delivery tool to express selected antigens on tumour cells.

In chapter 4, PAAV encoding *MUC1* or *PSMA* gene was used to mediate MUC1 and PSMA expression in several types of tumours. Although these two antigens are overexpressed in tumour cells and commonly used as a target for CAR T cell therapy, one obstacle in this treatment strategy is instability of the tumour antigen expression and antigen loss due to the tumour heterogeneity. It has been suggested that as few as one peptide-MHC complex is sufficient to trigger T-cell

activation, as well as, IL-2 and TNF-α secretion [332, 333]. However, this issue remains controversy. Watanabe *et al.* investigated the density of CD20 molecule required to activate CD20-specific CAR T cells and found that target cells expressing around 200 molecules/cell could induce lysis by CAR T cells [334]. This outcome was consistent with a previous finding from Stone *et al.* who suggested that CAR targeting a tumour-specific glycol-epitope of murine OTS8 could lyse target cells with similarly low density (~200 molecules/cell) of target antigen [335]. Despite those reports, it has been demonstrated that nearly 5,000 molecules/cell of CD20 were required for cytokine production and T cell proliferation [334]. In addition, Walker *et al.* investigated activation of ALK-specific CAR T cells on Nalm6 cells expressing various densities of ALK molecule (~18,000–450,000 molecules/cell) and found that CAR T cells could lyse the target cells at the lowest ALK expression in this target cell panel (~18,000 molecules/cell). However, approximately 60,000 and 30,000 molecules/cell of ALK were required for IL-2 and IFN-γ production, respectively [336]. According to the findings from Watanabe *et al.* and Walker *et al.*, there was a difference in threshold of IFN-γ production which may result from differences in the CAR constructs or the density of CAR expression [337]. Further, Liu *et al.* developed a strategy for CAR T cells to discriminate tumours overexpressing target antigen from normal tissues that express the antigen at basal levels. The study suggested that CARs have a considerably lower threshold of antigen expression for target cell lysis which may depend on CAR- or scFv-affinity [338]. From all these research it is suggested that each T cell subset or each single T cell has a distinct threshold to be activated, as well as, it is undoubted that target antigen density on tumour cells is one of a key factor contributing to a successful CAR T cell therapy [337]. By using PAAV as a delivery tool, it showed here that MUC1 and PSMA expression on the tumour cells tend to increase from their endogenous expression. Although we did not perform any experiments with CAR T cells, it is suggested that PAAV vector can contribute advantages in this field in the future particularly for treating solid tumours. For example, this application can be used to generate or enhance antigen expression on tumour cells conferring antigen loss and making the tumours more visible for CAR T cells. Also it can be applied to dual CARs T cell strategy for a double safety on normal cells.

PAAV vector was also used as a delivery tool for cancer vaccine combining with malaria vaccine. Generally, cancer vaccine requires two fundamentals, target antigen and vaccine platform, to accomplish anti-tumour immunity. Therefore, in chapter 5 of this thesis, a malarial epitope (Pb9) was chosen as a target antigen. As a foreign antigen, Pb9 provides more privilege in safety and immunogenicity for the therapy. The epitope was delivered by PAAV vector to present on tumour cells via restricted H2-K^d MHC class I molecules making Pb9 as an artificial tumour specific antigen. In the mean time, adenoviral vector encoding a malaria sequence (ME.TRAP) was used to stimulate an immune response against Pb9. In the field of malaria, Pb9 epitope is responsive compatibly with ME.TRAP vaccine to elicit a desirable anti-malarial immunity which, in this case, the combination was used to induce anti-tumour immunity. Cancer vaccine mainly relies on the interaction between tumours and tumour-specific effector immune cells. This activity initiates from the recognition of the antigen epitope-MHC complex on tumour cells by the specific immune cells and follows by the generation of tumour cell killing. Grossardt *et al*. constructed a therapeutic cancer vaccine from oncolytic measles viruses expressing granulocyte and macrophage colony-stimulating factor (GM-CSF). The vectors were targeted to MC38cea cells expressing human carcinoembryonic antigen (CEA) and showed promising therapeutic effect to delay tumour progression and prolong median overall survival compared to control virus-treated mice [339]. In addition, as mentioned before, matching the antigen epitope with MHC complex subclass is crucial for cancer vaccine strategy. The choice of target antigen is sometimes limited for some tumour types or some patients that lack the compatible MHC complex. Therefore, some researchers have applied various approaches to overcome the MHC restriction issue. Capasso *et al*. developed Peptide-coated Conditionally Replicating Adeno-viruses (PeptiCRAds) which coated with specific tumour epitope-MHC I complex on the viral surfaces. PeptiCRAds with SIINFEKL epitope showed a superior anti-tumour efficacy and increased the percentage of anti-tumour $CD8^+$ T cells and mature epitope-specific dendritic cells *in vivo*. In human melanoma-associated antigen A1 (MAGE-A1) targeting model, PeptiCRAds expressing GM-CSF eradicated established tumours and increased the human MAGE-A1-specific $CD8^+$ T cell population [340]. Regarding the results in this

thesis, it is shown that PAAV vector can mediate Pb9 expression in EF43.fgf4 breast tumour cells. The adeno.ME.TRAP vaccine can stimulate immune response according to *ex vivo* investigations of specific $CD8^+$T cell proliferation, activation and function. Pb9-specific tumour killing was also found both *ex vivo* and *in vivo*. The tumour cell death was mediated through caspase-3 dependent apoptosis which is the lower cascade of perforin/granzyme b pathway. All the findings here indicate the feasibility and efficiency of this therapeutic strategy for treating cancer. However, Pb9 epitope is restricted to H2-K^d MHC class I molecules of Balb/c mice. New target epitope compatible with human HLA allele is needed to perform further experiment in humanised mice.

According to the immune escape mechanisms and genomic instability of tumours, they sometime reduce or lose antigen expression and become invisible for the immune cells providing benefit for tumour progress. Applying PAAV vector as a delivery tool is considered to fulfil the target antigen issue for cancer immunotherapy. The vector encoding the tumour antigen sequence can be specifically targeted to tumour cells to mediate or enhance the antigen expression. Regarding previous *in vivo* experiments in our group, PAAV vector can be injected repeatedly to the animals without showing any harmful signs. Repeating the vector injection could further increase the expression level of target antigen and maximise the therapeutic potential. Furthermore, it is worth to mention that PAAV vector can be applied on many tumour cells expressing the specific integrins. This can fulfil the lack of target antigen in some tumour types and generalise the therapeutic approach on a wide range of cancer patients.

As mentioned before, PAAV vector is targeted to tumour cells through RGD4C ligands that bind to $\alpha_v\beta_3$ and $\alpha_v\beta_5$ integrins. These heterodimer integrins are prominently involved in tumourigenesis and overexpressed in a wide variety of cancer [341]. It is also well established that $\alpha_v\beta_3$ integrins are hallmarks of angiogenesis and highly expressed on tumour blood vessels. These provide double targeting of PAAV to not only tumour cells but also tumour blood vessels. In term of safety issues, all nanoparticles including PAAV are expected to be specific for their target cells but not harmful to normal cells. Unpublished data in

our group showed PAAV efficacy in a wide range of tumour types, such as brain tumours, melanoma, breast tumours, pancreatic tumours and lung cancer, as well as primary brain tumours and cancer stem cells. Interestingly, sets of experiments on lung fibroblasts, skin fibroblasts and astrocytes confirmed the vector safety on normal cells as none of reporter gene expression was detected when transducing with PAAV vector. These findings indicate specific efficacy of the vector for tumour cells while remaining safe for normal cells. Taken together, its efficacy, specificity and safety, the new hybrid vector, PAAV, shows promising aspects to make advancement in cancer gene therapy.

Regarding to the results in this thesis, there are some experiments suggested to complete in the future. For the PAAV vector modification by displaying H5WYG endosomal escape peptide, intracellular trafficking of the modified vector should be investigated in comparison to PAAV without H5WYG peptide. *In vivo* experiments of the modified vector is also needed for both reporter gene expression and therapeutic genes. For cancer vaccine strategy, it is suggested to use adeno/MVA prime-boost regimens instead of adenoviral vector alone. Also, the therapeutic effect should be confirmed in other tumour cell lines such as 4T1 breast tumour or CT26 colon carcinoma. Last, but not least, investigating the immune cell profiles and checkpoint inhibitors within the tumour microenvironment is believed to benefit the treatment and can improve the therapeutic impact in the future.

Bibliography

1. Sung, Y.K. and S.W. Kim, *Recent advances in the development of gene delivery systems.* Biomater Res, 2019. **23**: p. 8.
2. Goncalves, G.A.R. and R.D.A. Paiva, *Gene therapy: advances, challenges and perspectives.* Einstein-Sao Paulo, 2017. **15**(3): p. 369-375.
3. Han, S., et al., *Development of biomaterials for gene therapy.* Mol Ther, 2000. **2**(4): p. 302-17.
4. Moss, B., et al., *Live recombinant vaccinia virus protects chimpanzees against hepatitis B.* Nature, 1984. **311**(5981): p. 67-9.
5. Godbey, W.T., *An Introduction to Biotechnology*. 2015: Academic Press. 436.
6. Lehrman, S., *Virus treatment questioned after gene therapy death.* Nature, 1999. **401**(6753): p. 517-8.
7. Hidai, C. and H. Kitano, *Nonviral Gene Therapy for Cancer: A Review.* Diseases, 2018. **6**(3).
8. Nayerossadat, N., T. Maedeh, and P.A. Ali, *Viral and nonviral delivery systems for gene delivery.* Adv Biomed Res, 2012. **1**: p. 27.
9. Zhou, Z., et al., *Nonviral cancer gene therapy: Delivery cascade and vector nanoproperty integration.* Adv Drug Deliv Rev, 2017. **115**: p. 115-154.
10. Dormond, E., M. Perrier, and A. Kamen, *From the first to the third generation adenoviral vector: what parameters are governing the production yield?* Biotechnol Adv, 2009. **27**(2): p. 133-44.
11. Lang, F.F., et al., *Phase I trial of adenovirus-mediated p53 gene therapy for recurrent glioma: biological and clinical results.* J Clin Oncol, 2003. **21**(13): p. 2508-18.
12. Westphal, M., et al., *Adenovirus-mediated gene therapy with sitimagene ceradenovec followed by intravenous ganciclovir for patients with operable high-grade glioma (ASPECT): a randomised, open-label, phase 3 trial.* Lancet Oncol, 2013. **14**(9): p. 823-33.
13. Rodrigues, G.A., et al., *Pharmaceutical Development of AAV-Based Gene Therapy Products for the Eye.* Pharm Res, 2018. **36**(2): p. 29.
14. Yla-Herttuala, S., *Endgame: glybera finally recommended for approval as the first gene therapy drug in the European union.* Mol Ther, 2012. **20**(10): p. 1831-2.
15. Naso, M.F., et al., *Adeno-Associated Virus (AAV) as a Vector for Gene Therapy.* BioDrugs, 2017. **31**(4): p. 317-334.
16. Daya, S. and K.I. Berns, *Gene therapy using adeno-associated virus vectors.* Clin Microbiol Rev, 2008. **21**(4): p. 583-93.
17. Zincarelli, C., et al., *Analysis of AAV serotypes 1-9 mediated gene expression and tropism in mice after systemic injection.* Mol Ther, 2008. **16**(6): p. 1073-80.
18. Deyle, D.R. and D.W. Russell, *Adeno-associated virus vector integration.* Curr Opin Mol Ther, 2009. **11**(4): p. 442-7.
19. Kaeppel, C., et al., *A largely random AAV integration profile after LPLD gene therapy.* Nature Medicine, 2013. **19**(7): p. 889-+.

20. Daniel, R. and J.A. Smith, *Integration site selection by retroviral vectors: Molecular mechanism and clinical consequences.* Human Gene Therapy, 2008. **19**(6): p. 557-568.
21. Barquinero, J., H. Eixarch, and M. Perez-Melgosa, *Retroviral vectors: new applications for an old tool.* Gene Therapy, 2004. **11**: p. S3-S9.
22. Kay, M.A., J.C. Glorioso, and L. Naldini, *Viral vectors for gene therapy: the art of turning infectious agents into vehicles of therapeutics.* Nature Medicine, 2001. **7**(1): p. 33-40.
23. Salmond, G.P. and P.C. Fineran, *A century of the phage: past, present and future.* Nat Rev Microbiol, 2015. **13**(12): p. 777-86.
24. Clokie, M.R., et al., *Phages in nature.* Bacteriophage, 2011. **1**(1): p. 31-45.
25. Kazi, M. and U.S. Annapure, *Bacteriophage biocontrol of foodborne pathogens.* J Food Sci Technol, 2016. **53**(3): p. 1355-62.
26. Jepson, C.D. and J.B. March, *Bacteriophage lambda is a highly stable DNA vaccine delivery vehicle.* Vaccine, 2004. **22**(19): p. 2413-9.
27. Garcia, P., et al., *Bacteriophages and their application in food safety.* Lett Appl Microbiol, 2008. **47**(6): p. 479-85.
28. Clackson, T. and B.H. Lowman, *Phage Display: A Practical Approach*. 2004: Oxford University Press.
29. Bradbury, A.R.M., et al., *Beyond natural antibodies: the power of in vitro display technologies.* Nature Biotechnology, 2011. **29**(3): p. 245-254.
30. Larocca, D., et al., *Gene transfer to mammalian cells using genetically targeted filamentous bacteriophage.* Faseb Journal, 1999. **13**(6): p. 727-734.
31. Hajitou, A., et al., *A hybrid vector for ligand-directed tumor targeting and molecular imaging.* Cell, 2006. **125**(2): p. 385-98.
32. Hajitou, A., *Targeted systemic gene therapy and molecular imaging of cancer contribution of the vascular-targeted AAVP vector.* Adv Genet, 2010. **69**: p. 65-82.
33. Smith, T.L., et al., *AAVP displaying octreotide for ligand-directed therapeutic transgene delivery in neuroendocrine tumors of the pancreas.* Proc Natl Acad Sci U S A, 2016. **113**(9): p. 2466-71.
34. Paoloni, M.C., et al., *Launching a novel preclinical infrastructure: comparative oncology trials consortium directed therapeutic targeting of TNFalpha to cancer vasculature.* PLoS One, 2009. **4**(3): p. e4972.
35. Hajitou, A., et al., *A preclinical model for predicting drug response in soft-tissue sarcoma with targeted AAVP molecular imaging.* Proc Natl Acad Sci U S A, 2008. **105**(11): p. 4471-6.
36. Przystal, J.M., et al., *Efficacy of systemic temozolomide-activated phage-targeted gene therapy in human glioblastoma.* EMBO Mol Med, 2019. **11**(4).
37. Trepel, M., et al., *A heterotypic bystander effect for tumor cell killing after adeno-associated virus/phage-mediated, vascular-targeted suicide gene transfer.* Molecular Cancer Therapeutics, 2009. **8**(8): p. 2383-2391.
38. Tandle, A., et al., *Tumor Vasculature-targeted Delivery of Tumor Necrosis Factor-alpha.* Cancer, 2009. **115**(1): p. 128-139.
39. Pranjol, M.Z. and A. Hajitou, *Bacteriophage-derived vectors for targeted cancer gene therapy.* Viruses, 2015. **7**(1): p. 268-84.

40. Ferrari, M., *Frontiers in cancer nanomedicine: directing mass transport through biological barriers.* Trends in Biotechnology, 2010. **28**(4): p. 181-188.
41. Blanco, E., H. Shen, and M. Ferrari, *Principles of nanoparticle design for overcoming biological barriers to drug delivery.* Nat Biotechnol, 2015. **33**(9): p. 941-51.
42. Pecot, C.V., et al., *RNA interference in the clinic: challenges and future directions.* Nat Rev Cancer, 2011. **11**(1): p. 59-67.
43. Nishikawa, M., et al., *Targeted delivery of plasmid DNA to hepatocytes in vivo: optimization of the pharmacokinetics of plasmid DNA/galactosylated poly(L-lysine) complexes by controlling their physicochemical properties.* J Pharmacol Exp Ther, 1998. **287**(1): p. 408-15.
44. Choi, H.S., et al., *Renal clearance of quantum dots.* Nat Biotechnol, 2007. **25**(10): p. 1165-70.
45. Deen, W.M., M.J. Lazzara, and B.D. Myers, *Structural determinants of glomerular permeability.* Am J Physiol Renal Physiol, 2001. **281**(4): p. F579-96.
46. Yuan, F., et al., *Microvascular permeability and interstitial penetration of sterically stabilized (stealth) liposomes in a human tumor xenograft.* Cancer Res, 1994. **54**(13): p. 3352-6.
47. Csortos, C., I. Kolosova, and A.D. Verin, *Regulation of vascular endothelial cell barrier function and cytoskeleton structure by protein phosphatases of the PPP family.* Am J Physiol Lung Cell Mol Physiol, 2007. **293**(4): p. L843-54.
48. Yuan, F., et al., *Vascular permeability in a human tumor xenograft: molecular size dependence and cutoff size.* Cancer Res, 1995. **55**(17): p. 3752-6.
49. Cabral, H., et al., *Accumulation of sub-100 nm polymeric micelles in poorly permeable tumours depends on size.* Nat Nanotechnol, 2011. **6**(12): p. 815-23.
50. Jacobetz, M.A., et al., *Hyaluronan impairs vascular function and drug delivery in a mouse model of pancreatic cancer.* Gut, 2013. **62**(1): p. 112-U153.
51. Chauhan, V.P., et al., *Normalization of tumour blood vessels improves the delivery of nanomedicines in a size-dependent manner.* Nature Nanotechnology, 2012. **7**(6): p. 383-388.
52. Hobbs, S.K., et al., *Regulation of transport pathways in tumor vessels: Role of tumor type and microenvironment.* Proceedings of the National Academy of Sciences of the United States of America, 1998. **95**(8): p. 4607-4612.
53. Banks, W.A., *Characteristics of compounds that cross the blood-brain barrier.* Bmc Neurology, 2009. **9**.
54. Stylianopoulos, T., et al., *Diffusion of Particles in the Extracellular Matrix: The Effect of Repulsive Electrostatic Interactions.* Biophysical Journal, 2010. **99**(5): p. 1342-1349.
55. Whitehead, K.A., R. Langer, and D.G. Anderson, *Knocking down barriers: advances in siRNA delivery.* Nature Reviews Drug Discovery, 2009. **8**(2): p. 129-138.

56. Leopold, P.L. and R.G. Crystal, *Intracellular trafficking of adenovirus: Many means to many ends.* Advanced Drug Delivery Reviews, 2007. **59**(8): p. 810-821.
57. Luhmann, T., et al., *Cellular uptake and intracellular pathways of PLL-g-PEG-DNA nanoparticles.* Bioconjugate Chemistry, 2008. **19**(9): p. 1907-1916.
58. Hilgenbrink, A.R. and P.S. Low, *Folate receptor-mediated drug targeting: From therapeutics to diagnostics.* Journal of Pharmaceutical Sciences, 2005. **94**(10): p. 2135-2146.
59. Xu, L.A., et al., *Transferrin-liposome-mediated systemic p53 gene therapy in combination with radiation results in regression of human head and neck cancer xenografts.* Human Gene Therapy, 1999. **10**(18): p. 2941-2952.
60. Garanger, E., D. Boturyn, and P. Dumy, *Tumor targeting with RGD peptide Ligands-Design of new molecular conjugates for Imaging and therapy of cancers.* Anti-Cancer Agents in Medicinal Chemistry, 2007. **7**(5): p. 552-558.
61. Gao, H.J., W.D. Shi, and L.B. Freund, *Mechanics of receptor-mediated endocytosis.* Proceedings of the National Academy of Sciences of the United States of America, 2005. **102**(27): p. 9469-9474.
62. Huotari, J. and A. Helenius, *Endosome maturation.* Embo Journal, 2011. **30**(17): p. 3481-3500.
63. Scott, C.C., F. Vacca, and J. Gruenberg, *Endosome maturation, transport and functions.* Seminars in Cell & Developmental Biology, 2014. **31**: p. 2-10.
64. Huang, J.G., T. Leshuk, and F.X. Gu, *Emerging nanomaterials for targeting subcellular organelles.* Nano Today, 2011. **6**(5): p. 478-492.
65. Stewart, M., *Molecular mechanism of the nuclear protein import cycle.* Nat Rev Mol Cell Biol, 2007. **8**(3): p. 195-208.
66. Collas, P., H. Husebye, and P. Alestrom, *The nuclear localization sequence of the SV40 T antigen promotes transgene uptake and expression in zebrafish embryo nuclei.* Transgenic Res, 1996. **5**(6): p. 451-8.
67. Cho, Y.W., J.D. Kim, and K. Park, *Polycation gene delivery systems: escape from endosomes to cytosol.* J Pharm Pharmacol, 2003. **55**(6): p. 721-34.
68. Dimitrov, D.S., *Virus entry: molecular mechanisms and biomedical applications.* Nat Rev Microbiol, 2004. **2**(2): p. 109-22.
69. Varkouhi, A.K., et al., *Endosomal escape pathways for delivery of biologicals.* J Control Release, 2011. **151**(3): p. 220-8.
70. Mandal, M. and K.D. Lee, *Listeriolysin O-liposome-mediated cytosolic delivery of macromolecule antigen in vivo: enhancement of antigen-specific cytotoxic T lymphocyte frequency, activity, and tumor protection.* Biochim Biophys Acta, 2002. **1563**(1-2): p. 7-17.
71. Martens, T.F., et al., *Intracellular delivery of nanomaterials: How to catch endosomal escape in the act.* Nano Today, 2014. **9**(3): p. 344-364.
72. Lear, J.D. and W.F. DeGrado, *Membrane binding and conformational properties of peptides representing the NH2 terminus of influenza HA-2.* J Biol Chem, 1987. **262**(14): p. 6500-5.
73. Wiley, D.C. and J.J. Skehel, *The Structure and Function of the Hemagglutinin Membrane Glycoprotein of Influenza-Virus.* Annual Review of Biochemistry, 1987. **56**: p. 365-394.

74. Lin, C., et al., *Novel bioreducible poly(amido amine)s for highly efficient gene delivery.* Bioconjugate Chemistry, 2007. **18**(1): p. 138-145.
75. Boussif, O., et al., *A Versatile Vector for Gene and Oligonucleotide Transfer into Cells in Culture and in-Vivo - Polyethylenimine.* Proceedings of the National Academy of Sciences of the United States of America, 1995. **92**(16): p. 7297-7301.
76. Murata, M., et al., *pH-dependent membrane fusion activity of a synthetic twenty amino acid peptide with the same sequence as that of the hydrophobic segment of influenza virus hemagglutinin.* J Biochem, 1987. **102**(4): p. 957-62.
77. Wagner, E., et al., *Influenza-Virus Hemagglutinin-Ha-2 N-Terminal Fusogenic Peptides Augment Gene-Transfer by Transferrin Polylysine DNA Complexes - toward a Synthetic Virus-Like Gene-Transfer Vehicle.* Proceedings of the National Academy of Sciences of the United States of America, 1992. **89**(17): p. 7934-7938.
78. Lewin, M., et al., *Tat peptide-derivatized magnetic nanoparticles allow in vivo tracking and recovery of progenitor cells.* Nature Biotechnology, 2000. **18**(4): p. 410-414.
79. Lo, S.L. and S. Wang, *An endosomolytic Tat peptide produced by incorporation of histidine and cysteine residues as a nonviral vector for DNA transfection.* Biomaterials, 2008. **29**(15): p. 2408-2414.
80. Kamper, N., et al., *A membrane-destabilizing peptide in capsid protein L2 is required for egress of papillomavirus genomes from endosomes.* Journal of Virology, 2006. **80**(2): p. 759-768.
81. Kimura, T. and A. Ohyama, *Association between the Ph-Dependent Conformational Change of West Nile Flavivirus E-Protein and Virus-Mediated Membrane-Fusion.* Journal of General Virology, 1988. **69**: p. 1247-1254.
82. Tweten, R.K., *Cholesterol-dependent cytolysins, a family of versatile pore-forming toxins.* Infection and Immunity, 2005. **73**(10): p. 6199-6209.
83. Walton, C.M., C.H. Wu, and G.Y. Wu, *A DNA delivery system containing listeriolysin O results in enhanced hepatocyte-directed gene expression.* World Journal of Gastroenterology, 1999. **5**(6): p. 465-469.
84. Saito, G., G.L. Amidon, and K.D. Lee, *Enhanced cytosolic delivery of plasmid DNA by a sulfhydryl-activatable listeriolysin O/protamine conjugate utilizing cellular reducing potential.* Gene Therapy, 2003. **10**(1): p. 72-83.
85. Lorenzi, G.L. and K.D. Lee, *Enhanced plasmid DNA delivery using anionic LPDII by listeriolysin O incorporation.* Journal of Gene Medicine, 2005. **7**(8): p. 1077-1085.
86. Kullberg, M., J.L. Owens, and K. Mann, *Listeriolysin O enhances cytoplasmic delivery by Her-2 targeting liposomes.* Journal of Drug Targeting, 2010. **18**(4): p. 313-320.
87. Browne, K.A., et al., *Cytosolic delivery of granzyme B by bacterial toxins: Evidence that endosomal disruption, in addition to transmembrane pore formation, is an important function of perforin.* Molecular and Cellular Biology, 1999. **19**(12): p. 8604-8615.
88. London, E., *How Bacterial Protein Toxins Enter Cells - the Role of Partial Unfolding in Membrane Translocation.* Molecular Microbiology, 1992. **6**(22): p. 3277-3282.

89. Ariansen, S., et al., *Membrane Translocation of Diphtheria Toxin-a-Fragment - Role of Carboxy-Terminal Region.* Biochemistry, 1993. **32**(1): p. 83-90.
90. Day, P.J., et al., *Binding of ricin A-chain to negatively charged phospholipid vesicles leads to protein structural changes and destabilizes the lipid bilayer.* Biochemistry, 2002. **41**(8): p. 2836-2843.
91. Sun, J., et al., *Membrane destabilization by ricin.* European Biophysics Journal with Biophysics Letters, 2004. **33**(7): p. 572-579.
92. Vago, R., et al., *Saporin and ricin A chain follow different intracellular routes to enter the cytosol of intoxicated cells.* Febs Journal, 2005. **272**(19): p. 4983-4995.
93. Derossi, D., et al., *Cell internalization of the third helix of the antennapedia homeodomain is receptor-independent.* Journal of Biological Chemistry, 1996. **271**(30): p. 18188-18193.
94. Damante, G., et al., *A molecular code dictates sequence-specific DNA recognition by homeodomains.* Embo Journal, 1996. **15**(18): p. 4992-5000.
95. Dempsey, C.E., *The Actions of Melittin on Membranes.* Biochimica Et Biophysica Acta, 1990. **1031**(2): p. 143-161.
96. Ogris, M., et al., *Melittin enables efficient vesicular escape and enhanced nuclear access of nonviral gene delivery vectors.* Journal of Biological Chemistry, 2001. **276**(50): p. 47550-47555.
97. Rennert, R., I. Neundorf, and A.G. Beck-Sickinger, *Calcitonin-derived peptide carriers: Mechanisms and application.* Advanced Drug Delivery Reviews, 2008. **60**(4-5): p. 485-498.
98. Krauss, U., et al., *In vitro gene delivery by a novel human calcitonin (hCT)-derived carrier peptide.* Bioorganic & Medicinal Chemistry Letters, 2004. **14**(1): p. 51-54.
99. Lundberg, P., et al., *Delivery of short interfering RNA using endosomolytic cell-penetrating peptides.* Faseb Journal, 2007. **21**(11): p. 2664-2671.
100. Parente, R.A., S. Nir, and F.C. Szoka, *Mechanism of Leakage of Phospholipid Vesicle Contents Induced by the Peptide Gala.* Biochemistry, 1990. **29**(37): p. 8720-8728.
101. Futaki, S., et al., *Unique features of a pH-sensitive fusogenic peptide that improves the transfection efficiency of cationic liposomes.* Journal of Gene Medicine, 2005. **7**(11): p. 1450-1458.
102. Min, S.H., et al., *A composite gene delivery system consisting of polyethylenimine and an amphipathic peptide KALA.* Journal of Gene Medicine, 2006. **8**(12): p. 1425-1434.
103. Han, J. and Y.I. Yeom, *Specific gene transfer mediated by galactosylated poly-L-lysine into hepatoma cells.* International Journal of Pharmaceutics, 2000. **202**(1-2): p. 151-160.
104. Li, W.J., F. Nicol, and F.C. Szoka, *GALA: a designed synthetic pH-responsive amphipathic peptide with applications in drug and gene delivery.* Advanced Drug Delivery Reviews, 2004. **56**(7): p. 967-985.
105. Simoes, S., et al., *Mechanisms of gene transfer mediated by lipoplexes associated with targeting ligands or pH-sensitive peptides.* Gene Therapy, 1999. **6**(11): p. 1798-1807.

106. Lee, H., J.H. Jeong, and T.G. Park, *A new gene delivery formulation of polyethylenimine/DNA complexes coated with PEG conjugated fusogenic peptide.* Journal of Controlled Release, 2001. **76**(1-2): p. 183-192.
107. Moore, N.M., et al., *The effect of endosomal escape peptides on in vitro gene delivery of polyethylene glycol-based vehicles.* J Gene Med, 2008. **10**(10): p. 1134-49.
108. Midoux, P. and M. Monsigny, *Efficient gene transfer by histidylated polylysine pDNA complexes.* Bioconjugate Chemistry, 1999. **10**(3): p. 406-411.
109. Ghosn, B., S.P. Kasturi, and K. Roy, *Enhancing polysaccharide-mediated delivery of nucleic acids through functionalization with secondary and tertiary amines.* Current Topics in Medicinal Chemistry, 2008. **8**(4): p. 331-340.
110. Cheung, C.Y., et al., *A pH-sensitive polymer that enhances cationic lipid-mediated gene transfer.* Bioconjugate Chemistry, 2001. **12**(6): p. 906-910.
111. Mellman, I., R. Fuchs, and A. Helenius, *Acidification of the Endocytic and Exocytic Pathways.* Annual Review of Biochemistry, 1986. **55**: p. 663-700.
112. Siegel, R.L., K.D. Miller, and A. Jemal, *Cancer statistics, 2019.* CA Cancer J Clin, 2019. **69**(1): p. 7-34.
113. Urruticoechea, A., et al., *Recent advances in cancer therapy: an overview.* Curr Pharm Des, 2010. **16**(1): p. 3-10.
114. Mellman, I., G. Coukos, and G. Dranoff, *Cancer immunotherapy comes of age.* Nature, 2011. **480**(7378): p. 480-9.
115. Voena, C. and R. Chiarle, *Advances in cancer immunology and cancer immunotherapy.* Discov Med, 2016. **21**(114): p. 125-33.
116. Zhang, H. and J. Chen, *Current status and future directions of cancer immunotherapy.* J Cancer, 2018. **9**(10): p. 1773-1781.
117. Borghaei, H., M.R. Smith, and K.S. Campbell, *Immunotherapy of cancer.* Eur J Pharmacol, 2009. **625**(1-3): p. 41-54.
118. Dunn, G.P., L.J. Old, and R.D. Schreiber, *The immunobiology of cancer immunosurveillance and immunoediting.* Immunity, 2004. **21**(2): p. 137-48.
119. Dunn, G.P., et al., *Cancer immunoediting: from immunosurveillance to tumor escape.* Nature Immunology, 2002. **3**(11): p. 991-998.
120. Shankaran, V., et al., *IFN gamma and lymphocytes prevent primary tumour development and shape tumour immunogenicity.* Nature, 2001. **410**(6832): p. 1107-1111.
121. Teng, M.W.L., et al., *Immunotherapy of cancer using systemically delivered gene-modified human T lymphocytes.* Human Gene Therapy, 2004. **15**(7): p. 699-708.
122. Mittal, D., et al., *New insights into cancer immunoediting and its three component phases elimination, equilibrium and escape.* Current Opinion in Immunology, 2014. **27**: p. 16-25.
123. Aptsiauri, N., et al., *Cancer immune escape: implications for immunotherapy, Granada, Spain, October 3-5, 2011.* Cancer Immunol Immunother, 2012. **61**(5): p. 739-45.
124. Beatty, G.L. and W.L. Gladney, *Immune escape mechanisms as a guide for cancer immunotherapy.* Clin Cancer Res, 2015. **21**(4): p. 687-92.

125. Gun, S.Y., et al., *Targeting immune cells for cancer therapy.* Redox Biology, 2019. **In Press**(Available online 20 March 2019, 101174).
126. Kim, R., M. Emi, and K. Tanabe, *Functional roles of immature dendritic cells in impaired immunity of solid tumour and their targeted strategies for provoking tumour immunity.* Clin Exp Immunol, 2006. **146**(2): p. 189-96.
127. Amsen, D., C.G. Spilianakis, and R.A. Flavell, *How are T(H)1 and T(H)2 effector cells made?* Curr Opin Immunol, 2009. **21**(2): p. 153-60.
128. Sakaguchi, S., *Naturally arising CD4+ regulatory t cells for immunologic self-tolerance and negative control of immune responses.* Annu Rev Immunol, 2004. **22**: p. 531-62.
129. Qian, B.Z. and J.W. Pollard, *Macrophage diversity enhances tumor progression and metastasis.* Cell, 2010. **141**(1): p. 39-51.
130. Sica, A., et al., *Tumour-associated macrophages are a distinct M2 polarised population promoting tumour progression: potential targets of anti-cancer therapy.* Eur J Cancer, 2006. **42**(6): p. 717-27.
131. Pollard, J.W., *Tumour-educated macrophages promote tumour progression and metastasis.* Nat Rev Cancer, 2004. **4**(1): p. 71-8.
132. Burkholder, B., et al., *Tumor-induced perturbations of cytokines and immune cell networks.* Biochimica Et Biophysica Acta-Reviews on Cancer, 2014. **1845**(2): p. 182-201.
133. Dagogo-Jack, I. and A.T. Shaw, *Tumour heterogeneity and resistance to cancer therapies.* Nat Rev Clin Oncol, 2018. **15**(2): p. 81-94.
134. Campoli, M. and S. Ferrone, *HLA antigen changes in malignant cells: epigenetic mechanisms and biologic significance.* Oncogene, 2008. **27**(45): p. 5869-85.
135. Kitamura, H., et al., *Effect of human leukocyte antigen class I expression of tumor cells on outcome of intravesical instillation of bacillus calmette-guerin immunotherapy for bladder cancer.* Clin Cancer Res, 2006. **12**(15): p. 4641-4.
136. Sconocchia, G., et al., *HLA class II antigen expression in colorectal carcinoma tumors as a favorable prognostic marker.* Neoplasia, 2014. **16**(1): p. 31-42.
137. Shehata, M., et al., *Human leukocyte antigen class I expression is an independent prognostic factor in advanced ovarian cancer resistant to first-line platinum chemotherapy.* Br J Cancer, 2009. **101**(8): p. 1321-8.
138. Matsushita, H., et al., *Cancer exome analysis reveals a T-cell-dependent mechanism of cancer immunoediting.* Nature, 2012. **482**(7385): p. 400-4.
139. Vogelstein, B., et al., *Cancer genome landscapes.* Science, 2013. **339**(6127): p. 1546-58.
140. Coulie, P.G., et al., *Tumour antigens recognized by T lymphocytes: at the core of cancer immunotherapy.* Nat Rev Cancer, 2014. **14**(2): p. 135-46.
141. Taube, J.M., et al., *Association of PD-1, PD-1 ligands, and other features of the tumor immune microenvironment with response to anti-PD-1 therapy.* Clin Cancer Res, 2014. **20**(19): p. 5064-74.
142. Taube, J.M., et al., *Colocalization of inflammatory response with B7-h1 expression in human melanocytic lesions supports an adaptive resistance mechanism of immune escape.* Sci Transl Med, 2012. **4**(127): p. 127ra37.
143. Riley, R.S., et al., *Delivery technologies for cancer immunotherapy.* Nature Reviews Drug Discovery, 2019. **18**(3): p. 175-196.

144. Pardoll, D.M., *The blockade of immune checkpoints in cancer immunotherapy.* Nature Reviews Cancer, 2012. **12**(4): p. 252-264.
145. Webb, E.S., et al., *Immune checkpoint inhibitors in cancer therapy.* Journal of Biomedical Research, 2018. **32**(5): p. 317-326.
146. Granier, C., et al., *Mechanisms of action and rationale for the use of checkpoint inhibitors in cancer.* Esmo Open, 2017. **2**(2).
147. Alsaab, H.O., et al., *PD-1 and PD-L1 Checkpoint Signaling Inhibition for Cancer Immunotherapy: Mechanism, Combinations, and Clinical Outcome.* Frontiers in Pharmacology, 2017. **8**.
148. Vargas, F.A., et al., *Fc Effector Function Contributes to the Activity of Human Anti-CTLA-4 Antibodies.* Cancer Cell, 2018. **33**(4): p. 649-+.
149. Du, X.X., et al., *A reappraisal of CTLA-4 checkpoint blockade in cancer immunotherapy.* Cell Research, 2018. **28**(4): p. 416-432.
150. Byun, D.J., et al., *Cancer immunotherapy - immune checkpoint blockade and associated endocrinopathies.* Nat Rev Endocrinol, 2017. **13**(4): p. 195-207.
151. Ellis, P.M., E.T. Vella, and Y.C. Ung, *Immune Checkpoint Inhibitors for Patients With Advanced Non-Small-Cell Lung Cancer: A Systematic Review.* Clin Lung Cancer, 2017. **18**(5): p. 444-459 e1.
152. Naidoo, J., et al., *Pneumonitis in Patients Treated With Anti-Programmed Death-1/Programmed Death Ligand 1 Therapy.* J Clin Oncol, 2017. **35**(7): p. 709-717.
153. Friedman, C.F., T.A. Proverbs-Singh, and M.A. Postow, *Treatment of the Immune-Related Adverse Effects of Immune Checkpoint Inhibitors: A Review.* JAMA Oncol, 2016. **2**(10): p. 1346-1353.
154. Lee, S. and K. Margolin, *Cytokines in cancer immunotherapy.* Cancers (Basel), 2011. **3**(4): p. 3856-93.
155. Chapuis, A.G., et al., *Combined IL-21-primed polyclonal CTL plus CTLA4 blockade controls refractory metastatic melanoma in a patient.* Journal of Experimental Medicine, 2016. **213**(7): p. 1133-1139.
156. Cox, M.A., L.E. Harrington, and A.J. Zajac, *Cytokines and the inception of CD8 T cell responses.* Trends Immunol, 2011. **32**(4): p. 180-6.
157. Ben-Sasson, S.Z., et al., *IL-1 acts directly on CD4 T cells to enhance their antigen-driven expansion and differentiation.* Proceedings of the National Academy of Sciences of the United States of America, 2009. **106**(17): p. 7119-7124.
158. Trinchieri, G., *Interleukin-12 and the regulation of innate resistance and adaptive immunity.* Nature Reviews Immunology, 2003. **3**(2): p. 133-146.
159. Itoh, K. and S. Hirohata, *The Role of Il-10 in Human B-Cell Activation, Proliferation, and Differentiation.* Journal of Immunology, 1995. **154**(9): p. 4341-4350.
160. Berger, C., et al., *Safety and immunologic effects of IL-15 administration in nonhuman primates.* Blood, 2009. **114**(12): p. 2417-2426.
161. Hasan, A.N., et al., *Soluble and membrane-bound interleukin (IL)-15 R/IL-15 complexes mediate proliferation of high-avidity central memory CD8 T cells for adoptive immunotherapy of cancer and infections.* Clinical and Experimental Immunology, 2016. **186**(2): p. 249-265.
162. Enomoto, H., et al., *The in vivo antitumor effects of type I-interferon against hepatocellular carcinoma: the suppression of tumor cell growth and angiogenesis.* Scientific Reports, 2017. **7**.

163. Sun, T., et al., *Inhibition of Tumor Angiogenesis by Interferon-gamma by Suppression of Tumor-Associated Macrophage Differentiation.* Oncology Research, 2013. **21**(5): p. 227-235.
164. He, T.P., et al., *Interferon gamma stimulates cellular maturation of dendritic cell line DC2.4 leading to induction of efficient cytotoxic T cell responses and antitumor immunity.* Cellular & Molecular Immunology, 2007. **4**(2): p. 105-111.
165. Muller, L., P. Aigner, and D. Stoiber, *Type I Interferons and Natural Killer Cell Regulation in Cancer.* Frontiers in Immunology, 2017. **8**.
166. Quesada, J.R., et al., *Treatment of hairy cell leukemia with recombinant alpha-interferon.* Blood, 1986. **68**(2): p. 493-7.
167. Mehta, H.M., M. Malandra, and S.J. Corey, *G-CSF and GM-CSF in Neutropenia.* Journal of Immunology, 2015. **195**(4): p. 1341-1349.
168. Tanaka, J., M. Mielcarek, and B. Torok-Storb, *Impaired induction of the CD28-responsive complex in granulocyte colony-stimulating factor mobilized CD4 T cells.* Blood, 1998. **91**(1): p. 347-352.
169. Yan, W.L., et al., *Recent progress in GM-CSF-based cancer immunotherapy.* Immunotherapy, 2017. **9**(4): p. 347-360.
170. Alwan, L.M., et al., *Comparison of acute toxicity and mortality after two different dosing regimens of high-dose interleukin-2 for patients with metastatic melanoma.* Targeted Oncology, 2014. **9**(1): p. 63-71.
171. Kirchner, G.I., et al., *Pharmacokinetics of recombinant human interleukin-2 in advanced renal cell carcinoma patients following subcutaneous application.* British Journal of Clinical Pharmacology, 1998. **46**(1): p. 5-10.
172. Rosenberg, S.A., et al., *A Progress Report on the Treatment of 157 Patients with Advanced Cancer Using Lymphokine-Activated Killer-Cells and Interleukin-2 or High-Dose Interleukin-2 Alone.* New England Journal of Medicine, 1987. **316**(15): p. 889-897.
173. Lim, W.A. and C.H. June, *The Principles of Engineering Immune Cells to Treat Cancer.* Cell, 2017. **168**(4): p. 724-740.
174. Scholler, J., et al., *Decade-Long Safety and Function of Retroviral-Modified Chimeric Antigen Receptor T Cells.* Science Translational Medicine, 2012. **4**(132).
175. Neelapu, S.S., et al., *Axicabtagene Ciloleucel CAR T-Cell Therapy in Refractory Large B-Cell Lymphoma.* New England Journal of Medicine, 2017. **377**(26): p. 2531-2544.
176. Maude, S.L., et al., *Tisagenlecleucel in Children and Young Adults with B-Cell Lymphoblastic Leukemia.* New England Journal of Medicine, 2018. **378**(5): p. 439-448.
177. Linnemann, C., et al., *High-throughput identification of antigen-specific TCRs by TCR gene capture.* Nat Med, 2013. **19**(11): p. 1534-41.
178. van den Berg, J.H., et al., *Case Report of a Fatal Serious Adverse Event Upon Administration of T Cells Transduced With a MART-1-specific T-cell Receptor.* Molecular Therapy, 2015. **23**(9): p. 1541-1550.
179. Fitzgerald, J.C., et al., *Cytokine Release Syndrome After Chimeric Antigen Receptor T Cell Therapy for Acute Lymphoblastic Leukemia.* Crit Care Med, 2017. **45**(2): p. e124-e131.

180. Peggs, K.S., S.A. Quezada, and J.P. Allison, *Cancer immunotherapy: co-stimulatory agonists and co-inhibitory antagonists.* Clinical and Experimental Immunology, 2009. **157**(1): p. 9-19.
181. Buchan, S.L., A. Rogel, and A. Al-Shamkhani, *The immunobiology of CD27 and OX40 and their potential as targets for cancer immunotherapy.* Blood, 2018. **131**(1): p. 39-48.
182. Tolcher, A.W., et al., *Phase Ib Study of Utomilumab (PF-05082566), a 4-1BB/CD137 Agonist, in Combination with Pembrolizumab (MK-3475) in Patients with Advanced Solid Tumors.* Clinical Cancer Research, 2017. **23**(18): p. 5349-5357.
183. Segal, N.H., et al., *Results from an Integrated Safety Analysis of Urelumab, an Agonist Anti-CD137 Monoclonal Antibody.* Clinical Cancer Research, 2017. **23**(8): p. 1929-1936.
184. Zhang, P., et al., *Agonistic Anti-4-1BB antibody promotes the expansion of natural regulatory T cells while maintaining foxp3 expression.* Scandinavian Journal of Immunology, 2007. **66**(4): p. 435-440.
185. Hollingsworth, R.E. and K. Jansen, *Turning the corner on therapeutic cancer vaccines.* Npj Vaccines, 2019. **4**.
186. Lichty, B.D., et al., *Going viral with cancer immunotherapy.* Nature Reviews Cancer, 2014. **14**(8): p. 559-567.
187. Melero, I., et al., *Therapeutic vaccines for cancer: an overview of clinical trials.* Nature Reviews Clinical Oncology, 2014. **11**(9): p. 509-524.
188. van der Burg, S.H., et al., *Vaccines for established cancer: overcoming the challenges posed by immune evasion.* Nature Reviews Cancer, 2016. **16**(4): p. 219-233.
189. Disis, M.L., et al., *Concurrent trastuzumab and HER2/neu-specific vaccination in patients with metastatic breast cancer.* J Clin Oncol, 2009. **27**(28): p. 4685-92.
190. Karbach, J., et al., *Efficient in vivo priming by vaccination with recombinant NY-ESO-1 protein and CpG in antigen naive prostate cancer patients.* Clin Cancer Res, 2011. **17**(4): p. 861-70.
191. Finn, O.J., et al., *Importance of MUC1 and spontaneous mouse tumor models for understanding the immunobiology of human adenocarcinomas.* Immunol Res, 2011. **50**(2-3): p. 261-8.
192. Lam, K.W., et al., *Improved immunohistochemical detection of prostatic acid phosphatase by a monoclonal antibody.* Prostate, 1989. **15**(1): p. 13-21.
193. Correale, P., et al., *In vitro generation of human cytotoxic T lymphocytes specific for peptides derived from prostate-specific antigen.* J Natl Cancer Inst, 1997. **89**(4): p. 293-300.
194. Bakker, A.B., et al., *Melanocyte lineage-specific antigen gp100 is recognized by melanoma-derived tumor-infiltrating lymphocytes.* J Exp Med, 1994. **179**(3): p. 1005-9.
195. Chang, K. and I. Pastan, *Molecular cloning of mesothelin, a differentiation antigen present on mesothelium, mesotheliomas, and ovarian cancers.* Proc Natl Acad Sci U S A, 1996. **93**(1): p. 136-40.
196. Vonderheide, R.H., et al., *The telomerase catalytic subunit is a widely expressed tumor-associated antigen recognized by cytotoxic T lymphocytes.* Immunity, 1999. **10**(6): p. 673-9.

197. Lee, C.M., et al., *Age, gender, and local geographic variations of viral etiology of hepatocellular carcinoma in a hyperendemic area for hepatitis B virus infection.* Cancer, 1999. **86**(7): p. 1143-50.
198. Wang, J.W., et al., *Immunoprevention of human papillomavirus-associated malignancies.* Cancer Prev Res (Phila), 2015. **8**(2): p. 95-104.
199. de Vos van Steenwijk, P.J., et al., *The long-term immune response after HPV16 peptide vaccination in women with low-grade pre-malignant disorders of the uterine cervix: a placebo-controlled phase II study.* Cancer Immunol Immunother, 2014. **63**(2): p. 147-60.
200. Kim, T.J., et al., *Clearance of persistent HPV infection and cervical lesion by therapeutic DNA vaccine in CIN3 patients.* Nat Commun, 2014. **5**: p. 5317.
201. Alvarez, R.D., et al., *A pilot study of pNGVL4a-CRT/E7(detox) for the treatment of patients with HPV16+ cervical intraepithelial neoplasia 2/3 (CIN2/3).* Gynecol Oncol, 2016. **140**(2): p. 245-52.
202. Trimble, C.L., et al., *Safety, efficacy, and immunogenicity of VGX-3100, a therapeutic synthetic DNA vaccine targeting human papillomavirus 16 and 18 E6 and E7 proteins for cervical intraepithelial neoplasia 2/3: a randomised, double-blind, placebo-controlled phase 2b trial.* Lancet, 2015. **386**(10008): p. 2078-2088.
203. Castle, J.C., et al., *Exploiting the mutanome for tumor vaccination.* Cancer Res, 2012. **72**(5): p. 1081-91.
204. Kreiter, S., et al., *Targeting the tumor mutanome for personalized vaccination therapy.* Oncoimmunology, 2012. **1**(5): p. 768-769.
205. Melief, C.J., et al., *Therapeutic cancer vaccines.* J Clin Invest, 2015. **125**(9): p. 3401-12.
206. Kantoff, P.W., et al., *Sipuleucel-T immunotherapy for castration-resistant prostate cancer.* N Engl J Med, 2010. **363**(5): p. 411-22.
207. Taylor, M.W., *The Discovery of Bacteriophage and the d'Herelle Controversy*, in *Viruses and Man: A History of Interactions.* 2014, Springer, Cham.
208. Twort, F.W., *Further Investigations on the Nature of Ultra-Microscopic Viruses and their Cultivation.* J Hyg (Lond), 1936. **36**(2): p. 204-35.
209. Clark, J.R. and J.B. March, *Bacteriophages and biotechnology: vaccines, gene therapy and antibacterials.* Trends Biotechnol, 2006. **24**(5): p. 212-8.
210. Harada, L.K., et al., *Biotechnological applications of bacteriophages: State of the art.* Microbiol Res, 2018. **212-213**: p. 38-58.
211. Cuesta, A.M., et al., *Enhancement of DNA vaccine potency through linkage of antigen to filamentous bacteriophage coat protein III domain I.* Immunology, 2006. **117**(4): p. 502-6.
212. Hornung, V. and E. Latz, *Intracellular DNA recognition.* Nat Rev Immunol, 2010. **10**(2): p. 123-30.
213. Sartorius, R., et al., *Antigen delivery by filamentous bacteriophage fd displaying an anti-DEC-205 single-chain variable fragment confers adjuvanticity by triggering a TLR9-mediated immune response.* EMBO Mol Med, 2015. **7**(7): p. 973-88.
214. Hashiguchi, S., et al., *Immunological basis of M13 phage vaccine: Regulation under MyD88 and TLR9 signaling.* Biochem Biophys Res Commun, 2010. **402**(1): p. 19-22.

215. Willis, A.E., R.N. Perham, and D. Wraith, *Immunological properties of foreign peptides in multiple display on a filamentous bacteriophage.* Gene, 1993. **128**(1): p. 79-83.
216. De Berardinis, P., et al., *Phage display of peptide epitopes from HIV-1 elicits strong cytolytic responses.* Nat Biotechnol, 2000. **18**(8): p. 873-6.
217. Eriksson, F., et al., *Tumor specific phage particles promote tumor regression in a mouse melanoma model.* Cancer Immunol Immunother, 2007. **56**(5): p. 677-87.
218. Eriksson, F., et al., *Tumor-specific bacteriophages induce tumor destruction through activation of tumor-associated macrophages.* J Immunol, 2009. **182**(5): p. 3105-11.
219. Bazan, J., I. Calkosinski, and A. Gamian, *Phage display--a powerful technique for immunotherapy: 1. Introduction and potential of therapeutic applications.* Hum Vaccin Immunother, 2012. **8**(12): p. 1817-28.
220. Sioud, M. and M.H. Hansen, *Profiling the immune response in patients with breast cancer by phage-displayed cDNA libraries.* Eur J Immunol, 2001. **31**(3): p. 716-25.
221. Dantas-Barbosa, C., M. de Macedo Brigido, and A.Q. Maranhao, *Antibody phage display libraries: contributions to oncology.* Int J Mol Sci, 2012. **13**(5): p. 5420-40.
222. Thie, H., et al., *Phage display derived therapeutic antibodies.* Curr Pharm Biotechnol, 2008. **9**(6): p. 439-46.
223. Clark, J.R. and J.B. March, *Bacterial viruses as human vaccines?* Expert Rev Vaccines, 2004. **3**(4): p. 463-76.
224. Razazan, A., et al., *Lambda bacteriophage nanoparticles displaying GP2, a HER2/neu derived peptide, induce prophylactic and therapeutic activities against TUBO tumor model in mice.* Sci Rep, 2019. **9**(1): p. 2221.
225. Bartolacci, C., et al., *Phage-Based Anti-HER2 Vaccination Can Circumvent Immune Tolerance against Breast Cancer.* Cancer Immunol Res, 2018. **6**(12): p. 1486-1498.
226. Fang, J., et al., *The potential of phage display virions expressing malignant tumor specific antigen MAGE-A1 epitope in murine model.* Vaccine, 2005. **23**(40): p. 4860-6.
227. Xu, H., et al., *Engineering T7 bacteriophage as a potential DNA vaccine targeting delivery vector.* Virol J, 2018. **15**(1): p. 49.
228. Ghaemi, A., et al., *Recombinant lambda-phage nanobioparticles for tumor therapy in mice models.* Genet Vaccines Ther, 2010. **8**: p. 3.
229. Adhya, S., C.R. Merril, and B. Biswas, *Therapeutic and prophylactic applications of bacteriophage components in modern medicine.* Cold Spring Harb Perspect Med, 2014. **4**(1): p. a012518.
230. Karimi, M., et al., *Bacteriophages and phage-inspired nanocarriers for targeted delivery of therapeutic cargos.* Adv Drug Deliv Rev, 2016. **106**(Pt A): p. 45-62.
231. Larocca, D., et al., *Gene transfer to mammalian cells using genetically targeted filamentous bacteriophage.* FASEB J, 1999. **13**(6): p. 727-34.
232. Larocca, D., et al., *Targeting bacteriophage to mammalian cell surface receptors for gene delivery.* Hum Gene Ther, 1998. **9**(16): p. 2393-9.
233. Ashley, C.E., et al., *Cell-specific delivery of diverse cargos by bacteriophage MS2 virus-like particles.* ACS Nano, 2011. **5**(7): p. 5729-45.

234. Huang, R.K., et al., *Transferrin-mediated targeting of bacteriophage HK97 nanoparticles into tumor cells.* Nanomedicine (Lond), 2011. **6**(1): p. 55-68.
235. Choi, D.S., et al., *Cyclic RGD peptide incorporation on phage major coat proteins for improved internalization by HeLa cells.* Bioconjug Chem, 2014. **25**(2): p. 216-23.
236. Ziello, J.E., Y. Huang, and I.S. Jovin, *Cellular endocytosis and gene delivery.* Mol Med, 2010. **16**(5-6): p. 222-9.
237. Midoux, P., et al., *Membrane permeabilization and efficient gene transfer by a peptide containing several histidines.* Bioconjug Chem, 1998. **9**(2): p. 260-7.
238. Pichon, C., C. Goncalves, and P. Midoux, *Histidine-rich peptides and polymers for nucleic acids delivery.* Adv Drug Deliv Rev, 2001. **53**(1): p. 75-94.
239. Asseline, U., et al., *Improved nuclear delivery of antisense 2'-Ome RNA by conjugation with the histidine-rich peptide H5WYG.* J Gene Med, 2014. **16**(7-8): p. 157-65.
240. Harrison, E., et al., *Peptide functionalized gold nanoparticles: the influence of pH on binding efficiency.* Nanotechnology, 2017. **28**(29): p. 295602.
241. Alipour, M., et al., *Nano-biomimetic carriers are implicated in mechanistic evaluation of intracellular gene delivery.* Sci Rep, 2017. **7**: p. 41507.
242. Roberts, N.J., et al., *Systemic use of tumor necrosis factor alpha as an anticancer agent.* Oncotarget, 2011. **2**(10): p. 739-51.
243. van Horssen, R., T.L. Ten Hagen, and A.M. Eggermont, *TNF-alpha in cancer treatment: molecular insights, antitumor effects, and clinical utility.* Oncologist, 2006. **11**(4): p. 397-408.
244. Smith, G.P. and V.A. Petrenko, *Phage display.* Chemical Reviews, 1997. **97**(2): p. 391-410.
245. Danhier, F., A. Le Breton, and V. Preat, *RGD-based strategies to target alpha(v) beta(3) integrin in cancer therapy and diagnosis.* Mol Pharm, 2012. **9**(11): p. 2961-73.
246. Ooi, A., et al., *A Guide to Transient Expression of Membrane Proteins in HEK-293 Cells for Functional Characterization.* Frontiers in Physiology, 2016. **7**.
247. Thomas, P. and T.G. Smart, *HEK293 cell line: a vehicle for the expression of recombinant proteins.* J Pharmacol Toxicol Methods, 2005. **51**(3): p. 187-200.
248. Kondo, H., et al., *Differential Regulation of Gene Expression of Alveolar Epithelial Cell Markers in Human Lung Adenocarcinoma-Derived A549 Clones.* Stem Cells International, 2015.
249. Harishchandra, R.K., M. Saleem, and H.J. Galla, *Nanoparticle interaction with model lung surfactant monolayers.* J R Soc Interface, 2010. **7 Suppl 1**: p. S15-26.
250. Miliotou, A.N. and L.C. Papadopoulou, *CAR T-cell Therapy: A New Era in Cancer Immunotherapy.* Curr Pharm Biotechnol, 2018. **19**(1): p. 5-18.
251. Haji-Fatahaliha, M., et al., *CAR-modified T-cell therapy for cancer: an updated review.* Artificial Cells Nanomedicine and Biotechnology, 2016. **44**(6): p. 1339-1349.

252. Sharpe, M. and N. Mount, *Genetically modified T cells in cancer therapy: opportunities and challenges.* Disease Models & Mechanisms, 2015. **8**(4): p. 337-350.
253. Arabi, F., et al., *Antigenic targets of CAR T Cell Therapy. A retrospective view on clinical trials.* Exp Cell Res, 2018. **369**(1): p. 1-10.
254. Morgan, R.A., et al., *Recognition of glioma stem cells by genetically modified T cells targeting EGFRvIII and development of adoptive cell therapy for glioma.* Hum Gene Ther, 2012. **23**(10): p. 1043-53.
255. June, C.H., et al., *CAR T cell immunotherapy for human cancer.* Science, 2018. **359**(6382): p. 1361-1365.
256. O'Leary, M.C., et al., *FDA Approval Summary: Tisagenlecleucel for Treatment of Patients with Relapsed or Refractory B-cell Precursor Acute Lymphoblastic Leukemia.* Clin Cancer Res, 2019. **25**(4): p. 1142-1146.
257. Wohlfarth, P., N. Worel, and G. Hopfinger, *Chimeric antigen receptor Tcell therapy-a hematological success story.* Memo, 2018. **11**(2): p. 116-121.
258. D'Aloia, M.M., et al., *CAR-T cells: the long and winding road to solid tumors.* Cell Death Dis, 2018. **9**(3): p. 282.
259. Nath, S. and P. Mukherjee, *MUC1: a multifaceted oncoprotein with a key role in cancer progression.* Trends Mol Med, 2014. **20**(6): p. 332-42.
260. Fedorov, V.D., M. Sadelain, and C.C. Kloss, *Novel approaches to enhance the specificity and safety of engineered T cells.* Cancer J, 2014. **20**(2): p. 160-5.
261. McGranahan, N. and C. Swanton, *Clonal Heterogeneity and Tumor Evolution: Past, Present, and the Future.* Cell, 2017. **168**(4): p. 613-628.
262. Cheever, M.A., et al., *The prioritization of cancer antigens: a national cancer institute pilot project for the acceleration of translational research.* Clin Cancer Res, 2009. **15**(17): p. 5323-37.
263. Yata, T., et al., *Hybrid Nanomaterial Complexes for Advanced Phage-guided Gene Delivery.* Mol Ther Nucleic Acids, 2014. **3**: p. e185.
264. O'Rourke, D.M., et al., *A single dose of peripherally infused EGFRvIII-directed CAR T cells mediates antigen loss and induces adaptive resistance in patients with recurrent glioblastoma.* Sci Transl Med, 2017. **9**(399).
265. Farkona, S., E.P. Diamandis, and I.M. Blasutig, *Cancer immunotherapy: the beginning of the end of cancer?* BMC Med, 2016. **14**: p. 73.
266. Sanmamed, M.F. and L. Chen, *A Paradigm Shift in Cancer Immunotherapy: From Enhancement to Normalization.* Cell, 2018. **175**(2): p. 313-326.
267. Fishman, M., *Challenges facing the development of cancer vaccines.* Methods Mol Biol, 2014. **1139**: p. 543-53.
268. Cecco, S., et al., *Cancer vaccines in phase II/III clinical trials: state of the art and future perspectives.* Curr Cancer Drug Targets, 2011. **11**(1): p. 85-102.
269. Lundstrom, K., *Replicon RNA Viral Vectors as Vaccines.* Vaccines (Basel), 2016. **4**(4).
270. Pedersen, S.R., et al., *Comparison of vaccine-induced effector CD8 T cell responses directed against self- and non-self-tumor antigens: implications for cancer immunotherapy.* J Immunol, 2013. **191**(7): p. 3955-67.
271. Chang, M.H., et al., *Decreased incidence of hepatocellular carcinoma in hepatitis B vaccinees: a 20-year follow-up study.* J Natl Cancer Inst, 2009. **101**(19): p. 1348-55.
272. Klevorn, L.E. and R.M. Teague, *Adapting Cancer Immunotherapy Models for the Real World.* Trends Immunol, 2016. **37**(6): p. 354-363.

273. Schlom, J., et al., *Therapeutic cancer vaccines.* Adv Cancer Res, 2014. **121**: p. 67-124.
274. Laheru, D., et al., *Allogeneic granulocyte macrophage colony-stimulating factor-secreting tumor immunotherapy alone or in sequence with cyclophosphamide for metastatic pancreatic cancer: a pilot study of safety, feasibility, and immune activation.* Clin Cancer Res, 2008. **14**(5): p. 1455-63.
275. Small, E.J., et al., *Granulocyte macrophage colony-stimulating factor--secreting allogeneic cellular immunotherapy for hormone-refractory prostate cancer.* Clin Cancer Res, 2007. **13**(13): p. 3883-91.
276. Lipson, E.J., et al., *Safety and immunologic correlates of Melanoma GVAX, a GM-CSF secreting allogeneic melanoma cell vaccine administered in the adjuvant setting.* J Transl Med, 2015. **13**: p. 214.
277. Salgia, R., et al., *Vaccination with irradiated autologous tumor cells engineered to secrete granulocyte-macrophage colony-stimulating factor augments antitumor immunity in some patients with metastatic non-small-cell lung carcinoma.* J Clin Oncol, 2003. **21**(4): p. 624-30.
278. Lesterhuis, W.J., J.B. Haanen, and C.J. Punt, *Cancer immunotherapy--revisited.* Nat Rev Drug Discov, 2011. **10**(8): p. 591-600.
279. Disis, M.L., *Enhancing cancer vaccine efficacy via modulation of the tumor microenvironment.* Clin Cancer Res, 2009. **15**(21): p. 6476-8.
280. Bijker, M.S., et al., *Superior induction of anti-tumor CTL immunity by extended peptide vaccines involves prolonged, DC-focused antigen presentation.* Eur J Immunol, 2008. **38**(4): p. 1033-42.
281. Zhang, H., et al., *Comparing pooled peptides with intact protein for accessing cross-presentation pathways for protective CD8+ and CD4+ T cells.* J Biol Chem, 2009. **284**(14): p. 9184-91.
282. Jorritsma, S.H.T., et al., *Delivery methods to increase cellular uptake and immunogenicity of DNA vaccines.* Vaccine, 2016. **34**(46): p. 5488-5494.
283. Larocca, C. and J. Schlom, *Viral vector-based therapeutic cancer vaccines.* Cancer J, 2011. **17**(5): p. 359-71.
284. Hill, A.V., et al., *Prime-boost vectored malaria vaccines: progress and prospects.* Hum Vaccin, 2010. **6**(1): p. 78-83.
285. Hodgson, S.H., et al., *Evaluation of the efficacy of ChAd63-MVA vectored vaccines expressing circumsporozoite protein and ME-TRAP against controlled human malaria infection in malaria-naive individuals.* J Infect Dis, 2015. **211**(7): p. 1076-86.
286. Tiono, A.B., et al., *First field efficacy trial of the ChAd63 MVA ME-TRAP vectored malaria vaccine candidate in 5-17 months old infants and children.* PLoS One, 2018. **13**(12): p. e0208328.
287. Gilbert, S.C., et al., *A protein particle vaccine containing multiple malaria epitopes.* Nat Biotechnol, 1997. **15**(12): p. 1280-4.
288. Purbhoo, M.A., et al., *Quantifying and imaging NY-ESO-1/LAGE-1-derived epitopes on tumor cells using high affinity T cell receptors.* J Immunol, 2006. **176**(12): p. 7308-16.
289. Sadeghi, H. and M.M. Hitt, *Transcriptionally targeted adenovirus vectors.* Curr Gene Ther, 2005. **5**(4): p. 411-27.
290. Lee, A.S., *GRP78 induction in cancer: therapeutic and prognostic implications.* Cancer Res, 2007. **67**(8): p. 3496-9.

291. Dong, D., et al., *Spontaneous and controllable activation of suicide gene expression driven by the stress-inducible grp78 promoter resulting in eradication of sizable human tumors.* Hum Gene Ther, 2004. **15**(6): p. 553-61.
292. Stuber, G., et al., *Assessment of Major Histocompatibility Complex Class-I Interaction with Epstein-Barr-Virus and Human-Immunodeficiency-Virus Peptides by Elevation of Membrane H-2 and Hla in Peptide Loading-Deficient Cells.* European Journal of Immunology, 1992. **22**(10): p. 2697-2703.
293. Fox, B.S., *Interaction of Major Histocompatibility Complex-Molecules with Immunogenic Peptides.* Current Opinion in Immunology, 1988. **1**(1): p. 103-106.
294. Wang, X.L., et al., *Model for the interaction of gammaherpesvirus 68 RING-CH finger protein mK3 with major histocompatibility complex class I and the peptide-loading complex.* Journal of Virology, 2004. **78**(16): p. 8673-8686.
295. McConkey, S.J., et al., *Enhanced T-cell immunogenicity of plasmid DNA vaccines boosted by recombinant modified vaccinia virus Ankara in humans.* Nat Med, 2003. **9**(6): p. 729-35.
296. Kloetzel, P.M., *Antigen processing by the proteasome.* Nat Rev Mol Cell Biol, 2001. **2**(3): p. 179-87.
297. Altman, J.D., et al., *Phenotypic analysis of antigen-specific T lymphocytes.* Science, 1996. **274**(5284): p. 94-6.
298. Doolan, D.L. and S.L. Hoffman, *The complexity of protective immunity against liver-stage malaria.* J Immunol, 2000. **165**(3): p. 1453-62.
299. Ogwang, C., et al., *Prime-boost vaccination with chimpanzee adenovirus and modified vaccinia Ankara encoding TRAP provides partial protection against Plasmodium falciparum infection in Kenyan adults.* Sci Transl Med, 2015. **7**(286): p. 286re5.
300. Lane, P.J., F.M. Gaspal, and M.Y. Kim, *Two sides of a cellular coin: CD4(+)CD3- cells regulate memory responses and lymph-node organization.* Nat Rev Immunol, 2005. **5**(8): p. 655-60.
301. Castro, F., et al., *Interferon-Gamma at the Crossroads of Tumor Immune Surveillance or Evasion.* Front Immunol, 2018. **9**: p. 847.
302. Anderson, R.J., et al., *Enhanced CD8+ T cell immune responses and protection elicited against Plasmodium berghei malaria by prime boost immunization regimens using a novel attenuated fowlpox virus.* J Immunol, 2004. **172**(5): p. 3094-100.
303. Hermsen, C.C., et al., *Circulating concentrations of soluble granzyme A and B increase during natural and experimental Plasmodium falciparum infections.* Clin Exp Immunol, 2003. **132**(3): p. 467-72.
304. Chowdhury, D. and J. Lieberman, *Death by a thousand cuts: granzyme pathways of programmed cell death.* Annu Rev Immunol, 2008. **26**: p. 389-420.
305. Trapani, J.A. and V.R. Sutton, *Granzyme B: pro-apoptotic, antiviral and antitumor functions.* Curr Opin Immunol, 2003. **15**(5): p. 533-43.
306. Topham, N.J. and E.W. Hewitt, *Natural killer cell cytotoxicity: how do they pull the trigger?* Immunology, 2009. **128**(1): p. 7-15.

307. Chavez-Galan, L., et al., *Cell death mechanisms induced by cytotoxic lymphocytes.* Cell Mol Immunol, 2009. **6**(1): p. 15-25.
308. Martinez-Lostao, L., A. Anel, and J. Pardo, *How Do Cytotoxic Lymphocytes Kill Cancer Cells?* Clin Cancer Res, 2015. **21**(22): p. 5047-56.
309. Paul, S. and G. Lal, *The Molecular Mechanism of Natural Killer Cells Function and Its Importance in Cancer Immunotherapy.* Front Immunol, 2017. **8**: p. 1124.
310. Fell, A.H. and N.C. Smith, *Immunity to asexual blood stages of Plasmodium: is resistance to acute malaria adaptive or innate?* Parasitol Today, 1998. **14**(9): p. 364-9.
311. Russo, M.A., et al., *A small-molecule RGD-integrin antagonist inhibits cell adhesion, cell migration and induces anoikis in glioblastoma cells.* Int J Oncol, 2013. **42**(1): p. 83-92.
312. Yan, N. and Z.J. Chen, *Intrinsic antiviral immunity.* Nat Immunol, 2012. **13**(3): p. 214-22.
313. Zander, R.A., et al., *Th1-like Plasmodium-Specific Memory CD4(+) T Cells Support Humoral Immunity.* Cell Rep, 2017. **21**(7): p. 1839-1852.
314. Garg, A.D. and P. Agostinis, *Cell death and immunity in cancer: From danger signals to mimicry of pathogen defense responses.* Immunol Rev, 2017. **280**(1): p. 126-148.
315. Sheehy, S.H., et al., *ChAd63-MVA-vectored blood-stage malaria vaccines targeting MSP1 and AMA1: assessment of efficacy against mosquito bite challenge in humans.* Mol Ther, 2012. **20**(12): p. 2355-68.
316. O'Hara, G.A., et al., *Clinical assessment of a recombinant simian adenovirus ChAd63: a potent new vaccine vector.* J Infect Dis, 2012. **205**(5): p. 772-81.
317. Schofield, L., et al., *Gamma interferon, CD8+ T cells and antibodies required for immunity to malaria sporozoites.* Nature, 1987. **330**(6149): p. 664-6.
318. Russell, P.F. and B.N. Mohan, *The Immunization of Fowls against Mosquito-Borne Plasmodium Gallinaceum by Injections of Serum and of Inactivated Homologous Sporozoites.* J Exp Med, 1942. **76**(5): p. 477-95.
319. Barnes, E., et al., *Novel adenovirus-based vaccines induce broad and sustained T cell responses to HCV in man.* Sci Transl Med, 2012. **4**(115): p. 115ra1.
320. Ewer, K.J., et al., *Progress with viral vectored malaria vaccines: A multi-stage approach involving "unnatural immunity".* Vaccine, 2015. **33**(52): p. 7444-51.
321. Bliss, C.M., et al., *Assessment of novel vaccination regimens using viral vectored liver stage malaria vaccines encoding ME-TRAP.* Sci Rep, 2018. **8**(1): p. 3390.
322. Afolabi, M.O., et al., *Safety and Immunogenicity of ChAd63 and MVA ME-TRAP in West African Children and Infants.* Mol Ther, 2016. **24**(8): p. 1470-7.
323. Gilbert, S.C., et al., *Enhanced CD8 T cell immunogenicity and protective efficacy in a mouse malaria model using a recombinant adenoviral vaccine in heterologous prime-boost immunisation regimes.* Vaccine, 2002. **20**(7-8): p. 1039-45.
324. Rollier, C.S., A.V.S. Hill, and A. Reyes-Sandoval, *Influence of adenovirus and MVA vaccines on the breadth and hierarchy of T cell responses.* Vaccine, 2016. **34**(38): p. 4470-4474.

325. Green, C.A., et al., *Chimpanzee adenovirus- and MVA-vectored respiratory syncytial virus vaccine is safe and immunogenic in adults.* Sci Transl Med, 2015. **7**(300): p. 300ra126.
326. Swadling, L., et al., *A human vaccine strategy based on chimpanzee adenoviral and MVA vectors that primes, boosts, and sustains functional HCV-specific T cell memory.* Sci Transl Med, 2014. **6**(261): p. 261ra153.
327. Borthwick, N.J., et al., *Humoral responses to HIVconsv induced by heterologous vaccine modalities in rhesus macaques.* Immun Inflamm Dis, 2015. **3**(2): p. 82-93.
328. Sheehy, S.H., et al., *Phase Ia clinical evaluation of the safety and immunogenicity of the Plasmodium falciparum blood-stage antigen AMA1 in ChAd63 and MVA vaccine vectors.* PLoS One, 2012. **7**(2): p. e31208.
329. Ewer, K.J., et al., *Protective CD8+ T-cell immunity to human malaria induced by chimpanzee adenovirus-MVA immunisation.* Nat Commun, 2013. **4**: p. 2836.
330. Antrobus, R.D., et al., *A T cell-inducing influenza vaccine for the elderly: safety and immunogenicity of MVA-NP+M1 in adults aged over 50 years.* PLoS One, 2012. **7**(10): p. e48322.
331. Borthwick, N., et al., *Vaccine-elicited human T cells recognizing conserved protein regions inhibit HIV-1.* Mol Ther, 2014. **22**(2): p. 464-475.
332. Irvine, D.J., et al., *Direct observation of ligand recognition by T cells.* Nature, 2002. **419**(6909): p. 845-9.
333. Huang, J., et al., *A single peptide-major histocompatibility complex ligand triggers digital cytokine secretion in CD4(+) T cells.* Immunity, 2013. **39**(5): p. 846-57.
334. Watanabe, K., et al., *Target antigen density governs the efficacy of anti-CD20-CD28-CD3 zeta chimeric antigen receptor-modified effector CD8+ T cells.* J Immunol, 2015. **194**(3): p. 911-20.
335. Stone, J.D., et al., *A sensitivity scale for targeting T cells with chimeric antigen receptors (CARs) and bispecific T-cell Engagers (BiTEs).* Oncoimmunology, 2012. **1**(6): p. 863-873.
336. Walker, A.J., et al., *Tumor Antigen and Receptor Densities Regulate Efficacy of a Chimeric Antigen Receptor Targeting Anaplastic Lymphoma Kinase.* Mol Ther, 2017. **25**(9): p. 2189-2201.
337. Watanabe, K., et al., *Expanding the Therapeutic Window for CAR T Cell Therapy in Solid Tumors: The Knowns and Unknowns of CAR T Cell Biology.* Front Immunol, 2018. **9**: p. 2486.
338. Liu, X., et al., *Affinity-Tuned ErbB2 or EGFR Chimeric Antigen Receptor T Cells Exhibit an Increased Therapeutic Index against Tumors in Mice.* Cancer Res, 2015. **75**(17): p. 3596-607.
339. Grossardt, C., et al., *Granulocyte-macrophage colony-stimulating factor-armed oncolytic measles virus is an effective therapeutic cancer vaccine.* Hum Gene Ther, 2013. **24**(7): p. 644-54.
340. Capasso, C., et al., *Oncolytic adenoviruses coated with MHC-I tumor epitopes increase the antitumor immunity and efficacy against melanoma.* Oncoimmunology, 2016. **5**(4): p. e1105429.
341. Bianconi, D., M. Unseld, and G.W. Prager, *Integrins in the Spotlight of Cancer.* Int J Mol Sci, 2016. **17**(12).

Appendix

Nucleic Acid sequence for H5WYG gene

5’
GGCTTGTTCCACGCCATCGCGCACTTCATTCATGGGGGTTGGCACGGTCTCATCCATGGTTGGTAC
GGG 3’

Nucleic Acid sequence for IL-2 signal peptide gene

5’ ATGTACAGAATGCAACTCCTGTCTTGTATTGCACTAAGTCTCGCACTTGTCACAAACAGT 3’

Nucleic Acid sequence for secreted TNFα gene

5’
GTCAGATCATCTTCTCGAACCCCGAGTGACAAGCCTGTAGCCCATGTTGTAGCAAACCCTCAAGCT
GAGGGGCAGCTCCAGTGGCTGAACCGCCGGGCCAATGCCCTCCTGGCCAATGGCGTGGAGCTGAGA
GATAACCAGCTGGTGGTGCCATCAGAGGGCCTGTACCTCATCTACTCCCAGGTCCTCTTCAAGGGC
CAAGGCTGCCCCTCCACCCATGTGCTCCTCACCCACACCATCAGCCGCATCGCCGTCTCCTACCAGA
CCAAGGTCAACCTCCTCTCTGCCATCAAGAGCCCCTGCCAGAGGGAGACCCCAGAGGGGGCTGAGG
CCAAGCCCTGGTATGAGCCCATCTATCTGGGAGGGGTCTTCCAGCTGGAGAAGGGTGACCGACTCA
GCGCTGAGATCAATCGGCCCGACTATCTCGACTTTGCCGAGTCTGGGCAGGTCTACTTTGGGATCA
TTGCCCTGTGA 3’

Nucleic Acid sequence for luciferase gene

5’
ATGGAGGATGCCAAGAATATTAAGAAAGGCCCTGCCCCATTCTACCCTCTGGAAGATGGCACTGCT
GGTGAGCAACTGCACAAGGCCATGAAGAGGTATGCCCTGGTCCCTGGCACCATTGCCTTCACTGAT
GCTCACATTGAGGTGGACATCACCTATGCTGAATACTTTGAGATGTCTGTGAGGCTGGCAGAAGC
CATGAAAAGATATGGACTGAACACCAACCACAGGATTGTGGTGTGCTCTGAGAACTCTCTCCAGT
TCTTCATGCCTGTGTTAGGAGCCCTGTTCATTGGAGTGGCTGTGGCCCCTGCCAATGACATCTACA
ATGAGAGAGAGCTCCTGAACAGCATGGGCATCAGCCAGCCAACTGTGGTCTTTGTGAGCAAGAAG
GGCCTGCAAAAGATCCTGAATGTGCAGAAGAAGCTGCCCATCATCCAGAAGATCATCATCATGGA
CAGCAAGACTGACTACCAGGGCTTCCAGAGCATGTATACCTTTGTGACCAGCCACTTACCCCCTGG
CTTCAATGAGTATGACTTTGTGCCTGAGAGCTTTGACAGGGACAAGACCATTGCTCTGATTATGA
ACAGCTCTGGCTCCACTGGACTGCCCAAAGGTGTGGCTCTGCCCCACAGAACTGCTTGTGTGAGAT
TCAGCCATGCCAGAGACCCCATCTTTGGCAACCAGATCATCCCTGACACTGCCATCCTGTCTGTGG
TTCCATTCCATCATGGCTTTGGCATGTTCACAACACTGGGGTACCTGATCTGTGGCTTCAGAGTGG
TGCTGATGTATAGGTTTGAGGAGGAGCTGTTTCTGAGGAGCCTACAAGACTACAAGATCCAGTCT
GCCCTGCTGGTGCCCACTCTGTTCAGCTTCTTTGCCAAGAGCACCCTCATTGACAAGTATGACCTG
AGCAACCTGCATGAGATTGCCTCTGGAGGAGCACCCCTGAGCAAGGAGGTGGGTGAGGCTGTGGC
AAAGAGGTTCCATCTCCCAGGAATCAGACAGGGCTATGGCCTGACTGAGACCACCTCTGCCATCCT
CATCACCCCTGAAGGAGATGACAAGCCTGGTGCTGTGGGCAAGGTGGTTCCCTTTTTTGAGGCCAA
GGTGGTGGACCTGGACACTGGCAAGACCCTGGGAGTGAACCAGAGGGGTGAGCTGTGTGTGAGGG
GTCCCATGATCATGTCTGGCTATGTGAACAACCCTGAGGCCACCAATGCCCTGATTGACAAGGATG
GCTGGCTGCACTCTGGTGACATTGCCTACTGGGATGAGGATGAGCACTTTTTCATTGTGGACAGGC
TGAAGAGCCTCATCAAGTACAAAGGCTACCAAGTGGCACCTGCTGAGCTAGAGAGCATCCTGCTCC
AGCACCCCAACATCTTTGATGCTGGTGTGGCTGGCCTGCCTGATGATGATGCTGGAGAGCTGCCTG
CTGCTGTTGTGGTTCTGGAGCATGGAAAGACCATGACTGAGAAGGAGATTGTGGACTATGTGGCC
AGTCAGGTGACCACTGCCAAGAAGCTGAGGGGAGGTGTGGTGTTTGTGGATGAGGTGCCAAAGGG
TCTGACTGGCAAGCTGGATGCCAGAAAGATCAGAGAGATCCTGATCAAGGCCAAGAAGGGTGGCA
AA 3’

Nucleic Acid sequence for MUC1 gene

5’
ATGGCTCTCCCAGTGACTGCCCTACTGCTTCCCCTAGCGCTTCTCCTGCATGCAACCGCCCCTCCAG
CCCACGGAGTGACCAGCGCCCCTGACACCCGGCCTGCTCCTGGAAGCACAGCTCCACCTGCCCACGG
CGTTACCTCTGCACCAGATACTAGGCCTGCTCCAGGCTCCATCGAGGTGATGTACCCCCCCCCCTAC
CTGGACAACGAGAAGAGCAACGGCACCATCATCCACGTGAAGGGCAAGCACCTGTGCCCCAGCCCC
CTGTTCCCCGGCCCCAGCAAGCCCTTCTGGGTGCTGGTGGTGGTGGGCGGCGTGCTGGCCTGCTAC
AGCCTGCTGGTGACCGTGGCCTTCATCATCTTCTGGGTGCGGAGCAAGAGGAGAAAGCGCAGCGGT
TCCGGC 3’

Nucleic Acid sequence for PSMA gene

5’
ATGTGGAACCTGCTGCACGAGACTGACAGCGCCGTGGCAACCGCACGGAGACCCCGGTGGCTGTGC
GCTGGCGCACTGGTGCTGGCCGGCGGGTTCTTTCTGCTGGGGTTCCTGTTTGGATGGTTTATCAAA
AGCTCCAACGAGGCCACCAATATTACACCTAAGCACAATATGAAAGCATTCCTGGATGAACTGAA
GGCCGAGAACATCAAGAAATTCCTGTACAACTTTACTCAGATTCCACATCTGGCTGGCACCGAGCA
GAACTTTCAGCTGGCAAAACAGATCCAGAGCCAGTGGAAGGAATTCGGGCTGGACTCCGTGGAGC
TGGCCCACTACGATGTCCTGCTGAGTTATCCAAATAAGACACATCCCAACTATATCTCAATCATTA
ACGAAGACGGAAATGAGATTTTCAACACTTCACTGTTTGAACCCCCTCCACCCGGCTACGAGAACG
TGAGCGACATCGTCCCTCCATTCTCAGCCTTTAGCCCACAGGGAATGCCTGAGGGGGATCTGGTGT
ACGTCAATTATGCTCGCACCGAAGACTTCTTTAAGCTGGAGCGAGATATGAAAATCAACTGTAGC
GGCAAGATCGTGATTGCCAGATACGGCAAAGTGTTTCGCGGGAATAAGGTCAAAAACGCTCAGCT
GGCCGGGGCTAAGGGAGTGATTCTGTACTCTGACCCCGCTGATTATTTCGCACCTGGAGTGAAGAG
TTATCCAGACGGATGGAATCTGCCAGGAGGAGGAGTGCAGCGAGGAAACATCCTGAACCTGAATG
GGGCCGGAGATCCTCTGACCCCAGGATACCCCGCCAACGAATACGCTTATAGGCGAGGAATTGCAG
AGGCAGTGGGACTGCCTTCCATCCCAGTCCACCCCATTGGCTACTATGACGCCCAGAAGCTGCTGG
AGAAAATGGGAGGCTCTGCTCCCCCTGATTCTAGTTGGAGAGGCAGTCTGAAGGTGCCTTACAAT
GTCGGCCCAGGGTTCACAGGGAACTTTTCAACTCAGAAGGTGAAAATGCACATCCATAGCACTAA
TGAAGTGACCAGGATCTATAACGTCATTGGAACTCTGCGAGGCGCCGTGGAGCCTGACAGATACG
TCATTCTGGGGGGACACCGCGACTCCTGGGTGTTTGGCGGGATCGATCCACAGTCTGGCGCCGCTG
TGGTCCATGAAATTGTGCGGTCTTTCGGCACACTGAAGAAAGAGGGGTGGAGACCCCGACGGACT
ATCCTGTTTGCAAGTTGGGATGCCGAGGAATTCGGCCTGCTGGGGAGTACAGAATGGGCCGAGGA
AAATTCACGGCTGCTGCAGGAGAGAGGGGTGGCTTACATCAATGCAGACTCAAGCATTGAAGGAA
ACTATACACTGCGGGTGGATTGCACTCCCCTGATGTACAGCCTGGTCCACAACCTGACCAAGGAGC
TGAAATCCCCTGACGAGGGATTCGAAGGCAAAAGCCTGTATGAATCCTGGACAAAGAAAAGTCCA
TCACCCGAGTTTAGCGGAATGCCTCGAATCTCTAAGCTGGGAAGTGGCAATGATTTCGAAGTGTTC
TTTCAGAGACTGGGGATTGCCTCCGGAAGAGCTAGGTACACCAAAAATTGGGAGACAAACAAGTT
CTCCGGCTACCCACTGTATCACAGCGTGTACGAGACTTATGAACTGGTCGAGAAATTCTACGACCC
CATGTTTAAGTATCATCTGACCGTGGCACAGGTCAGGGGAGGCATGGTGTTTGAGCTGGCCAATT
CCATCGTCCTGCCATTCGACTGTAGAGATTATGCTGTGGTCCTGAGGAAGTACGCAGACAAAATCT
ATAGCATTTCCATGAAACATCCCCAGGAGATGAAGACCTACTCTGTGAGTTTCGATTCCCTGTTTT
CTGCCGTCAAAAACTTCACAGAAATCGCTAGTAAGTTTTCAGAGCGCCTGCAGGACTTCGATAAGT
CTAATCCCATTGTGCTGAGGATGATGAACGACCAGCTGATGTTCCTGGAACGCGCCTTTATCGACC
CTCTGGGGCTGCCTGATCGCCCCTTCTACCGACACGTGATCTACGCACCTTCCTCTCATAACAAGT
ACGCCGGAGAGTCTTTTCCAGGCATCTATGACGCTCTGTTCGATATTGAATCAAAGGTCGATCCCA
GCAAAGCATGGGGCGAGGTCAAGAGACAGATCTACGTGGCAGCCTTCACCGTCCAGGCTGCAGCCG
AAACACTGAGCGAGGTGG 3’

Nucleic Acid sequence for Grp78 promoter gene

5’
CGCGTGCAGGGCCCACTAGTCGGGAGCGCGTACTTCTTCCGAGTGAGAGACAGAAAGAGAGGACCC
GAGTCTCACAGCCCTGAGGGAACTGACACGCAGACCCCACTCCAGTCCCCGGGGGCCCAACGTGAG
GGGAGGACCTGGACGGTTACCGGCGGAAACGGTTTCCAGGTGAGAGGTCACCCGAGGGACAGGCA
GCTGCTCAACCAATAGGACCAGCTCTCAGGGCGGATGCTGCCTCTCATTGGCGGCCGTTAAGAATG
ACCAGTAGCCAATGAGTCGGCCTGGGGGGCGTACCAGTGACGTGAGTTGCGGAGGAGGCCGCTTCG
AATCGGCAGCGGCCAGCTTGGTGGCATGAACCAACCAGCGGCCTCCAACGAGTAGCGAGTTCACCA
ATCGGAGGCCTCCACGACGGGGCTGCGGGGAGGATATATAAGCCGAGTCGGCGACCGGCGCGCTCG
ATACTGGCTGTGACTACACTGACTTGGACACTTGGCCTTTTGCGGGTTTGAGAGGTAAGCGTCGCG
GCCTGCTTCCAGGCCTACCCTGATTTTGGTTCGTGGCTCCTCCTGACCCTGAGACCTCTGTCGCCCT
CAGATCAGAACCGTCGTCGCGTTTCGGGGCTACAGCCTGTTGCTGGACTCTGTGAGACACCTGACC
GACCGCTGAGCGACTGACTGGTCCACAGCGCCGGCACCATGGGGGGTTCTCATCATCATCATCATC
ATGGTATGGCTAGCATGACTGGTGG 3’

Nucleic Acid sequence for Pb9 gene

5’ TCATACATCCCGAGCGCAGAGAAGATT 3’

Nucleic Acid sequence for TIP gene

5’
ATGACCTTTCTTACCTCTGAGCTACCCGGCTGGTTGCAAGCAAACCGCCATGTAAAACCCACAGCA
GCGTATGCGGCCGTGAAAAATTGGATGACACAAACCTTAGCAGCCTAC 3’

Nucleic Acid sequence for ubiquitin gene

5’
ATGCAAATTTTTGTTAAAACTTTAACTGGTAAGACAATTACACTCGAGGTGGAACCCTCTGACAC
AATAGAGAATGTTAAGGCCAAGATTCAAGACAAGGAGGGCATACCACCCGATCAGCAGAGACTTA
TATTTGCGGGAAAACAATTAGAGGATGGACGAACACTCTCGGATTATAATATCCAGAAAGAATCT
ACCTTGCACCTAGTCCTTCGATTAAGGGGTGGA 3’

Nucleic acid sequence for puromycin-resistance gene:

5’
CTCAGGTTTAAGCTCCAGGCTTCCTTGTCATGCACCAAGTTCTTGGGCCTTCTGGAACCTCAACAT
CAGCTGTCACAGTGAATCCCAGTCTTTCATAAAAAGGCAGGTTTCTGGGAGCAGAAGTTTCCAGA
AAGGCAGGAACTCCAGCCCTTCAGCAGCTTCAACTCCAGGCAGAACAACAGCAGATCCCAGACCCT
TTCCCTGGTGGTCAGGGCTCACTCCAACAGTTGCCAGAAACCAAGCTGGCTCTTTTGGCCTGTGTG
GTGCCAGCAGACCTTCCATTTGTTGTTGTGCTGCCAGCCTGCTTCCAGAGAGCTCAGCCATTCTTG
GTCCAATTTCAGCAAAAACAGCACCAGCTTCAACAGACTCAGGTGTTGTCCAAACTGCAACAGCAG
CTCCATCATCTGCAACCCAAACTTTTCCAATGTCCAGTCCCACTCTGGTGAGGAAGAGTTCTTGCA
GTTCTGTCACCCTCTCAATGTGCCTGTCAGGGTCAACTGTGTGCCTTGTTGCAGGGTAGTCTGCAA
AAGCAGCAGCCAGTGTTCTCACAGCTCTTGGAACATCATCTCTGGTTGCCAGCCTCACTGTGGGTT
TGTACTCAGTCAT 3’

Scientific contributions

Conferences

Waramit S, Suwan K, Asavarut A, Ashfield R, Draper SJ and Hajitou A. *New strategy of cancer vaccination by a hybrid bacteriophage vector and a malaria vaccine*. BSGCT Annual Conference 2019, Sheffield, UK (Oral presentation)

Waramit S, Suwan K, Asavarut A and Hajitou A. *The augmentation of tumour-associated antigen expression by hybrid bacteriophage/adeno-associated virus vector for CAR T cell therapy*. ESGCT Annual Congress 2017, Berlin, Germany (Poster presentation)

Publications

Suwan K, Yata T, Waramit S, Przystala JM, Chongchai A, Asavarut P,Bentayebi K, Lee KY, Stoneham CA, Topanurak S, Pothachareon P, Smith TL, Gelovani JG, Sidman RL, Pasqualinie R, Araph W, and Hajitou A. *A next-generation of targeted AAVP vectors for systemic transgene delivery against cancer.* Accepted manuscript PNAS July 2019.

Przystal JM, Waramit S, Pranjol MZI, Yan W, Chu G, Chongchai A, Samarth G, Olaciregui NG, Tabatabai G, Carcaboso AM, Aboagye EO, Suwan K and Hajitou A. *Efficacy of systemic temozolomide-activated phage-targeted gene therapy in human glioblastoma*. EMBO Mol Med. 2019 Apr;11(4). pii: e8492.

Campbell S, Suwan K, Waramit S, Aboagye EO and Hajitou A. *Selective Inhibition of Histone Deacetylation in Melanoma Increases Targeted Gene Delivery by a Bacteriophage Viral Vector*. Cancers (Basel). 2018 Apr 21;10(4). pii: E125.

Patent Application

Hajitou A, Suwan K, Albahrani M and Waramit S. *Cancer treatment*. WO/2018/197859.